CANADIAN THESES

THÈSES CANADIENNES

NOTICE

The quality of this microfiche is heavily dependent upon the quality of the original thesis submitted for microfilming. Every effort has been made to ensure the highest quality of reproduction possible.

If pages are missing, contact the university which granted the degree.

Some pages may have indistinct print especially if the original pages were typed with a poor typewriter ribbon or if the university sent us an inferior photocopy.

Previously copyrighted materials (journal articles, published tests, etc.) are not filmed.

Reproduction in full or in part of this film is governed by the Canadian Copyright Act, R.S.C. 1970, c. C-30.

AVIS

La qualité de cette microfiche dépend grandement de la qualité de la thèse soumise au microfilmage. Nous avons tout fait pour assurer une qualité supérieure de reproduction.

S'il manque des pages, veuillez communiquer avec l'université qui a conféré le grade.

La qualité d'impression de certaines pages peut laisser à désirer, surtout si les pages originales ont été dactylographiées à l'aide d'un ruban usé ou si l'université nous a fait parvenir une photocopie de qualité inférieure.

Les documents qui font déjà l'objet d'un droit d'auteur (articles de revue, examens publiés, etc.) ne sont pas microfilmés.

La reproduction, même partielle, de ce microfilm est soumise à la Loi canadienne sur le droit d'auteur, SRC 1970, c. C-30.

THIS DISSERTATION
HAS BEEN MICROFILMED
EXACTLY AS RECEIVED

LA THÈSE A ÉTÉ
MICROFILMÉE TELLE QUE
NOUS L'AVONS REÇUE

NL-339 (r.86/06)

Canada

ISBN 0-315-33324-3

UNIVERSITÉ D'OTTAWA
UNIVERSITY OF OTTAWA

To

NanKai University

(China)

ACKNOWLEDGEMENTS

I wish to express my sincere appreciation to my supervisor, Emeritus Professor K. J. Laidler, for his constant guidance, encouragement and patience throughout the research and during the preparation of this thesis. I gratefully acknowledge his many invaluable suggestions, critical comments, and discussions. His untiring work in research and education will forever remain my model and my inspiration. It has been an honour and pleasure working with Professor Laidler, such an outstanding researcher and scientific teacher.

I am indebted to Dr. Y. L. Yao and Mrs. Yao for encouraging me to work towards a Ph.D. degree, and thank them for their financial support at the beginning of my studies.

I am grateful to Dr. M. H. Back for offering me a very good place in her laboratory and for her concern and encouragement.

Thanks are due to Dr. J. M. J. Fréchet for his friendly help, and also to Dr. B. E. Conway, Dr. J. L. Holmes, Dr. B. A. Morrow and Dr. T. Durst for their assistance in their courses; thanks also to all members of the Chemistry Department of the University of Ottawa for their friendship. I am thankful to Dr. D. K. Banerjee for our fruitful exchange of views.

Special gratitude goes to my husband Nai-Hong, I deeply appreciate his understanding, exceptional patience and constant encouragement, also to my sons Young and Qing for their tolerance and understanding. Their love is my moral support.

TABLE OF CONTENTS

List of Figures

List of Tables

ABSTRACT

The kinetics of the hydrolysis of cellobiose catalyzed by β-glucosidase has been investigated both in free solution and in a tubular reactor, with the enzyme chemically attached to a surface.

The enzyme reaction in free solution was studied by experimental techniques which allow the course of reaction to be followed continuously. They involve assaying the product glucose by a continuous procedure involving the use of a coupled system containing ATP, hexokinase, glucose-6-phosphate dehydrogenase and NADP; the latter is converted into its reduced form NADPH and determined spectrometrically at 340 nm where it absorbs strongly.

Two procedures, referred to as the glucose-concentration method and the glucose-slope method, have been devised for the determination of initial rates of the enzyme reaction under different conditions. These procedures are based on the use of different types of calibration curves. One is the conventional calibration curve with absorbance plotted against concentration; the other one involves the initial slope of absorbance-time curves plotted against concentration.

Kinetic measurements were carried out at eight pH values varying from 5 to 6.9, at temperatures varying from 10°C to 37°C, and at substrate concentrations varying from 0.2 mM to 4.8 mM. In all of the measurements the enzyme concentration was 0.1 mg/mL. The pH-dependences of Michaelis parameters show a maximum at a pH

value of 5.76 at 18°C and at pH values between 5.5 and 5.6 at 24° and 31°C. The pK values for catalytically important groups were determined at three temperatures, 18°, 24° and 31°C, by a computerized statistical procedure. The pK values 4.9 and 6.4 at 24°C suggest a carboxylate group and an imidazolium group involved at the active centre of the enzyme. The Michaelis constant K_m increases with pH and the limiting rate V_m passes through a maximum as the pH is varied; this indicates that the imidazole group is probably implicated in the binding of substrate to form the enzyme-substrate complex, whereas both active groups are involved in the decomposition of the complex.

The studies of temperature effects were made at different pH values for various substrate concentrations. Arrhenius plots of initial rates and of Michaelis parameters consistently show a change in slope at about 23°C, under all conditions. The variation of activation energy with pH was investigated. The activation energies and entropies of activation in the higher temperature range do not vary much with pH, but those in the lower temperature range pass through a minimum at around pH 5.9. The results were first analyzed on the basis of the theory of temperature effect in terms of a mechanism involving two intermediates:

$$E + S \underset{k_{-1}}{\overset{k_1}{\rightleftharpoons}} ES \xrightarrow{k_2} ES' \xrightarrow{k_3} E + \text{products}$$

but this theory did not satisfactorily interpret the dependence

of activation energy on pH.

The cooperative effects of temperature and pH were then considered and an unified treatment of both effects was developed to interpret the Arrhenius behaviour and the variation of activation energy with pH. Equations were obtained which indicate how the apparent activation energy varies with pH and temperature, for one-intermediate and two-intermediate mechanisms. It was shown that Arrhenius plots are in general concave towards the axes. The application of this treatment to the β-glucosidase results showed that a two-intermediate mechanism was required to interpret both the concave Arrhenius behaviour and the variation of the apparent activation energy with pH. It was found possible to obtain, for the four elementary reactions, activation energies and entropies of activation, by a successive approximation procedure.

The temperature effects on the dissociation constants of active groups were studied and the results analyzed to give the thermodynamic parameters associated with these dissociation processes for the free enzyme and the enzyme-substrate complex. The first ionization is accompanied by a substantial entropy increase, 109 J $K^{-1}mol^{-1}$, the second with a large entropy decrease -283 J $K^{-1}mol^{-1}$. The entropy changes are too large to be attributed to electrostriction effects, and suggest structural changes in the enzyme molecules; the first ionization probably involves the conformational change from an expanded to a coiled form, while the second ionization involves a change from a random

coiled to an expanded form.

The enzyme β-glucosidase was attached covalently to the inner surface of nylon tubing. Flow kinetic studies were carried out at a range of temperatures from 5 to 45°C, pH values from 4.44 to 6.90, flow rates varying from 0.98 to 9.18 cm s^{-1} and substrate concentrations ranging from 1.3 mM to 13.3 mM.

The extent of diffusion control was investigated. Various tests on the basis of the Kobayashi-Laidler treatment of flow systems showed that diffusion control was negligible.

The inherent Michaelis constants, obtained at different temperatures and different pH values, are higher than the corresponding values for the enzyme in free solution. However, the differences are small, again indicating little diffusion control and showing that the immobilized system is quite efficient.

A comparison was made between the immobilized and free enzyme with particular reference to pH and temperature effects and to stability. The pH-rate profiles for the immobilized enzyme were similar to that for free enzyme. However there is a small difference between the patterns of the pH curves for Michaelis parameters, in that the immobilized enzyme shows greater relative activity at lower pH and smaller relative activity at higher pH, and has an optimum pH higher by about 0.3 units. The pK values are slightly lowered as a result of the immobilization. These differences are attributed to a small positive residual charge on the surface of the support.

The temperature dependence of the enzyme reaction remains much the same after immobilization. The Arrhenius plots showed intersections at about 22°C, as with the free enzyme, the changes in slope being small at the pH optimum of about 5.9 and becoming much more pronounced as the pH is increased or decreased. The activation energies for the immobilized enzyme are close to those for the free enzyme.

Tests were made to determine the stability of the enzyme-coated tube used in the experiments. The immobilized enzyme is substantially more stable than the free enzyme, both on storage at low and higher temperatures, and its thermal stability is greater. The enzyme tube can be used a considerable number of times before becoming inffective; its half life on re-use is about 200 hours.

The similar kinetic behaviour of the immobilized enzyme to that of free enzyme indicates that the attachment procedure does not affect significantly the function and activity of the enzyme.

CHAPTER I

GENERAL INTRODUCTION

The enzymes are important constituents of living systems, their function being to catalyze the chemical processes that occur. They are remarkable for their specificity, and a very large number of enzymes have now been identified. They are also unusual in their high catalytic efficiency. Kinetic and mechanistic studies of enzyme systems are important in leading to valuable insight into the general problem of catalytic efficiency, and also in throwing light on the functioning of living systems. This thesis describes a detailed kinetic study of the enzyme β-glucosidase, both in free solution and attached to a surface.

1.1 Enzymic hydrolysis of cellulose and the role of β-glucosidase

The enzymic conversion of cellulose to D-glucose and its fermentation to ethanol, a liquid fuel, has great potential as a significant source of renewable energy as well as a feedstock for chemicals, since about half of Biomass, accumulated by photosynthetic storage of solar energy in green plants, is in the form of cellulose. Cellulose, a biopolymer, must be broken into smaller sugar molecules before it can be converted to liquid

fuel by fermentation. Although this can be accomplished by acid hydrolysis, enzymic hydrolysis has recently received much attention because it forms fewer by-products and proceeds under milder conditions. The enzymic degradation of cellulose therefore has important practical implications. Intensive research efforts are in progress to make the technology viable.

Cellulase, the enzyme system which hydrolyzes cellulose to glucose, ordinarily contains three major components:

(1) exo-β-1,4-glucanase or β-1,4-glucan cellobiohydrolase (EC.3.2.1.91), which splits off cellobiose from the nonreducing end of the cellulose chain(1-5).

(2) endo-β-1,4-glucanase(EC.3.2.1.4), which cleaves the cellulose chain at random positions and produces more chain ends on which exo-β-glucanase may act(2,5,6).

(3) β-glucosidase or cellobiase(EC.3.2.1.21), which catalyzes the hydrolysis of cellobiose and cellodextrins to glucose (7,8,9,11,12).

The hydrolysis of native cellulose thus involves a sequential action(10) by an endo-glucanase which attacks at random the 1,4-β-linkage along the cellulose chain. The structure is opened in this way, and exo-β-glucanase splits off cellobiose units from the non-reducing ends of the cellulose chain. The continued cooperative action of the endo-glucanase and exo-glucanase results in the coversion of cellulose into cellobiose and small oligosaccharides which are finally hydrolyzed to glucose by β-glucosidase. This process may be envisaged as follows:

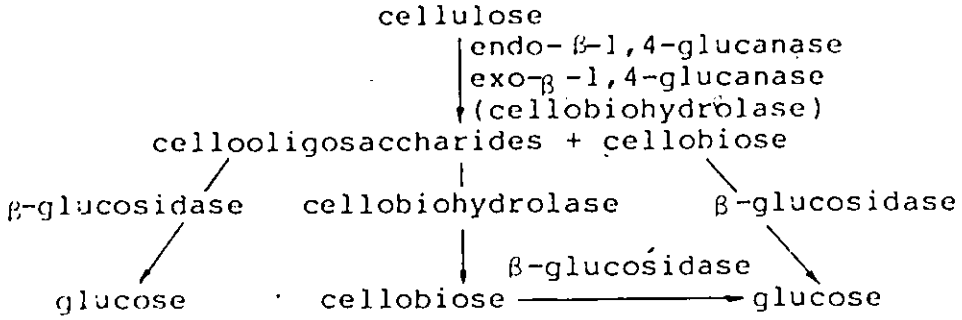

However, cellobiose, the intermediate of cellulose hydrolysis, is an inhibitor for cellobiohydrolase by product inhibition(5,13,14) and it is also an inhibitor for β-glucosidase by substrate inhibition(7,15,17). Because of these inhibiting effects the accumulation of cellobiose in the process slows the enzymic degradation, and lowers the yield of glucose. Therefore, β-glucosidase in high levels in cellulase complex plays a crucial role in large-scale saccharification of cellulose by removing inhibitory cellobiose(4-8,15,16). Indeed, it has been demonstrated that the rate of saccharification of cellulose and the yield of glucose can be significantly improved by supplementation of cellulase with β-glucosidase(17-22).

The kinetics of the action of β-glucosidase is therefore a matter of considerable practical significance.

1.2 Previous studies on β-glucosidase

β-glucosidase(β-D-glucoside glucohydrolase, EC 3.2.1.21) is an enzyme which catalyzes the hydrolysis of various compounds having β-D-glucosidic linkages; it acts on aryl and alkyl β-D-

glucosides as well as on cellobiose. This enzyme is stereospecific for the hydroxyl groups at the positions C-1, C-2 and C-4 of the aldohexose ring. In general, the interchange of hydrogen and hydroxyl groups on any carbon atom in the hexose ring of glucoside substrate is sufficient to prevent the action of the enzyme; thus β-glucosidase does not act on β-D-mannosides or on β-D-galactosides, nor does it act on β-D-glucosides. However, the existence of different types of β-glucosidase, from different sources, with variations in C-4 specificity, has been clearly established. For example, β-glucosidase from almond emulsin has been shown to hydrolyze both β-D-glucosides and β-D-galactosides(25,46).

Substitution on the hydroxyl groups of the glucosyl moiety usually has a profound effect. Any substitution at C-2, C-3 or C-4 completely prevents hydrolysis, while substitution at C-6 lowers the rate of hydrolysis. Replacement of the $-CH_2OH$ group attached to C-5 by -H, i.e. conversion to a β-D-xyloside, produces a 200-fold reduction in rate. Thus, in general, an intact unsubstituted hexose ring is required for the action of β-glucosidase.

β-glucosidase can tolerate a wide variety of aglycones, but the nature of the aglycone has a marked influence on the rate of hydrolysis. Positional isomerism is not critical, and β-glucosidase hydrolyzes all disaccharides of glucose: sophorose(β-1,2), laminaribiose(β-1,3), cellobiose(β-1,4) and gentiobiose(β-1,6).

The enzyme β-glucosidase can be obtained from a variety of sources: fungi, bacteria, yeast and plants. Its physical, chemical and enzymic properties depend on the source and on the conditions under which the enzyme is produced and/or purified. For example, the molecular weight, the optimum pH, the substrate specificity, the inhibition by product or by substrate, and the values of the dissociation constants of catalytically active groups may differ for the enzymes obtained from different sources.

A great many studies on this enzyme have been published in the literature. However, most of these were concerned with its isolation, purification and characterization, and with the functional properties of the enzyme from different sources(7,15,23,24,26,27,29,30,31,32,33). The substrate specificity has been extensively studied. The inhibition by substrate and substrate analogues, and by the product glucose, has also been investigated(7,15,17,25,34-39,41-47). Little information about the structure is available in the literature. As far as structural aspects are concerned, most of the work has concentrated on whether the enzyme has one or two catalytic sites responsible for both the β-glucosidase and β-galactosidase activities; this has been done for enzyme types which showed both these two activities(25,46,47). There are opposing views: one is that there are two catalytic sites, one for the β-glucosidase and the other for the β-galactosidase activity(25); the alternative view is that there is a single catalytic site for both

activities(46). It has also been suggested that the enzyme molecule has two substrate binding sites and a single catalytic site(47), the binding sites being specific for a β-glucoside or a β-galactoside.

Some work has been concerned with the identification of catalytically active groups(15,26,48-52). From the determination of K_m and V_m at different pH values for the hydrolysis of salicin(48), cellobiose(49) and o-nitrophenyl-β-D-glucopyranoside (50-52), a carboxylate group and an imidazolium group have been indicated as being involved in catalysis. In one investigation(15) it is has been suggested that only carboxylate groups are involved in the catalytic role. This suggestion was based on the measurements of pK values for the enzyme from S. rolfsii; these were 4.2 and 4.7 for groups in the free enzyme, and 3.2 and 3.8 for groups in the enzyme-substrate complex.

The mechanism of the action of β-glucosidase is not well known. Most previous work was done with aryl β-D-glucosides, and a two-step mechanism for the hydrolysis has been proposed (1,3,52,54,55). The first step involves splitting of an aglycon moiety with simultaneous formation of an enzyme-glucosyl complex; this intermediate complex then reacts with water, yielding glucose. Umezurike(50,51,52) investigated the effect of varying the solvent composition: he increased the concentration of dioxan on the activity of β-glucosidase from Botryodiplodia theobromae Pat, and suggested a carboxyl group and an imidazole group as being at the active centre. On the basis of inhibition studies,

and studies of the effect of added acceptors on the rate of the hydrolysis of o-nitrophenyl β-D-glucopyranoside, he proposed a reaction scheme for the hydrolytic and transferase activities of β-glucosidase in the presence of an added acceptor A:

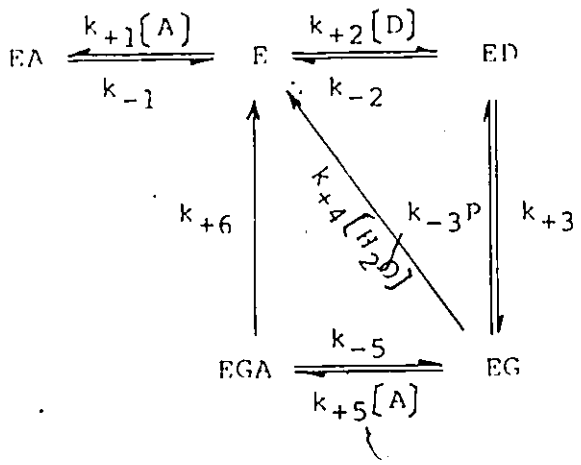

Here D is the substrate, and ED is an enzyme-bound glucosyl cation-carboxylate ion-pair which is formed by acid catalysis of imidazolium group on the enzyme.

However, no mechanism of the hydrolysis of cellobiose by β-glucosidase has yet been proposed. Most studies on cellulose degradation have focused on the initiation of the hydrolysis (56,57), and on the hydrolysis catalyzed by cellulase. With regard to the hydrolysis of cellobiose catalyzed by β-glucosidase, most previous work has been on stability, activity and applications of different immobilized preparations. Some investigations were concerned with kinetic aspects(58-64), but no detailed kinetic studies have been reported.

1.3 Objectives and outline of present work

The present work was concerned with investigating the kinetics of the hydrolysis of cellobiose by β-glucosidase in more detail, in order to understand the mechanism and the kinetic and thermodynamic behavior of the enzyme.

A comprehensive experimental study of the hydrolysis reaction, with both free and immobilized enzyme, will be described in subsequent chapters. The studies were made at different pH values, at different temperatures, and at different substrate concentrations. This allows the evaluation of dissociation constants for the catalytically important groups on the enzyme and therefore allows the identification of these active groups. In addition, based on the temperature dependence of the corresponding dissociation constants, these studies provide an estimate of the entropy and enthalpy changes associated with the dissociation processes, and therefore provide some information about the change of the enzyme conformation during the dissociation processes, and during the formation and breakdown of the enzyme-substrate complex.

Such comprehensive experimental studies on both pH and temperature effects not only allow the calculation of activation energies under different conditions, but also provide the possibility of investigation and analysis of the cooperative effects of temperature and pH; the latter is more important for establishing the reaction mechanism. Theories in enzyme kinetics

are either only on pH effects or temperature effects; no consideration of cooperation of both temperature and pH effects appears to have been made.

The immobilization of an enzyme can offer particular advantages in the stability and repetitive use of the enzyme, and the employment of immobilized β-glucosidase is of considerable significance in the industrial saccharification of cellulose on a large scale. This enzyme has previously been attached to different supports, but no attempt has been made to attach it to a nylon tube. One objective of the present work was to find a suitable procedure and optimum conditions for stable attachment of β-glucosidase inside nylon tubing. Kinetic studies were undertaken with the immobilized preparation, and were concerned with the activity, stability and flow kinetics over a range of temperatures, pH and flow rates. The extent of diffusion control was also determined.

The methods previously employed for following the hydrolysis of cellulose by cellulase or of cellobiose by β-glucosidase, usually involved stopping the reaction after various times and then performing an analysis; such methods are inconvenient for kinetic investigations. Another important objective of this work was to devise a more rapid and satisfactory method for following the reaction continuously.

1.4 General aspects of enzyme kinetics

It has been well established that enzyme reactions proceed in at least two well-defined steps(65): the first is the formation of a complex between enzyme E and substrate S, and the second is the decomposition of the complex into the products of the reaction with the regeneration of enzyme. This may be represented by the following reaction schemes

$$E + S \underset{k_{-1}}{\overset{k_1}{\rightleftharpoons}} ES \xrightarrow{k_2} P + E$$

Often there are three steps, as in the scheme

$$E + S \underset{k_{-1}}{\overset{k_1}{\rightleftharpoons}} ES \xrightarrow{k_2} ES' \xrightarrow{k_3} P + E$$

The concept of the enzyme-substrate complex has been of enormous importance in enzyme kinetics, and has been supported by a great deal of evidence from the kinetics found for a large variety of reactions, and by experimental demonstrations of the existence of intermediates by spectroscopy(66), spectral shifts(67), fluorescence(68), light scattering(69) and chromatography(70) etc.

For one-substrate reactions involving one intermediate and uncomplicated by the reverse reactions or the effects of modifiers,

$$E + S \underset{k_{-1}}{\overset{k_1}{\rightleftharpoons}} ES \xrightarrow{k_2} P + E$$

the following rate equations can be easily formulated by means of steady-state treatment

$$v = \frac{k_2[E]_o[S]}{\frac{k_{-1}+k_2}{k_1} + [S]} \qquad (1)$$

or

$$v = \frac{V_m[S]}{K_m + [S]} \qquad (2)$$

In this equation

$$V_m = k_2[E]_o \qquad (3)$$

$$K_m = \frac{k_{-1}+k_2}{k_1} \qquad (4)$$

Here $[E]_o$ is the total concentration of the enzyme. Eq.(2) is known as the Michaelis-Menten equation and the constant K_m as the Michaelis constant; it has the same units as a concentration.

Equations (1) and (2) are the equations of a rectangular hyperbola. Thus, at low substrate concentrations the rate of an enzyme reaction rises with [S], at first linearly, but at high concentrations it levels off at a limiting rate, equal to V_m ($=k_2[E]_o$).

For the two-intermediate mechanism

$$E + S \underset{k_{-1}}{\overset{k_1}{\rightleftharpoons}} ES \overset{k_2}{\underset{P_1}{\rightleftharpoons}} ES' \xrightarrow{k_3} E + P_2$$

the steady-state treatment leads to an equation of the same form as that given by the single-intermediate mechanism,

$$v = \frac{k_2k_3/(k_2+k_3)\ [E]_o[S]}{\{(k_{-1}+k_2)/k_1\}\cdot\{k_3/(k_2+k_3)\} + [S]} \qquad (5)$$

or

$$v = \frac{V\ [S]}{K_m + [S]} \qquad (2)$$

The significance of the parameters V and K_m is now different:

$$V = \frac{k_2k_3}{k_2 + k_3}[E]_o \qquad (6)$$

$$K_m = \frac{k_{-1}+k_2}{k_1}\cdot\frac{k_3}{k_2+k_3} \qquad (7)$$

Steady-state studies of influence of substrate concentration on rate can not therefore provide information about the number of intermediates.

In the analysis of experimental data from kinetic measurements of enzyme reactions the most commonly employed procedure is the Lineweaver-Burk method(71), in which the rate equation(2) is used in reciprocal form as

$$\frac{1}{v} = \frac{K_m}{V}\cdot\frac{1}{[S]} + \frac{1}{V} \qquad (8)$$

If the Michaelis- Menten equation is obeyed a plot of 1/v against 1/[S] gives a straight line with slope K_m/V and intercept 1/V on the 1/v axis. The kinetic parameters K_m and V can therefore be calculated from the slopes and intercepts of such Lineweaver-Burk plots. Another procedure, proposed by Eadie(74), is also used in the analysis of experimental data; it is based on equation(2) in the following form

$$\frac{v}{[S]} = \frac{V}{K_m} - \frac{v}{K_m} \qquad (9)$$

If the equation is obeyed, v/[S] plotted against v also gives a straight line. In the present work we used the Lineweaver-Burk method to deal with the experimental data.

Because product interference is commonly found in an enzyme reaction the most useful kinetic method for analyzing results is the differential method, the rates (slopes) being measured at the very beginning of the reactions for a series of initial concentrations. It is often very convenient in studying enzyme systems to cause the reaction to occur sufficiently slowly (e.g. by reducing the enzyme concentration) so that a number of measurements can be made during the very early stages of reaction. In this way it is possible for the initial rates to be determined very accurately. In addition, in order to satisfy the steady-state hypothesis, the concentrations of substrate are

usually made sufficiently large compared with the enzyme concentration, the ratio $[S]/[E]_o$ being 10^3 or greater.

Enzymes are particularly sensitive to their environment, and readily undergo subtle changes in structure which lead to an alteration in activity and kinetic properties. Changes in pH, for example, can produce drastic changes in activity, both directly (by altering the ionization of groups involved in catalysis) and indirectly (through a change in conformation). Also, enzymes undergo conformational changes very easily at higher temperatures. Ionic strength is also known to have effects on the activities of many enzymes, such as chymotrypsin(72), trypsin and ribonuclease(73).

Three factors, temperature, pH and ionic strength are therefore critical in carrying out an enzyme kinetic study. These factors require even more stringent control than in the case of ordinary chemical reactions.

Depending on the properties of the substrate and the products of enzyme reactions, several methods can be used for following the progress of the reaction, namely

(1) spectrophotometry: measurements of absorbance of radiation or fluorescence at certain wavelength.

(2) methods employing electrodes: pH measurements or conductimetry measurements of the system.

(3) magnetic measurements: electron spin resonance(e.s.r.) and nuclear magnetic resonance(n.m.r.), particularly proton magnetic resonance.

In the case of the hydrolysis of cellobiose by β-glucosidase, both the substrate and the product glucose do not give an obvious absorbance peak in the range of 200-700 nm, so that the reaction cannot simply and continuously be followed by spectrophotometry. This problem will be discussed in the next chapter.

CHAPTER II

KINETIC PROCEDURE

2.1 Three-step (reaction-stop-analysis) method

Glucose is the only product of cellobiose hydrolysis, so that an accurate and specific method for glucose determination is of great importance in the kinetic study of the hydrolysis of cellobiose.

Several methods for glucose determination have been described in the literature:

(1) Enzymic determination by a coupled glucose oxidase-peroxidase system(75-78).

This method is based on the following reaction scheme.

$$\text{Glucose} + O_2 + H_2O \xrightarrow{\text{glucose oxidase}} H_2O_2 + \text{gluconic acid}$$

$$H_2O_2 + \text{reduced chromogen} \xrightarrow{\text{peroxidase}} \text{oxidized chromogen} + H_2O$$

The oxidized chromogen formed in the final reaction absorbs at 420 nm. Its concentration is proportional to the glucose concentration, and the absorbance measured at 420 nm therefore gives the concentration of glucose.

(2) Enzymic determination by a coupled glucose-6-phosphate dehydrogenase-NADP system(79,80).

This procedure comprises the following steps

$$\text{glucose} + \text{ATP} \xrightarrow{\text{hexokinase}} \text{ADP} + \text{glucose-6-phosphate}$$

$$\text{glucose-6-phosphate} + \text{NADP} \xrightarrow{\text{G6PDH}} \text{NADPH} + \text{6-phosphogluconate}$$

The NADPH absorbs strongly at 340 nm, and its concentration and the glucose concentration can therefore be determined at this wavelength.

(3) Chemical determinations of glucose(81-84).

These chemical determinations employ condensation reactions between glucose and certain aromatic amines, e.g. p-aminobenzoic acid or m-aminophenol(81), or ortho-toluidine(82,83), to give coloured products; these colours are characteristic and the products can be measured colorimetrically.

All of these methods have been used extensively for the determination of glucose in serum, plasma and urine; they are accurate, specific and reproducible, and are convenient for clinical purposes. However, these techniques are not readily adaptable to kinetic measurements.

The activities of β-glucosidase or cellulase are commonly evaluated by endpoint analysis of the product or by stopping the reaction and analyzing the product. The reactions catalyzed by cellulase or β-glucosidase are usually followed by assaying the product after various periods of time. In the past this has been done by the following procedure(18,58,60,61,85,86,87):

(1) The enzyme is first incubated with its substrate(e.g. cellulose or cellobiose) in buffered solution;

(2) The enzyme reaction is then stopped by inactivation of enzyme by heat or by addition of an inhibitor, e.g.trichloroacetic acid or sodium carbonate;

(3) The glucose formed is then measured spectrophotometrically(18,58,60,85,87,88), using the coupled glucose oxidase system, a coupled glucose 6-phosphate dehydrogenase-NADP system, or chemically(86,89,90).

Even for a reaction with a product that absorbs at some wavelength (e.g. the hydrolysis of p-nitrophenyl-D-glucoside by β-glucosidase), the usual kinetic procedures also consist of stopping the reaction and then carrying out an analysis.

These methods are inconveniently laborious and time-consuming for a kinetic investigation and it is advantageous to have available a more rapid method.

We therefore explored an alternative method which allows the reaction to be followed continuously, by continuous determination of the product glucose.

2.2 The glucose concentration method and glucose slope method

In these new methods, the coupled system,containing ATP, hexokinase, glucose-6-phosphate dehydrogenase and NADP was used as an assay reagent for glucose determination. The following successive reactions are involved:

$$\text{Cellobiose} + H_2O \xrightarrow{\beta\text{-glucosidase}} 2\ \text{glucose}$$

$$\text{glucose} + \text{ATP} \xrightarrow{\text{hexokinase}} \text{ADP} + \text{glucose-6-phosphate (G-6-P)}$$

$$\text{G-6-P} + \text{NADP} \xrightarrow{\text{glucose-6-phosphate dehydrogenase (G-6-PD)}} \text{6-phosphogluconic acid} + \text{NADPH}$$

(no A_{340}) (high A_{340})

The NADPH formed is then determined spectrophotometrically at 340 nm.

Materials

The β-glucosidase(β-D-glucoside glucohydrolase, EC 3.2.1.21), type 1 derived from almonds, was obtained as a lyophilized powder from the Sigma Chemical Co. It had been purified chromatographically and was essentially salt-free. The specific activity was 30 units/mg with salicin as subtrate at pH 5.0 and at 37°C. The substrate, D(+)cellobiose (β-D(+)cellobiose; 4-O-β-D-glucopyranosyl-D-glucose) was also obtained from Sigma, as was the reagent for glucose determination. According to the specifications the reagent should be reconstituted with 31 mL water. However, in order to optimize the amount of assay reagent for the glucose determination, various amounts of reagent for a series of standard glucose concentrations were tested. It was found that in the range of substrate concentrations investigated in the present work the best amount of reagent is 1 mL which was obtained by reconstituting the reagent with 15.5 mL, for a total volume of 3 mL of the enzyme system. Thus the resulting reagent

solution contains the following:

2.0 mmol/L	ATP
1.0 mmol/L	NADP
1600 U/L	yeast hexokinase
1000 U/L	G-6-PDH (yeast)
4.0 mmol/L	Mg^{2+}

together with buffers.

The enzyme solution and the substrate solution were both prepared in 0.2 M acetate buffers at the pH values required.

The absorbances were measured by the double beam SP 1800 U.V. Spectrophotometer connected to a Unicam AR 25 linear chart Recorder. The sample chamber of the spectrophotometer was thermostatted by the use of a HAAKE Refrigerated Bath and a F3-C Circulator. Micropipettes were used to transfer appropriate portions of the stock solutions of the reactants.

Procedure

Calibration curves were obtained with standard glucose solution at different pH values and different temperatures; this was done for each new batch of assay reagent.

Standard 0.556 mM and 0.0556 mM glucose solutions were prepared by diluting a standard glucose solution (containing 5.56 mM glucose in saturated benzoic acid) with 0.2 M acetate buffer, at a desired pH. A cuvette of 3 mL capacity and a light path of 1 cm was used to mix 1 mL of the assay reagent with an

appropriate amount of buffer solution at the desired pH. The mixture was incubated at the temperature to be used in the kinetic measurement. After 4 minutes a certain aliquot of a standard glucose solution was made up to a total volume of 3 mL, the final concentrations being between 2.97 μM and 37.1 μM, or between 37.1 μM and 371 μM (for pH 5.0). The absorbance at 340 nm, as compared with a glucose-free blank solution, was automatically recorded as a function of time.

For pH values above 6.2, calibration curves were prepared by plotting absorbance against glucose concentration. For pH values below 6.2, initial slopes of absorbance-time curves were plotted against glucose concentration. An example of each type of calibration curves is shown in Fig. 1 and Fig. 2.

Kinetic runs with the enzyme were also carried out in cuvettes, 1 mL assay reagent being mixed with 0.5 mL of 0.6 mg/mL enzyme solution and with an appropriate aliquot of 0.2 M acetate buffer to make the final total volume 3 mL after adding substrate solution. The addition of the appropriate amount of 5.99 mM substrate solution started the reaction, which was followed by recording, as a function of time, the changes of absorbance at 340 nm; a mixture of 1 mL assay, 0.5 mL enzyme solution and 1.5 mL buffer was used as a blank.

Calculation of initial rates of enzyme reactions

(1) Reactions at pH values above 6.2; the glucose-concentration-method

At pH values above 6.2, the reaction of the assay reagent

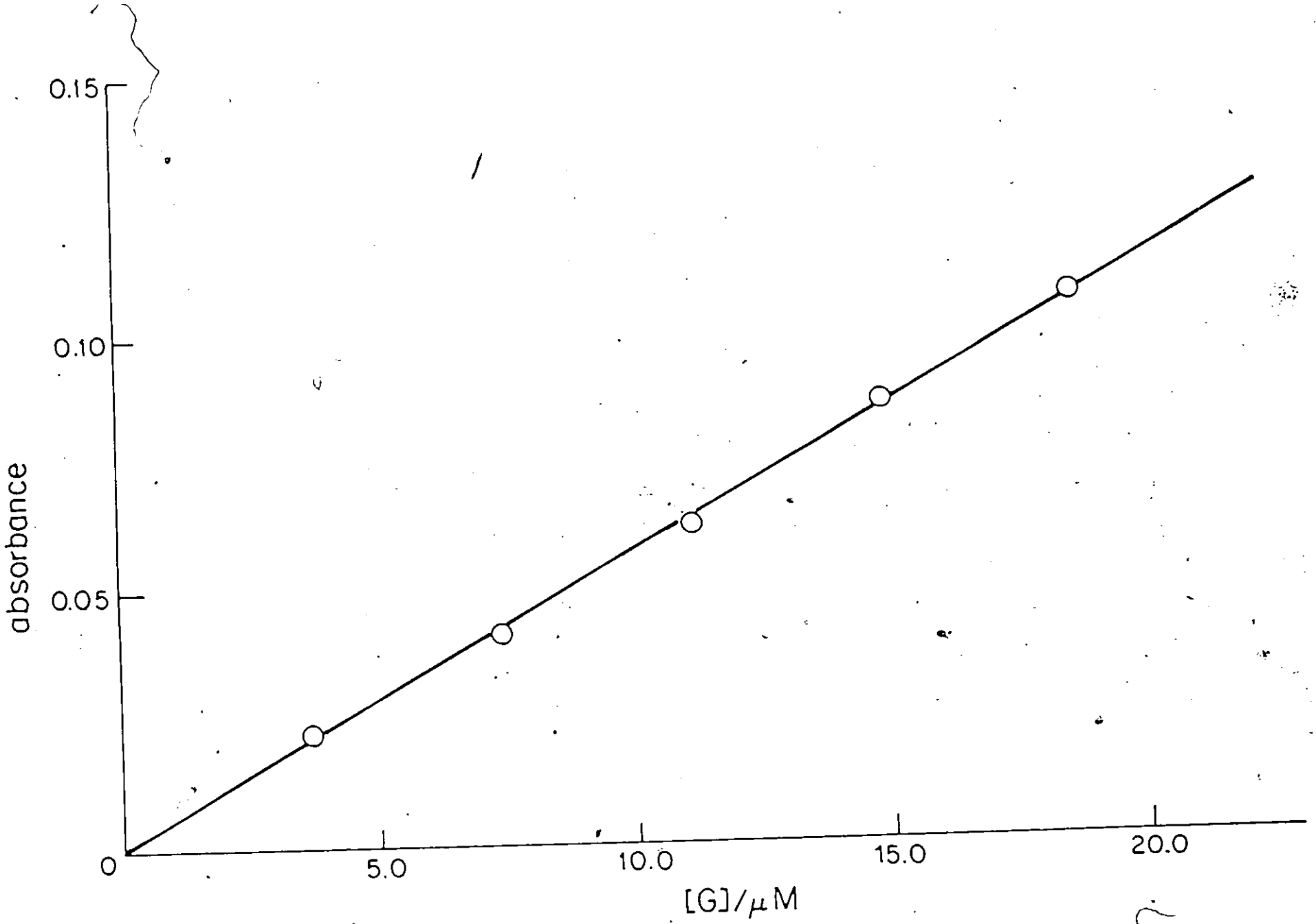

Figure 1. Calibration curve with absorbance plotted against glucose concentration; pH 6.39 T=10.1°C.

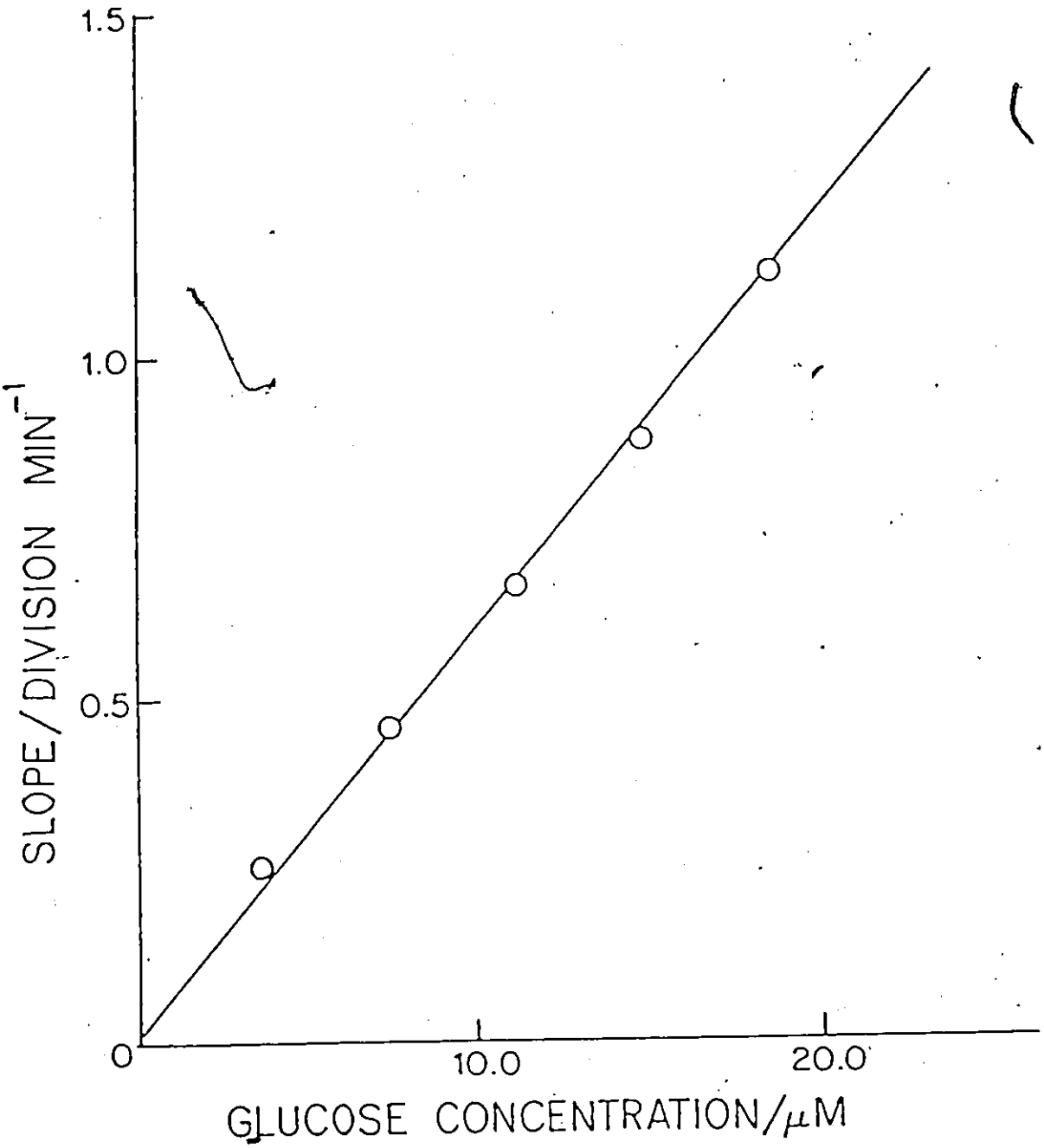

Figure. 2 Calibration curve with initial slope of absorbance-time curves plotted against glucose concentration; pH=5.76 T=18.0^{o}C.

with glucose is very fast, being essentially complete in 2—2.5 mins as shown in curve A of Fig. 3. On the other hand, during the course of the ß-glucosidase reaction system the absorbance increases steadly with time, with no induction period (Fig. 4). In this situation the initial rates of the ß-glucosidase reaction were therefore calculated from the initial slopes of the corresponding absorbance time curves, use being made of the conventional calibration curves with the absorbance plotted against the glucose concentration. This procedure will be referred to as the 'glucose-concentration method'(GCM).

(2) **Reactions at pH values below 6.2; the glucose-slope-method**

At pH values below 6.2, it was observed from the records of absorbance against time that there was a distinct lag phase, of length dependent upon the pH; later the absorbance (corresponding to the apparent amount of glucose produced) became linear with the reaction time(Fig. 5). The lag phase is due to the fact that the reaction of the assay reagent with glucose is slow at pH values below 6.2, as shown in curve B of Fig. 3. At the beginning of the enzyme reaction, the quantities of glucose produced are too small for reaction with the assay reagent to occur sufficiently rapidly. After an accumulation of glucose to a certain amount during the lag phase, the assay reagent reacts with glucose at a constant rate, which is equal to the rate of glucose formation, and the absorbance of the system changes linearly with time.

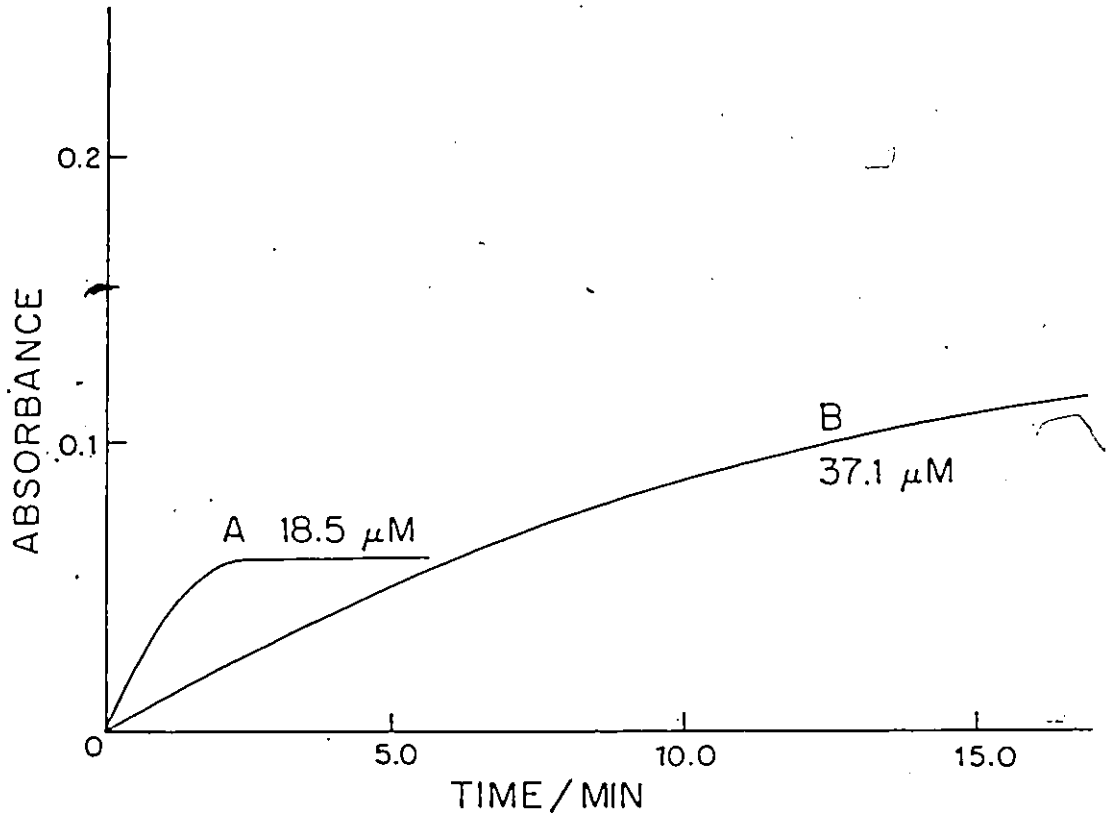

Figure. 3 Absorbance-time curves for the reaction between standard glucose and assay reagent; the glucose concentrations are shown on the curves.

A. pH 6.48; T = 24.0°C
B. pH 5.35; T = 24.0°C

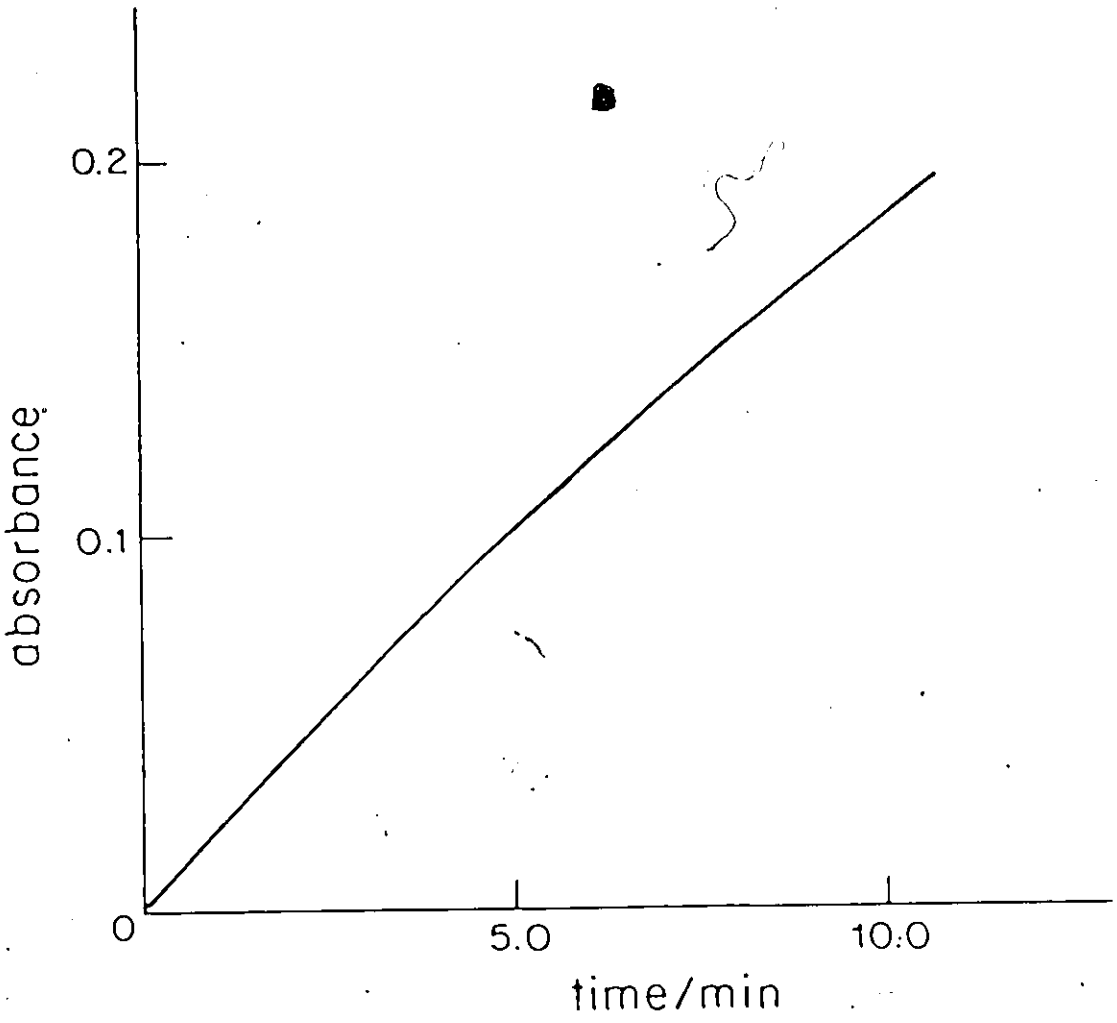

Figure 4. Absorbance-time curve for the enzyme-catalyzed reaction.
[β-glucosidase] = 0.1 mg/mL; [cellobiose] = 0.699 mM; T=24.0°C; pH 6.48.

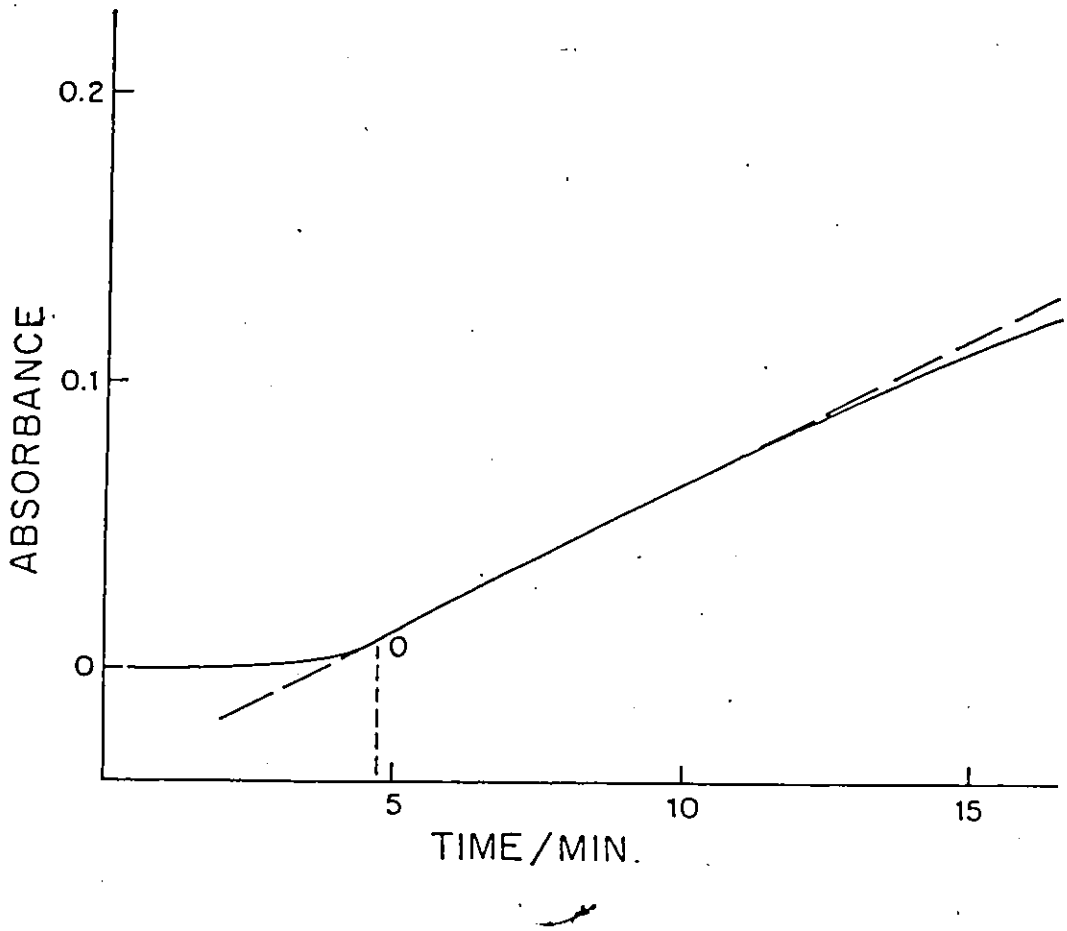

Figure 5. Absorbance-time curve for the enzyme-catalyzed reaction.

{β-glucosidase} = 0.1 mg/mL;
{cellobiose} = 0.699 mM;
T = 24.0°C; pH 5.35.

In this situation the rate would be seriously underestimated if it were obtained from the calibration curve of absorbance against glucose concentration. The reason is that at point O, after which the absorbance changes proportionally with time, the time is shorter than that required for the completion of the assay-glucose reaction. We devised a new method for calculating the initial rate in such a situation. This method was to obtain an average rate at a sufficiently early period of the reaction, so that the rate is nearly equal to the initial rate. The calibration curves were made by plotting the initial slope of the absorbance-time curve against the glucose concentration. The average rate was obtained in the following way. The concentration of glucose accumulated at the point O (see Fig. 5) was first determined; it was given by the slope of the straight portion of the time course of the enzyme reaction, use being made of a calibration curve with slope plotted against glucose concentration. The glucose concentration so obtained was then divided by the length of lag phase, to give the average rate. This procedure involves the approximation, which introduces negligible error, of neglecting the glucose that has reacted with the assay reagent during the lag phase. The term 'glucose-slope-method,'GSM', will be used to describe this procedure.

2.3 Discussion and experimental tests

No interference between the glucose reaction with assay and the enzyme reaction

In the one step assay procedures used , the reaction system contains not only β-glucosidase and cellobiose, but also the assay reagent which contains two additional enzymes (hexokinase and G-6-PD), ATP, and NADP. The system is therefore kinetically complicated, and it was necessary to investigate whether the assay reagent interferes with the β-glucosidase system, and whether either the β-glucosidase or cellobiose interferes with the glucose determination. A series of measurements of absorbance given by certain amounts of standard glucose were therefore made, both in the absence and the presence of enzyme or substrate of different concentrations. The results are shown in Table 1.

The first effect, the interference of assay reagent with the β-glucosidase system was shown to be unimportant by the following facts:

a. No absorbance was observed with a mixture containing 2 mL assay reagent and 1 mL β-glucosidase of 1.2 mg/mL in a total volume of 3 mL (this amount of enzyme was four times that in the kinetic experiments), compared with an enzyme-free blank solution, indicating no reaction between assay and β-glucosidase.

b. Cellobiose reacts with assay only at high concentrations. Substrate at a concentration of 5 mM (which is higher than that used in the enzyme reaction) with 1 mL assay in a total volume of 3 mL gave an absorbance of 0.04, which, compared with the absorbance of 1.58 given by the enzyme system containing 5 mM

Table 1.

Absorbance of standard glucose solution in the absence and presence of enzyme or substrate at different concentrations

T = 25.0°C pH : 6.39

Sample*	absorbance**	Blank
2 mL assay; 1 mL emzyme	0	2 mL assay; 1 mL buffer
1 mL assay; 0.5 mL substrate	0.04	1 mL assay; 2 mL buffer
1 mL assay; 0.5 mL substrate 0.25 mL enzyme	1.58	1 mL assay; 2 mL buffer
1 mL assay; 0.3 mL glucose	0.35	" ; "
1 mL assay; 0.3 mL glucose 0.1 mL enzyme	0.35	" ; "
1 mL assay; 0.3 mL glucose 0.5 mL enzyme	0.35	" ; "
1 mL assay; 0.5 mL glucose	0.58	" ; "
1 mL assay; 0.5 mL glucose 0.1 mL enzyme	0.58	" ; "
1 mL assay; 0.5 mL glucose 0.5 mL enzyme	0.58	" ; "
1 mL assay; 0.5 mL glucose	0.58	" ; "
1 mL assay; 0.5 mL glucose 0.1 mL substrate	0.58	" ; "
1 mL assay; 0.5 mL glucose 0.5 mL substrate	0.59	" ; "

* All of the samples were made up to a total volume of 3 mL by adding an appropriate amount of buffer solution.

** Absorbance was measured at 340 nm.

Concentration of standard glucose [G] = 0.556 mM
Concentration of enzyme solution [E] = 1.2 mg/mL
Concentration of substrate solution [S] = 30 mM

cellobiose, 0.1 mg/mL β-glucosidase and 1 mL assay in the same total volume, can be neglected without serious error (0.04/1.58 = 2.5 %).

The second possibility was eliminated by the following facts:

c. The absorbance developed by standard glucose was found to be the same in the presence of the enzyme as it was in its absence, indicating that in the glucose determination there was no interference by β-glucosidase.

d. Cellobiose of a concentration of 5 mM gave rise to only a 1.7 % change in the absorbance given by 0.093 mM glucose solution.

It might be concluded that, although the system is quite complicated, the coupled assay reagent can be used to monitor the continuous production of glucose in the one-step method during the enzymic hydrolysis of cellobiose.

'GCM' and 'GSM' procedures

The reaction sequence involved in this one-step method can be expressed in simplified form as follows:

$$E + S \xrightarrow[(1)]{k_S} G \xrightarrow[(2)\ \text{assay}]{k_A} A$$

where E refers to the enzyme, S, to the substrate, G to glucose and A to the compound measured spectrophotometrically at 340 nm. The total reaction rate , i.e. the rate of change of absorbance is mainly determined by the slowest step, step (1) or step (2).

Glucose-Concentration Method (GCM)

Various possibilities must be considered.

$k_A \gg k_S$

If k_A is sufficiently large and k_S sufficiently small, even at the early stage of reaction, when the substrate concentration is large and the glucose concentration is small, the hydrolysis of cellobiose catalyzed by β-glucosidase is the slow step. Once the glucose is formed, the assay reagent reacts with it immediately, giving a measurable absorbance. Therefore, the rate of the hydrolysis of cellobiose is given by the rate of formation of A, as measured by the change of absorbance. In addition, the reaction of assay with glucose is fast enough that the calibration curve, of absorbance plotted against glucose concentration, can be used for initial rate calculations without serious error.

This is the situation that applies at pH values higher than 6.2, when the absorbance increases steadily with time, with no lag phase (Fig. 4).

Glucose-Slope Method (GSM)

$k_A > k_S$, but k_A is smaller than that under the above condition.

In this situation, at the beginning of the reaction the assay cannot respond immediately to the formation of glucose, because the amount of glucose is too small. In the early period of the reaction the first step is faster than the second one because the substrate concentration is much larger than the glucose

concentration; thus the amount of glucose in the system, and therefore the rate of reaction of the assay with glucose, increases with time. When the rate of the second step becomes equal to that of the first step, the glucose concentration and the rate of reaction of the assay with glucose reach a value that is constant for some time (Fig. 5). Therefore, a lag phase appears in the time course, and the curve of absorbance against time in the lag phase corresponds to the rate of the second step, not the rate of the enzyme reaction. The straight line portion is related to the rates of both the first and second steps, i.e. k_A and k_S. Therefore the rate of change of absorbance does not measure the rate of the enzyme reaction.

Because the reaction of the assay reagent with glucose is slow, being completed in 20-25 mins (see Fig. 3 curve B), the use of the calibration curve showing absorbance against glucose concentration may cause error in the calculation of the initial rate. On the other hand the use of a calibration curve of initial slope against standard glucose concentration gives the amount of glucose present in the system corresponding to the straight line portion, which makes it possible to calculate the average rate in the early period of reaction. The fact that the curves were always linear after the lag phase was completed indicates that there is little error in considering the average rate as the initial rate. This condition was satisfied at pH values higher than 5.

Some typical results indicate that the 'GSM' procedure is

practical. For example at pH. 5.35 and 5.00 the Lineweaver-Burk plots of v^{-1} against $[S]^{-1}$ are curves (one of them is shown in Fig. 6) when the initial rates were calculated from calibration curves of absorbance against glucose concentration. However, the application of the 'GSM' for calculation of initial rates gave linear of Lineweaver-Burk plots, as shown in Fig. 7.

It is obvious that the enzyme reaction also contributes to the lag phase when the value of k_s is small.

When $k_A < k_s$ and k_A is small the lag phase will be longer, and when the reaction rate of the assay with glucose is equal to the rate of glucose formation, the rate of the enzyme reaction has changed from the initial rate. Accordingly, the average rate cannot be considered as the initial rate. There still is a straight portion on the time course, and the amount of glucose consumed by the assay in the lag phase cannot be neglected. Thus 'GSM' can not be used at pH values at which the reaction of the assay reagent with glucose is too slow. In the case of β-glucosidase the limiting pH is about 5.00 .

Experimental comparison of k_A with k_s

In order to test experimentally the validity of the 'GCM' and 'GSM' methods the apparent rate constants k_A and k_s were estimated by the following procedures. The magnitude of k_A was estimated from the kinetic studies of standard glucose with the assay reagent.

The rates of reaction of standard glucose were measured at

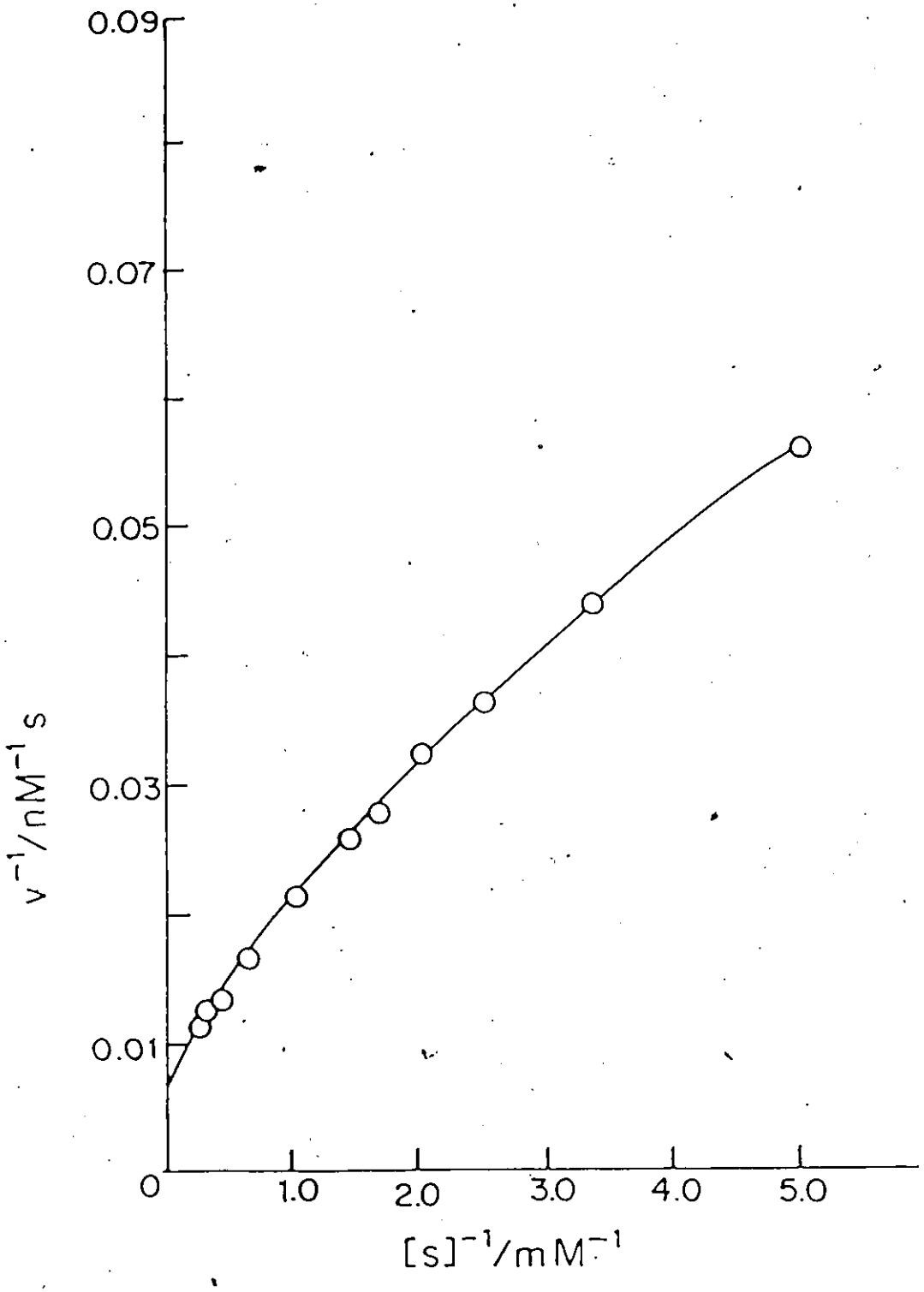

Figure 6. Lineweaver-Burk plot for the free enzyme system. [α-glucosidase] = 0.1 mg/mL; T=24.0°C; pH 5.35. The initial rates calculated by using the conventional calibration curve with absorbance plotted against concentration.

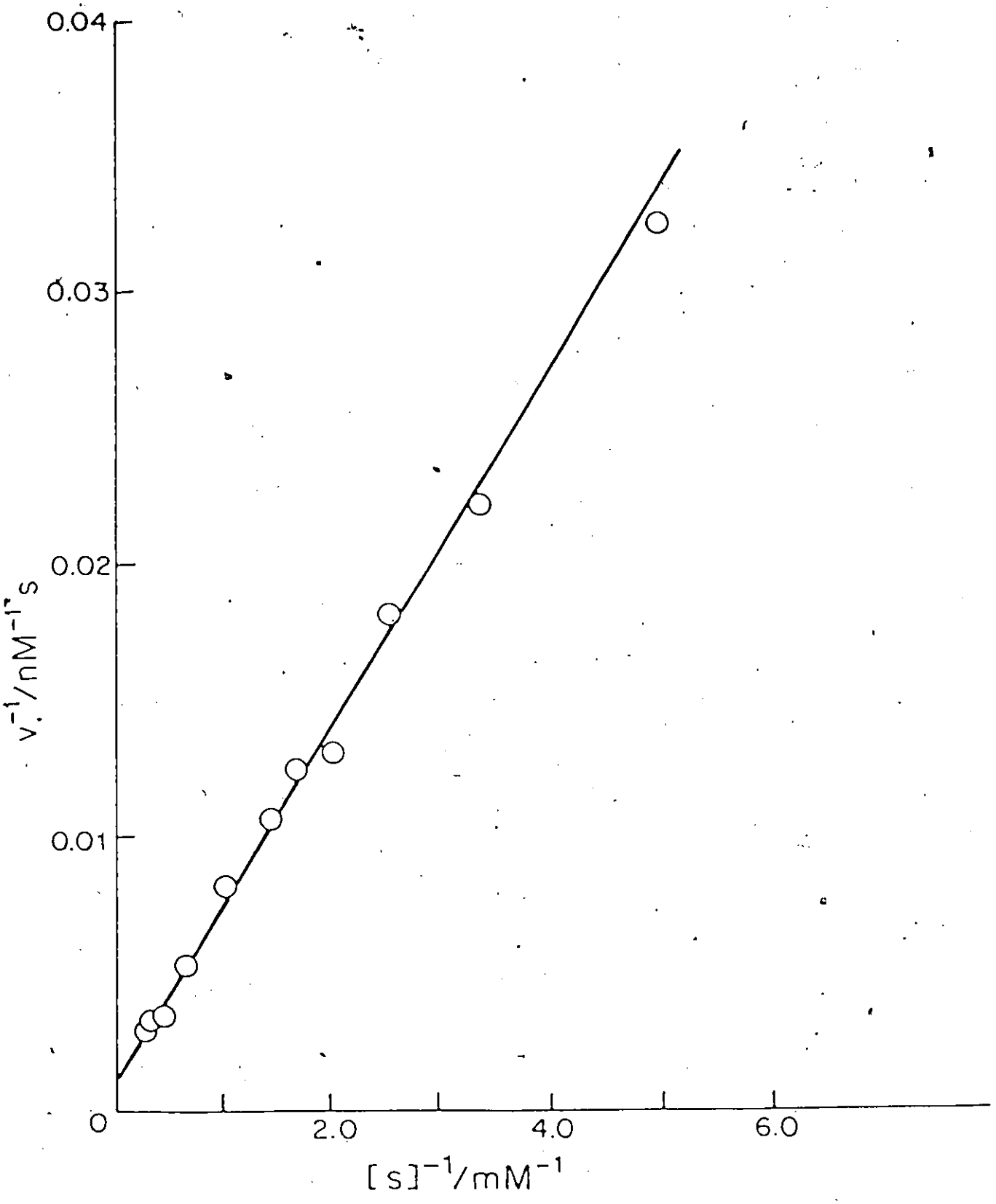

Figure 7. Lineweaver-Burk plot for the enzyme system, [β-glucosidase] = 0.1 mg/mL; T=24.0°C; pH 5.35, which was obtained on the basis of the initial rates calculated by using calibration curve with slope plotted against concentration.

different concentrations in the same pH range and the same temperature range as that used in the kinetic studies of the enzyme reaction. The rates obtained as initial slopes of absorbance-time curves are given in Table 2. The values of k_A were determined from plots of the slopes of absorbance-time curves against glucose concentrations and are listed in Table 3.

The constant k_S was obtained in the following way. At first the initial slopes, k_T, of plots of the slopes of absorbance-time curves against substrate concentrations were determined. The k_T value corresponds to the overall rate constant and is related to k_A and k_S by the equation

$$\frac{1}{k_T} = \frac{1}{k_A} + \frac{1}{k_S} \qquad (10)$$

Therefore the magnitude of k_S can be calculated from values of k_T and k_A. Examples are shown in Fig. 8 and for comparison the values of k_A and k_S at three different pH values are given in Table 4. In all cases k_A is greater than k_S; at pH 6.19 it is much greater, and at the lower pH values it is substantially greater. The results of a comparison between k_A and k_S provide powerful evidence for the reliability and the validity of the 'GCM-GSM' procedure.

Furthermore, the glucose-slope method with the glucose-concentration procedure led to completely self-consistent results, and gave a similar pH-activity profile of β-glucosidase to that reported in the literature(46,61,62,111). This method is

much simpler and less time-consuming than the previous method of taking samples at various times.

There has been a little work reported on the continuous analysis of glucose and cellobiose. Morris and coworkers(91) reported an automated analysis of glucose in serum by means of nylon tube on which the hexokinase and glucose-6-phosphate dehydrogenase are coimmobilized. Day and Workman(92) recently reported a linked assay system containing glucose oxidase and peroxidase which can be used for rapid, continuous kinetic assays for cellobiose-producing enzymes. However, these procedures have not been used for studying the hydrolysis of cellobiose. Danielsson et al.(93) developed a calorimetric assay procedure for the determination of cellobiose. The cellobiose is hydrolyzed by β-glucosidase and the glucose formed is measured calorimetrically by an enzyme thermistor containing coimmobilized glucose oxidase and catalase. This method might be used for the kinetic study of the cellulose degradation or cellobiose hydrolysis; however the sensitivity of this method is low, especially for small-scale studies. The present method is faster and simpler and it is suitable for use on the micro scale.

One of the limitations of the method is that because of the rapid inactivation of the assay reagent, it cannot be used satisfactorily at temperatures above 40°C. The method is also unsuitable for pH values below 5.0, because then the assay mixture reacts too slowly with glucose.

Table 2.

Initial slope of absorbance-time curves for standard glucose with assay reagent under different conditions

T/°C	[G]/μM \ pH	5.22	5.50	5.57	5.76	6.19	6.61	6.91
18.0	3.71	0.020	0.086	0.118	0.226	0.736	0.992	1.38
	7.41	0.040	0.171	0.236	0.453	1.47	1.99	2.75
	11.1	0.060	0.257	0.353	0.679	2.21	2.98	4.13
	14.8	0.080	0.343	0.470	0.906	2.94	3.97	5.50
31.0	3.71	0.064	0.215	0.277	0.524	1.28	1.64	2.12
	7.41	0.128	0.427	0.553	1.05	2.57	3.28	4.25
	11.1	0.192	0.645	0.830	1.57	3.85	4.93	6.37
	14.8	0.255	0.858	1.110	2.10	5.13	6 57	8.50
	pH	5.32	5.35	5.47	5.53	5.92	6.19	
24.0	3.71	0.065	0.098	0.093	0.139	0.85	2.06	
	7.41	0.129	0.192	0.182	0.267	1.69	4.12	
	11.1	0.194	0.290	0.270	0.396	2.54	6.20	
	14.8	0.260	0.388	0.362	0.525	3.38	8.30	
	18.5	0.365	0.490	0.448	0.657			

pH 5.00

[G]/mM \ T/°C	18.0	24.0	31.0
0.0371	0.049	0.097	0.182
0.0927	0.122	0.251	0.454
0.148	0.195	0.397	0.724
0.175	0.230	0.470	0.856

Table 3.

Apparent rate constant k_A for the reaction of standard glucose with assay reagent under different conditions

k_A / division $min^{-1} \mu M^{-1}$

pH	18.0°C	31.0°C	pH	24.0°C
5.00	1.32×10^{-3}	4.90×10^{-3}	5.00	2.68×10^{-3}
5.22	5.36×10^{-3}	1.72×10^{-2}	5.32	1.74×10^{-2}
5.52	2.31×10^{-2}	5.80×10^{-2}	5.35	2.64×10^{-2}
5.57	3.17×10^{-2}	7.46×10^{-2}	5.47	2.42×10^{-2}
5.76	6.11×10^{-2}	1.43×10^{-1}	5.53	3.54×10^{-2}
6.19	1.99×10^{-1}	3.46×10^{-1}	5.92	2.29×10^{-1}
6.61	2.68×10^{-1}	4.43×10^{-1}	6.19	5.59×10^{-1}
6.91	3.71×10^{-1}	5.73×10^{-1}	6.90	3.51×10^{-1}

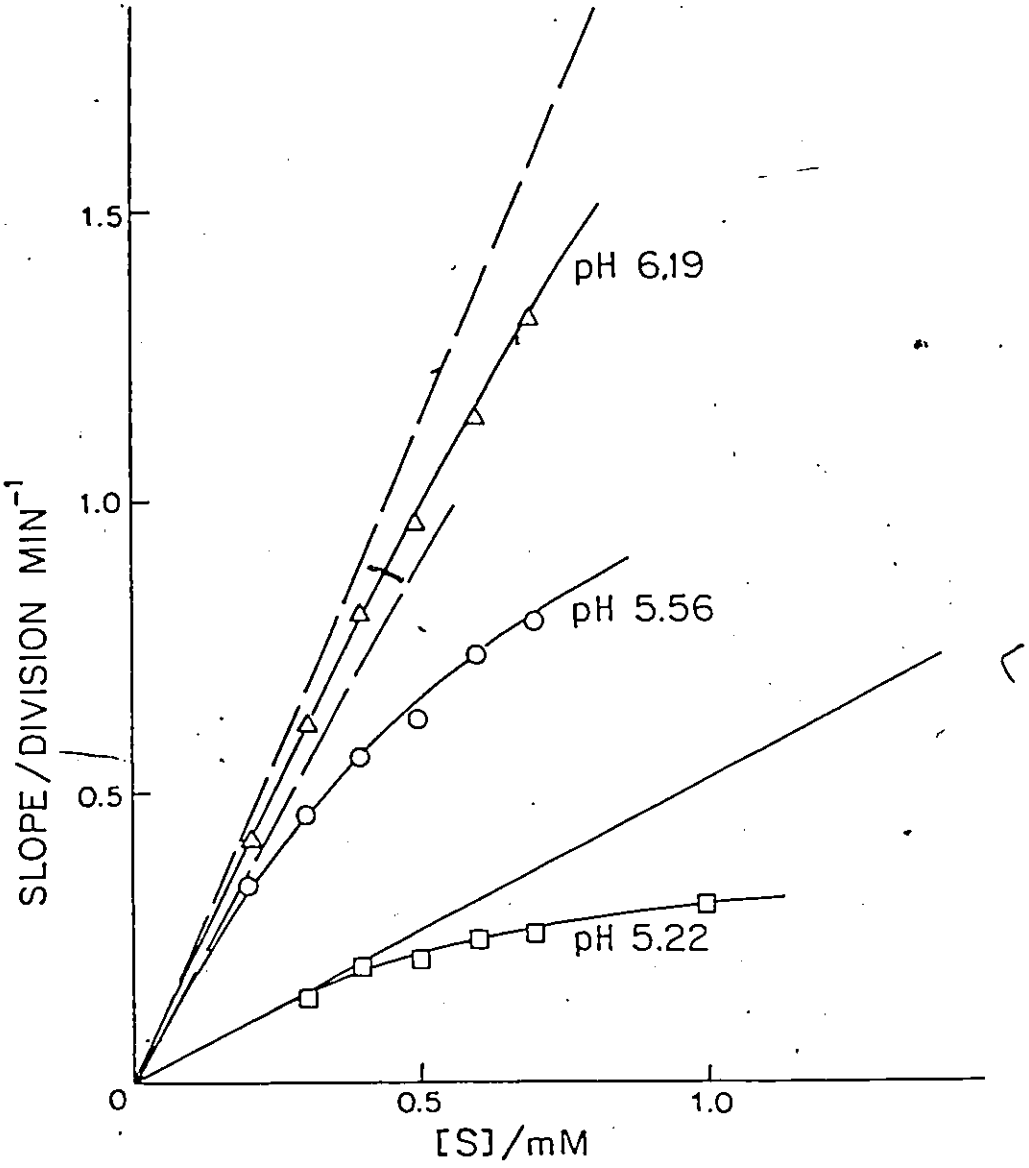

Figure 8-a. Plots of slopes of absorbance-time curves (e.g. Fig. 4, Fig. 5) against the substrate concentration.
[β-glucosidase] = 0.1 mg/mL;
[cellobiose] = 0.2-3.2 mM;
the pH values are shown;
T = 18.0°C.

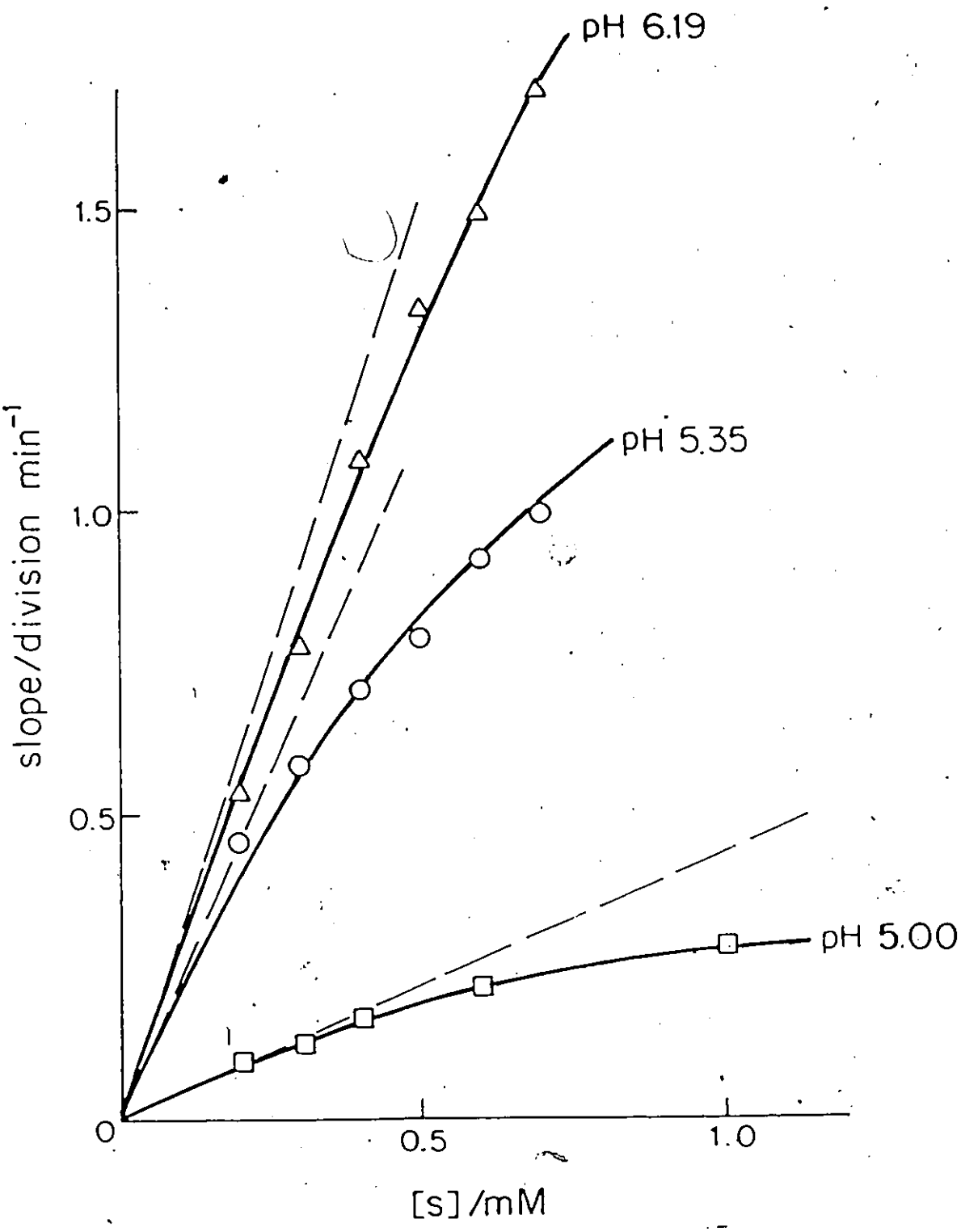

Figure 8-b. Plots of slopes of absorbance-time curves (e,g, Fig. 4, Fig. 5) against the substrate concentration.
[β-glucosidase] = 0.1 mg/mL;
[cellobiose] = 0.2-3.2 mM;
the pH values are shown;
T = 24.0°C.

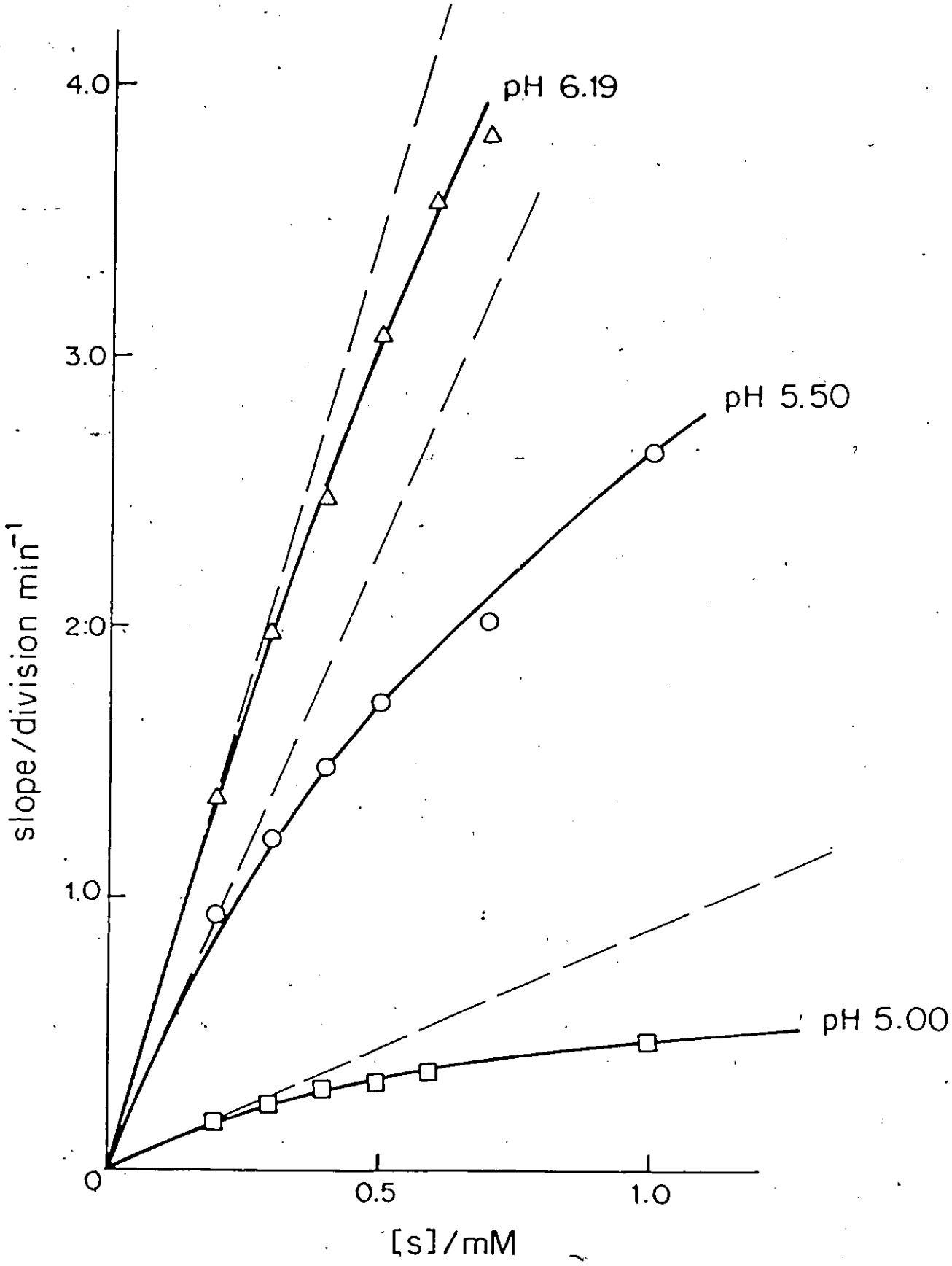

Figure 8-c. Plots of slopes of absorbance-time curves (e,g, Fig. 4, Fig. 5) against the substrate concentration.
[β-glucosidase] = 0.1 mg/mL;
[cellobiose] = 0.2-3.2 mM;
the pH values are shown;
T = 31.0°C.

Table 4.

Rate constants k_A, k_T and k_s under different conditions

T/℃	pH	$10^3 k_A$*	$10^3 k_T$*	$10^3 k_s$*	k_A/k_s
18	6.19	200	2.26	2.29	87
18	5.56	31.7	1.77	1.87	17
18	5.22	5.4	0.52	0.58	9.2
24	6.19	560	3.05	3.07	182
24	5.35	26	2.29	2.51	10
24	5.00	2.71	0.44	0.525	5
31	6.19	346	6.94	7.04	50
31	5.50	58.0	4.60	4.99	11.6
31	5.00	4.9	0.88	1.07	4.6

* The units of k_A, k_T and k_s are divisions $min^{-1}\mu M^{-1}$

CHAPTER III

INFLUENCE OF SUBSTRATE CONCENTRATION AND pH ON THE KINETICS OF β-GLUCOSIDASE IN FREE SOLUTION

3.1 Introduction

The hydrogen ion concentration has a very marked effect on the activity and kinetic behaviour of enzyme systems. Enzyme reactions usually have a pH optimum, having a bell-shaped profile of activity against pH, as a result of the activation and inhibition of the enzyme by hydrogen ions(94).

Based on the pH-activity profiles one can evaluate the dissociation constants of ionizing groups at or near the active centre and therefore gain information about the groups involved in the enzyme catalysis(65,95). Furthermore, the studies of the pH dependence of enzyme reactions can provide a good deal of information about the reaction sequence, involving substrate binding and subsequent catalytic process. From the analysis of pH effects on the kinetic parameters one can determine whether a particular ionizing group of an enzyme is involved in the binding of a substrate, or in the catalysis of the subsequent reaction, or both. A systematic study of the effects of pH on the kinetic behaviour is thus of importance for establishing the mechanism of an enzyme reaction.

Some previous studies(15,18,48,49,50,59,60,63,113,116) have

been concerned with the influence of pH on the activity of β-glucosidase, in either the free or immobilized form. However, only a few(15,48,49,50) have been concerned with the evaluation of dissociation constants and the identification of catalytically important groups on the enzyme. Some results of previous studies are given in Table 5. The differences among the reported pK values are large, up to 2.6 pH units. This is probably because of the differences in the source of enzyme, in the nature of the substrate and in the experimental conditions. No detailed pH studies have been reported on the kinetics of the β-glucosidase catalyzed hydrolysis of cellobiose . In the present work, studies on the pH dependence of the rate of hydrolysis of cellobiose, at various substrate concentrations and at three temperatures 18°, 24°, 31°C, were carried out with both free and immobilized β-glucosidase. This chapter will report the results obtained with enzyme in free solution and Chapter VIII will give the results with immobilized β-glucosidase.

3.2 Theoretical principles

Enzyme molecules contain a number of ionizing groups which are very important in the function of the enzyme. The active centre usually consists of some acidic groups such as -COOH and basic groups such as NH_2, so that enzymes exhibit amphoteric properties, being polyampholytes. Therefore, changes in hydrogen ion concentration, by causing changes in the ionization state of these active groups and in the folding and conformation of enzyme

Table 5(a).
A summary of literature data on K_m values for β-glucosidase

source	matrix	pH	T/°C	K_m/mM	V (μM/mgmin)	Ref.
Sclerotium rolfsii	free	3.5 4.5 5.5	65	1.5 5.6 7.3	305 183 76	15
Trichoderma viride	free	4.75	50	2.65 2.5 2.74	66.2 116 44.6	59
Trichoderma viride	free	5.0	40	1.5	33	7
Trichoderma viride	free	4.94	25	2.68		49
Aspergillus niger	free	4.8	26	1.5	0.44	63
Aspergillus phoenicis	free	4.8	50	0.75	164	17
Aspergillus phoenicis QM329	free	4.8	50	0.8		60
Penicillium funiculosum	free	4.8	40	2	0.4	113
Pyricularia oryzae	free	5.5	40	0.9		116
Aspergillus phoenicis	chitosan	4.8	50	5.0		60
Aspergillus phoenicis	alumina	3.5	50	2.7		18
Penicillium funicilosum	poly-amide	4.8	40	4	0.16	113

Table 5(b).

A summary of literature data on pK values for β-glucosidase

source	T/°C	pK_a	pK_b	pK_a'	pK_b'	Ref.
Trichoderma viride	25	3.5	6.8			*49
Botryodiplodia theobromae Pat	40	4.1	6.0	3.65	6.75	*** 50
Pyricularia oryzae	40	4.8	7.4	4.2	7.5	** 48
Sclerotium rolfsii	65	4.3	4.8	3.2	3.8	*15

* cellobiose as substrate

** cellobiose and salicin as substrate

*** o-nitrophenyl- β-D-glucopyranoside as substrate

molecules, will affect the ease of binding of enzyme with substrate and therefore affect the activity of the enzyme.

Michaelis and coworkers(96,97,98) first emphasized the importance of the amphoteric properties of the protein and first advanced an explanation for pH effects on the enzyme activity. Since then a large number of workers have investigated this problem and various workers have presented the theory of pH effects in enzyme kinetics.

Von Euler, Josephson and Myrback(99), on the basis of the proposals of Michaelis and Davidsohn(96) and of Michaelis and Rothstein(98), proposed the following reaction scheme to explain the pH effect:

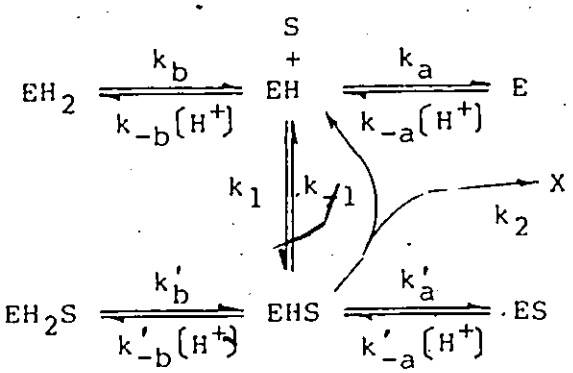

Later Waley(100) developed the rate equation for this scheme on the basis of the steady-state treatment:

$$v = \frac{k_2[E]_o[S]}{K_m\left(1 + \frac{K_a}{[H^+]} + \frac{[H^+]}{K_b}\right) + [S]\left(1 + \frac{K'_a}{[H^+]} + \frac{[H^+]}{K'_b}\right)} \qquad (11)$$

This rate equation gives a satisfactory interpretation for many

enzyme reactions. A more general formulation of this problem was given by Laidler(101) with reference to the following reaction scheme:

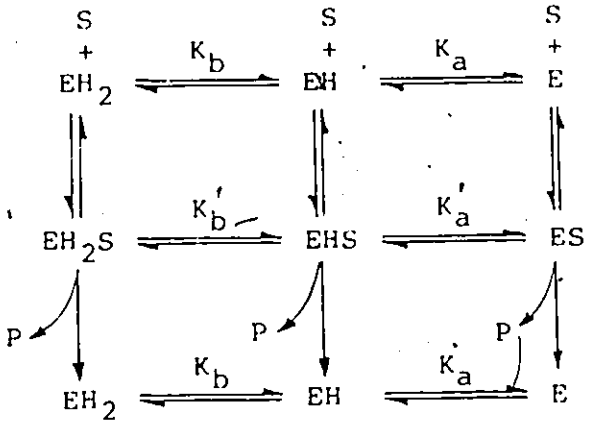

In this scheme the vertical reactions involving the extreme ionized forms of the enzyme are included, which was not taken into account in the proposal of Von Euler, Josephson and Myrback, and of Waley. Laidler also discussed the exact conditions under which it is legitimate to neglect the vertical reactions.

For a more general reaction scheme with two intermediates

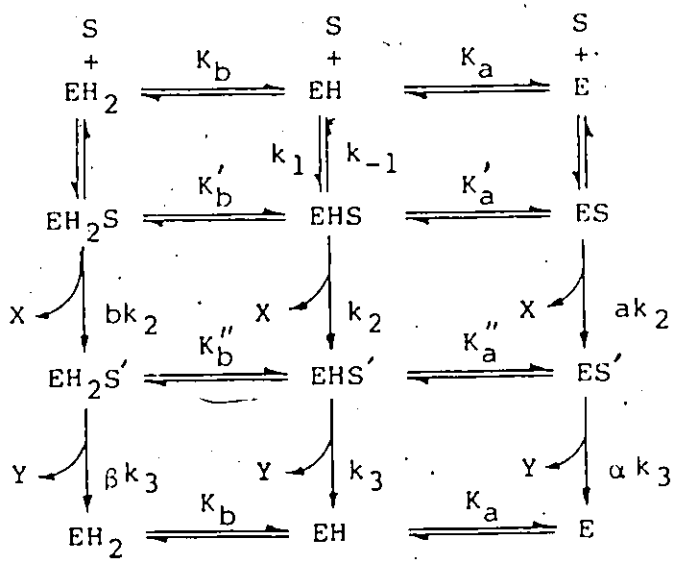

Kaplan and Laidler(102) developed a general formulation for the pH effects on the rate and on the Michaelis parameters;

$$v = \frac{\tilde{k}_c [E]_o \cdot [S]}{\tilde{K}_m + [S]} \qquad (12)$$

$$\tilde{k}_c = \frac{k_2}{\left(1 + \frac{K'_a}{[H^+]} + \frac{[H^+]}{K'_b}\right)\cdot \frac{}{\left(1 + \frac{aK'_a}{[H^+]} + \frac{b[H^+]}{K'_b}\right)} + \frac{k_2}{k_3}\cdot \frac{\left(1 + \frac{K''_a}{[H^+]} + \frac{[H^+]}{K''_b}\right)}{\left(1 + \frac{\alpha K''_a}{[H^+]} + \frac{\beta[H^+]}{K''_b}\right)}} \qquad (13)$$

$$\tilde{K}_m = \frac{\left(\frac{k_{-1}+k_2}{k_1}\right)\frac{\left(1 + \frac{K_a}{[H^+]} + \frac{[H^+]}{K_b}\right)}{\left(1 + \frac{aK'_a}{[H^+]} + \frac{b[H^+]}{K'_b}\right)}}{\frac{\left(1 + \frac{K'_a}{[H^+]} + \frac{[H^+]}{K'_b}\right)}{\left(1 + \frac{aK'_a}{[H^+]} + \frac{b[H^+]}{K'_b}\right)} + \frac{k_2}{k_3}\cdot \frac{\left(1 + \frac{K''_a}{[H^+]} + \frac{[H^+]}{K''_b}\right)}{\left(1 + \frac{\alpha K''_a}{[H^+]} + \frac{\beta[H^+]}{K''_b}\right)}} \qquad (14)$$

$$\frac{\tilde{k}_c}{\tilde{K}_m} = \left(\frac{k_1 k_2}{k_{-1}+k_2}\right)\cdot \frac{\left(1 + \frac{aK'_a}{[H^+]} + \frac{b[H^+]}{K'_b}\right)}{\left(1 + \frac{K_a}{[H^+]} + \frac{[H^+]}{K_b}\right)} \qquad (15)$$

By distinguishing kinetically inessential and kinetically essential groups and taking into account the possibilities of different rate-determining steps, Kaplan and Laidler discussed different types of pH behaviour and classified them in a table. The pH dependence of the overall rates was also discussed by Krupka and Laidler(103) in terms of the nature of the ionizations of the free enzyme and the enzyme-substrate complexes.

It should be emphasized that not all the groups participating in the catalysis are revealed by the pH dependence of the kinetics; only those groups for which a change in state of ionization has some effect on the rate of reaction can be revealed by a kinetic study.

It is obvious that from equations (13), (14), (15) the ionization constants in enzyme systems can be obtained from studies of the effect of pH on kinetic parameters. Theoretical considerations indicate that the ionization constants obtained from k_c/K_m or V/K_m relate to the free enzyme, while those from k_c or V relate to the enzyme-substrate complex.

Usually the ionization constants are obtained graphically from plots of the common logarithms of the kinetic parameters against pH, generally known as Dixon plots(104). According to this method, the values of pK are formed from the intersections of tangent lines. Similar results can also be obtained from plots of pK_m against pH; these plots, being the difference between the plots of $\log_{10}V$ and $\log_{10}V/K_m$ against pH, show many patterns of

behaviour. However the graphical methods are reliable only when the difference between the dissociation constants of ionizing groups are several units of pH. In such cases, fairly reliable estimates of the pK values may also be obtained by plotting the kinetic parameter itself against pH and finding the pH values at which it has half its maximum value. If the dissociation constants of active groups are not well separated, they can be obtained by the method of Alberty and Massey(105). This method is based on the fact that the hydrogen ion concentration at the maximum activity is the geometric mean of the two dissociation constants, the latter values being obtained from the pH values at which a kinetic parameter has half its maximum value.

3.3 Analysis of data: Determination of Ionization Constants

For a reaction obeying the Michaelis-Menten equation, the simplest pH effect can be represented by equation(11):

$$v = \frac{V\,[S]}{K_m\left(1 + \frac{K_a}{[H^+]} + \frac{[H^+]}{K_b}\right) + [S]\left(1 + \frac{K_a'}{[H^+]} + \frac{[H^+]}{K_b'}\right)} \qquad (11)$$

The rate in the limit of high substrate concentrations is therefore

$$\tilde{V} = \frac{V}{1 + \frac{K_a'}{[H^+]} + \frac{[H^+]}{K_b'}} \qquad (16)$$

That at sufficiently low substrate concentrations is

$$\frac{\tilde{V}}{\tilde{K}_m} = \frac{V}{K_m} \frac{1}{1 + \frac{K_a}{[H^+]} + \frac{[H^+]}{K_b}} \qquad (17)$$

where K_a and K_b are the acid dissociation constants for two ionizing groups at the active centre of the free enzyme, and K_a' and K_b' are the corresponding dissociation constants for the groups on the enzyme-substrate complex(65,95,106) according to the following scheme:

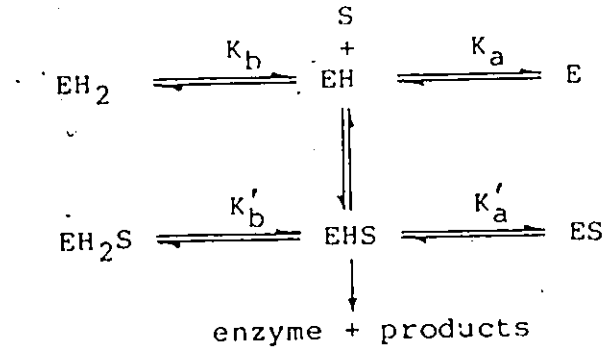

V and K_m are the pH-independent parameters. It follows that the pH-dependent parameters $\tilde{K}_m/\tilde{V}$ and $1/\tilde{V}$ both vary with pH according to an equation of the general form

$$Y = C(1 + \frac{K_a}{[H^+]} + \frac{[H^+]}{K_b}) \qquad (18)$$

where C is a pH-independent parameter and Y is either $\tilde{K}_m/\tilde{V}$ or $1/\tilde{V}$. In the former case K_a and K_b are the acid dissociation constants relating to the free enzyme. When $Y=1/\tilde{V}$, the constants

K_a and K_b relate to the enzyme-substrate complex or some other enzyme-substrate intermediate. The analysis of the pH dependence of the kinetic parameters will therefore give the values of dissociation constants.

The Michaelis constant K_m itself shows more complex behaviour, and has been analyzed in terms of Dixon's plot; however, this procedure sometimes leads to difficulty because of the masking of the dissociation constants. We have therefore carried out the analysis of the data using $\tilde{K}_m/\tilde{V}$ and $1/\tilde{V}$. In general, any graphical method such as the logarithmic plots of the kinetic parameters against pH leads to only approximate values for the dissociation constants; for more reliable values a statistical treatment is necessary.

Statistical analyses of the pH dependence of kinetic parameters were previously made by Wilkinson(107), by Hinberg and Laidler(108), and by Mazid and Laidler(109). The treatment of data in the present work is based on the method of Hinberg and Laidler, modified and improved by Mazid and Laidler, which involves the least squares procedure. The deviation D_i of the experimental value Y_i of the parameter Y from the value calculated by the use of Eq. 18 is

$$D_i = y_i - C - \frac{CK_a}{[H^+]_i} - \frac{C[H^+]_i}{K_b} \qquad (19)$$

so that

$$\sum_{i=1}^{n} D_i^2 = \sum_{i=1}^{n} \left(y_i - C - \frac{CK_a}{[H^+]_i} - \frac{C[H^+]_i}{K_b} \right)^2 \qquad (20)$$

In order to satisfy the least-squares criterion for the best fit, that the sum of the squares of the deviations is minimized, the partial derivative of this expression with respect to K_a is set equal to zero:

$$\frac{\partial \sum_{i=1}^{n} D_i^2}{\partial K_a} = 2 \sum_{i=1}^{n} \left(- \frac{C}{[H^+]_i} \right) \left(y_i - C - \frac{CK_a}{[H^+]_i} - \frac{C[H^+]_i}{K_b} \right) = 0 \qquad (21)$$

Similarly, after partial differentiation with respect to K_b,

$$\frac{\partial \sum_{i=1}^{n} D_i^2}{\partial K_b} = 2 \sum_{i=1}^{n} \left(\frac{C[H^+]_i}{K_b^2} \right) \left(y_i - C - \frac{CK_a}{[H^+]_i} - \frac{C[H^+]_i}{K_b} \right) = 0 \qquad (22)$$

Solving Eq.(21) and (22) for C leads to

$$C = \frac{\sum_{i=1}^{n} (y_i / [H^+]_i)}{\sum_{i=1}^{n} \left[\frac{1}{[H^+]_i} + \frac{n}{K_b} + K_a \sum_{i=1}^{n} \left(\frac{1}{[H^+]_i^2} \right) \right]} = \frac{\sum_{i=1}^{n} (y_i [H^+]_i)}{\sum_{i=1}^{n} [H^+]_i + \frac{1}{K_b} \sum_{i=1}^{n} [H^+]_i^2 + nK_a} \qquad (23)$$

where n is the number of data points. This gives a relationship between K_a and K_b. Partial differentiation of Eq.(20) with respect to C gives

$$\sum_{i=1}^{n} \left(y_i - C - \frac{C[H^+]_i}{K_b} - \frac{CK_a}{[H^+]_i} \right) \left(1 + \frac{K_a}{[H^+]_i} + \frac{[H^+]_i}{K_b} \right) = 0 \qquad (24)$$

Equation 23 gives expressions for C as well as the relationship between K_a and K_b. This equation can be rearranged to give K_a as

a function of K_b, or K_b as a function of K_a. Thus the substitution of an expression for C into Eq.24, followed by the substitution of the expression for K_b as a function of K_a into the resulting equation, gives a quadratic in K_b, and this quadratic equation can be solved for K_b; K_a can then be obtained. The solution of this quadratic equation is quite lengthy, and a computer program in Fortran IV language was used to perform the calculations.

The approximate 100(1-q)% confidence contours, as described by Draper and Smith(110), were obtained by finding the values of K_a and K_b which satisfy the equation

$$\sum^{n} D_i^2(K_a,K_b) = \sum^{n} D_i^2(\tilde{K}_a,\tilde{K}_b)\left(1 + \frac{p}{n-p} F(p,n-p,1-q)\right) \qquad (25)$$

Here $\tilde{K}_a$ and $\tilde{K}_b$ are the dissociation constants obtained by the least-squares treatment; the parameter p is the number of variables, which is 2 in the present case. The function F is the distribution used for the F-test, and tables for this F distribution are given in statistical texts. The right-hand side of Eq.25 is therefore known, while the left-hand side is given by Eq.20 into which the value of C, corresponding to the least-squares values $\bar{K}_a$ and $\bar{K}_b$, has been substituted. Equation 25 therefore yields an expression involving only the two unknowns K_a and K_b, and this can be rearranged to give a quadratic equation in either K_a or K_b. From the least-squares estimates of K_a the quadratic then yields the two limiting values of K_b, and vice versa.

3.4 Experimental Procedure

By use of the one-step methods, the 'GCM' and 'GSM' procedures described in Chapter II, kinetic experiments for the hydrolysis of cellobiose catalyzed by β-glucosidase in free solution were carried out, at temperatures 18°C, 24°C and 31°C, at pH values ranging from 5.0 to 6.9, and at substrate concentrations ranging from 0.2 mM to 4.8 mM. In all measurements, the enzyme concentration is 0.1 mg/mL. The buffer used was 0.2 M acetate-acetic acid.

The kinetic procedure has been described in Chapter II. The rate measurements were carried out in a thermostatted cuvette with 3 mL capacity and 1 cm light path. In this reaction cuvette 1 mL assay reagent was mixed with 0.5 mL 0.6 mg/mL enzyme solution, and with an appropriate aliquot of 0.2 M acetate buffer at the desired pH value to make the final total volume 3 mL after adding substrate solution. Before starting the reaction, the reaction cuvette and reference cuvette, which contains 1 mL assay reagent and certain amounts of buffer solution and substrate solution to make the substrate concentration the same as that in reaction cuvette, were kept inside the spectrophotometer at the required temperature for 4 mins to allow thermal equilibrium to be attained. The enzyme reaction was then started by the addition of an appropriate amount of 5.99 mM substrate solution and the change of absorbance at 340 nm, as a function of time, was recorded automatically by means of a PYE UNICAM SP 1800 UV spectrophotometer.

The initial rates, at pH values above 6.2, were calculated from the initial slopes of the corresponding absorbance-time curves by using a conventional calibration curve with the absorbance plotted against concentration (the 'glucose-concentration method'). However at pH values below 6.2, the initial rates were obtained as average rates by using calibration curves with initial slopes plotted against concentration ('glucose-slope method').

3.5 Results and Discussion

pH-rate profiles

Tables 6(a),(b) and (c) list the initial rates obtained at temperatures 18.0°, 24.0° and 31.0°C , for different substrate concentrations ; the plots against pH of initial rates are shown in Fig. 9(a), (b) and (c). The initial rates listed in Table 6 are the average values for several runs.

Lineweaver-Burk plots and Michaelis parameters

The Lineweaver-Burk plots at different pH values for three temperatures are shown in Fig.10(a), (b) and (c). The linearity of these plots under all conditions indicates that the kinetic behaviour of β-glucosidase closely follows the Michaelis-Menten equation. Table 7 gives the Michaelis parameters obtained from such Lineweaver-Burk plots. Fig.11 shows the plots of $\log_{10}V$ against pH and Fig.12 the plots of $\log_{10}V/K_m$ against pH. The optimum pH for β-glucosidase at temperatures 24.0° and 31°C is between 5.5 and 5.6, which agrees well with values reported by

Heyworth and Walker(46), Venardos et al(62), Barker et al.(111) and by Moyairi et al.(61), while at temperature 18.0° the optimum pH is around 5.76 .

Table 6(a).

Initial rates of reaction of β-glucosidase at a concentration of 0.1 mg/mL

T : 18.0°C

pH / [S]/mM	Initial rates (v/nM s^{-1})							
	4.99	5.22	5.50	5.56	5.76	6.19	6.61	6.91
0.200	9.17	12.4	17.0	17.0	19.6	13.0	6.76	4.09
0.299	13.9	17.7	25.5	24.8	28.2	19.9	9.96	6.00
0.399	18.6	22.3	32.0	34.6	39.1	26.4	13.7	7.83
0.499		27.9		44.0	44.3	35.0	16.9	9.78
0.599	25.0	34.3	46.3	47.9	55.0	38.0	21.0	11.5
0.699	30.8	39.0	52.4	57.6	58.7	46.0	22.6	13.8
0.998	41.3	54.4	71.5	74.8	87.0	60.6	31.1	19.9
1.60	59.4	77.5	107	109	132	85.8	49.6	29.5
2.40	80.7	110	148	142	174	131	73.5	45.6
3.19	95.2	140	144	190	260	158	94.7	60.7

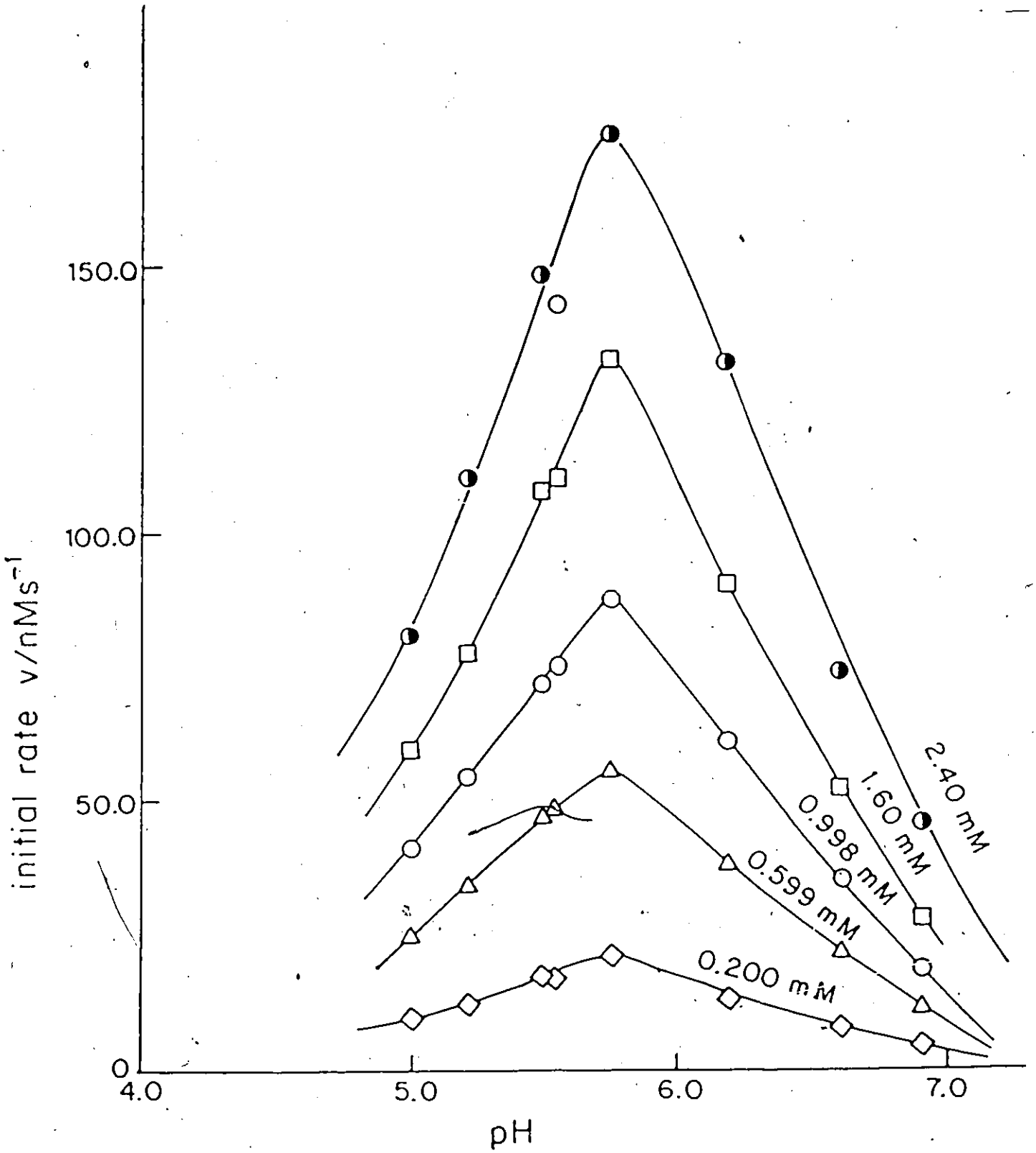

Figure 9a. pH dependence of initial rates for β-glucosidase in free solution at different substrate concentrations as indicated and at T=18.0°C

Table 6(b).

Initial rates of reaction of β-glucosidase at a concentration of 0.1 mg/mL

T : 24.0°C

pH / [S]/mM	Initial rates (v/nM s^{-1})							
	5.00	5.32	5.35	5.53	5.92	6.19	6.48	6.90
0.200	25.1	32.8	31.0	38.0	27.3	22.1	17.9	10.1
0.299	36.0	47.7	45.5	53.0	35.8	31.4	25.3	13.9
0.399	45.9	61.1	55.6	73.2	52.4	45.6	34.1	19.6
0.499		73.6	77.2	87.3	68.0	55.1	42.4	24.6
0.599	68.5	82.4	80.6	105	74.9	61.9	52.4	29.1
0.699		94.8	94.5	117		70.5	59.1	34.9
0.799	89.0				104			
0.998	92.1	138	124	168	125	96.0	82.8	48.1
1.60	152	225	194	296	201	172	118	74.4
2.40	195	286	308	363	278	235	171	108
3.19	234	329	311	435	357	309	208	115

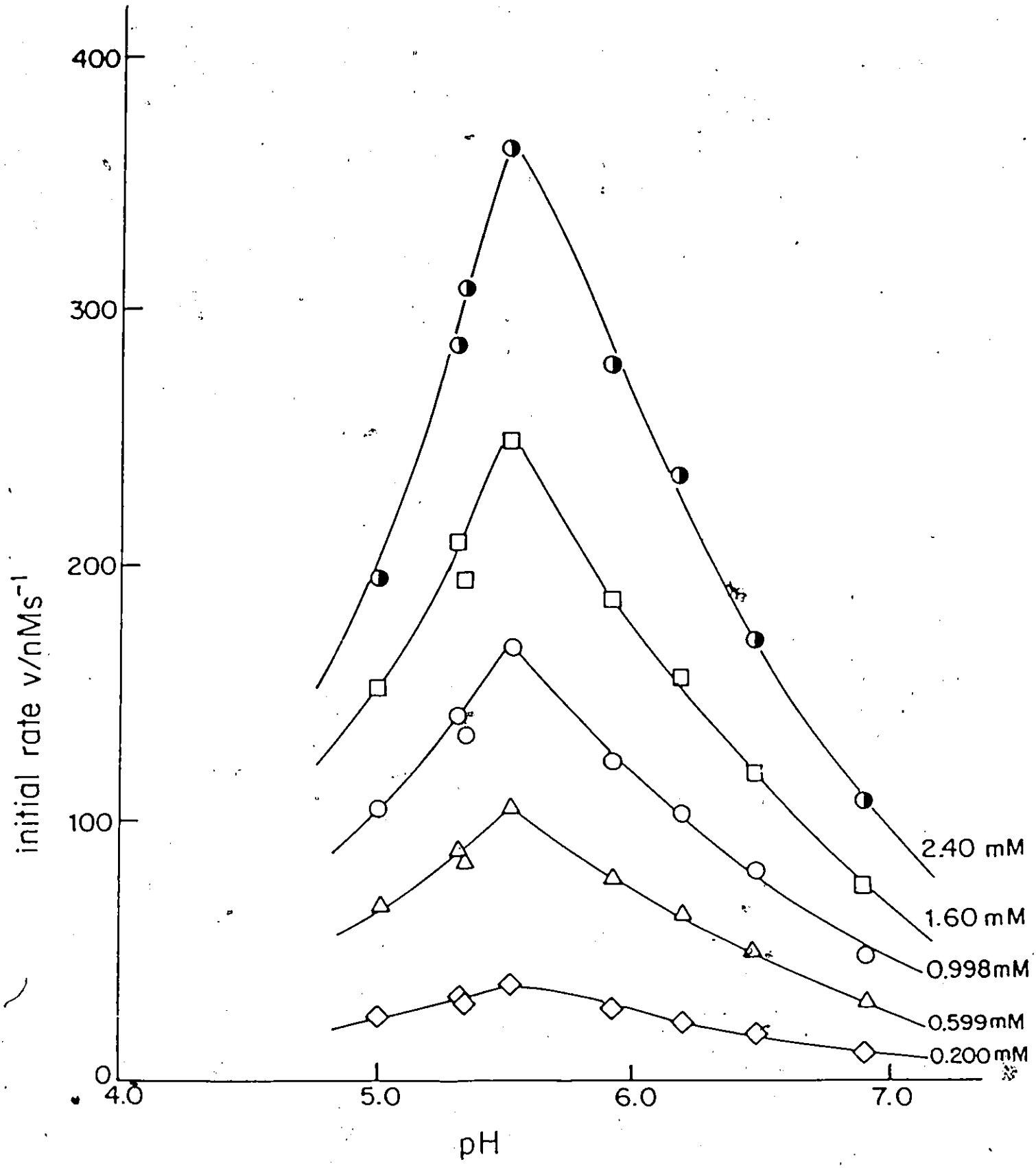

Figure 9b. pH dependence of initial rates for β-glucosidase in free solution at different substrate concentrations as indicated and at T=24.0°C

Table 6(c).

Initial rates of reaction of β-glucosidase at a concentration of 0.1 mg/mL

T : 31.0°C

pH / [S]/mM	Initial rates (v/nM s^{-1})							
	5.04	5.22	5.50	5.57	5.76	6.19	6.61	6.91
0.200	31.2	43.0	54.1	56.9	52.3	31.9	22.4	14.8
0.299	45.7	66.8	82.3	84.8	74.3	55.2	36.7	22.1
0.399	60.2	84.5	107	112	93.0	74.2	47.6	29.2
0.499	70.1	111	118	131	116	84.7	58.1	35.9
0.599	84.1	119	155	158	137	99.2	66.1	45.8
0.699		133	166	180	160	104	77.8	49.2
0.998	141	193	248	254	221	157	114	72.9
1.60	207	285	372	372	327	232	151	116
2.40	286	403	565	493	575	288	220	156
3.19	345	521	577	654			278	227

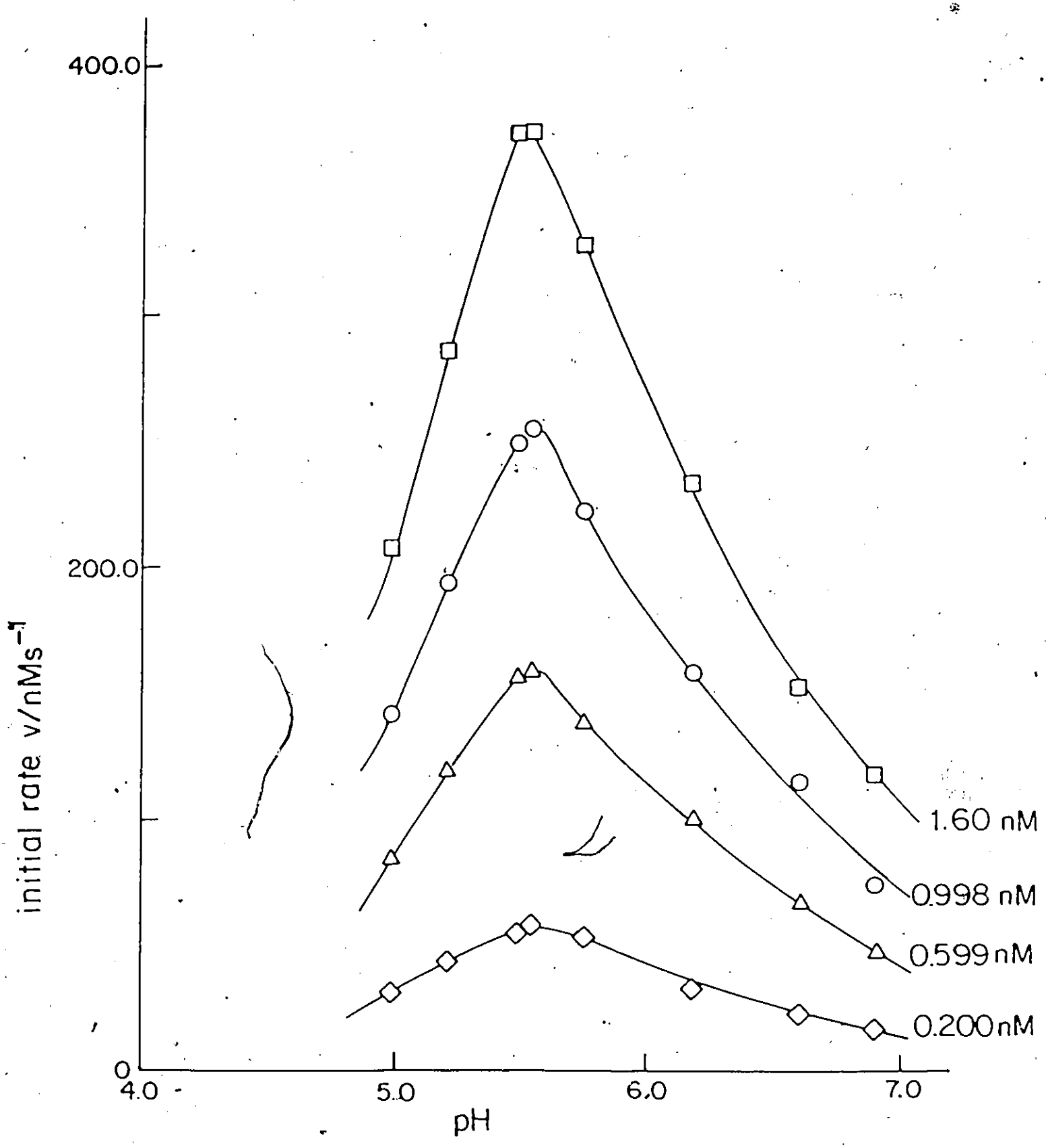

Figure 9c. pH dependence of initial rates for β-glucosidase in free solution at different substrate concentrations as indicated and at T=31.0°C.

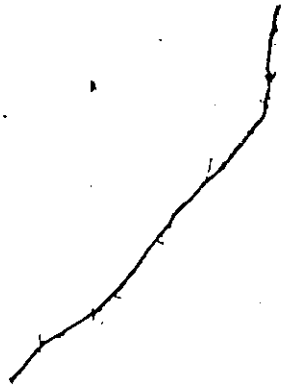

Figure 10a. Lineweaver-Burk plots for β-glucosidase in free solution at various pH values; T = 18.0°C.

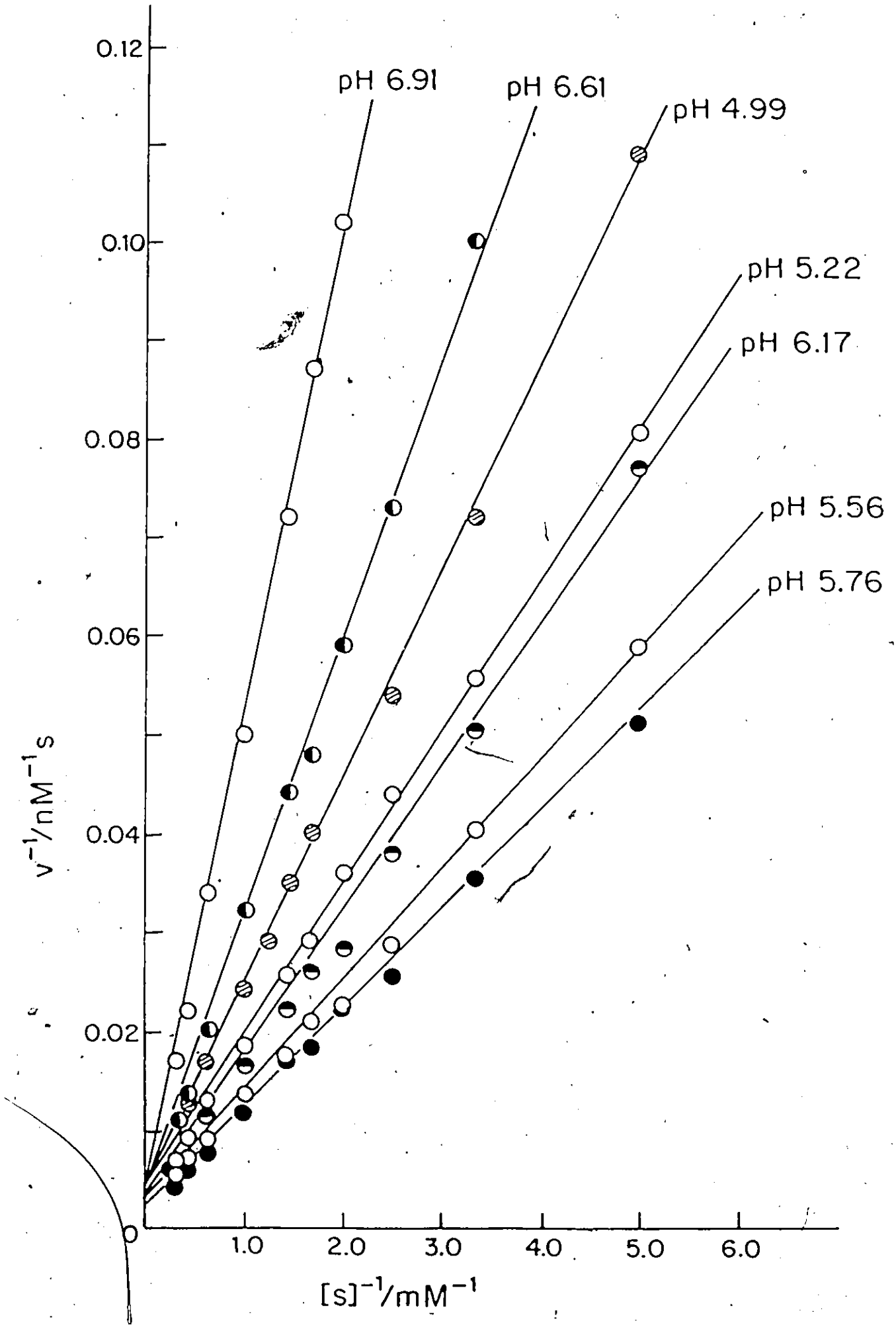
0.12
0.10
0.08
0.06
0.04
0.02
pH 6.91
pH 6.61
pH 4.99
pH 5.22
pH 6.17
pH 5.56
pH 5.76
1.0
2.0
3.0
4.0
5.0
6.0
$v^{-1}/nM^{-1}s$
$[s]^{-1}/mM^{-1}$

Figure 10b. Lineweaver-Burk plots for β-glucosidase in free solution at various pH values. T = 24.0°C.

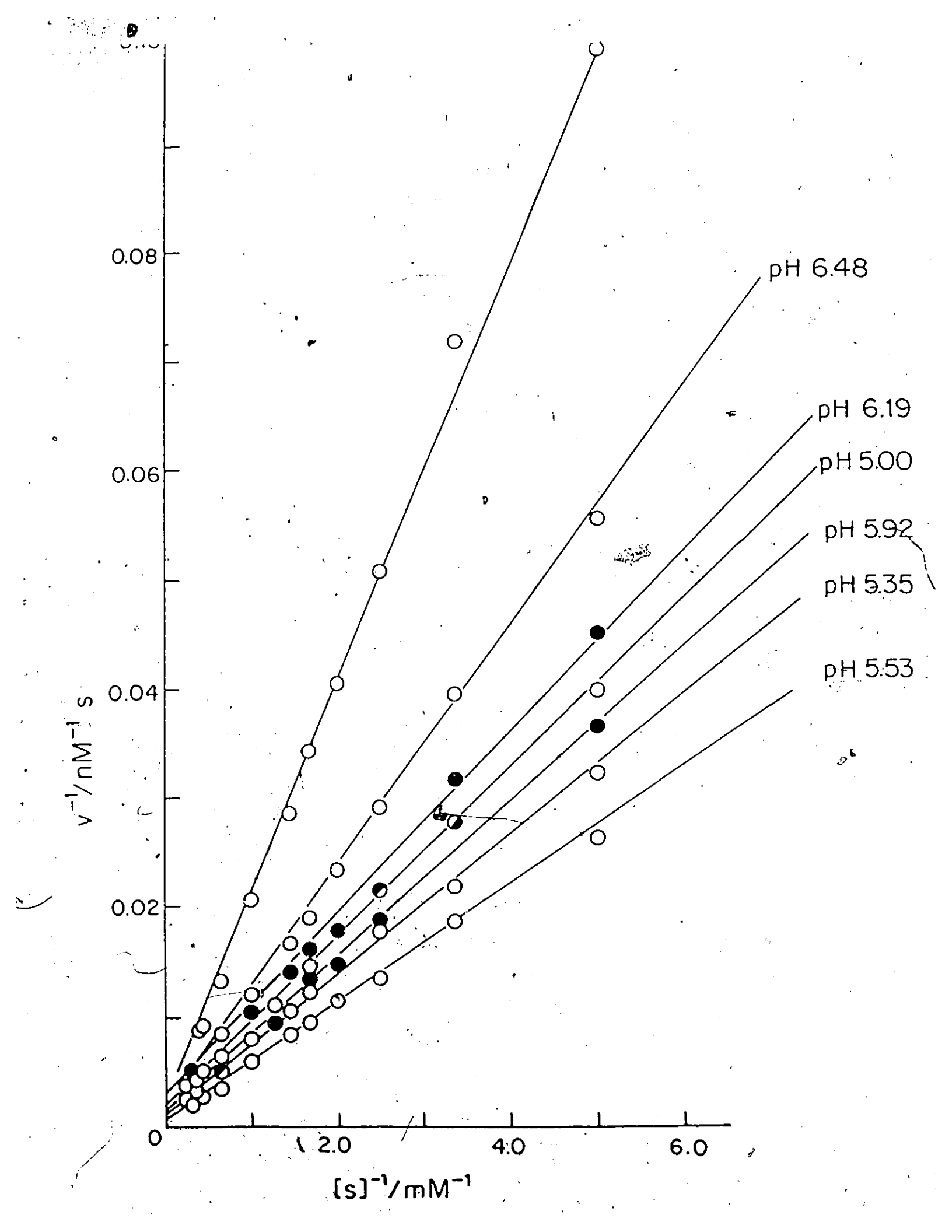
0.08
0.06
0.04
0.02
0
2.0
4.0
6.0
v^{-1}/nM^{-1} s
$[s]^{-1}/mM^{-1}$
pH 6.48
pH 6.19
pH 5.00
pH 5.92
pH 5.35
pH 5.53

Figure 10c. Lineweaver-Burk plots for β-glucosidase in free solution at various pH values T = 31.0°C.

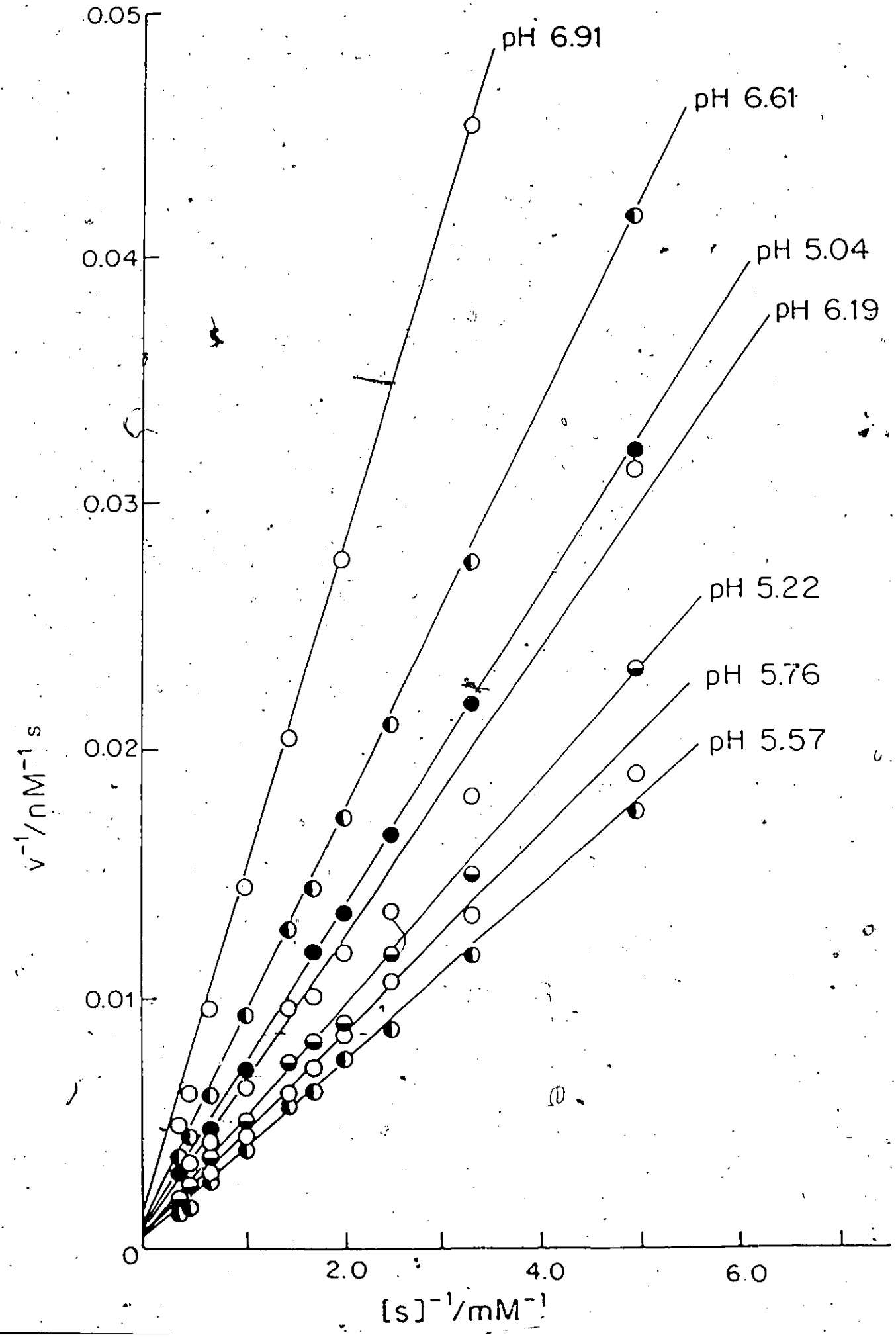
0.05
0.04
0.03
0.02
0.01
0
pH 6.91
pH 6.61
pH 5.04
pH 6.19
pH 5.22
pH 5.76
pH 5.57
2.0
4.0
6.0
$v^{-1}/nM^{-1}s$
$[s]^{-1}/mM^{-1}$

Table 7(a).

Values of V and K_m under different conditions for β-glucosidase in free solution

T : 24.0°C

pH	V /mM·s^{-1}	K_m/mM
5.00	667 ± 4.5%	5.38 ± 4.5%
5.32	952 ± 4.7%	5.80 ± 4.7%
5.35	935 ± 4.8%	6.13 ± 4.8%
5.53	1250 ± 3.2%	6.60 ± 3.2%
5.92	980 ± 4.9%	7.05 ± 4.9%
6.19	870 ± 5.3%	7.62 ± 5.3%
6.48	714 ± 3.1%	7.93 ± 3.1%
6.90	606 ± 2.7%	11.96 ± 2.7%

The errors given are standard deviations, obtained by the method of least squares on the basis of the Lineweaver-Burk equation.

Table 7(b).

Values of V and K_m under different conditions for β-glucosidase in free solition

	T: 18.0°C		T: 31.0°C	
pH	V/nM s^{-1}	K_m/mM	V /nM s^{-1}	K_m/mM
5.00	233 ± 3.7%	4.78 ± 3.7%	1099 ± 1.6%	6.92 ± 1.6%
5.22	328 ± 3.3%	5.07 ± 3.3%	1370 ± 4.2%	6.22 ± 4.2%
5.50	526 ± 2.7%	6.15 ± 2.7%	1923 ± 4.5%	6.91 ± 4.5%
5.56	588 ± 3.9%	6.58 ± 3.9%	1887 ± 2.1%	6.47 ± 2.1%
5.76	769 ± 3.9%	7.85 ± 3.9%	1724 ± 2.6%	6.68 ± 2.6%
6.19	541 ± 3.0%	7.97 ± 3.0%	1250 ± 5.4%	7.03 ± 5.4%
6.61	323 ± 4.4%	9.21 ± 4.4%	926 ± 1.4%	7.49 ± 1.4%
6.91	208 ± 5.3%	9.97 ± 5.3%	769 ± 2.1%	10.09 ± 2.1%

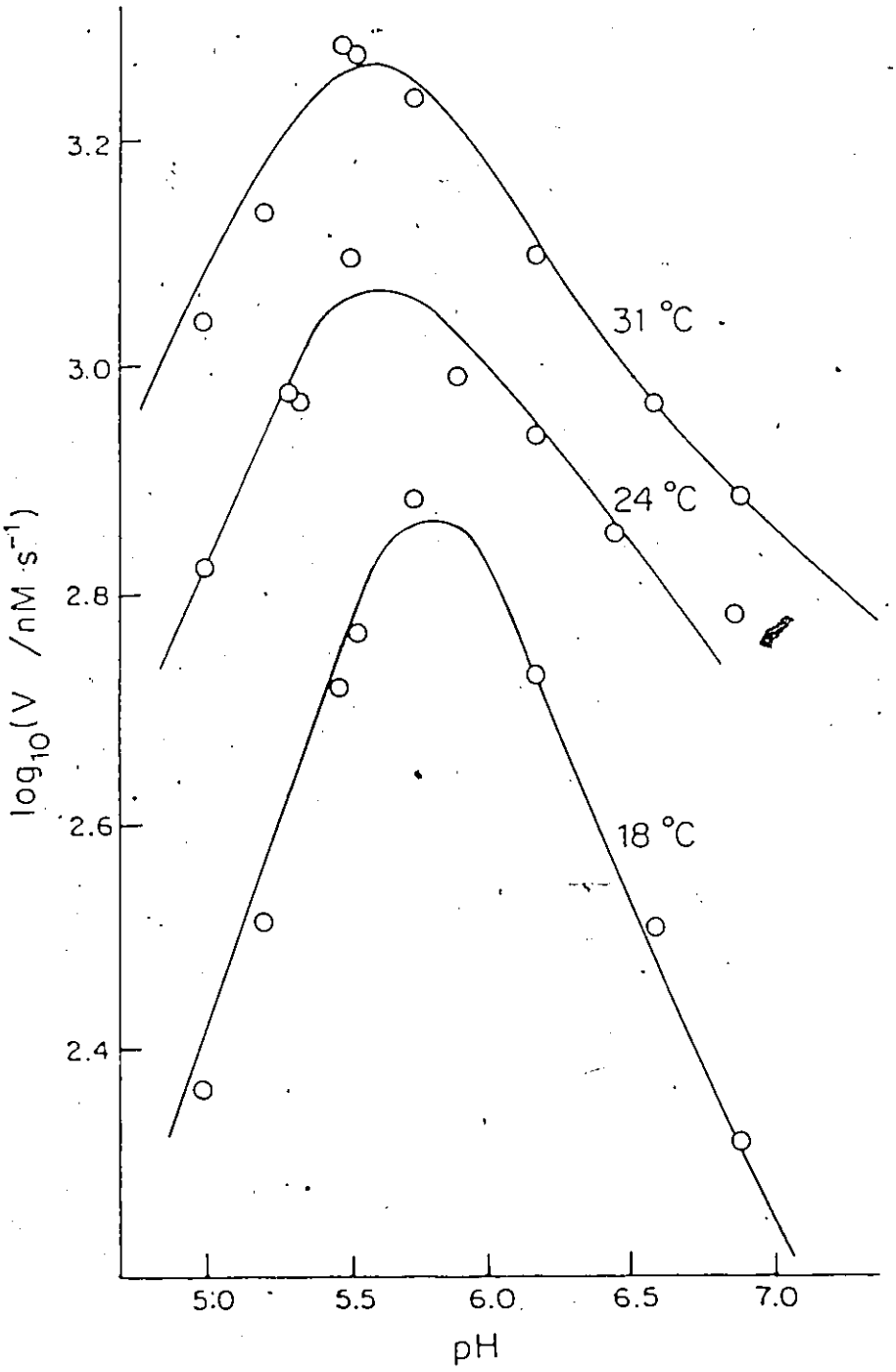

Figure 11. Plots of $\log_{10}V$ against pH for β-glucosidase in free solution at three temperatures.

The curves are the theoretical curves, based on the pK values given in Table 8.

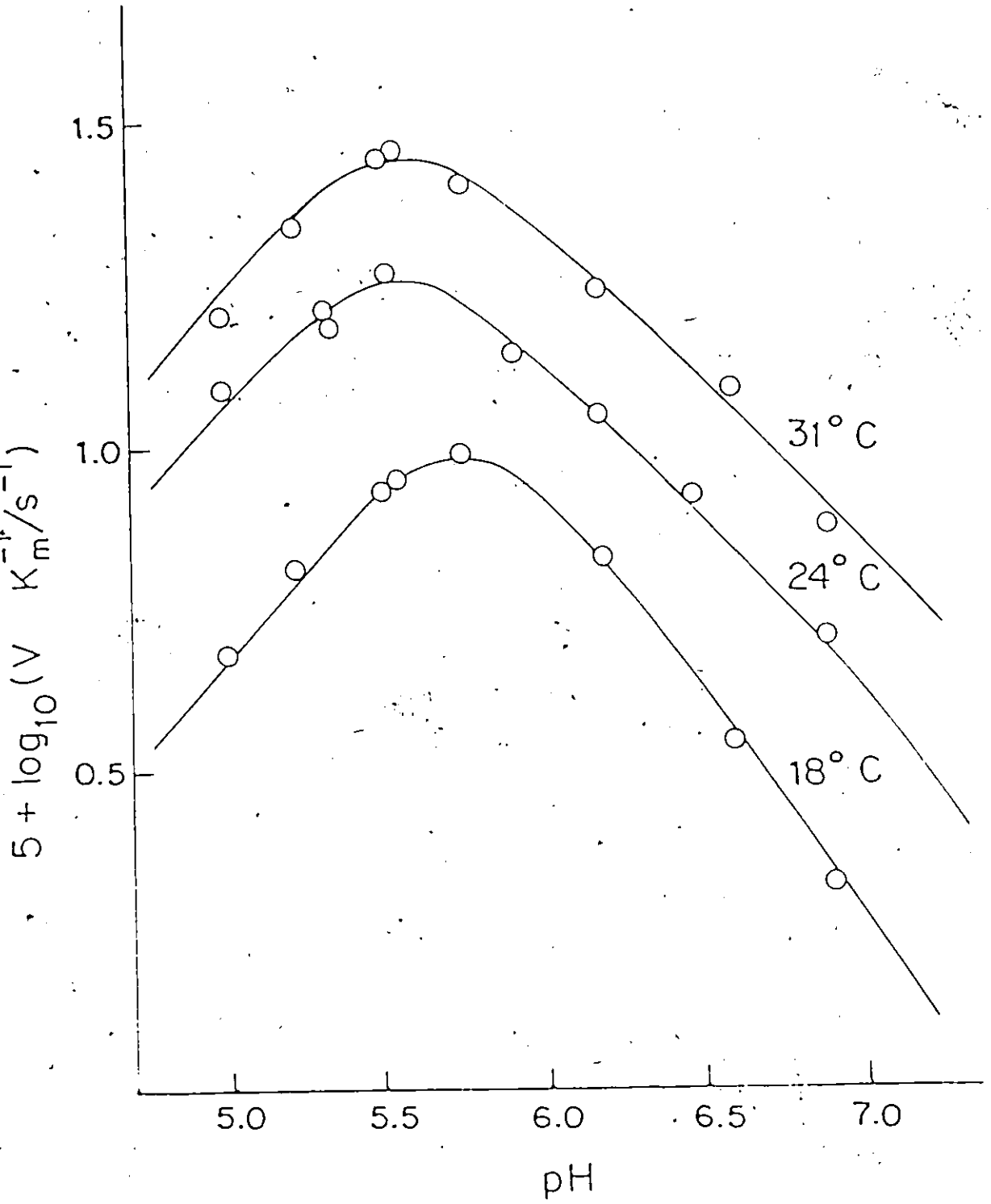

Figure 12. Plots of $\log_{10}(V/K_m)$ against pH for free β-glucosidase at three temperatures. The curves are the theoretical curves, based on the pK values given in Table 8.

Ionization constants of catalytically important groups

The ionization constants of catalytically important groups were obtained from the Michaelis parameters at different pH values. In the present system, reliable values cannot be obtained directly either from the logarithmic plots of V and V/K_m against pH or from pHs at half maximal values of the rates and Michaelis parameters, although very approximate estimates can be made and provide a useful check of the calculations based on statistical treatments. Use was made of a computerized least-squares procedure, already described above. Table 8 gives the values of dissociation constants so obtained, at three temperatures. The pK values are those related to the enzyme itself while pK' values related to the enzyme-substrate complex. These values are rounded-off at the first place after the decimal point and the 95% confidence limits for these values were less than ±0.2 units.

Discussion

It seems that the affinity of β-glucosidase from almond (K_m=5.38 ~12.0 mM from the present work) is lower than that of β-glucosidase from some fungi : Trichoderma viride (K_m=1.5 ~2.74) (7,36,49,59), Aspergillus niger (K_m=1.5 mM)(63), Aspergillus phoenicis (K_m=0.75 ~ 0.8 mM)(18,60,113), Penicillium funiculosum (K_m=2 mM)(113), A.funigatus (K_m=0.84 mM)(114), and Lenzites trabea (K_m=1.64 mM)(115).

The pK_b values about 5 at 25°C suggest that a carboxyl group

Table 8

Dissociation constants for free enzyme obtained by use of statistical procedures

Temperature (°C)	Free enzyme		Enzyme-substrate complex	
	pK_b	pK_a^*	pK_b'	pK_a'
18.0	5.4±0.1	6.0±0.1	5.3±0.1	6.3±0.1
24.0	4.9±0.1	6.4±0.1	5.0±0.1	6.5±0.1
31.0	4.9±0.1	6.4±0.1	4.8±0.2	6.6±0.2

The errors quoted are 95% confidence limits, obtained from the computerized least-squares treatment described in the text.

is involved at the active center, which is catalytically active when in the basic form $-COO^-$ and inactive in the protonated form $-COOH$. The other active group, corresponding to the pK_a value of 6.4, is presumably an imidazole group, which is active in its protonated form. The dissociations of β-glucosidase may therefore be represented schematically as follows:

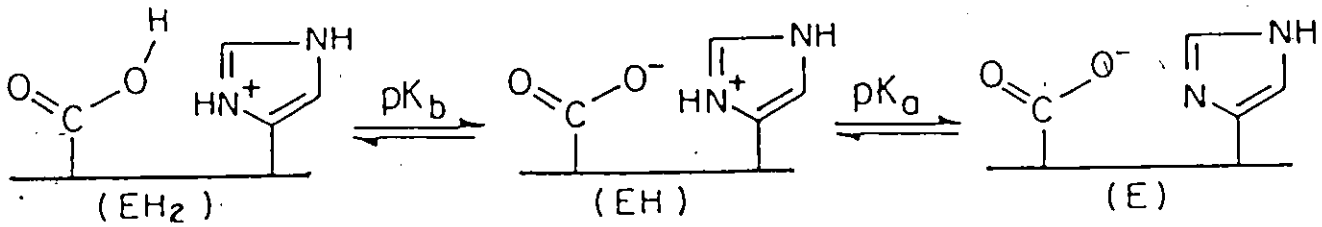

The pK_b values at three temperatures are little changed when the enzyme-substrate complex is formed, suggesting that the carboxyl group is probably not directly involved in the binding of the substrate. However there is some change in the pK_a values on complex formation; in addition, K_m, of which the pH dependence as a plot of pK_m against pH is shown in Fig.13 , increases with pH; this means that the affinity of β-glucosidase for cellobiose decreases with pH, suggesting that the imidazole group is probably implicated in the binding of substrate to form the complex. On the other hand, the pH dependence of log V (Fig. 11) with a maximum at around pH 5.6 indicates that both active

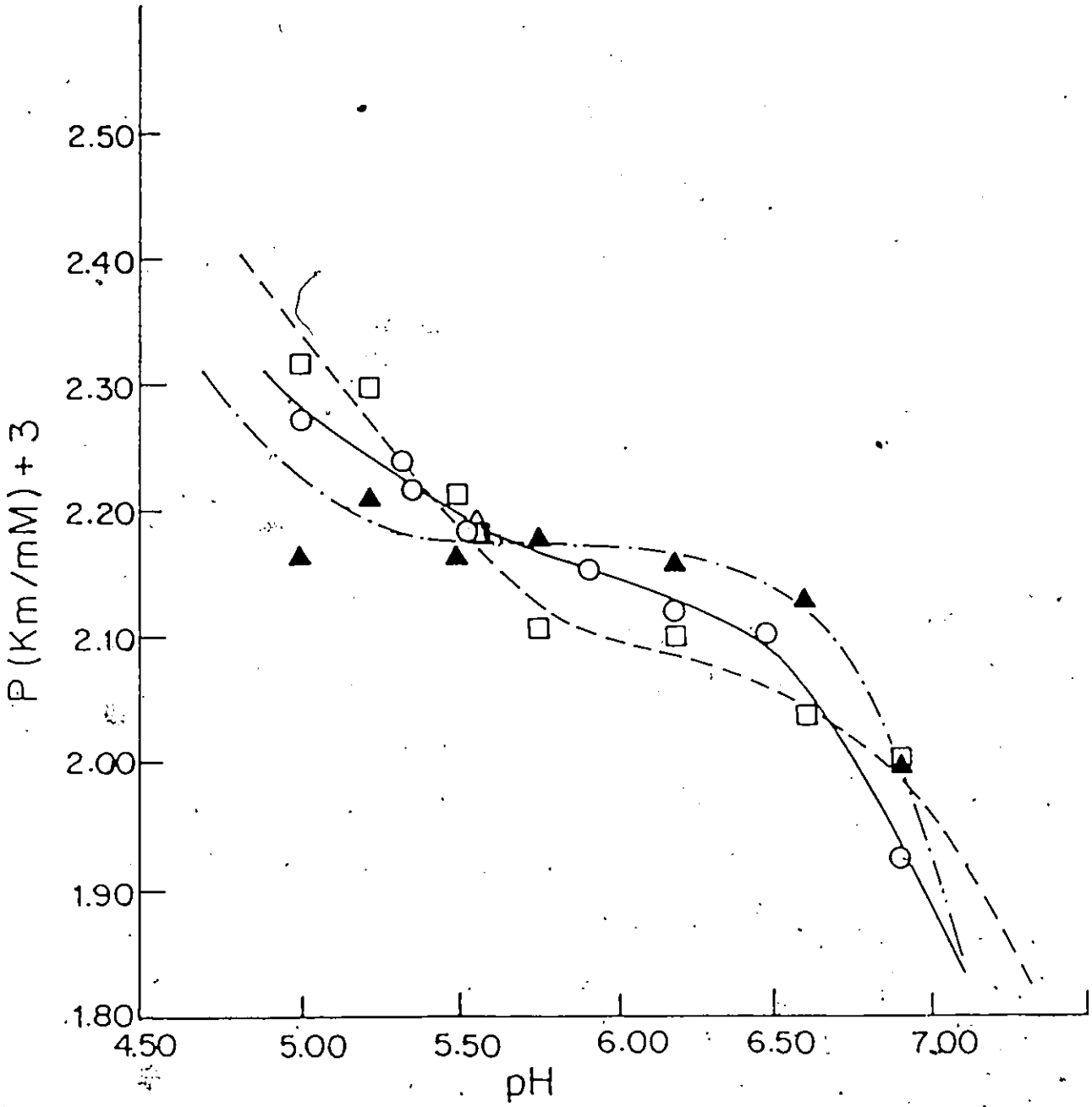

Figure 13. Plots of pK_m against pH at three temperatures. ---□--- 18.0°C; ---○--- 24.0°C; --▲-- 31.0°C.

groups, the carboxylate group and the imidazolium group are involved in the decomposition of the enzyme-substrate complex.

In the literature various pK values for catalytically important groups on β-glucosidase have been reported. Maguire(49) determined the pK values for β-glucosidase from Trichoderma viride, being 3.5 and 6.8 , and suggested that a carboxylate group and a protonated nitrogen atom of an imidazole group of histidine play the catalytic role in the hydrolysis of cellobiose. Umezurike (50) has reported pK values of 4.1 and 6.0 for the enzyme itself, and 3.65 and 6.75 for the enzyme-substrate complex, with β-glucosidase from Botryodiplodia theobromae pat, and also suggested that carboxyl and imidazole groups are responsible for the hydrolysis of p-nitrophenyl-β-D-glucoside. Hiroyama and coworkers(48) reported 4.2-4.8 and 7.4-7.5 for the pK values and considered that the carboxyl group is strongly implicated in the formation and dissociation of the enzyme-substrate complex for β-glucosidase of P.oryzae, and that the ionization of an imidazole group or sulfhydryl group is also responsible for the hydrolyses of salicin and cellobiose.

However, in contrast, Shewale and Sadana (15) recently measured pK values of 4.2-4.3 and 4.7-4.9 for the free enzyme, and 3.2 and 3.8 for the enzyme-substrate complex, with β-glucosidase from S.rolfsii, and suggested that only the carboxylate group is involved in the catalytic role. On the basis of the variation of K_m, which is greater on both sides of the optimum pH, and on the basis of the variation of log V with pH,

they proposed that the ionizing groups in the free enzyme control the binding of the substrate and also the next step, the decomposition of the enzyme-substrate complex.

The results obtained from the present studies on the pK values, and on the entropy change $\triangle S$ and the enthalpy change $\triangle H$ associated with these ionization processes (which will be discussed in the next chapter), suggest that a carboxyl group and an imidazole group are involved at the active center. The imidazole group may be responsible for both the formation and decomposition of enzyme-substrate complex, while the carboxyl group is probably only implicated in the splitting of the bond in the complex.

CHAPTER IV

THERMODYNAMICS OF THE IONIZATION PROCESSES OF β-GLUCOSIDASE IN FREE SOLUTION

4.1 Introduction

The studies of the pH dependence of the kinetic parameters make possible the evaluation of dissociation constants and lead to suggestions as to the identity of the ionizing groups constituting the active center of the enzyme. However, in order to obtain valuable information about the mechanism of enzymic reactions, the systematic studies of pH effects on the detailed kinetics must include also an investigation of the effect of temperature on the ionizations of the active groups; this provides the thermodynamic parameters for the dissociation processes. Unfortunately few previous studies on the temperature dependence of the ionization constants have been made for any enzyme system; therefore the thermodynamic quantities, enthalpies and entropies of the ionization processes are not available for most enzyme systems.

With the particular object of investigating the temperature dependence of the dissociation constants, the kinetic measurements were carried out at different pH values for three temperatures, 18.0°, 24.0° and 31.0°C; and the results were

analyzed to obtain the enthalpy changes and entropy changes accompanying the dissociations of catalytically active groups in the free enzyme, and the corresponding values for the dissociations of the enzyme-substrate complex.

4.2 Values of the thermodynamic parameters ΔH_d, ΔS_d associated with ionization processes

Figure 14 shows the plots of four pK values against 1/T. The enthalpies ΔH_d for the dissociation processes were obtained from the slope of these plots, according to the van't Hoff equation.

$$\frac{d\ \ln K}{dT} = \frac{\Delta H_d}{RT^2}$$

The entropy changes ΔS_d for the dissociations were obtained from the slope of plots of ΔG_d against T (Fig. 15)

$$\frac{d\ \Delta G_d}{dT} = -\Delta S_d$$

Table 9 lists these thermodynamic parameters so obtained for free β-glucosidase and the enzyme-substrate complex.

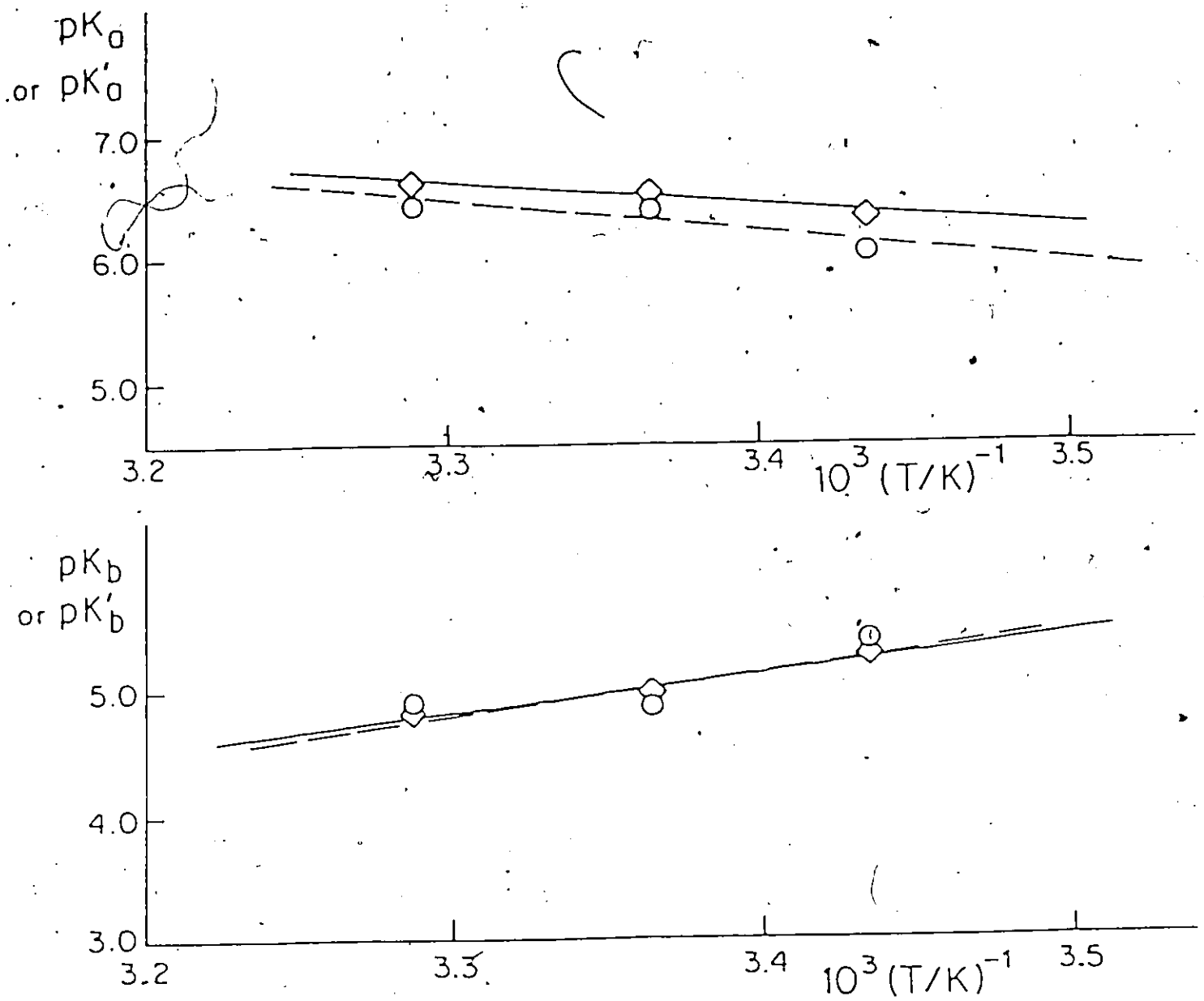

Figure 14. Plots of pK_a and pK_b against 1/T, for the free enzyme(○) and the enzyme-substrate complex(◇).

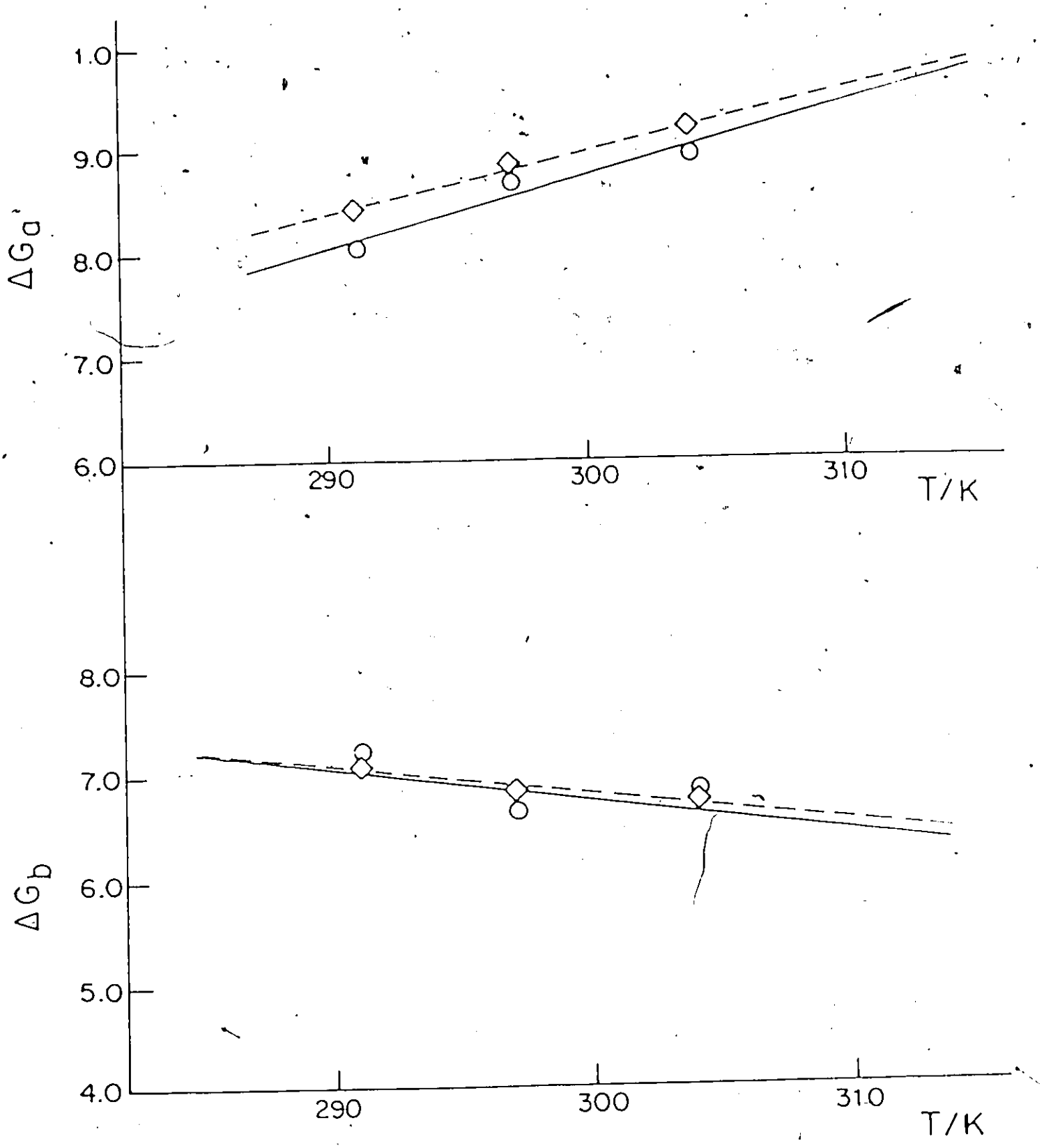

Figure 15. Plots of ΔG against T, for the dissociation processes of free enzyme(○) and the enzyme-substrate complex(◇)

Table 9

Thermodynamic parameters for free β-glucosidase and for the enzyme-substrate complex.

	pK(25.0°C)	ΔG(25.0°C) kJ mol^{-1}	ΔH_d kJ mol^{-1}	ΔS_d J K^{-1} mol^{-1}
Free enzyme:				
pK_b	5.0	28.8	61.3±12	109±41
pK_a	6.3	35.9	-48.5±9	-283±36
Enzyme-substrate complex:				
pK_b'	5.1	28.9	60.8±27	107±62
pK_a'	6.5	37.0	-35.5±21	-243±66

The error was estimated as the difference between the largest and smallest slopes which could arise on the basis of the values of pK or ΔG.

4.3 Discussion.

The most significant feature of the thermodynamic parameters obtained (Table 9) is that there is a large entropy increase associated with the first ionization, for both the enzyme and the enzyme-substrate complex. An entropy decrease, of even greater magnitude, is associated with the second ionization. For the ionic dissociation of a simple neutral acid such as acetic acid there is always a substantial entropy decrease, owing to the electrostriction of water molecules by the ions produced from the neutral molecule (117). For the ionic dissociation of a cationic acid such as NH_4^+ there is a much smaller entropy change, since an ion has given rise to an ion and a neutral molecule(117). The following table(183) gives the values of ΔH°, and ΔS° for the dissociation process of some simple neutral and cationic acids.

	ΔH°/kJ mol^{-1}	pK	ΔS°/J $K^{-1}mol^{-1}$	T/^{0}C
CH_3COOH	2.0	4.762	-84.5	10
NH_4^+	52.5	9.90	-0.9	5
$CH_3NH_3^+$	54.0	11.31	-22.2	5
imidazole	36.7	6.993(pK_1)	-10.5	25

Since the X-ray structure of β-glucosidase is unknown, no firm conclusions can yet be drawn as to the nature of the ionizing groups at the active centre of this enzyme. The pK values of 5.0 and 6.3 that have been obtained in the present work are consistent with those obtained by other workers(48,49,52), and it has usually been supposed that a carboxyl group and an imidazole group are involved at the active centre. The active centre at an intermediate pH value would thus be as follows:

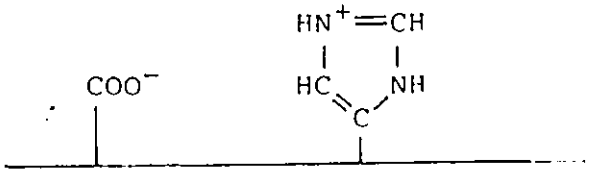

The $-COO^-$ group plays the basic role, and the imidazole group the acidic role, in the catalytic process. Alternatively, one investigator(15) has suggested that two carboxyl groups are involved, one in its protonated form and the other in its unprotonated form:

However, this suggestion is based on work with an enzyme preparation obtained from S. roefii; in this study the pK values obtained were 4.2 and 4.7, substantially lower than the values found in the present work and in other investigations(48,49,52); this suggestion therefore may not apply to the present enzyme.

In view of the uncertainty as to the nature of the ionizing

groups at the active centre its is impossible at the present time to draw any firm conclusions from the entropy changes observed. However, some comments may be useful. The group of pK 5.0 is probably a carboxyl group, and if its ionization were a simple one there would be an entropy decrease, as a result of the electrostriction of water, as previously noted. There is, however, a substantial entropy increase for this ionization. This may be due to structural changes occurring at the same time.

The substantial entropy decrease of $-283\ J\ K^{-1}mol^{-1}$ that occurs in the ionization of the second group is consistent in sign with the ionization of a -COOH group, but the magnitude of the change is much too great. If the group is an imidazole ring the entropy change is of the wrong sign to be explained by a simple ionization process. In either case the results cannot be explained except in terms of complications such as interactions between charged groups or structural changes in the enzyme.

Further elucidation of this problem must await structural work on the enzyme. The entropy and enthalpy values obtained are, however, of significance in connection with the temperature and pH effects to be discussed in the next two chapters.

CHAPTER V

TEMPERATURE EFFECTS WITH FREE β-GLUCOSIDASE

5.1 Introduction

Investigations of temperature effects on enzyme kinetics, by providing the details of kinetic constants and thermodynamic parameters such as enthalpies and entropies, can throw light on the details of enzyme-substrate interactions, and therefore on the mechanism of enzyme action. Such investigations make a very significant contribution to the understanding of the kinetics of enzyme systems.

It is well known that the overall rate of an enzyme—catalyzed reaction passes through a maximum as the temperature is increased. This universal phenomenon of the optimum temperature for an enzyme system is due to the fact that raising the temperature affects two independent processes, the catalyzed reaction itself and the thermal inactivation of the enzyme. Usually the thermal inactivations of enzymes have much higher temperature coefficients than do the enzyme-catalyzed reactions. In the lower temperature range, the inactivation is slow compared with the enzyme reaction; the overall rate therefore increases with increase in temperature, as with ordinary chemical reactions. However, at higher temperatures inactivation becomes more and more important, so that the concentration of active enzyme falls

during the course of reaction; this results in a decrease in the overall reaction rate.

Most kinetic studies with enzyme systems have been performed at a single temperature, or else the temperature effects were limited to a single pH to give an estimate of activation energies. As mentioned above, studies of temperature effects on reaction rates can provide important information about the reaction mechanism. However, enzymic catalysis is very complicated and is controlled by the ionization states of the active groups on the enzyme, which in turn depend on enzyme ionization constants and the pH of the system; the rate constant of an enzyme-catalyzed reaction is therefore a complex function of temperature, pH and the pK values. It is thus desirable to carry out studies of temperature effects not at a single pH, but over a range of pH values, in order to obtain valuable information about the intermediates and the mechanism of the reaction.

In the present work, the kinetic measurements with β-glucosidase were carried out over a temperature range at different pH values and the results were analyzed to obtain the enthalpies of activation and entropies of activation at different pH values. The theory of temperature effects on the rates of enzyme catalyzed reactions provided a good interpretation for the non-Arrhenius behaviour, but could not give an explanation for the dependence of activation energy on pH. A unified theory of both pH and temperature effects was therefore developed and will

be discussed in the next chapter.

5.2 Theoretical principles

The kinetic equation for an enzyme-catalyzed reaction is always complex, containing at least three kinetic constants. In the simplest case, when the simple Michaelis-Menten mechanism applies, the rate equation

$$v = \frac{k_2[E_o][S]}{K_m + [S]} = \frac{K_2[E_o][S]}{\frac{k_{-1}+k_2}{k_1} + [S]} \qquad (1)$$

involves three rate constants k_1, k_{-1} and k_2. These individual rate constants vary with temperature according to the Arrhenius equation:

$$k = A\, e^{-E/RT} \qquad (26)$$

where E is the energy of activation for the reaction and A is the pre-exponential factor. The variation with temperature of the overall rate, v, for an enzyme reaction is therefore complicated, and the plot of the logarithm of the rate against the reciprocal of the absolute temperature may be linear or curved depending upon the relative magnitudes of the individual rate constants. The observed activation energy may correspond to one of the individual activation energies or be a function of more than one individual activation energy.

For example, for the simplest case above, the limiting rate at low substrate concentrations is

$$v_o = \frac{k_1 k_2}{k_{-1}+k_2}[E]_o[S] \qquad (27)$$

The second-order rate constant k_o, equal to $k_1k_2/(k_{-1}+k_2)$, is composite so that it is not necessarily the case that the Arrhenius equation will apply to it directly. There are, however, two special cases under which this composite constant will obey the equation;

(1) When $k_2 \gg k_{-1}$, k_{-1} may be neglected in comparison with k_2, so that k_o is equal to k_1. This means that the rate constant for the overall reaction at low substrate concentrations is simply that for the first step, the formation of the complex. The Arrhenius equation should apply to k_o, and the observed activation energy corresponding to k_o will be E_1, the activation energy for the initial complex formation.

(2) When $k_{-1} \gg k_2$, the constant k_o is now equal to k_1k_2/k_{-1}. The application of the Arrhenius equation to the individual rate constants k_1, k_2 and k_{-1} leads to

$$k_o = \frac{k_1 k_2}{k_{-1}} = \frac{A_1 A_2}{A_{-1}} e^{-(E_2+E_1-E_{-1})/RT}$$

In this extreme case, the Arrhenius law should also apply to this

composite constant k_o i.e. (k_1k_2/k_{-1}), but the activation energy for k_o does not correspond to a single elementary step; it is the sum of the activation energy E_2 for the second step (EA → E+P) and the total energy increase E_1-E_{-1} for the first step (E+A ⇌ EA).

cases, the plots of $\log_{10}k_o$ against 1/T will not necessarily be linear and the observed activation energy E_o is related to the individual values by the following equation(65):

$$E_0 = \frac{k_{-1}(E_1+E_2-E_{-1})+k_2E_1}{k_{-1}+k_2} \qquad (28)$$

In other words, the overall activation energy E_0 is the weighted mean of the values E_1 and $E_1+E_2-E_{-1}$ for the extreme cases (1) and (2), the weighting factors being

$$\frac{k_2}{k_{-1}+k_2} \quad \text{and} \quad \frac{k_{-1}}{k_{-1}+k_2}$$

The overall activation energy will therefore vary with temperature and the plot of log v against 1/T will be curved.

In the investigation of temperature effects, a careful analysis of kinetic data is important for obtaining correct information as to the reaction mechanism.

5.3 Experimental measurements and Results

The materials and kinetic procedures used for the present studies are essentially the same as those given in Chapter II and

III. The methods for the calculation of initial rates have been described in Chapter II. The calibration curves were made for each temperature used in the kinetic measurement, with standard glucose solutions.

Rates were measured at eleven temperatures ranging from 10°C to 37°C, and at an enzyme concentration of 0.1 mg/mL, for a variety of substrate concentrations ranging from 0.2 mM to 3.2 mM.

Temperature dependence of initial rates and Michaelis parameters

The initial rates obtained at different temperatures and at pH 6.39 are listed in Table 10; some of the initial rates are shown in Figure 16 as plots of $\log_{10} v$ against 1/T. Such plots consistently show a change in slope, and appear to consist of two straight lines with an intersection at about 23°C.

The Michaelis parameters (V and K_m) at the eleven temperatures were obtained from the corresponding Lineweaver-Burk plots, examples of which are shown in Figure 17. The values of V and K_m are listed in Table 11. The temperature dependences at pH 6.39 of the Michealis parameters are shown as Arrhenius plots in Figure 18. These plots also show an intersection at 23°C. The intersections in Arrhenius plots indicate that there are two temperature regions with different activation energies for free β-glucosidase, one below 23°C and another above 23°C. Some previous studies have also reported a transition temperature; Mayaiki et al.(61) obtained an intersection at 27°C, and Venardo

Table 10.

Initial rates of reaction (nM s^{-1}) for free β-glucosidase at a concentration 0.1 mg/mL at various temperatures and at pH 6.39

T°C / [S]/mM	10.2	13.0	15.2	18.1	20.2	23.0	25.2	28.0	31.0	34.0	37.0
0.200	4.73	6.07	8.60	11.4	12.3	18.1	21.7	25.7	31.1	43.7	50.6
0.299	6.69	9.09	12.3	16.1	18.9	26.9	31.3	40.9	47.6	60.2	68.6
0.399	8.82	11.9	16.1	21.3	24.3	32.8	40.8	49.1	58.2	76.9	91.4
0.499	11.1	14.1	19.8	25.5	30.8	41.6	50.7	63.5	71.7	94.3	106
0.599	13.6	17.6	22.5	31.0		50.9	57.4	70.7	84.6	118	120
0.699	15.4	22.7	27.7	34.4	43.9	60.9	67.9	81.9	94.0	138	122
0.998	23.9	34.1	41.4	52.1	62.6	82.1	99.5	120	144	184	202
1.60	34.7	44.9	58.3	77.8	96.4	122	146	166	205	254	304
2.40	47.5	62.6	78.7	105	133	162	190	230	266	324	401
3.19	59.8	80.2	105	139	158	197	228	279	307	385	439

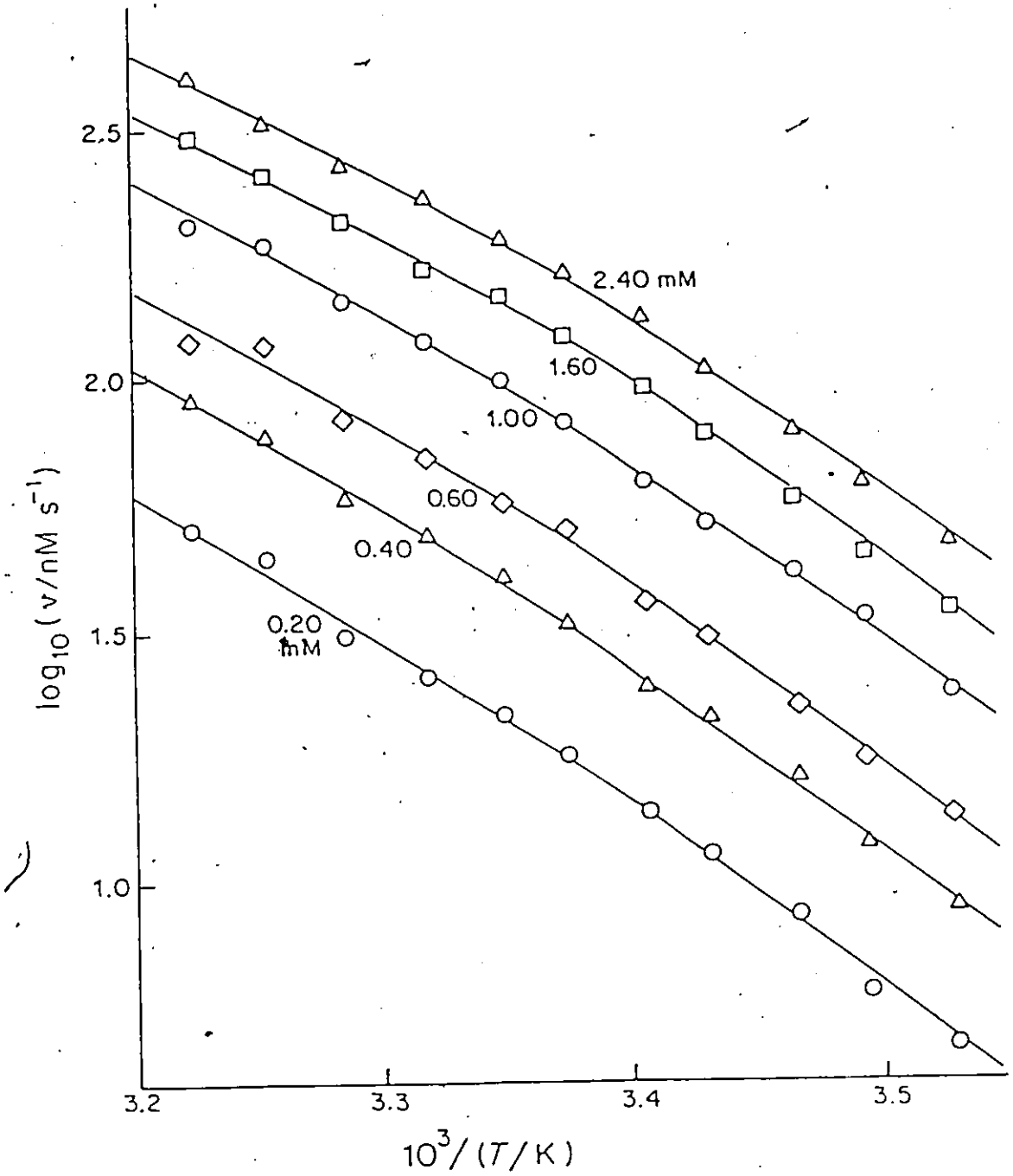

Figure 16. Arrhenius plots of the initial rates for free β-glucosidase, at pH 6.39 and at the substrate concentrations indicated.

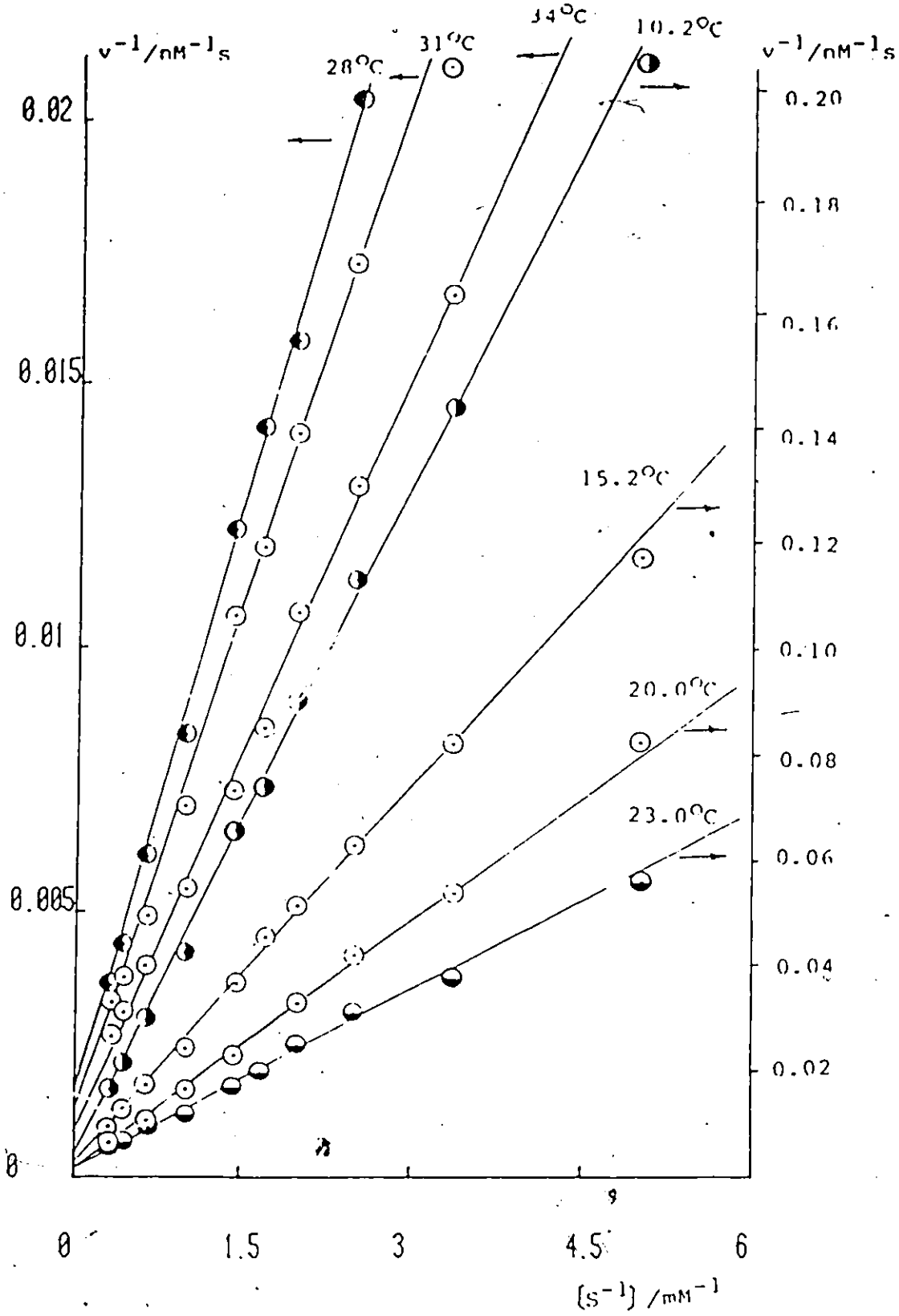

Figure 17. Lineweaver-Burk plots at different temperatures for free enzyme [E] = 0.1 mg/mL, pH = 6.39

Table 11.

Values of V and K_m for the free enzyme; [E] = 0.1 mg/mL; at pH = 6.39 and at various temperatures

Percentage error in both V and $K_m < \pm 5\%$

T (^{o}C)	V (nM S^{-1})	K_m (mM)
10.2	256	10.91
13.0	303	9.65
15.2	370	8.74
18.1	476	8.58
20.2	556	8.44
23.0	690	7.63
25.2	730	6.69
28.0	909	6.82
31.0	1010	6.40
34.0	1234	5.85
37.0	1408	6.03

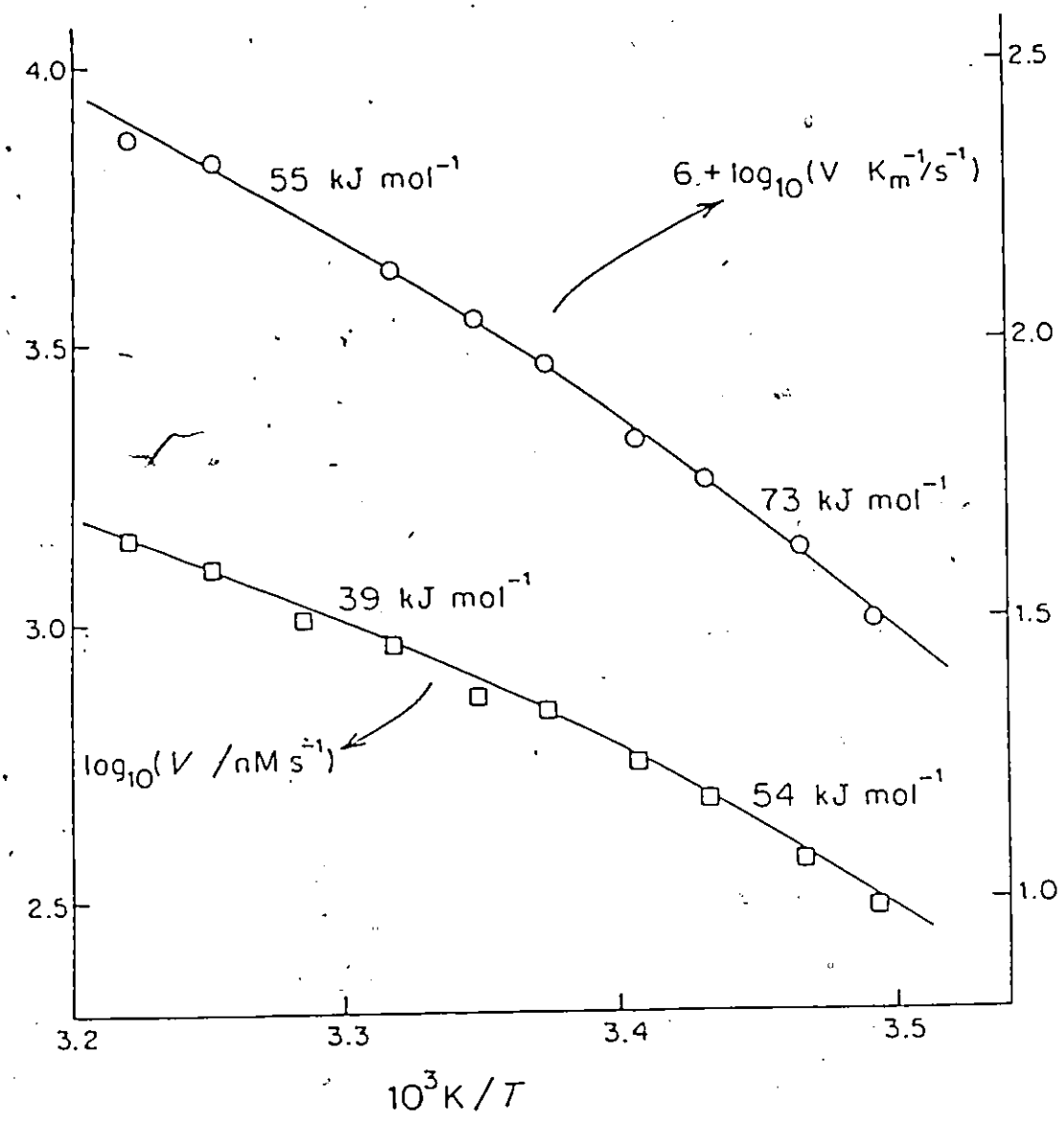

Figure 18. Plots of $\log_{10}V$ and of $\log_{10}(V/K_m)$ against $1/T$, $[E] = 0.1$ mg/mL pH = 6.39.

et al.(62) at 45°C.

The reaction rates were also measured at different temperatures (18°, 24° and 31°C) for 8 other pH values. The results, the initial rates and the Michaelis parameters have been given in Table 6 and 7 in Chapter III. Some of the results, as plots of $\log_{10}V$, $\log_{10}V$ and $\log_{10}V/K_m$ against 1/T for different pH values, are presented in Figure 19 and Figure 20. It is interesting to note that all of these plots at different pH values consistently show a change in slope. The change in slope becomes much more pronounced as the pH value either increases or decreases from the optimum pH value.

Activation energies and entropies of activation

The activation energies obtained at different pH values are given in Table 12. The values designated E_c are those obtained from the plots of $\log_{10}V$ against 1/T, which means that they were obtained from rates when $[S] \gg K_m$; the subscript ℓ indicates the activation energy in the lower temperature range (below 23°C) and h that in the higher temperature range (about 23°C). The $E_{0,\ell}$ and $E_{0,h}$ values are those obtained from the $\log_{10}(V/K_m)$ plots, that is, obtained from rates when $[S] \ll K_m$.

Figure 21 shows the variations of the activation energies with pH. It is to be seen that $E_{c,h}$ and $E_{o,h}$, the activation energies in the higher temperature range corresponding either to V or to V/K_m, do not vary much with pH. The activation energies in the lower temperature range, $E_{c,\ell}$ and $E_{o,\ell}$ pass through a

Figure 19. Plots of $\log_{10} v$ against 1/T at various pH values
(a) pH 5.00 (b) pH 5.22 (c) pH 5.50 (d) pH 5.56
(e) pH 5.76 (f) pH 6.19 (g) pH 6.61 (h) pH 6.91

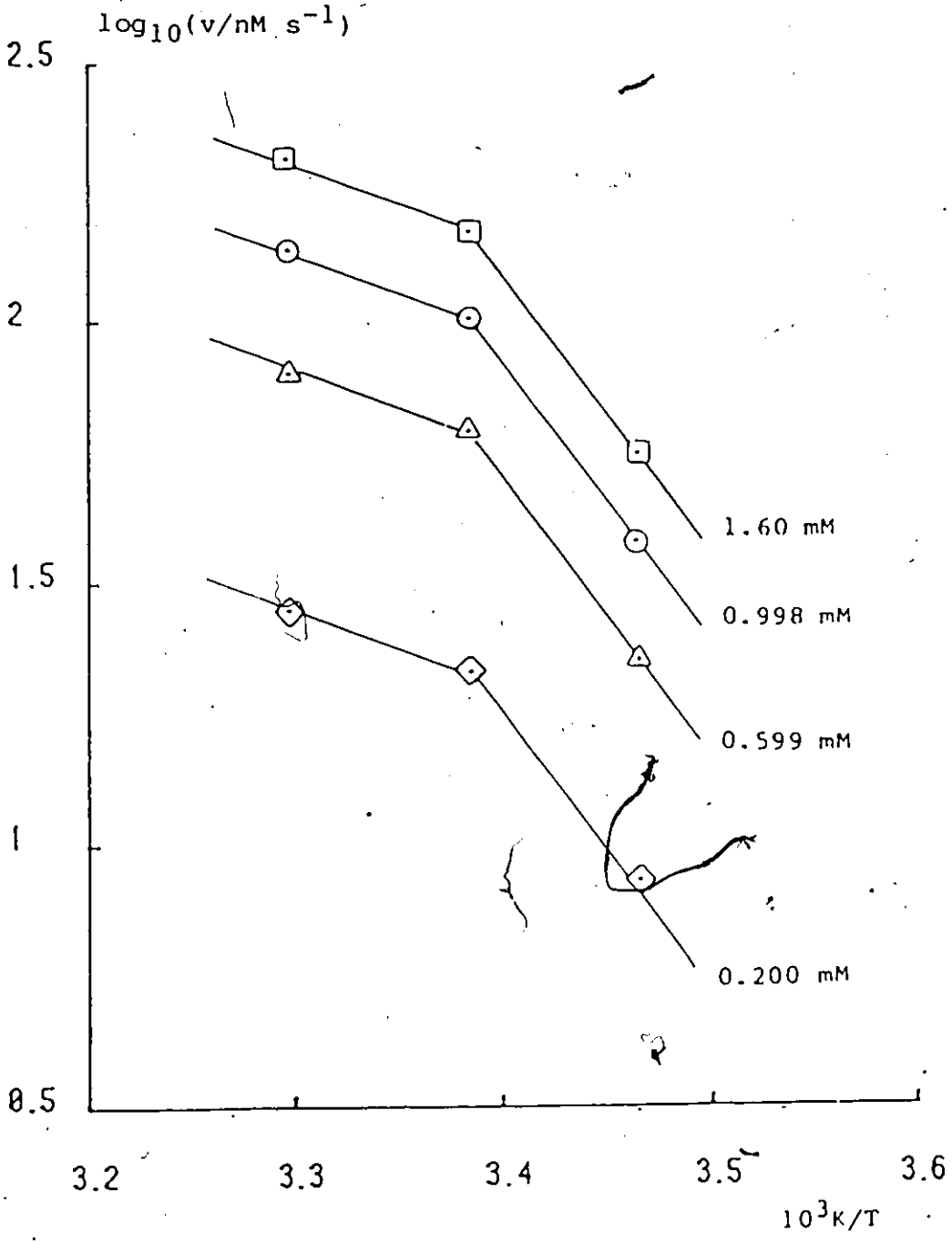

Figure 19(a) pH = 5.00

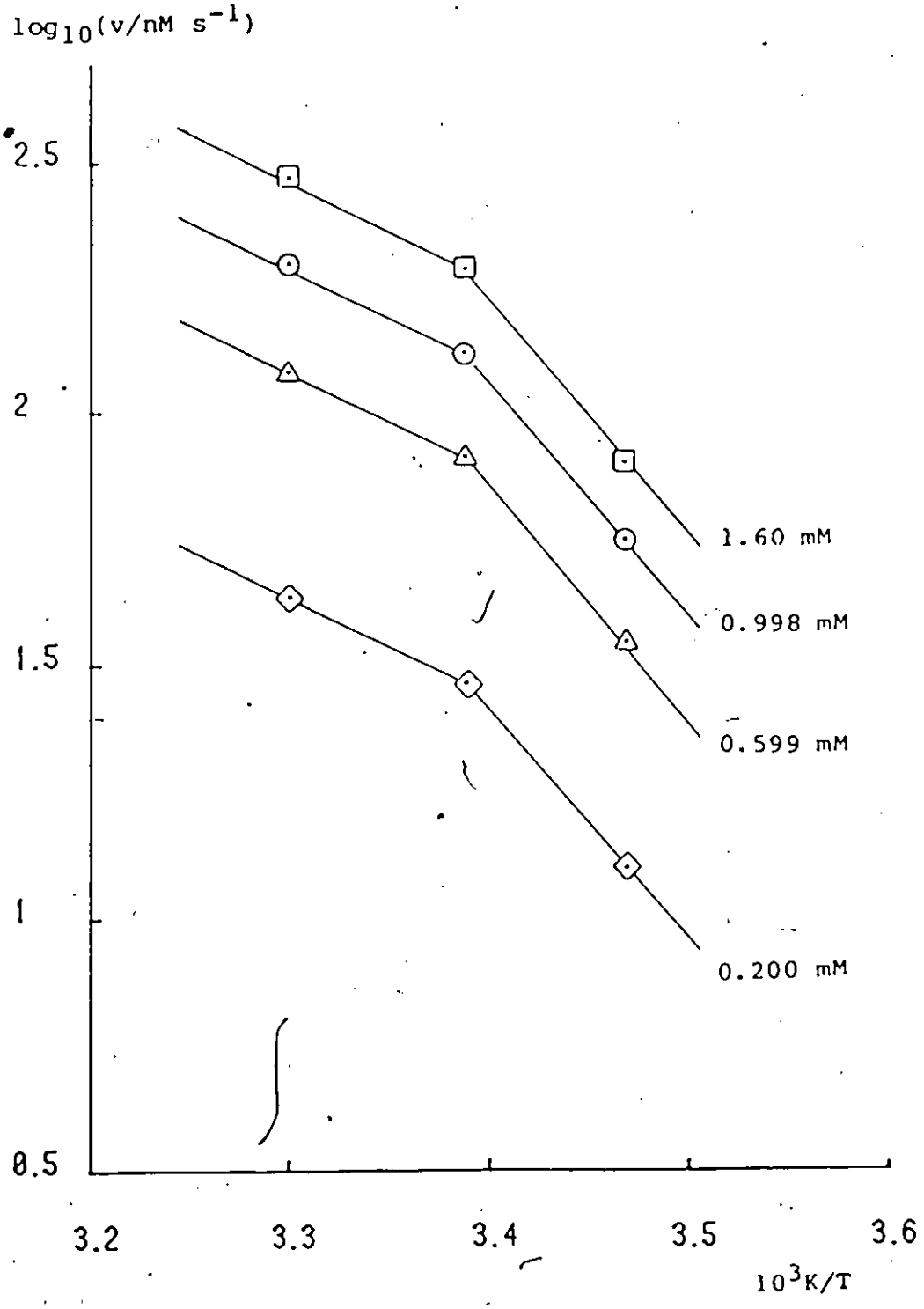

Figure 19(b) pH = 5.22

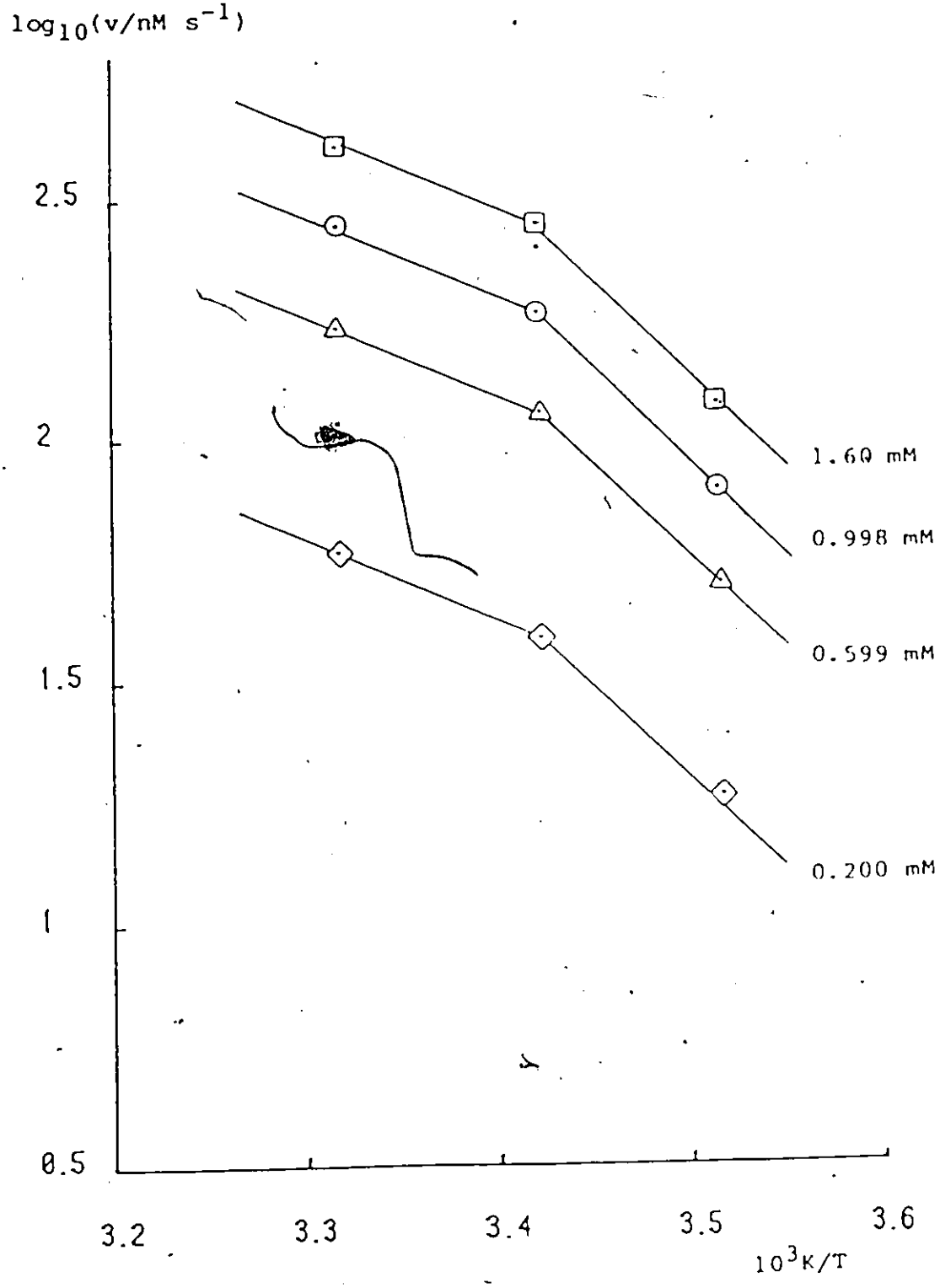

Figure 19(c) pH = 5.50

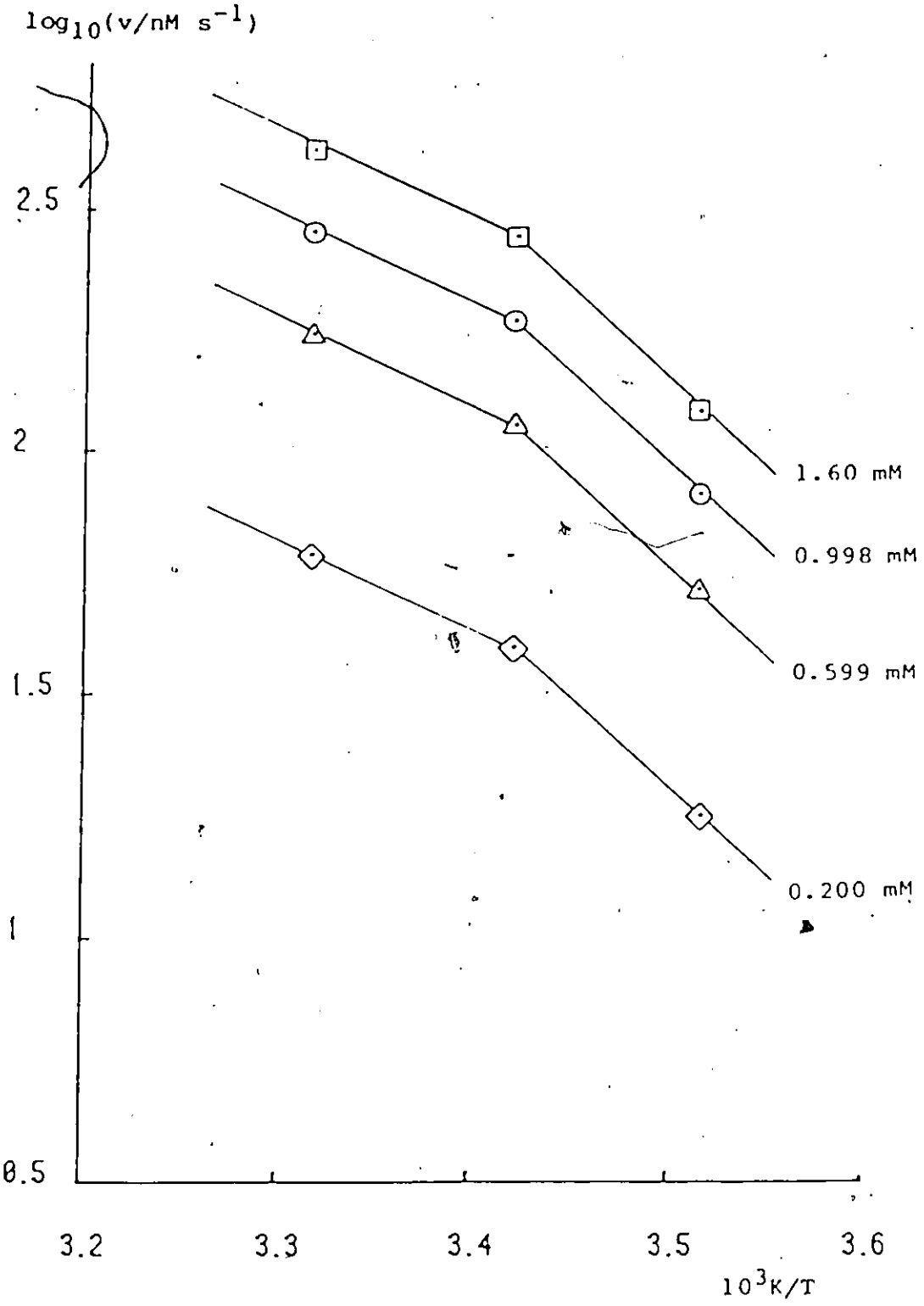

Figure 1º(d) pH = 5.56

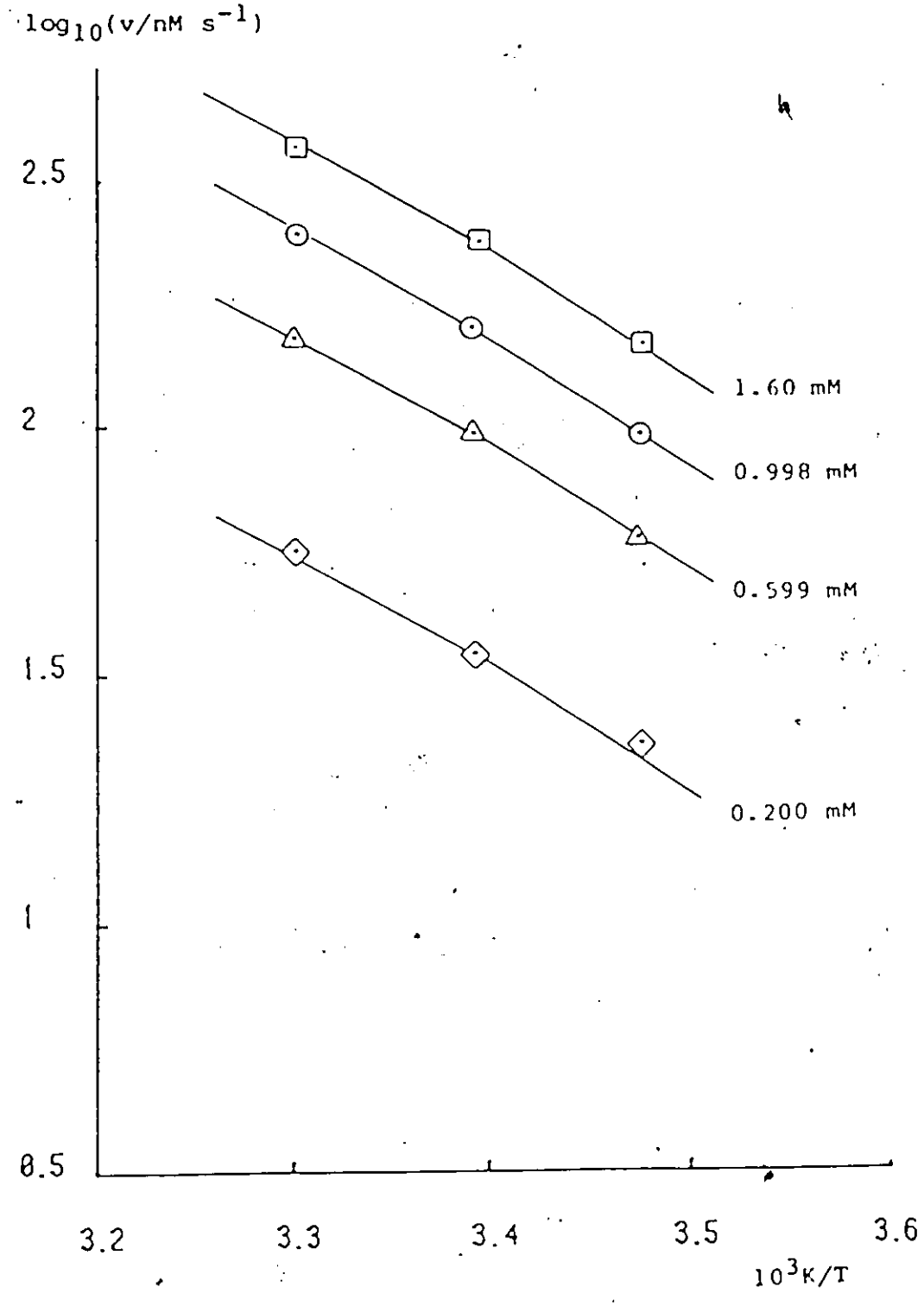

Figure 19(e) pH = 5.76

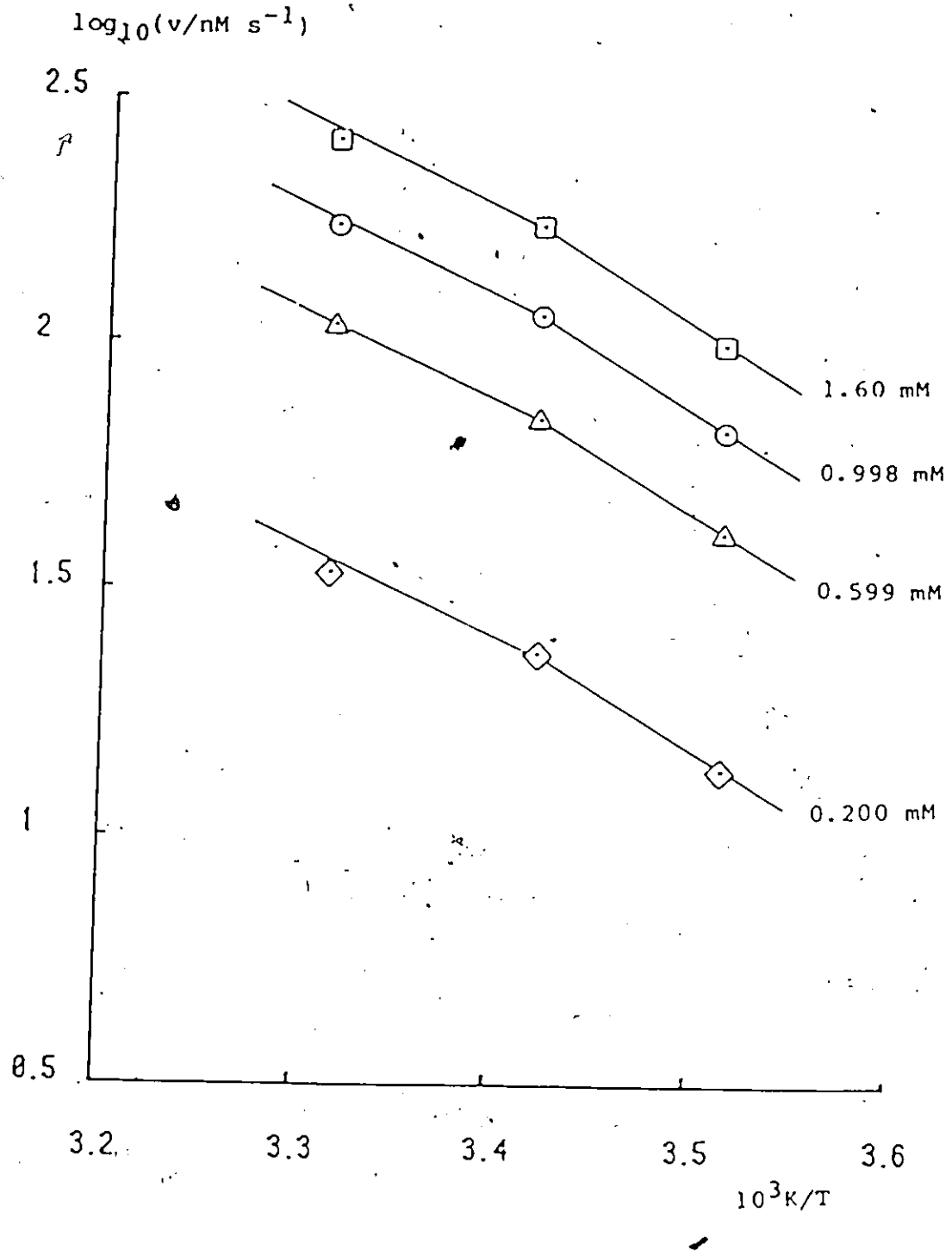

Figure 19(f) pH = 6.19

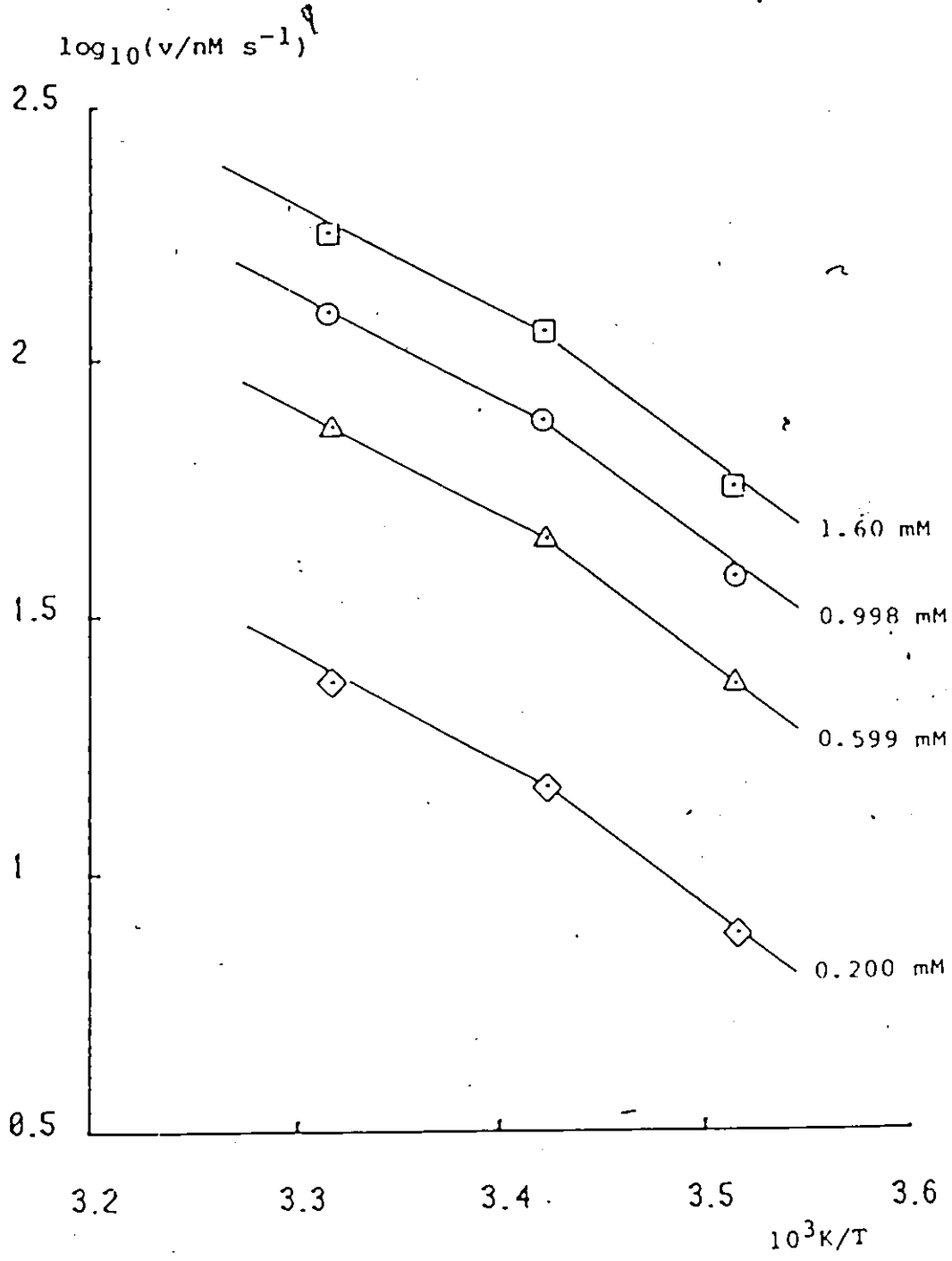

Figure 19(g) pH = 6.61

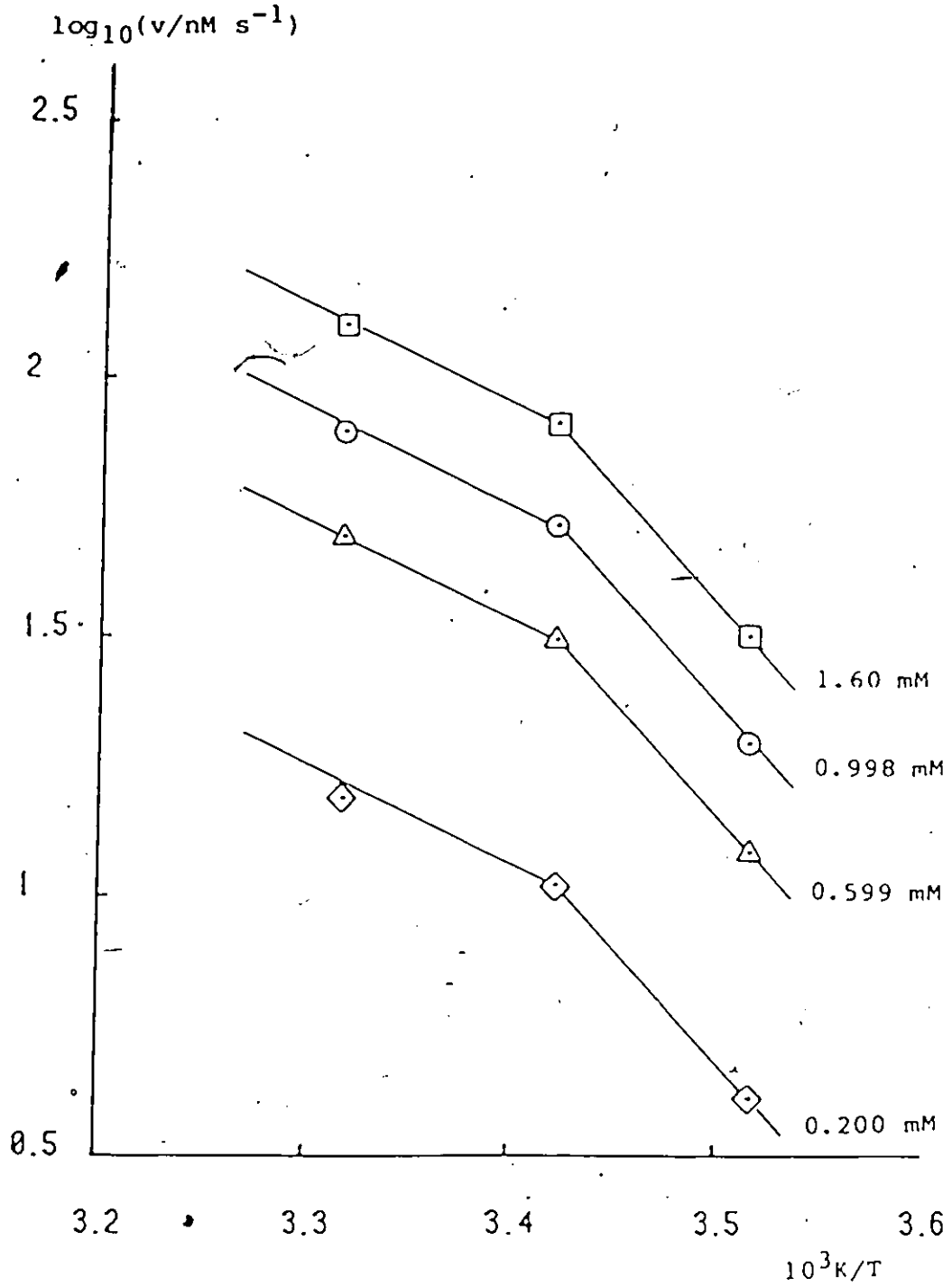

Figure 19(h) pH = 6.91

Figure 20. Plots of $\log_{10}V$ and of $\log_{10}(V/K_m)$ against $1/T$ at various pH values
(a) pH 5.00 (b) pH 5.22 (c) pH 5.50 (d) pH 5.56
(e) pH 5.76 (f) pH 6.19 (g) pH 6.61 (h) pH 6.91

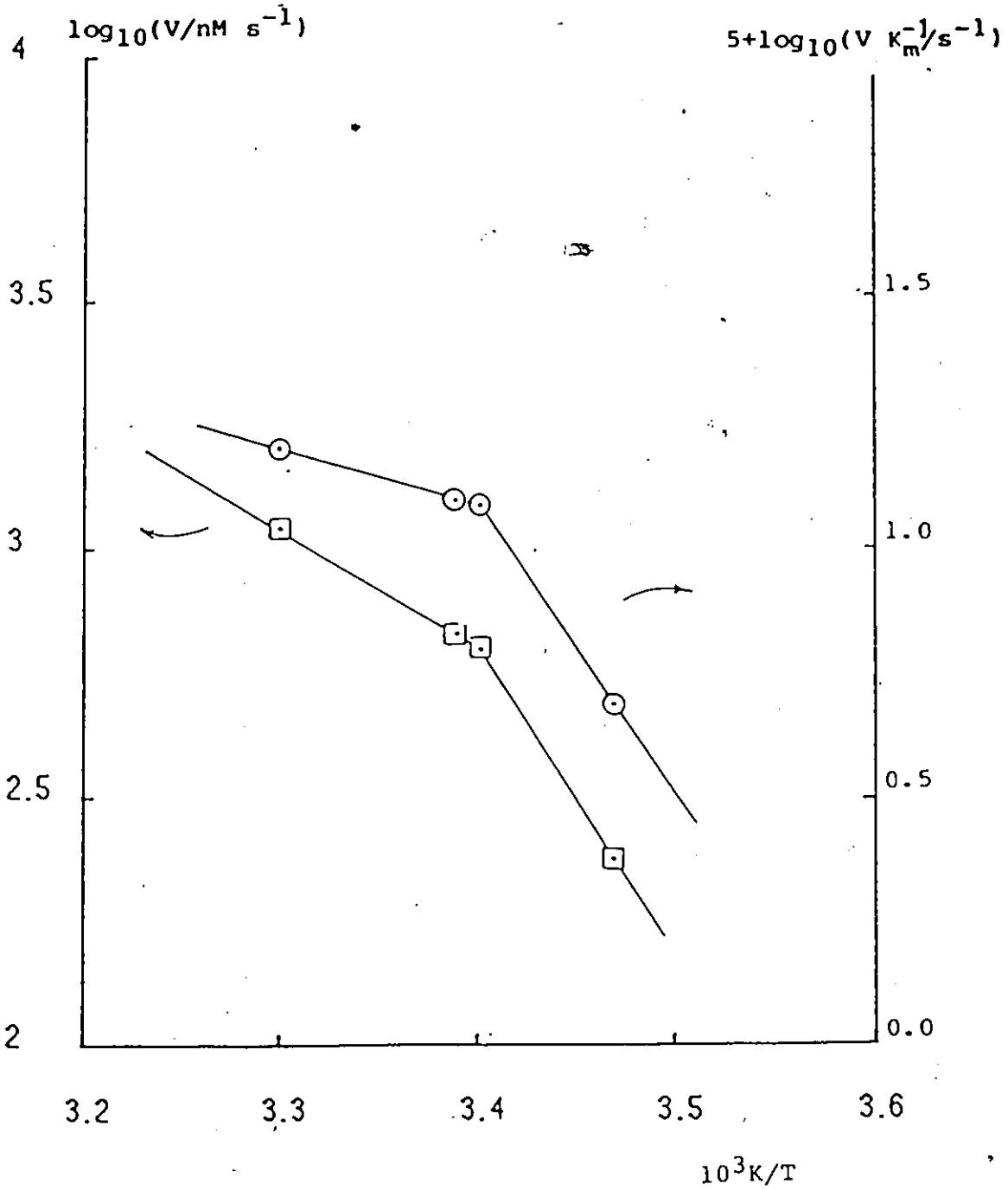

Figure 20(a) pH = 5.00

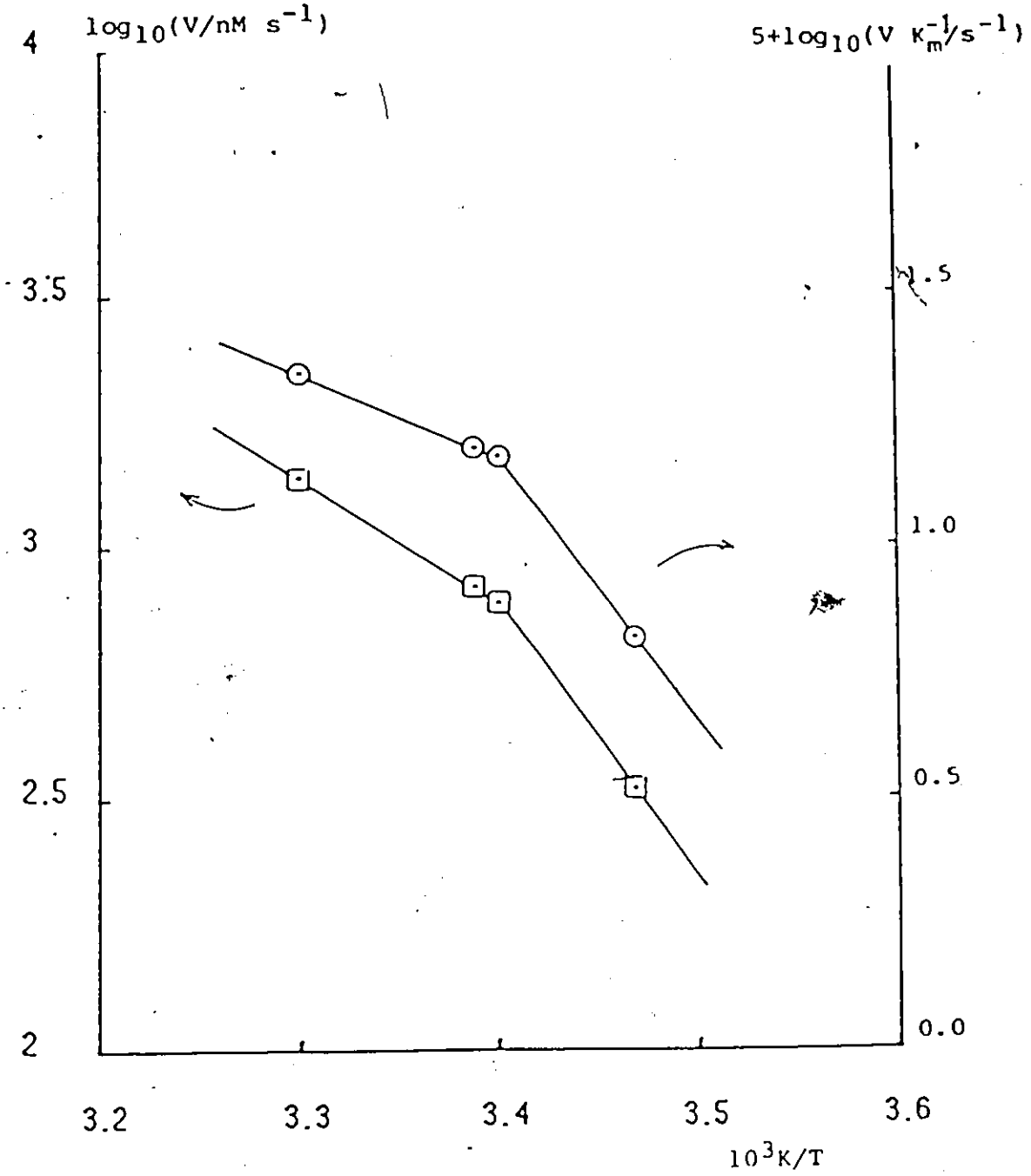

Figure 20(b) pH = 5.22

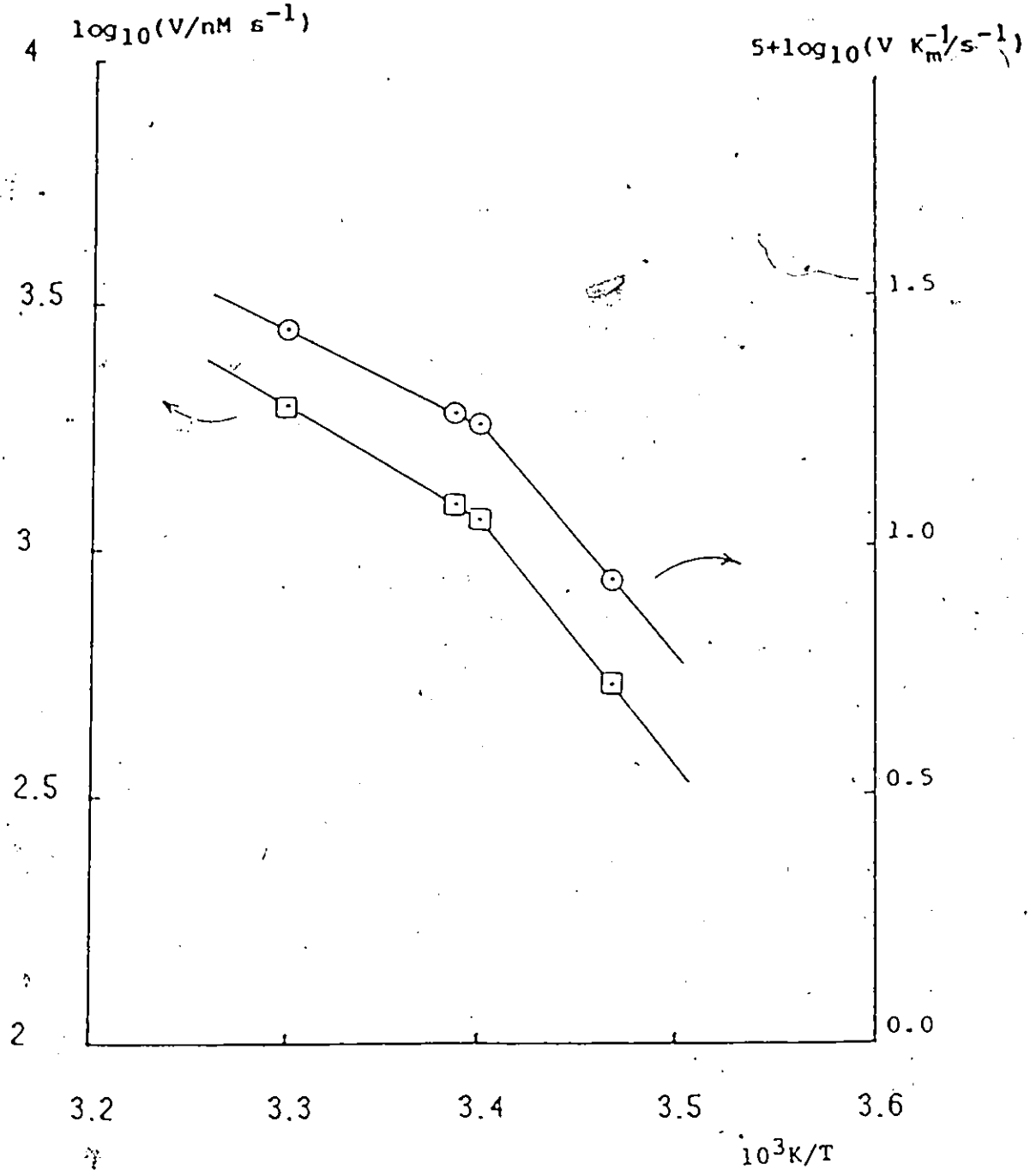

Figure 20(c) pH = 5.50

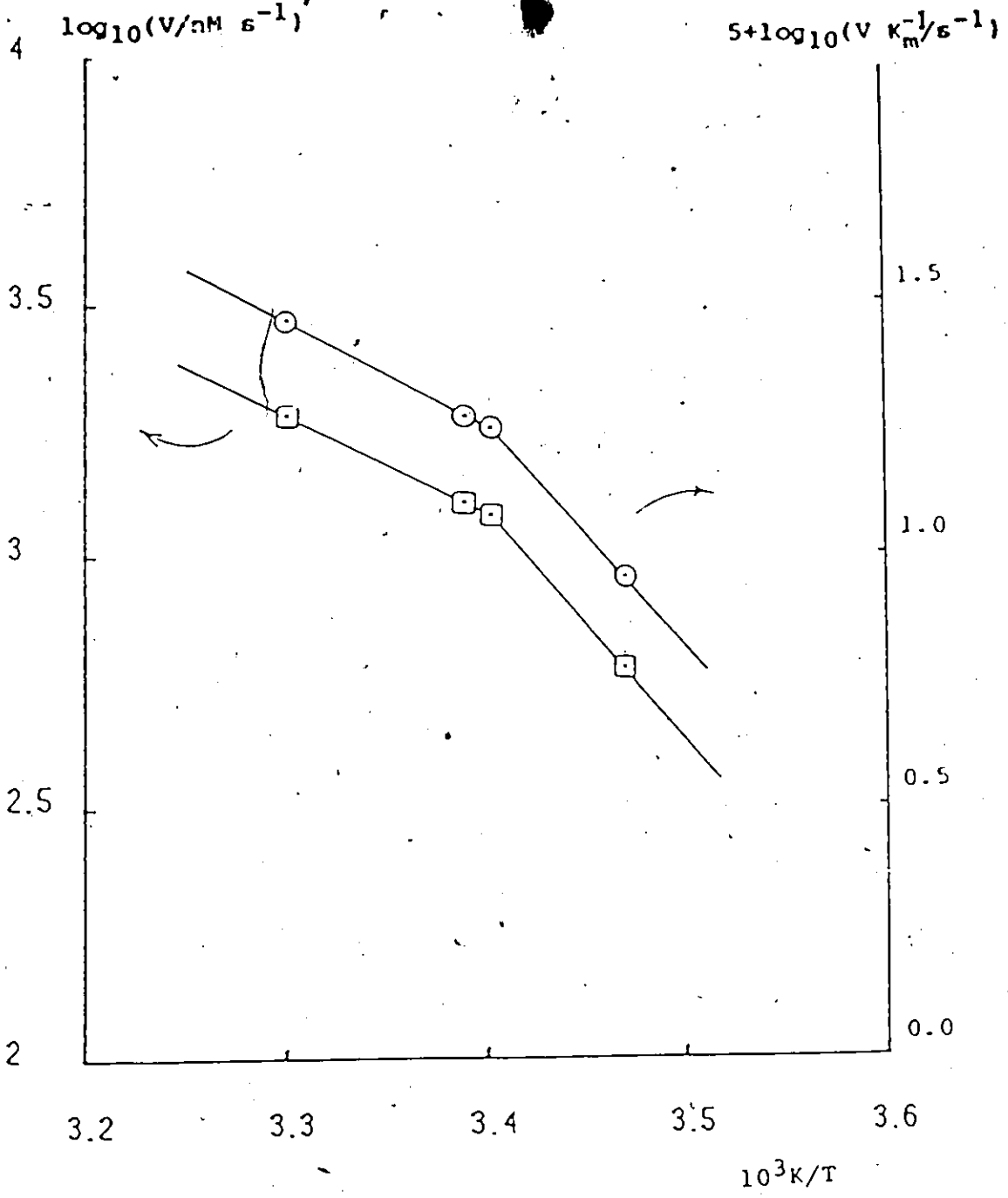

Figure 20(d) pH = 5.56

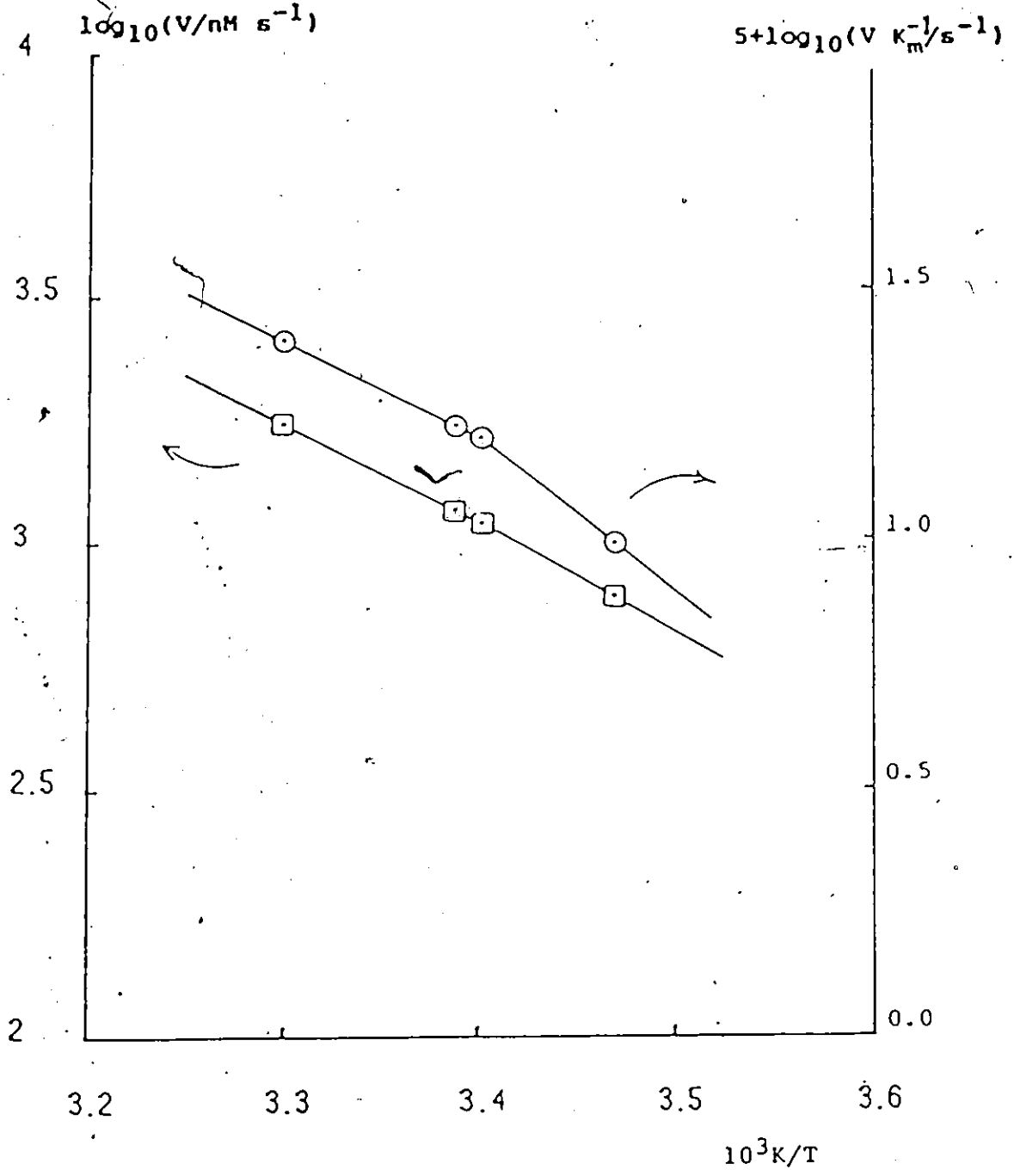

Figure 20(e) pH = 5.76

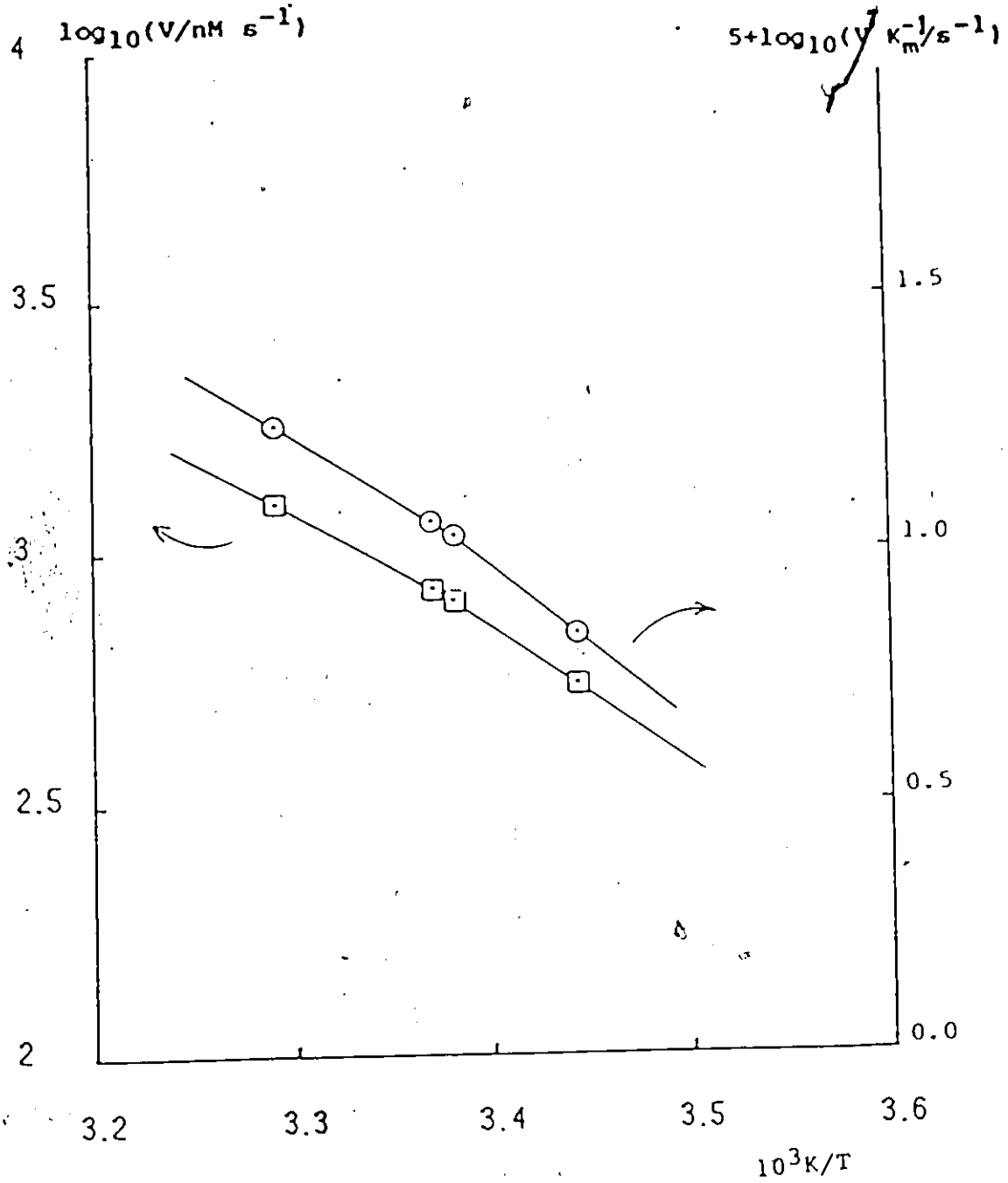

Figure 20(f) pH = 6.19

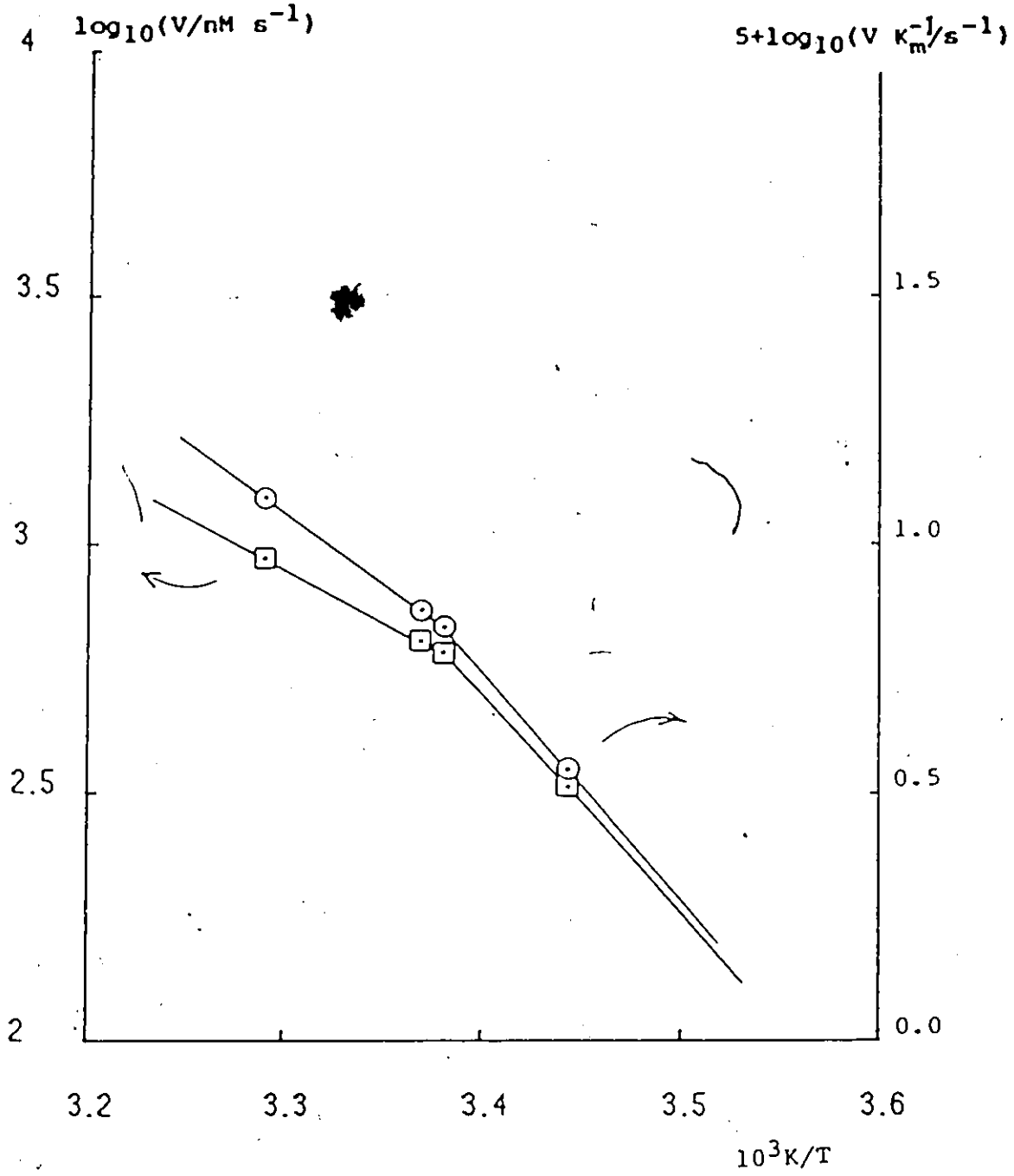

Figure 20(g) pH = 6.19

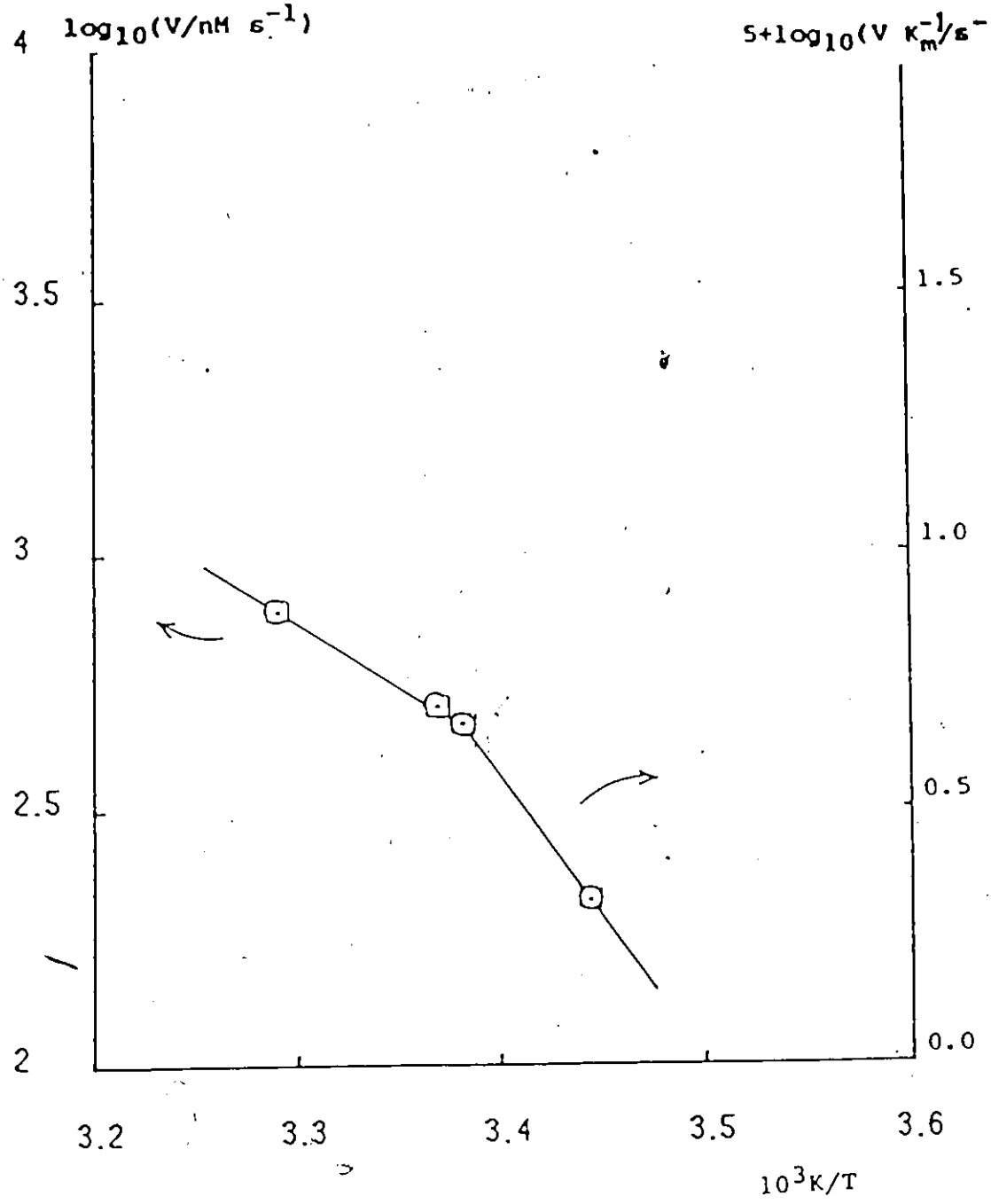

Figure 20(h) pH = 6.91

Table 12.

Activation energies at different pH values
Estimated error $< \pm 6\%$

pH	$E_{c,\ell}$/kJ mol^{-1}	$E_{c,h}$/kJ mol^{-1}	$E_{o,\ell}$/kJ mol^{-1}	$E_{o,h}$/kJ mol^{-1}
5.00	137	54	129	27
5.22	119	55	116	37
5.50	99	50	94	43
5.56	90	44	88	48
5.76	49	44	70	44
6.19	55	42	65	47
6.39	54	39	73	55
6.61	89	42	92	57
6.91	112	48	112	48

The error of $< \pm$ 6% was estimated from the errors in V and V/K_m (Table 7), by determining the largest and smallest slopes that could arise on the basis of these errors.

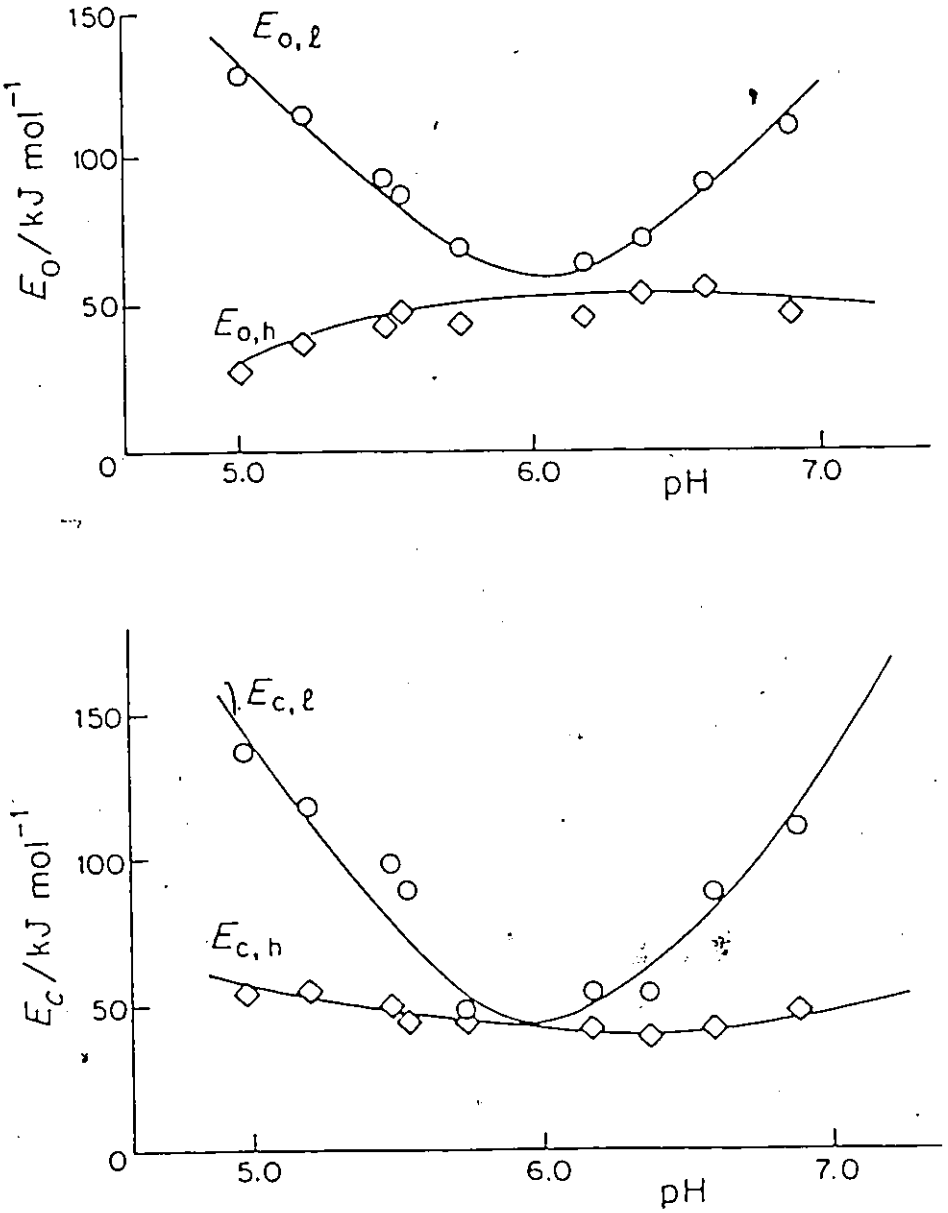

Figure 21. Plots of the activation energies against the pH. The subscript ℓ refers to temperatures below 23°C, and h to those above. The first subscript ○ refers to values obtained from rates when $[s] \ll K_m$; the subscript c relates to $[s] \gg K_m$.

minimum at around pH 6.

Using a molecular weight of 85000 for β-glucosidase (44), entropies of activation $\Delta^{\ddagger}S$ were calculated on the basis of the transition-state equation

$$k = e \frac{\tilde{k}T}{h} e^{\Delta^{\ddagger}S/R} e^{-E/RT} \qquad (29)$$

The values obtained for different pH values are shown in Table 13 and are plotted against pH in Figure 22. Again there is little dependence of $\Delta^{\ddagger}S_{o,h}$ and $\Delta^{\ddagger}S_{c,h}$ on pH, but the $\Delta^{\ddagger}S_{o,\ell}$ and $\Delta^{\ddagger}S_{c,\ell}$ values pass through a minimum at around pH 6.

5.4 Interpretation of Arrhenius behaviour

The existence of the intersection at 23°C in the Arrhenius plots, found at both low and high substrate concentrations, can be explained (65,123) in terms of a mechanism involving a second intermediate:

$$E + S \underset{k_{-1}}{\overset{k_1}{\rightleftharpoons}} ES \xrightarrow{k_2} ES' \xrightarrow{k_3} E + Y + Z$$

Application of the steady-state treatment leads to

$$v = \frac{\frac{k_2 k_3}{k_2 + k_3}[E]_o[S]}{\frac{k_{-1}+k_2}{k_1}\frac{k_3}{k_2+k_3} + [S]} \qquad (5)$$

Table 13.

Entropies of activation at different pH values
Estimated error < 10 J $K^{-1}mol^{-1}$

pH	$\Delta S_{c,R}$ / J $K^{-1}mol^{-1}$	$\Delta S_{c,A}$ / J $K^{-1}mol^{-1}$	$\Delta S_{o,R}$ / J $K^{-1}mol^{-1}$	$\Delta S_{o,A}$ / J $K^{-1}mol^{-1}$
5.00	203.9	-75.5	221	-123.5
5.22	145.4	-70.3	180.1	-87.5
5.50	115.1	-85.6	137.7	-68
5.56	82.5	-105.8	114.3	-50.1
5.76	-89.6	-106.4	23.7	-63.1
6.19	-66.5	-115.6	2.2	-57.5
6.39	-74	-125.9	29 5	-32.5
6.61	43.3	-114.9	91.5	-26.9
6.91	116.6	-98	154.8	-59.8

The error of <10 J K^{-1} mol^{-1} is consistent with the estimated error in the activation energies (Table 12).

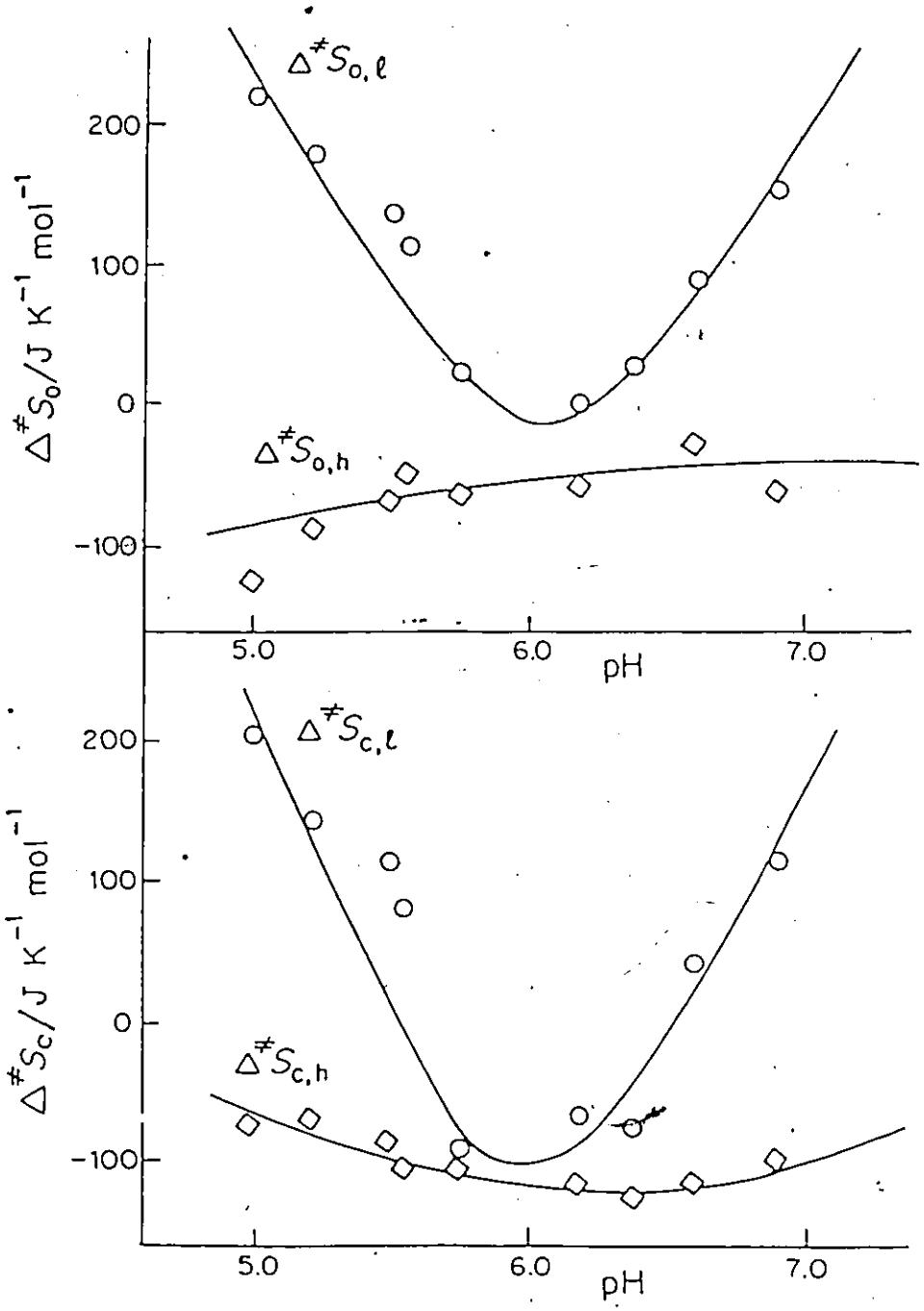

Figure 22. Plots of entropies of activation $\Delta^{\neq}S$ against pH.

where $[E]_o$ is the total enzyme concentration. The rate in the limit of high substrate concentrations is therefore

$$v = \frac{k_2 k_3}{k_2 + k_3}[E]_o \qquad (6)$$

while that at low substrate concentrations is

$$v_0 = \frac{k_1 k_2}{k_{-1} + k_2}[E]_0[S] \qquad (27)$$

The rate coefficient of the overall reaction contains two or three rate constants in these cases.

The experimental activation energy E_a is defined as

$$E_a = RT^2 \frac{d \ln k}{d T}$$

where the k is the rate coefficient of the overall reaction. For the limit of high substrate concentration

$$k = k_c = \frac{k_2 k_3}{k_2 + k_3} \qquad (30)$$

or $$\ln k = \ln k_2 + \ln k_3 - \ln(k_2 + k_3)$$

Therefore,

$$\frac{E_a}{RT^2} = \frac{d \ln k_2}{dT} + \frac{d \ln k_3}{dT} - \frac{d \ln(k_2+k_3)}{dT}$$

$$= \frac{1}{k_2}\frac{d\,k_2}{dT} + \frac{1}{k_3}\frac{d\,k_3}{dT} - \frac{1}{k_2+k_3}\left(\frac{d\,k_2}{dT} + \frac{d\,k_3}{dT}\right)$$

$$= \frac{k_3}{k_2 + k_3}\frac{d\ln k_2}{dT} + \frac{k_2}{k_2 + k_3}\frac{d\ln k_3}{dT}$$

The temperature dependences of the rate constants k_2 and k_3 are given by

$$\frac{d\ln k_2}{dT} = \frac{E_2}{RT^2} \quad \text{and} \quad \frac{d\ln k_3}{dT} = \frac{E_3}{RT^2}$$

Thus

$$E_a = \frac{k_3E_2 + k_2E_3}{k_2 + k_3} \qquad (31)$$

The observed activation energy at any temperature is thus the weighted mean of the values E_2 and E_3, the elementary activation energies, the weighting factors being $k_3/(k_2 + k_3)$ and $k_2/(k_2 + k_3)$ respectively.

Similarly for the limiting rate at low substrate concentration

$$E_a = \frac{k_{-1}(E_1+E_2-E_{-1}) + k_2E_1}{k_{-1} + k_2} \qquad (28)$$

the weighting factors now being $k_{-1}/(k_{-1}+k_2)$ and $k_2/(k_{-1}+k_2)$. The weighting factors vary with temperature; the observed activation energy therefore varies with temperature and the

Arrhenius plot will be curved.

However the variation of activation energy with pH can not be interpreted in terms of equations (28) and (31). A theoretical treatment involving a consideration of both pH and temperature effects on the rates of enzyme-catalyzed reactions was therefore developed and will be discussed in the next chapter.

5.5 Enthalpy-entropy compensation effect

It has been shown that both the activation energy and the entropy of activation in the lower temperature range pass through a minimum at about the optimum pH. The actual rates show a maximum at this pH, and in the case of the results at the lower temperatures this is largely due to the variations in activation energy. However, there is a partly compensating variation in the entropies of activation. Figure 24 shows the plots of entropy of activation against the activation energy.

The plot shows that the enthalpy-entropy compensation effect in the present system is very striking. This is to be attributed (124) to structural effects accompanied by changes in vibrational frequencies and restricted rotations in the enzyme molecules. A pH change that brings about a loosening of the enzyme structure, for example, and which therefore gives an entropy increase, will at the same time produce an enthalpy increase because of the necessity for the breaking of secondary bonds such as hydrogen bonds.

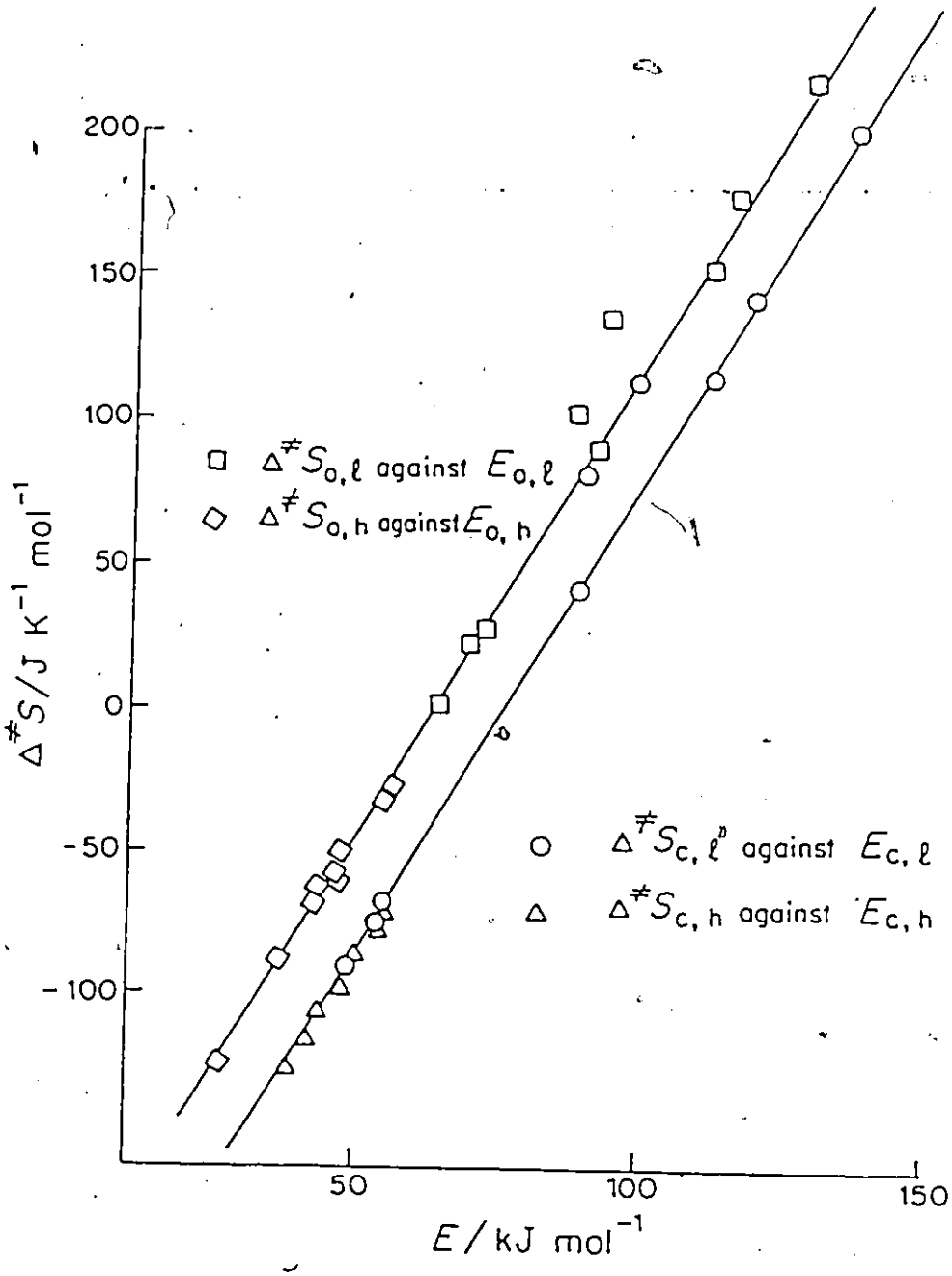

Figure 23. Plots of $\Delta^{\neq}S$ against energy of activation E, for different pH values, showing the compensation effect.

CHAPTER VI

UNIFIED TREATMENT OF pH AND TEMPERATURE EFFECTS ON THE RATES OF ENZYME-CATALYZED REACTIONS

6.1 Introduction

The pH effects and temperature effects on the kinetics of β-glucosidase have been discussed in previous chapters. There have been a number of treatments of the influence of pH on the rates of enzyme reactions, for various mechanisms. Temperature dependence has also been treated for a variety of enzyme systems, including those in which there are two intermediates.

However, these treatments were concerned either with pH or with temperature effects; so far no unified treatment of both effects appears to have been presented. The rate constant of an enzyme reaction is a complex function of temperature, pH and dissociation constants of active groups of the enzyme; as a result the effects of pH and temperature are interrelated. In some situations a proper understanding of the kinetic behaviour of enzyme systems can only be achieved if both effects are considered together. For example, in the present work on β-glucosidase the non-Arrhenius behaviour can be interpreted in terms of a mechanism with two intermediates, but the values of activation energies for individual steps, which were estimated by a successive approximation procedure, vary with pH; the experimental activation energy measured at higher temperatures

showed little pH dependence, but values measured at lower temperatures passed through a minimum. This behaviour can not be satisfactorily interpreted without considering pH and temperature together.

Cooperative effects of both pH and temperature were therefore considered and a unified treatment of both effects was developed Equations were obtained which indicate how the apparent activation energy varies with pH and temperature, for one-intermediate and two-intermediate mechanisms. This chapter describes this new treatment and its application to the results on β-glucosidase. The unified treatment will first be discussed with reference to the one-intermediate mechanism; then a similar treatment will be applied to the two-intermediate mechanism.

6.2 One-intermediate mechanism

The simplest single-intermediate mechanism which accounts for pH dependence may be written as

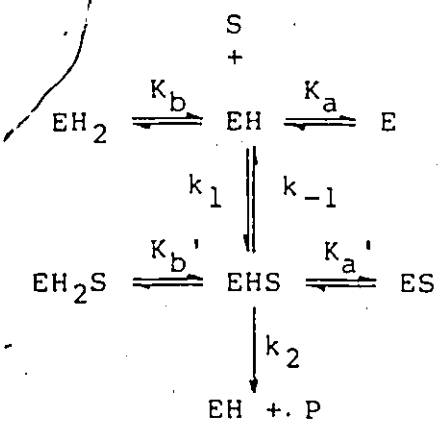

Here EH_2, EH, and E are three ionizing forms of the free enzyme

and EH_2S, EHS and ES are three forms of the enzyme-substrate complex; the K's are the acid dissociation constants. The steady-state rate is

$$v = \frac{k_2[E]_o[S]}{K_m\left(\frac{[H^+]}{K_b} + 1 + \frac{K_a}{[H^+]}\right) + [S]\left(\frac{[H^+]}{K_b'} + 1 + \frac{K_a'}{[H^+]}\right)} \qquad (11)$$

where $K_m = \frac{k_{-1}+k_2}{k_1}$ and $[E]_o$ is the total enzyme concentration.

High substrate concentrations

For limiting high substrate concentrations the rate, designated as V , becomes

$$V = \frac{k_2[E]_o}{\frac{[H^+]}{K_b'} + 1 + \frac{K_a'}{[H^+]}} \qquad (16)$$

The temperature dependence of k_2 can be expressed by the Arrhenius equation

$$k_2 = A_2 e^{-E_2/RT} \qquad (26)$$

where the activation energy E_2 relates to the reaction of the

enzyme-substrate addition complex. Similarly the temperature dependences of the equilibrium constants K_a' and K_b' may be expressed by the van't Hoff equations

$$K_a' = e^{\triangle S_a'/R} \cdot e^{-\triangle H_a'/RT} = B_a' e^{-\triangle H_a'/RT}$$

and

$$K_b' = e^{\triangle S_b'/R} \cdot e^{-\triangle H_b'/RT} = B_b' e^{-\triangle H_b'/RT}$$

The entropy changes $\triangle S$ and the enthalpy changes $\triangle H$ can be treated as constant within a fairly small temperature range, although in aqueous systems there are significant variations over a wider range, as a result of changes in the structure of water. Whereas E_2 is necessarily a positive quantity, the enthalpy changes $\triangle H_a'$ and $\triangle H_b'$ may be positive or negative; details are considered later.

Dependence of apparent activation energy on pH

A general expression for the variation of activation energy with pH may be obtained as follows. The apparent activation energy E_{app} at any temperature is defined by the equation

$$\frac{d \ln v}{dT} = \frac{E_{app}}{RT^2} \quad , \qquad (32)$$

Differentiation of the logarithmic form of eq. (16) leads to

$$\frac{d \ln V}{dT} = \frac{d \ln k_2}{dT} + \frac{\frac{[H^+]}{k_b'} \frac{d \ln K_b'}{dT} - \frac{K_a'}{[H^+]} \frac{d \ln K_a'}{dT}}{\frac{[H^+]}{K_b'} + 1 + \frac{K_a'}{[H^+]}}$$

The apparent activation energy $E_{c,app}$ under these conditions is thus

$$E_{c,app} = E_2 + \frac{\frac{[H^+]}{K_b'} \Delta H_b' - \frac{K_a'}{[H^+]} \Delta H_a'}{\frac{[H^+]}{K_b'} + 1 + \frac{K_a'}{[H^+]}} \qquad (33)$$

It follows that the apparent activation energy is pH dependent. At sufficiently high pH values the term $K_a'/[H^+]$ predominates in the second term of equation (33); the activation energy is thus $E_2 - \Delta H_a'$. At very low pH values, on the other hand, the term $[H^+]/K_b'$ predominates, and the apparent activation energy then approaches $E_2 + \Delta H_b'$. At intermediate pH values the term unity may predominate, and the apparent activation energy is then close to E_2.

Since $\Delta H_b'$ and $\Delta H_a'$ may be either positive or negative, there are four different patterns of behaviour of the apparent activation energy as the pH is varied. These four patterns are illustrated in Fig. 24. The firm lines show the variations to be expected when activation energies are measured at intermediate temperatures and the value at a given temperature is plotted

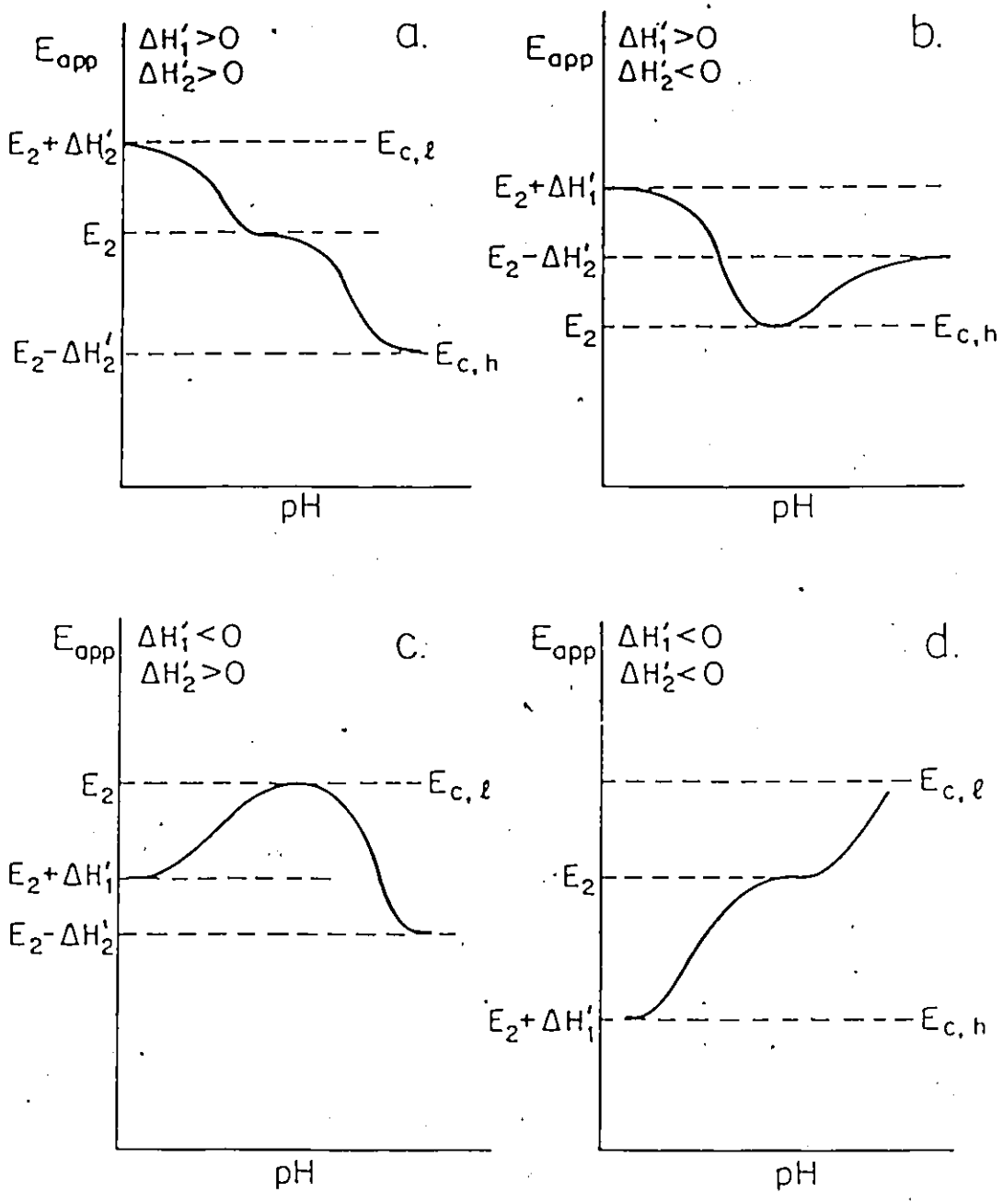

Figure 24. The theoretical variations of apparent activation energy with pH, for various sign combinations of the thermodynamic parameters for the acid dissociation constants. These curves relate to the activation energies in the limit of high substrate concentrations. Similar variations are obtained in the limit of low substrate concentrations, but E_2 is replaced by E_0 (defined by eq.(28)) and the primes are dropped from enthalpy changes, which now relate to the free enzyme.

against the pH. If, on the other hand, activation energies are measured at very high or very low temperatures, within an intermediate pH range, certain terms in eq.(33) will predominate and the activation energy will show little dependence on pH. The dashed horizontal lines in Fig. 24, designated $E_{c,h}$ (at high temperature) and $E_{c,\ell}$ (at low temperatures), show the expressions to which these apparent activation energies correspond.

Non-linear Arrhenius behaviour

It follows from eqs.(11) and (33) that non-linear Arrhenius plots are in general to be expected, as a result of the pH-dependent terms. At very low or very high pH values, the Arrhenius plots may be fairly linear, provided that the ΔH values themselves do not vary greatly with temperature. However in certain pH ranges there may be significant non-linearity in Arrhenius plots as a result of the effect of temperature itself on the relative magnitudes of the terms in the denominator of eq.(33). This will first be illustrated for the case in which $\Delta H_b'$ is positive and $\Delta H_a'$ is negative, this case being chosen since it applies to the β-glucosidase system, to be considered in detail in the next section.

In the higher pH range the term $1+K_a'/[H^+]$ is more important than $[H^+]/K_b'$, and if the pH is not too high the terms unity and $K_a'/[H^+]$ will be of comparable importance; moreover their relative importance changes with the temperature. If $\Delta H_a'$ is negative the term $K_a'/[H^+]$ decreases with increasing temperature, and at

sufficiently high temperatures the term unity predominates in the denominator of eq.(33); the activation energy therefore approaches E_2. At lower temperatures the term $K'_a/[H^+]$ is of greater importance, and the activation energy approaches $E_2-\Delta H'_a$; since $\Delta H'_a$ is negative this is greater than E_2. The Arrhenius plotes is therefore concave to the axes, as shown schematically in Figure 25.

Concave Arrhenius plots are in fact expected whatever the sign of the ΔH values. For example, if the higher pH range is considered and $\Delta H'_a$ is positive, the term $K'_a/[H^+]$ predominates at higher temperatures and the activation energy approaches $E_2-\Delta H'_a$, which is lower than E_2, the limiting value at the lower temperatures. Similar conclusions apply to the lower pH range, where it is the relative importance of unity and $[H^+]/K'_b$ that is significant. At high temperatures the activation energy approaches E_2, and at lower temperatures it approaches $E_2+\Delta H'_b$. The various possibilities are summarized in Figure 25 .

Although these concave Arrhenius plots are continuous, they often have the appearance of consisting of two intersecting straight lines, especially if there is a substantial difference between the two limiting activation energies. The dashed lines in Figure 25 correspond to the limiting slopes at high and low temperatures, and these intersect at what will be referred to as an intersection. In the high pH range these lines correspond to k_2 and to $[H^+]k_2/K'_a$ respectively, and the lines therefore intersect at a 1/T value at which $[H^+] = K'_a$. Similarly in the

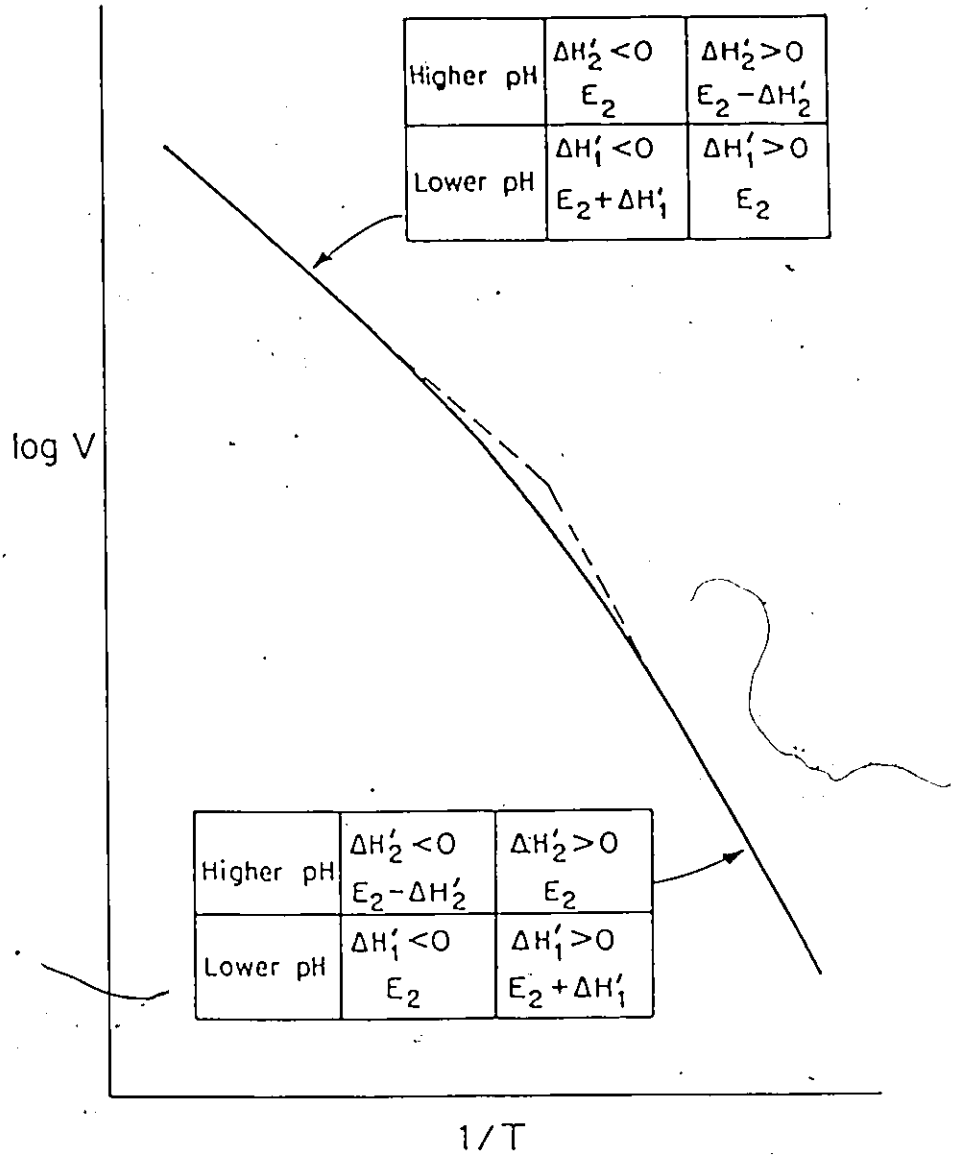

Figure 25. A schematic concave Arrhenius plot, arising from pH dependent terms in the rate equation. The conditions indicated apply to the limit of high substrate concentrations. In the limit of low substrate concentration E_2 is replaced by E_0 (defined by eq.(28)), and the primes are dropped from the enthalpy changes.

lower pH range the intersection corresponds to $[H^+] = K_b'$.

Low substrate concentrations

The situation is somewhate analogous but more complicated in the limit of very low substrate concentrations. The rate expression is now

$$v_o = \frac{k_2[E]_o[S]}{K_m(1 + \frac{K_a}{[H^+]} + \frac{[H^+]}{K_b})} \qquad (34)$$

There is the additional complication that K_m is composite and may itself give rise to non-Arrhenius behaviour, as discussed in the previous chapter . For the single-intermediate mechanism $K_m = (k_{-1} + k_2)/k_1$, and therefore k_2/K_m is $k_1k_2/(k_{-1}+k_2)$. As long as the temperature dependences of k_{-1} and k_2 are different, this also gives rise to concave Arrhenius plots. It has been shown that in general the activation energy is

$$E_o = \frac{k_{-1}(E_1+E_2-E_{-1}) + k_2E_1}{k_{-1} + k_2} \qquad (28)$$

If k_{-1} has a stronger temperature dependence than k_2 the activation energy will range from $E_1+E_2-E_{-1}$ at high temperatures to E_1 at low temperatures; conversely, it will be E_1 at high temperatures and $E_1+E_2-E_{-1}$ at low. In either case the Arrhenius plot is concave. There may again be the appearence of two intersecting straight lines in the Arrehenius plot, the point of

intersection corresponding to the temperature at which $k_{-1} = k_2$.

Even if this effect is insignificant, concave behaviour may still be obtained because of the pH-dependent term in eq.(34). The argument is much the same as for the high substrate concentration case (Figure 24); however, the rate and E_{app} are now

$$v_o = \frac{k_2 k_1 [E]_o [S]}{(k_{-1}+k_2)\left(1 + \frac{K_a}{[H^+]} + \frac{[H^+]}{K_b}\right)}$$

$$E_{app} = E_o + \frac{\frac{[H^+]}{K_b}\Delta H_b - \frac{K_a}{[H^+]}\Delta H_a}{\frac{[H^+]}{K_b} + 1 + \frac{K_a}{[H^+]}}$$

Thus, k_2 is replaced by $k_1k_2/(k_{-1}+k_2)$ and E_2 by E_o as defined in eq.(28), and the dissociation constants that are involved are K_b and K_a, relating to the free enzyme.

6.3 Two enzyme-substrate intermediates

For two enzyme-substrate intermediate systems, similar principles apply, but the relationships are considerably more complex and could not readily be applied to experimental results, except for some limiting cases, which will be considered.

The simplest mechanism involving two intermediates is

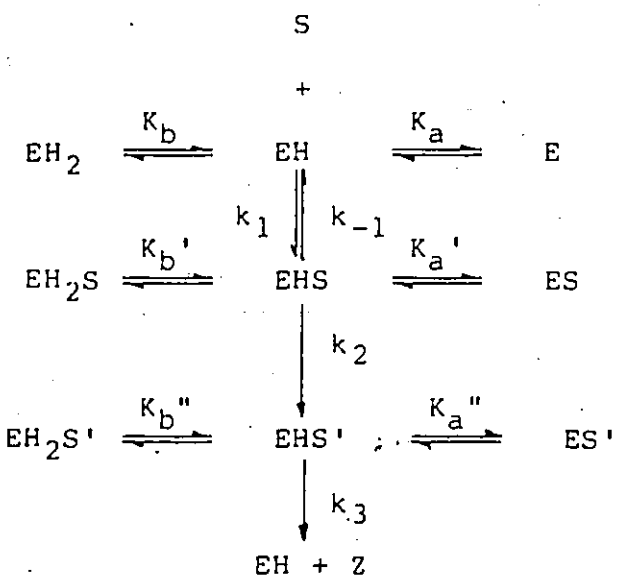

In the limit of high substrate concentrations the steady-state rate is

$$V_m = \frac{k_2 k_3 [E]_o}{k_2\left(\frac{[H^+]}{K_b''} + 1 + \frac{K_a''}{[H^+]}\right) + k_3\left(\frac{[H^+]}{K_b'} + 1 + \frac{K_a'}{[H^+]}\right)} \qquad (35)$$

Use of eq.(32) leads to

$$E_{app} = \frac{k_3 E_2 f' + k_2 E_3 f'' + [H^+]\left(\frac{k_2 \Delta H_b''}{K_b''} + \frac{k_3 \Delta H_b'}{K_b'}\right) - \frac{1}{[H^+]}\left(k_2 K_a'' \Delta H_a'' + k_3 K_a' \Delta H_a'\right)}{k_3 f' + k_2 f''} \qquad (36)$$

where f' and f" are the pH-dependent functions:

$$f' = \frac{[H^+]}{K_b'} + 1 + \frac{K_a'}{[H^+]} \quad \text{and} \quad f'' = \frac{[H^+]}{K_b''} + 1 + \frac{K_a''}{[H^+]} \qquad (37)$$

Equation (36) reduces to eq.(33) in the event that $k_3 \gg k_2$. In

the special case that the two intermediates ionize in the same way, i.e. $K_b' = K_b''$, $K_a' = K_a''$, $\Delta H_b' = \Delta H_b''$ and $\Delta H_a' = \Delta H_a''$, equation(36) reduces to

$$E_{app} = \frac{k_3E_2+k_2E_3}{k_2 + k_3} + \frac{\frac{[H^+]\Delta H_b'}{K_b'} - \frac{K_a'\Delta H_a'}{[H^+]}}{\frac{[H^+]}{K_b'} + 1 + \frac{K_a'}{[H^+]}} \qquad (38)$$

At intermediate pH values the first term will predominate, especially if the pH profile has a flat maximum. At extreme pH values there will be more contribution from the second, pH-dependent, term.

6.4 Application to β-glucosidase

The non-Arrhenius behaviour and the variation of activation energy with pH obtained with β-glucosidase can be satisfactorily interpreted in terms of the theory that has been outlined.

The one intermediate mechanism

We consider first the dependence on pH of activation energies $E_{c,h}$, $E_{c,\ell}$, corresponding to high substrate concentrations, and discuss them with reference to the single-intermediate mechanism.

For this system $\Delta H_b'$ is positive and $\Delta H_a'$ is negative (Table 9), so that the predicted pattern for the results at high substrate concentrations is that shown in Figure 24(b). The

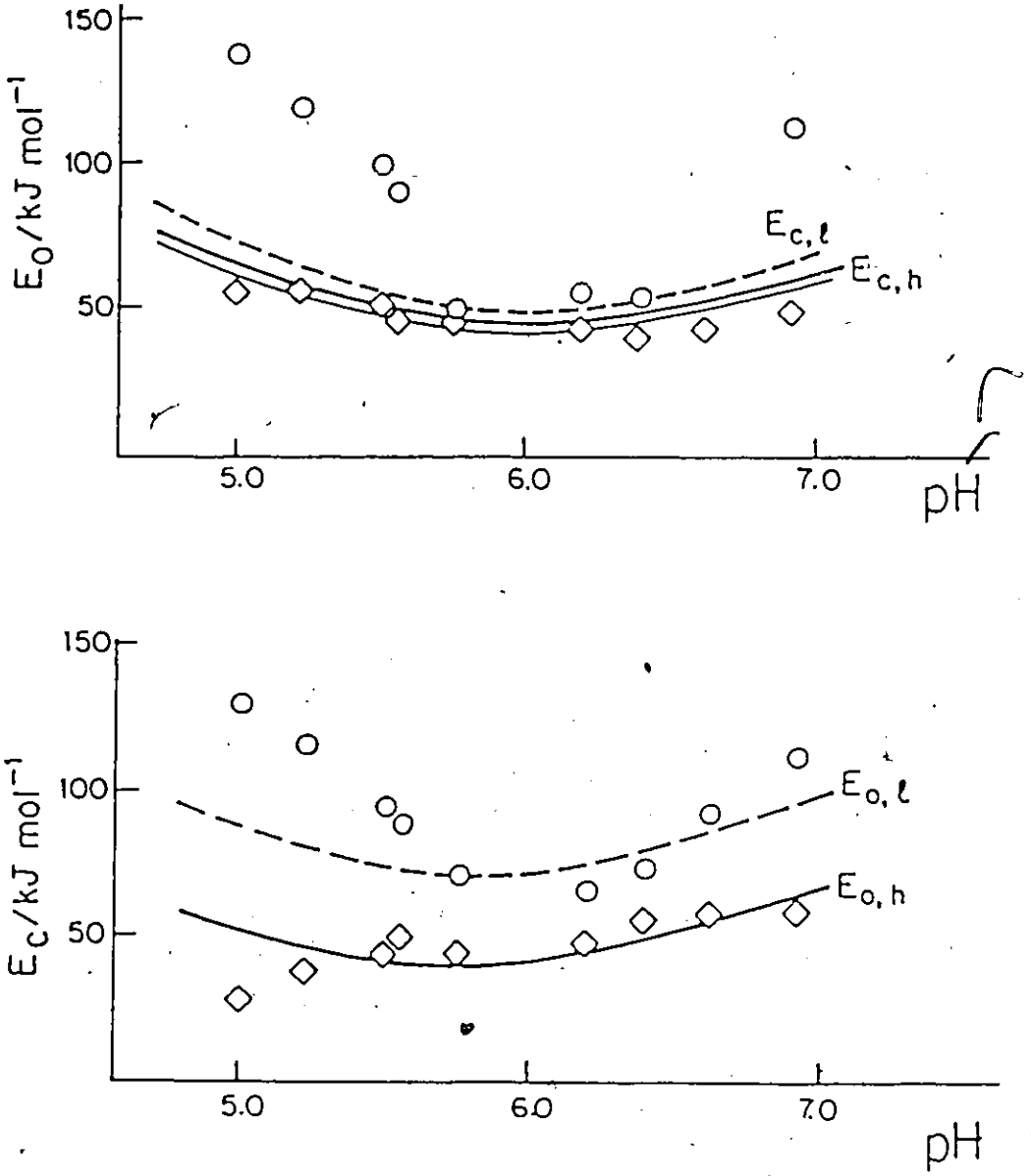

Figure 26. Plots of activation energies against pH.
(a) Results at high substrate concentrations.
◇, experimental values at higher temperatures($E_{c,h}$); the firm line shows the theoretical prediction, based on the one-intermediate mechanism.
○, experimental values at low temperatures($E_{c,l}$); the dashed line shows the theoretical prediction.
(b). Results at low substrate concentrations.
◇, $E_{o,h}$ values; the firm line gives the theoretical prediction.
○, $E_{o,l}$ values; the dashed line gives the theoretical prediction.

values of $E_{c,h}$ obtained at high temperatures are expected to show little variation with pH, and this is confirmed by the experimental results plotted in Figure 26. The values $E_{c,\ell}$, on the other hand, are expected to pass through a minimum corresponding to $E_{c,h}'$, and the results again show this behaviour. The experimental results are thus in qualitative agreement with the theoretical treatment.

Good quantitative agreement could not, however, be obtained on the basis of the single intermediate assumption. The calculations were based on E_2 = 31 kJ mol^{-1}, which was deduced from the fit of the theoretical values of $E_{c,\ell}$ and $E_{c,h}'$ to the experimental data. The prediction of the variation of $E_{c,h}$ with pH was made using eq.(33) with the following values of the dissociation constants at 25°C:

$$K_b'(25^oC) = 7.9X10^{-6} \text{ mol dm}^{-3}$$
$$K_a'(25^oC) = 3.0X10^{-7} \text{ mol dm}^{-3}$$

these being the values deduced from the parameters in Table 9. The firm line in Figure 26a shows the variation of $E_{c,h}$ deduced on this basis, and it passes reasonably close to the experimental points. For the $E_{c,\ell}$ values the theory (see Figure 24b) predicts that they should vary from $E_2 + \Delta H_b' \approx E_2 + 60.8$ kJ mol^{-1} at low pH values to $E_2 - \Delta H_a' = E_2 + 35.5$ kJ mol^{-1} at high values, passing at intermediate values through a minimum close to E_2. Caluclations were made based on the following values:

$K_b'(18^oC) = 5.0X10^{-6}$ mol dm^{-3}

$K_a'(18^oC) = 5.0X10^{-7}$ mol dm^{-3}

The dashed line in Figure 26 shows the minimum, but the curve is much too shallow compared with the experimental points.

The same pattern is expected in the limit of low substrate conentrations, and Figure 26b shows the corresponding analysis, based on the single-intermediate mechanism for the results. The agreement is reasonably good for $E_{o,h}$, but again the predicted curve for $E_{o,\ell}$ is much too shallow.

The fact that the results, although following the predicted pattern, deviate from the theoretical values based on the single-intermediate mechanism shows that the simple mechanism is inadequate for this particular reaction.

The same conclusion was also obtained from attempts to interpret the non-linear Arrhenius behaviour in terms of the single-intermediate mechanism. Figure 27 shows the Arrhenius plots at pH 6.4, the points being the experimental ones obtained in the limit of high substrate concentrations.

The dashed curve was obtained on the basis of the single intermediate mechanism, use being made of equation (16). The values of K_a' and K_b' for different temperatures were calculated using the $\Delta H_b'$ and $\Delta H_a'$ values in Table 9. The activation energy E_2 used in these calculations was 31 kJ mol^{-1}, which was obtained from the fit to the experimental data of theoretical calculations of E_{app}. The calculated values of v do give a

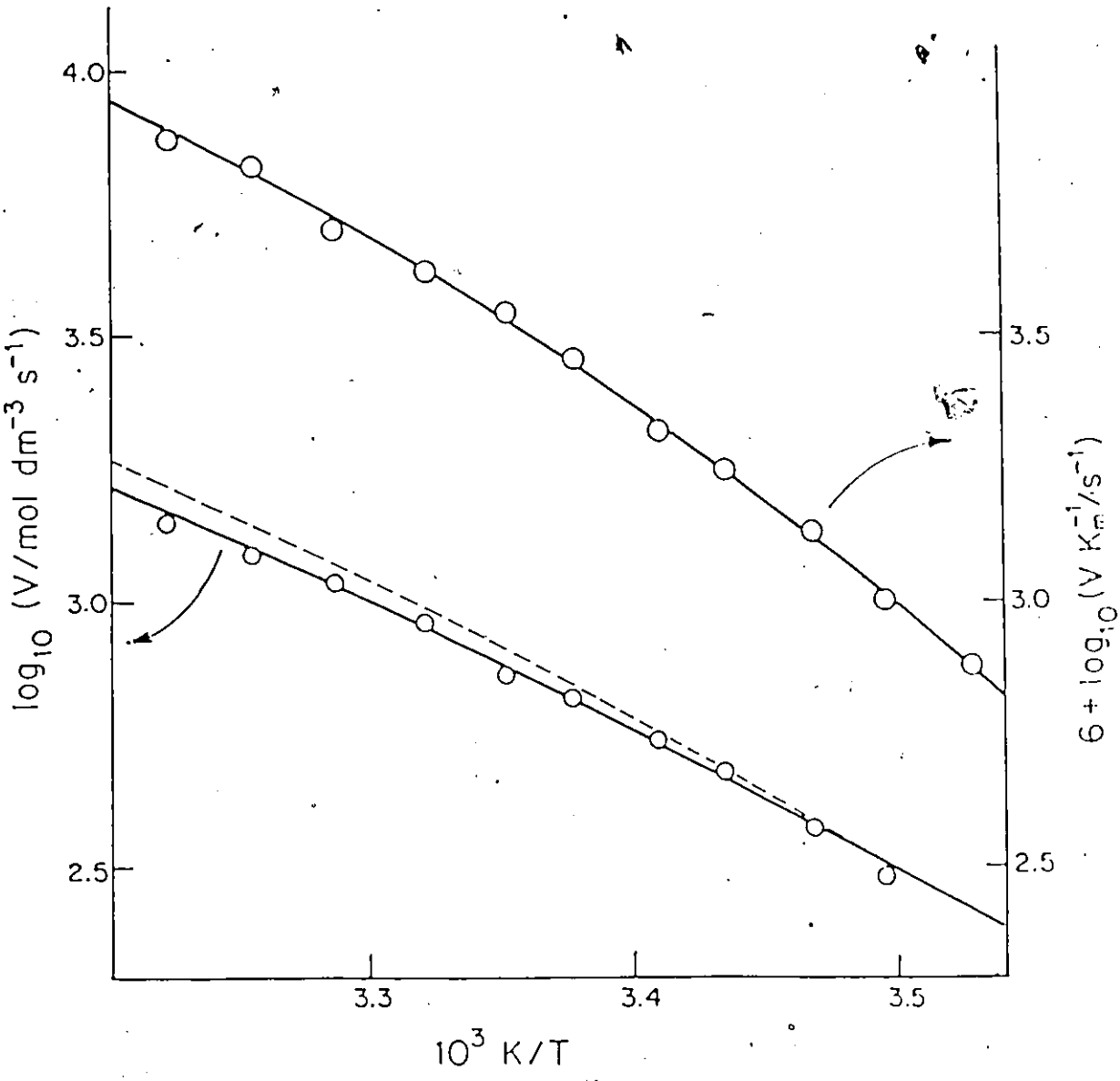

Figure 27. Arrhenius plots of $\log_{10}V$ and $\log_{10}(V/K_m)$ against 1/T. The dashed line shows the estimate based on the one-intermediate mechanism. The firm lines are based on the two intermediate mechanism, including the pH-dependent factors.

concave Arrhenius plot, with an intersection at 23°C rather than at 25°C. However, the slopes at both high and low temperatures differ significantly from those found experimentally.

This lack of agreement confirms the conclusion from the pH-dependent activation energies that the single-intermediate mechanism is inadequate. We therefore attempted a fit of the data in which both the pH-dependent terms and the two rate constants k_2 and k_3 are taken into account, i.e., in which use is made of eq.(35)—(38).

The two-intermediate mechanism

It did not prove possible in the present investigation to determine the four ionization constants K_a', K_b', K_a'' and K_b'' and the corresponding ΔH values; to do so would require stopped-flow measurements to be made, and the available analytical techniques for following the reaction (involving the case of a subsidiary reaction that is not extremely rapid) do not make this feasible. It was therefore necessary to make the assumption that $\Delta H_b' = \Delta H_b''$ and $\Delta H_a' = \Delta H_a''$, in other words to use the equation

$$v = \frac{k_2 k_3 [E]_o}{(k_2+k_3)\left(\frac{[H^+]}{K_b'} + 1 + \frac{K_a'}{[H^+]}\right)} \qquad (39)$$

which is the reduced from of eq.(35) for this special case. As previously noted, this equation leads to eq.(38) for the apparent

activation energy.

The curve fitting was done by a successive approximation method. In order for there to be an intersection at 23.0°C (=296.15°K), it follows that $k_2=k_3$ at this temperature ($k_2=A_2e^{-E_2/RT}$; $k_3=A_3e^{-E_3/RT}$), so that

$$\frac{A_2}{A_3} = e^{-(E_3-E_2)/R\cdot 296.15}; \qquad (40)$$

By a procedure of successive approximations with the use of equations (39) and (40), the two activation energies 20.5 kJ mol^{-1} and 38.5 kJ mol^{-1} are found to give excellent agreement with the results for this particular case; the line drawn in Figure 27 in fact corresponds to these values.

Since equation (39) is symmetrical in k_2 and k_3, as far as this analysis alone is concerned it is immaterial which reaction has the higher activation energy. One possibility is

$$E_2 = 38.5 \text{ kJ mol}^{-1}; \quad E_3 = 20.5 \text{ kJ mol}^{-1}$$

The actual values of preexponential factors A_2 and A_3 may be obtained by making use of the fact that $k_2 = k_3$ at 23°C, so that, from eq.(39),

$$V = \frac{k_2[E]_o}{2\left(\frac{[H^+]}{K_b'} + 1 + \frac{K_a'}{[H^+]}\right)} = \frac{k_3[E]_o}{2\left(\frac{[H^+]}{K_b'} + 1 + \frac{K_a'}{[H^+]}\right)} \qquad (41)$$

The use of the value of V measured at 23°C, and the known concentration of enzyme solution $(E)_o$, with the value E_2 or E_3 and K_b', K_a', then gives

$$A_2 = 1.49\times10^7\ s^{-1}; \quad A_3 = 9.93\times10^3\ s^{-1}$$

The analysis of the rates at low substrate concentration proceeds similarly. A successive approximation procedure now led to

$$E_1 = 22.5\ kJ\ mol^{-1}; \quad E_1 + E_2 - E_{-1} = 49.0\ kJ\ mol^{-1}$$

Use of the E_2 value obtained previously then gave

$$E_{-1} = 12.0\ kJ\ mol^{-1}$$

The upper curve of $\log V/K_m$ against $1/T$ shown in Figure27 is plotted on the basis of these values, and is seen to pass very well through the experimental points.

The preexponential factors were again calculated from the rate at the intersection. In this case, at the intersection temperature

$$\therefore\ k_1 = \frac{k_1k_2}{k_{-1}} \qquad \text{or} \qquad k_2 = k_{-1}$$

so that from the equation

$$\frac{V}{K_m} = \frac{k_1k_2(E)_o}{(k_{-1}+k_2)\left(1 + \frac{K_a}{[H^+]} + \frac{[H^+]}{K_b}\right)}$$

we can obtain the following equation:

$$\frac{V}{K_m} = \frac{k_1 [E]_o}{2\left(1 + \frac{K_a}{[H^+]} + \frac{[H^+]}{K_b}\right)} \qquad (42)$$

Use of the value of V/K_m at 23°C gives

$$A_1 = 4.02 \times 10^6 \text{ dm}^3\text{mol}^{-1}\text{s}^{-1}; \quad A_{-1} = 3.14 \times 10^2 \text{ s}^{-1}$$

This procedure then gives the rate constant for individual steps as follows:

$$k_1 = 4.02 \times 10^6 e^{-22500/RT} \qquad k_{-1} = 3.14 \times 10^2 e^{-12000/RT}$$

$$k_2 = 1.49 \times 10^7 e^{-38500/RT} \qquad k_3 = 9.93 \times 10^3 e^{-20500/RT}$$

The two-intermediate mechanism provides a better fit than that based on the one-intermediate assumption, especially at the higher temperatures. The small deviations observed in the lower temperature range may result from inadequacy of the assumption that the dissociation parameters are the same for the two intermediates.

Unfortunately, for the dependence of E_{app} on pH a satisfactory quantitative treatment is now impossible because of our ignorance of the individual temperature dependences of the dissociation constants for the two intermediates. For a treatment of the non-Arrhenius behaviour (Figure 27) the assumption that the temperature dependences are the same for the two intermediates does not introduce a serious error. For the

treatment of pH dependence, however, the use of eq.(38) involves a much greater approximation, since the first term in that expression should really be $(k_3f'E_2 + k_2f"E_3)/(k_3f' + k_2f")$, which itself shows considerable pH dependence. When the approximate eq.(38) is used the only pH dependence included is that from the second term, and an important contribution has been neglected. In fact, the pH dependence predicted by eq.(38) is exactly the same as that predicted by the one-intermediate equation(33).

The unified treatment of both pH and temperature effects has provided a satisfactory semi-quantitative interpretation for the variation of activation energy with pH for β-glucosidase system. For a quantitative agreement with experiment, more detailed studies are necessary to determine separately the values of K_b', $K_b"$, K_a' and $K_a"$; this requires the use of transient-kinetic techniques.

6.5 Construction of entropy and enthalpy profiles

From the values of preexponential factors obtained from this analysis, the entropies of activation for individual steps were calculated. In addition, the enthalpies of activation and Gibbs energies of activation were also obtained on the basis of the following equations:

$$\Delta^{\ddagger}H = E - RT \qquad \Delta^{\ddagger}G = \Delta^{\ddagger}H - T\Delta^{\ddagger}S$$

These values with the kinetic parameters are summarized in Table 14, and are presented in Figure 28 as reaction profiles.

Table 14.

Kinetic parameters obtained from analysis of the temperature dependence

(pH 6.4)

Reaction	pre-exponential factor	Activation energy, E $kJ\ mol^{-1}$	$\Delta^{\ddagger}G(23^{o}C)$ $kJ\ mol^{-1}$	$\Delta^{\ddagger}S$ $J\ K^{-1}mol^{-1}$	$\Delta^{\ddagger}H$ $kJ\ mol^{-1}$
(1)E+S→ES	$4.02X10^{6}$ $dm^{3}mol^{-1}s^{-1}$	22.5	57.6	-127	20.0
(-1)ES→E+S	$3.14X10^{2}\ s^{-1}$	12	70.4	-205	9.5
(2)ES→ES'	$1.49X10^{7}\ s^{-1}$	38.5	70.3	-116	36.0
(3)ES'→E+Y+Z	$9.93X10^{3}\ s^{-1}$	20.5	70.3	-177	18.0

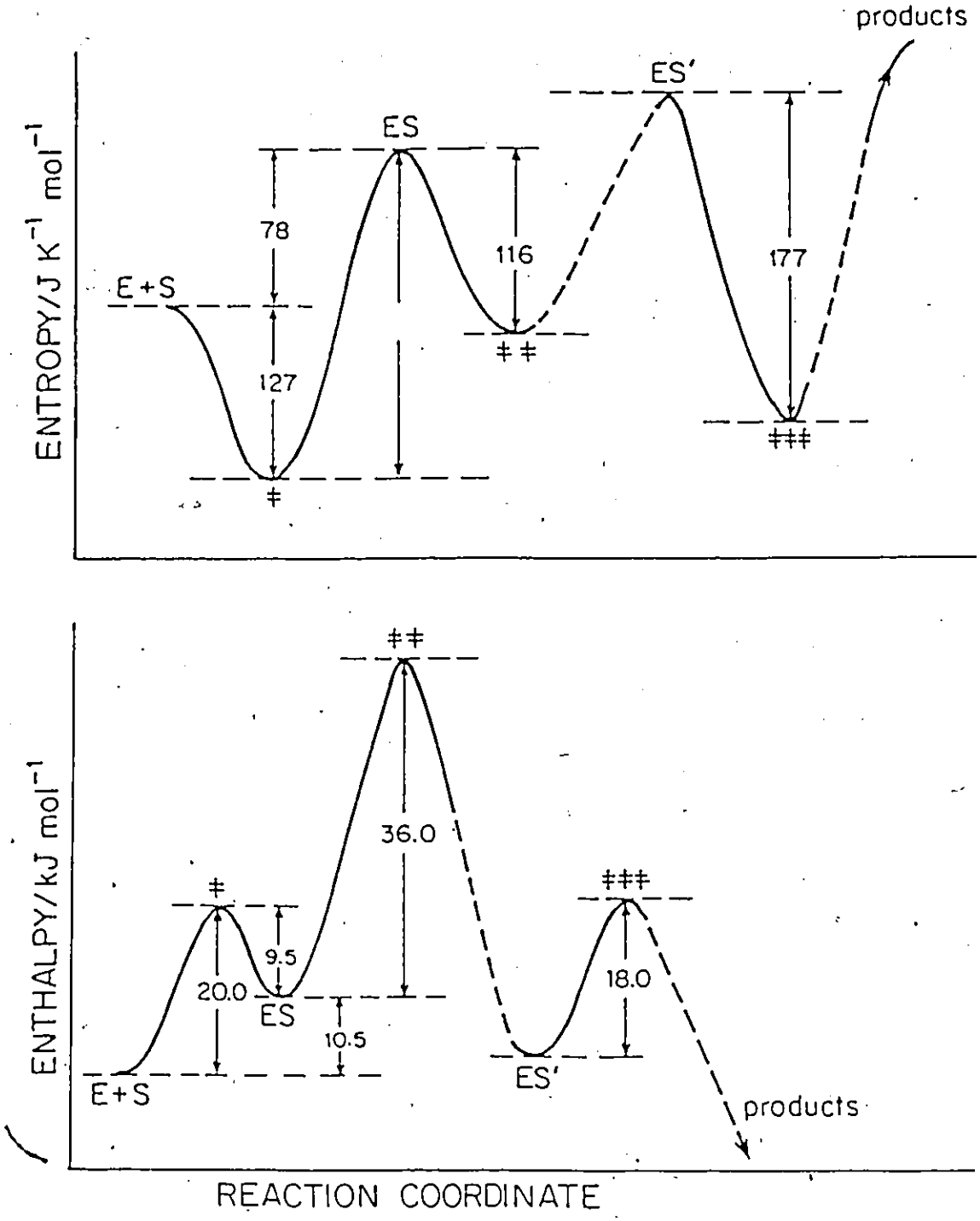

Figure 28. Reaction profiles, showing the variations of Gibbs energy, entropy, and enthalpy during the course of the process E + S → ES → ES' → E + Y + Z.

6.6 Conclusion

From the results obtained in this work it may be concluded that the hydrolysis of cellobiose catalyzed by β-glucosidase follows a two-intermediate mechanism. First the Michaelis enzyme-substrate complex is formed. In the second step a glucosyl group is split off with simultaneous formation of an enzyme-glucosyl complex, the second intermediate; this intermediate then reacts with water to produce another glucose molecule. The imidazolium group probably acts as a general acid protonating the leaving group; and the second intermediate is probably an enzyme-bound glucosyl cation-carboxylate ion-pair as postulated by Umezurike in the β-glucosidase catalyzed hydrolysis of o-nitrophenyl-β-D-glucopyranoside (51,52). This may be represented as follows:

$$EC^-(IMH^+) + GOG \rightleftharpoons EC^-(IMH^+ \text{——} GOG)$$

$$EC^-(IMH^+ \text{——} GOG) \longrightarrow EC^-(IM) \text{——} G^+ + GOH$$

$$EC^-(IM) \text{——} G^+ + H_2O \longrightarrow EC^-(IMH^+) + GOH$$

In these equations $EC^-(IMH^+)$ refers to the free enzyme with its carboxylate group (C^-) and protonated imidazolium group (IMH^+), GOG is the substrate cellobiose, $EC^-(IMH^+ \text{——} GOG)$ is the Michaelis enzyme-substrate complex, $EC^-(IM) \text{——} G^+$ is the enzyme bound glucosyl cation stabilized by intimate ion-pairing with the carboxylate ion, and GOH is the product glucose.

CHAPTER VII

FLOW KINETICS OF β-GLUCOSIDASE CHEMICALLY ATTACHED ON NYLON TUBING

7.1 Introdution

As has been discussed in Chapter I, the enzymic degradation of cellulose is of considerable technical importance, and β-glucosidase plays an important role in that process, being essential for the hydrolysis of the intermediate cellobiose. The rate of cellulose degradation and the yield of the product glucose can be increased significantly by adding β-glucosidase to cellulase. However, β-glucosidase is costly and is expended when used in soluble form. In addition, the enzyme activity is strongly inhibited by glucose and the activity therefore decreases during cellulose degradation. The use of immobilized β-glucosidase, which can be separated from the soluble product for reuse and can be protected from product inhibition, will bring about a considerable economic improvement in the technical saccharification process.

Because of this, and because kinetic studies of immobilized enzymes also provide significant information on the features and the mechanism of the enzyme reaction, and provide the knowledge necessary for the design of a reactor and for obtaining the optimal operating conditions, investigations on the method of immobilization and the stabilities and kinetics of immobilized

β-glucosidase were also undertaken in the present work.

General aspects of enzyme immobilization

Immobilization of biocatalysts has gained considerable scientific and technical importance in the last decade. Immobilized enzyme systems have been extensively used in various areas: research, chemical process industry and clinical medicine, because they are readily recoverable for reuse, and because they often possess greater stability than the native form. These practical applications have provided the impetus for the enormous research activity in this field. In addition, in biological systems the enzymes are often not in free solution but are attached to structural material, e.g. the membranes of cells, tissues or vessels. An understanding of the kinetics of immobilized enzyme systems will therefore lead to a deeper knowledge of the function and behaviour of enzymes in vivo (125-129). Thus intensive research efforts have been directed towards the kinetic studies of immobilized enzymes (63,130-137). As a result investigations of immobilized enzymes(138-142) have rapidly developed, and now constitute one of the most important aspects of enzymology. The industrial applications of immobilized enzymes (142-146), of immobilized whole microbial cells (147-157), or of the coimmobilizates of whole cells(158-160) or parts of the cells and additional enzymes, have led to the development of a new area, enzyme biotechnology, in the last few years.

A variety of techniques for enzyme immobilization have been developed from simple flocculation to specific covalent attachment. A number of reviews (60,161-164) on the immobilization methods have been published.

The methods can be classified into three basic categories as follows (40):

(1) Support-binding method: the binding of enzymes to water-insoluble supports. This method can be further subdivided into 'physical adsorption', 'ionic binding' and 'covalent binding', according to the binding mode of the enzyme.

(2)Cross-linking method: intermolecular cross-linking of enzymes by means of bifunctional or multifunctional reagents.

(3) Entrapping method: (1) incorporating enzymes into the lattice of a semipermeable gel, 'lattice type'; or (2) enclosing the enzymes in a semipermeable polymer membrane, 'microencapsulation type'. These categories are shown schematically in Figure 29.

A specific conformation and an active centre are regarded as essential features of the catalytic activity of enzymes; if the amino acid residues at the active centre, or the tertiary structure of the enzyme, are altered, the catalytic activity may decrease and changes of enzymic properties such as substrate specificity may occur. Therefore in order to retain the catalytic activity of the enzyme in the immobilized state, it is necessary that the functional groups in the active centre should not be

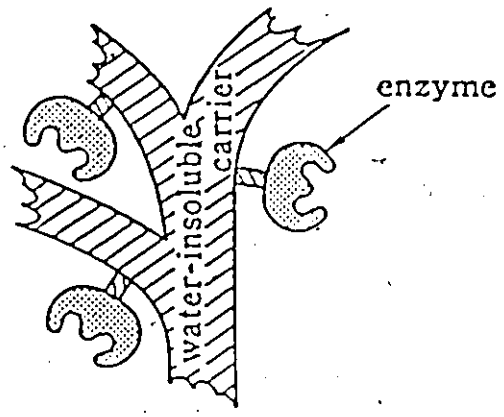

(a) Support-binding method

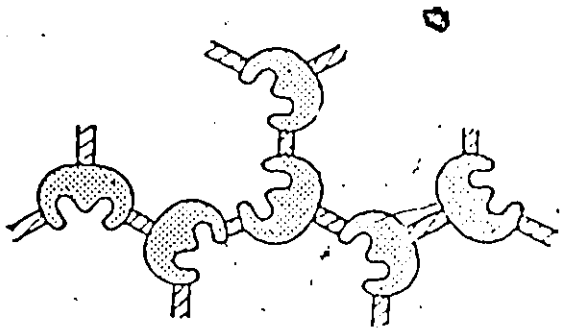

(b) Cross-linking method

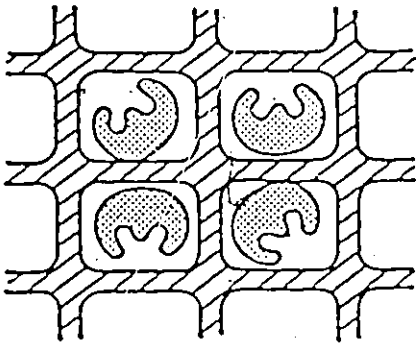

i) Lattice type

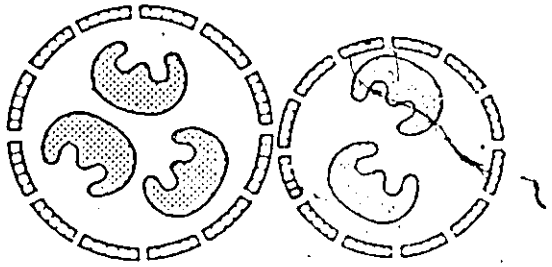

ii) microencapsulation type

(c) Entrapping methods

Figure 29. Schematic diagrams of immobilized enzymes

involved in the reaction leading to immobilization of the enzyme, and that the immobilization should be carried out under very mild and extremely well-controlled conditions; high temperature and strong acid or alkali treatments must be avoided so that the structural integrity of enzymes can be preserved.

Some immobilization methods, such as physical adsorption and ionic binding, cause little or no conformational change or destruction of the active centre of the enzyme, and therefore yield immobilized enzymes having high activity in many cases. However, these methods have the disadvantage that the immobilized enzyme may leak from the support during the utilization, because the binding forces between the enzyme and the supports are not strong. On the other hand, some techniques such as covalent binding and cross-linking involve the formation of covalent bonds between enzymes and water-insoluble supports or between the enzyme molecules, use being made of bi- or multifunctional reagents. The reaction conditions for chemical bonds are relatively severe and complicated. Thus, in some cases, the conformational structure and the active centre of the enzyme may be altered by the immobilization reactions, leading to significant loss of activity. However, when there is covalent binding the force between enzyme and carrier is strong and leakage of the bound enzyme may not occur even in the presence of substrate or salt solution of high ionic strength.

In the choice of an immobilization method for a particular application, both high activity and long life of the immobilized

enzyme should be taken into account.

However, the immobilization of an enzyme is a very complex problem, and the activity and the life time of immobilized preparation are affected by a number of factors, depending markedly on the nature of the support, the attachment technique, and the nature of the enzyme itself. Care is therefore required regarding the selection of the support, the method of immobilization, and the attachment procedure.

Factors influencing activity of immobilized enzymes

Most immobilized enzymes exhibit altered kinetic behaviour as compared with the corresponding free enzyme. For this, there are four main reasons:

(1) Immobilization may cause the three-dimensional conformation of the enzyme protein to change, so that the immobilized enzyme may be conformationally different from that present in free solution. It has been explained above that kinetic behaviour depends very critically on enzyme conformation, and certain changes may lead to a complete loss of activity.

(2) In the support, the interaction between the enzyme and the substrate takes place in a different environment from that existing in free solution. Sometimes some of the active centres of the enzyme may be shielded by the support and the substrate may suffer steric hindrances in approaching the active centre.

(3) In the immobilized state the substrate concentration in the neighbourhood of the enzyme may be different from what it

is away from the enzyme, because of partitioning of the substrate between the support and the free solution. The partitioning effects depend on the characteristics of the substrate and of the support. For example, a relatively non-polar substrate will be more concentrated in the vicinity of a support containing a number of non-polar groups than in aqueous solution, while a polar substrate will be more concentrated in solution than in the neighbourhood of the support. The kinetic effects of partitioning of substrate have been discussed by several workers (60,116,130,132). When both the substrate and the support are electrically charged, the partitioning effects will be much more profound(28).

(4) The fourth factor that may be responsible for the different kinetic behaviour of an immobilized enzyme is the diffusion effect. In an immobilized enzyme system, a diffusion layer may be established between the support and the solution, so that the rate of transport of the substrate to the enzyme, or of the product from enzyme, through the diffusion layer may be rate limiting(131). Therefore the reaction of immobilized enzyme may be, to some extent, diffusion-controlled. Only in the case of an exceedingly slow enzyme reaction will the reaction be other than diffusion-controlled in the immobilized state.

The kinetic parameters for an immobilized enzyme will be different from those obtained with the free enzyme, as a result of these conformational, environmental, partitional and diffusional effects. It is usually difficult to assess the extent

of each effect on a particular parameter. However, an estimate as to which one plays the most important role can be made from a theoretical analysis of the kinetic results.

Previous work on immobilization of β-glucosidase.

This enzyme has previously been attached to supports in different ways. Barker et al.(111) attached β-glucosidase chemically to microcrystalline cellulose, while Srinivasan and Bumm (112) coupled it to cellulose activated by cyanogen bromide. By cross-linking with glutaraldehyde, Bissett and Sternberg (19) attached the enzyme to chitoson, while Mala Rao et al.(113) immobilized it on polyamide. In addition to covalent attachment, entrapment into gels and polymers(56,165,166), and adsorption on supports(18,62,167), have also been brought about. Venardos et al.(62) immobilized β-glucosidase on a cation exchange resin. Sundstrom et al.(18) attached it on controlled pore alumina by sorption, and Lomako et al. immobilized it on an inorganic carrier, Silochrom S-80(167). Although β-glucosidase has been used in a hollow fiber reactor to hydrolyze Salicin(175), no attempt has been made to attach the enzyme to nylon tubing. Nylon, as supporting material for the immobilization of enzymes, possesses a number of advantages, such as mechanical strength, non-biodegradable properties and potential chemical reactivity which is important for covalent attachment of enzymes. Among various reaction configurations, the tubular reactor has proved to be superior in the automated

analysis of specific substrates (91,148,168-173) in clinical medicine, food industry and drug technology, because of its convenience of operation, its ability to withstand clogging in crude solution, and its low pressure drop and favourable hydrodynamic properties. The tubular reactor is particularly valuable for fundamantal kinetic investigations on immobilized enzymes, and has been extensively used in this laboratory(176-180).

In the present work β-glucosidase was attached covalently to the inner surface of nylon tubing. The studies involved optimizing the reaction conditions to obtain an efficient immobilized preparation and studying the flow kinetics over a range of temperatures, pH values, flow rates and substrate concentrations. The extent of diffusion control was also investigated. In addition a comparison was made between the immobilized and free enzyme with particular reference to pH and temperature effects and to stability. No previous studies along these lines appear to have been made.

7.2 Theoretical considerations

Because of conformational, partitional, environmental, and diffusional effects the parameters in the Michaelis-Menten equation

$$v = \frac{k_c'[E][S]}{K_m(app)+[S]} = \frac{V'[S]}{K_m(app)+[S]} \qquad (43)$$

are different for an immobilized enzyme from those that apply to the enzyme in free solution (135). In this equation [E] is the concentration of the immobilized enzyme and [S] that of the substrate in solution. The catalytic constant k'_c is modified by conformational, partitional and environmental effects but not by diffusional effects; the apparent Michaelis constant $K_m(app)$ is influenced by all these effects: conformational, environmental, partitional and diffusional.

A detailed treatment of the flow kinetics for an enzyme immobilized on the inner surface of a tube, with full derivations, has been given by Kobayashi and Laidler(174); only a very brief outline, sufficient to explain the procedures used in the present work, will be given here. Between the bulk solution and the surface a diffusion layer is established; the concentration of substrate within the diffusion layer may differ from its value in the bulk of the solution due to the fact that the rate of disappearence of the substrate by enzymic reaction is not necessarily the same as the rate of diffusion of the substrate through the layer to the enzyme. The diffusion layer and concentration profile are shown schematically in Figure 30 (129). The thickness of the diffusion layer depends on the magnitude of the mass transfer coefficient k_L, defined as

$$k_L = \text{constant} \left(\frac{D^2 v_f}{r L}\right)^{1/3} \qquad (44)$$

where D is the diffusion coefficient of the substrate, v_f the

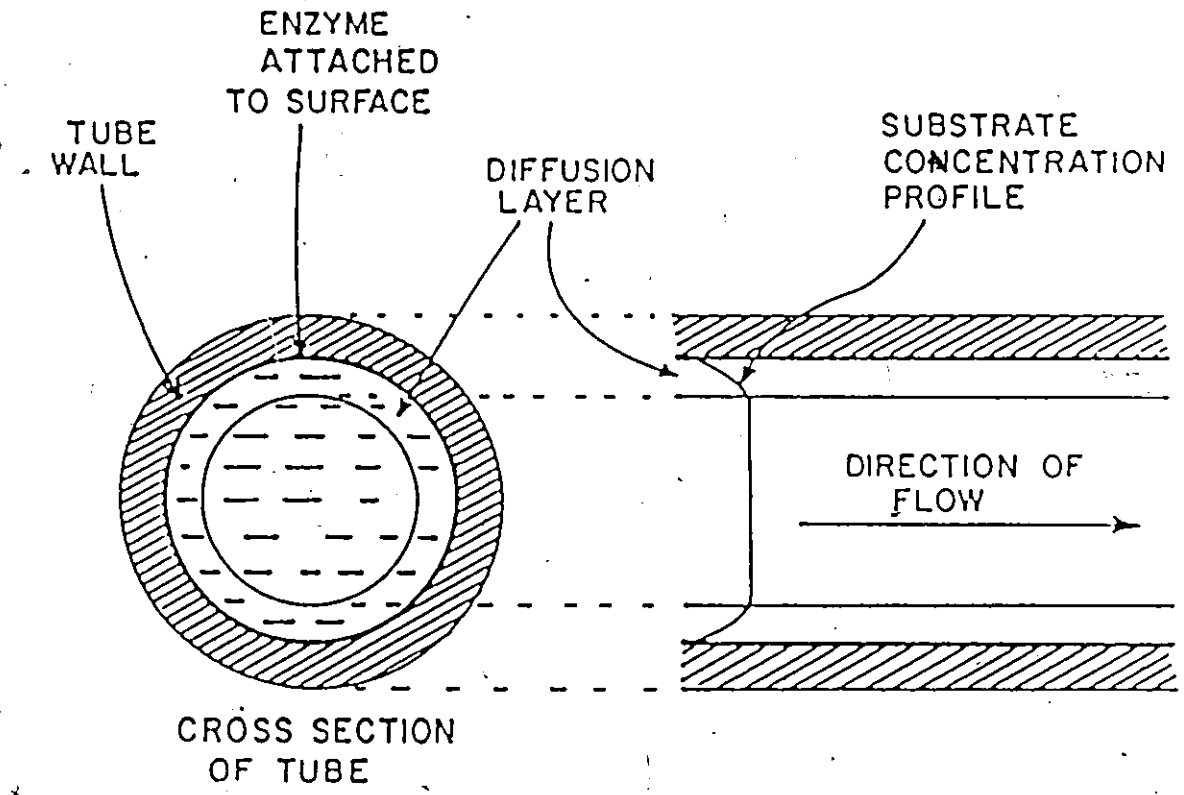

Figure 30. A tube with enzyme attached to the inner surface, showing the diffusion layer and the concentration profile of substrate (129).

flow rate of the substrate through the tube, r the radius of the tube, and L its length. Thus, k_L is a measure of the rate at which the substrate diffuses through the layer..

Equation (44) shows that decreasing the flow rate and increasing the diameter of the tube or its length decreases the mass transfer coefficient, and therefore increases the extent of the diffusional effect. Conversely, increasing the flow rate will increase the rate of diffusion of the substrate, and consequently decreases the relative effect of diffusion on the overall rate of reaction. Diffusional effects are also unimportant at sufficiently high substrate concentrations. Aside from the dependence on experimental conditions, the extent of the diffusion effect also depends on the nature of the substrate and the enzyme activity. Under limiting conditions of complete diffusion control e.g., at low [S] and low v_f, the concentration of product formed at the exit of the tube, $P_e(D)$, is predicted by the theory to be

$$P_{e(D)} = 2.56\left(\frac{D\ L}{r^2 v_f}\right)^{2/3}[S] \qquad (45)$$

or

$$P_{e(D)} = 2.56\left(\frac{D}{r^2}\right)^{2/3}[S]\left(\frac{v_f}{L}\right)^{1/3}t_r \qquad (46)$$

where t_r is the residence time of the substrate in the tube:

$$t_r = \frac{L}{v_f} \qquad (47)$$

The rate of product formation is given by

$$v_D = 8.06(v_f D^2 r^2 L^2)^{1/3}[S] \qquad (48)$$

At the other extreme, at the limit of high substrate concentrations and high flow rates, there is no influence of diffusion. The concentration of product formed at the exit, $P_e(O)$, is then given by

$$P_e(O) = \frac{2L}{rv_f} v_r = \frac{2v_r}{r} t_r \qquad (49)$$

where v_r, the inherent rate of the immobilized enzyme-substrate reaction, is given by

$$v_r = \frac{k'_c[E][S]}{K'_m + [S]} \qquad (50)$$

This differs from the expression in eqn.(43) in involving the intrinsic Michaelis constant K'_m and not $K_m(app)$; the latter includes the diffusional effects. The rate in the enzyme-tube system is now given by

$$v_o = 2\pi r L v_r \qquad (51)$$

Based on this theory several procedures can be used to determine the extent of diffusion control in a particular system.

(1) Plots of $\log_{10}P_e$ against $\log_{10}v_f$. If eq.(45) applies, that is, if there is full diffusion control, the plot will have a slope of -0.67, while if there is no diffusion control (eq.(49)), the slope will be -1.0 .

(2) Double-logarithmic plots of reaction rate v against flow rate v_f . The slopes are now 1/3(eq.(48)) or zero(eq.(51)) for complete or no diffusion control, respectively.

(3) Another simple way to examine the extent of diffusion control is based on plots of concentration of product against the residence time. If the reaction is diffusion-free the plot will be a straight line (eq.(49)), while if the reaction is affected by diffusion the plot will be curved(eq.(46)).

(4) Lineweaver-Burk plots of 1/v against 1/(S). For the diffusion-free reactions the plot will be a straight line. Because the extent of diffusion control varies with concentration of substrate, being greater at lower concentrations, the Lineweaver-Burk plot shows curvature for a diffusion-controlled process. The theory(174) predicts that $K_m(app)$ is related to the intrisic(diffusion-free) Michaelis constant for the immobilized enzyme, K'_m, by the equation

$$K_m(app) = K'_m + \frac{V'}{2.58}\left(\frac{rL}{D^2}\right)^{1/3} v_f^{-1/3} \qquad (52)$$

where V' is the maximal rate for the immobilized enzyme. When there is no diffusion control, the $K_m(app)$ value approaches the K'_m value.

(5) A special procedure by use of dimensionless parameters, ϕ and ρ.

These parameters are defined by the Kobayashi-Laidler theory as follows:

$$\phi = \frac{P_e}{[S]}\left(\frac{v_f r^2}{DL}\right)^{2/3} \qquad (53)$$

and

$$\rho = \frac{K_m(app)}{[S]} \qquad (54)$$

A theoretical plot of ϕ against ρ can be divided into regions by means of the utilization factor η, which is defined as the ratio of the actual rate to that in the absence of diffusion effects and therefore is a measure of the extent of diffusion control. Figure 35 is an example of such a diagram;it is divided into three regions by two lines corresponding to the utilization factors shown. These regions correspond to small(1), moderate(2) and large(3) diffusion effects. Thus, the extent of diffusion control in a particular experiment can be determined from where the experimental values of ϕ and ρ (eq.(53) and eq.(54)) lie on the theoretical $\phi-\rho$ diagram.

7.3 Experimental: Materials and Methods

Materials

The enzyme, β-glucosidase (EC 3.2.1.21) used for immobilization contained 24 units per milligram protein with

salicin as substrate at pH 5.0 and at 37°C. The substrate and the reagent for glucose determination are the same as that described in Chapter II. The nylon tubing, of 0.155cm internal diameter, used for the immobilization of the enzyme, was obtained from Canus Plastics Company, Ottawa. Benzidine for the coupling processes was obtained from Sigma Company, while the glutaraldehyde as 25% aqueous solution was obtained from J. T. Baker Chem. Co., Phillipsburg, N. J., and dicyclohexylcarbodiimide from Fisher Scientific Company. Sodium phosphate used for the preparation of buffer were obtained from Fisher Scientific Company, sodium borate from J. T. Baker Chemical Co., Phillipsburg, N.J., and boric acid from British Drug Houses Ltd. All chemicals were analytical reagents. The water used to make buffer solutions was doubly distilled and cartridges packed with ion exchange resins (products of the Rybron Corporation, U.S.A.) were used to deionize the water.

Attachment procedure

The attachment procedure used in the present study was a modification of the techniques devised by Daka and Laidler(181). The surface of the nylon tubing is partially hydrolyzed with cleavage of amide bonds, followed by coupling of the carboxyl groups with benzidine in the presence of dicyclohexylcarbodiimide and subsequent coupling of amino groups with glutaraldehyde. The enzyme is attached finally to the active surface of the tubing. This procedure, shown in Figure 31(182), tends to leave a surface

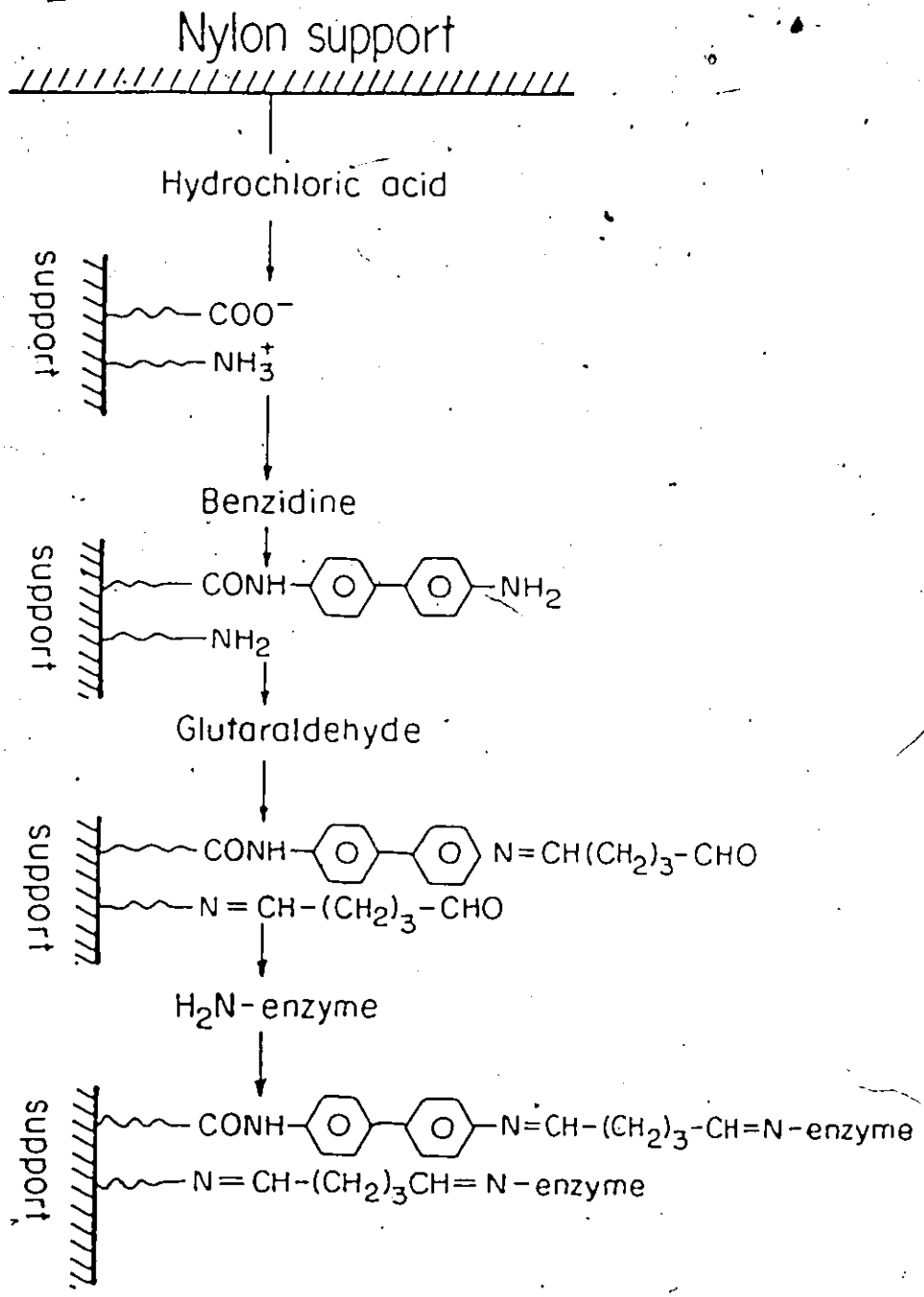

Figure 31. Summary of the immobilization technique employed in the present study.

that is fairly neutral electrically, thereby improving the enzymic stability (182).

A 2 m portion of the tube was first filled with a mixture of 18%(w/w) $CaCl_2$ in water and 18%(V/V) water in methanol, and incubated for 30 min at 40°C to etch the nylon surface. The tube was then perfused with water for 30 min at a flow rate of 4 mL min^{-1}. Partial hydrolysis of the inner surface was carried out at 40°C by pumping about 4 M HCl for 22 min at a flow rate of 4 mL min^{-1}. After washing for 30 min with ice-cold distilled water, the tube became quite opaque, indicating successful hydrolysis.

After perfusion with acetone for 5 min and methylene chloride for 5 min, at flow rates of 4 mL min^{-1}, a mixture of 1%(w/v) benzidine with 1% (w/v) dicyclohexylcarbodiimide in methylene chloride was passed through the tube at 1 mL min^{-1} for 5 hours at 10°C in order to couple benzidine with carboxyl groups of the surface. In this step, because tygon tubing and silicon tubing are both attacked by methylene chloride, the solution passing through the tube was not driven by pumping but by hydrostatic pressure; this was brought about by controlling the difference between the surface level of feed solution and the level at the exit. After removal of the unreacted benzidine by successive perfusions with 50 mL methylene chloride, 50 mL acetone at 1 mL min^{-1}, and 100 mL ice-cold distilled water at 4 mL min^{-1}, a solution of 12.5%(v/v) glutaraldehyde in 0.2M borate buffer (pH 8.5) was passed through the tube at 1 mL min^{-1} for 1 hr and at

3°C, in order to block all the amino groups, those produced by partial hydrolysis and those derived by benzidine attachment. The excess of glutaraldehyde was washed away by pumping 0.1 M phosphate buffer(pH 7.5) for 15 min at 4 mL min^{-1}.

Immediately afterwards the tube was perfused with an enzyme solution of 50 mg in 25 mL 0.1 M phosphate buffer at pH 5.95, containing 1 mM EDTA, and 1 mM ß-mercapto-ethanol. To ensure complete reaction, the enzyme solution was circulated through the tube at 0.5 mL min^{-1} for 24 hours, the temperature being maintained at 3°C. Enzyme that was not bound chemically was removed by washing the tube with 1 L of 0.5 M NaCl solution in 0.1 M phosphate buffer at pH 7.0 at 4 mL min^{-1}. When not in use the tube was filled with 0.1 M phosphate buffer at pH 5.87 and stored below 5°C.

The activity of the enzyme-tube was determined by measuring the rate of formation of glucose, when a 5.99 mM substrate solution in 0.1 M phosphate buffer at pH 5.87 was passed through the tube at a flow rate of 2.74 cm s^{-1}, and at 25.0°±0.1°C.

Kinetic procedure

The substrate solutions, at various concentrations, were prepared in two different buffers, according to the pH desired. For pH values below 5.6, the buffer used was 0.2 M acetate-acetic acid, while at higher pH values 0.1 M phosphate buffer was used. Kinetic runs were carried out at temperatures ranging from 5°C to 45°C, flow rates from 0.98 to 9.18 cm s^{-1} and concentrations from

1.50 to 13.3 mM. A 1 m length of coiled enzyme tube with 1 mm internal diameter was immersed in a thermostatted bath. One end was connected by tygon tubing to the thermostatted substrate solution through a LKB Varioperpex II peristaltic pump, which was used for pumping the substrate solution through the enzyme-tube at desired flow rate. The product was collected at the other end of the tube and analyzed spectrophotometrically after the steady state had become established. The data for all the concentrations of substrate and for all flow rates were the average of three such measurements. Since the flow rates changed slightly with the usage time of the tygon tubing they were determined for each kinetic run.

After each kinetic determination the tube was washed thoroughly with buffer to remove all traces of product and substrate.

Determination of glucose and reaction rate

The product glucose was determined by measuring the absorbance at 340 nm by use of the assay reagent. In the analysis of the sample solution 1 mL of the assay reagent was added to 1 mL or 2 mL of effluent in a certain amount of buffer to make the final total volume 3 mL.

The absorbance was recorded as a function of time by means of a Pye Unicam SP 1800 UV Spectrophotometer. The reading was taken when the absorbance attained a constant value.

A calibration curve, covering the range of glucose

concentrations produced in these studies, was obtained with standard glucose solution.

The reaction rate was determined by dividing the product concentration at the exit by the residence time of the substrate solution in the enzyme-tube, the latter was obtained from the length of the reactor and the linear flow rate of the solution passing through it.

Some batches of substrate gave absorbance at 340 nm with the assay; it was therefore necessary to measure the absorbance given by the substrate together with the assay reagent. Separate determinations for substrate at different concentrations were performed, and a correction for the absorbance due to the substrate was made for every kinetic measurement.

7.4 Results and Discussion

For each kinetic measurement, the time required for a steady-state rate of cellobiose hydrolysis to be attained was first determined by measuring the amounts of product formed after various time intervals. The time required depends on the substrate concentrations and flow rates, and ranges from 24 mins to 60 mins.

Dependence of product concentration and reaction rate on flow velocity

For the investigation on the extent of diffusion the enzyme-

Table 15.

Product concentrations $[P]_e$ at the exit of the tube, and reaction rates v for different substrate concentrations at various flow rates v_f;

T = 25.0°C pH = 5.87

$[S]_0$/mM	v_f/cm s^{-1}	t_r/s	P_e/μM	v/μM s^{-1}
	6.93	14.4	3.94	0.27
	4.88	20.5	6.15	0.30
1.50	3.54	28.3	9.11	0.32
	2.16	46.3	15.0	0.32
	1.52	65.8	20.9	0.32
	0.84	119.1	36.5	0.31
	8.58	11.7	3.62	0.31
	6.18	16.2	6.03	0.37
1.82	4.40	22.7	7.79	0.34
	2.66	37.6	13.8	0.37
	1.83	54.6	20.8	0.38
	0.98	101.6	36.6	0.36
	9.17	10.9	4.52	0.42
	6.57	15.2	8.37	0.55
3.00	4.73	21.1	12.2	0.57
	2.84	35.2	20.4	0.58
	1.97	50.9	29.8	0.59
	1.06	94.7	51.6	0.55

[S]/mM	v_f/cm s^{-1}	t_r/s	P_e/μM	v/μM s^{-1}
	8.99	11.1	6.19	0.56
	6.35	15.8	11.9	0.76
4.17	4.56	21.9	17.3	0.79
	2.74	36.5	28.7	0.79
	1.88	53.2	41.4	0.78
	0.99	100.9	80.5	0.80
	8.96	11.2	7.11	0.64
	6.44	15.5	13.3	0.85
5.00	4.58	21.8	19.7	0.90
	2.78	36.0	33.4	0.92
	1.92	52.1	47.9	0.92
	1.02	98.0	92.0	0.94
	9.14	10.9	8.71	0.80
	6.53	15.3	13.5	0.88
5.99	4.69	21.3	21.4	1.03
	2.85	35.1	37.2	1.03
	1.95	51.3	54.7	1.05
	1.06	94.4	96.6	1.03

[S]/mM	v_f/cm s^{-1}	t_r/s	P_e/μM	v/μM s^{-1}
	8.82	11.3	12.4	1.10
	6.25	16.0	20.7	1.29
7.49	4.51	22.2	31.0	1.40
	2.71	36.9	50.7	1.37
	1.85	54.1	74.5	1.38
	0.99	101.2	142.6	1.41
	8.65	11.6	22.8	1.97
	6.24	16.0	36.2	2.26
13.3	4.45	22.5	52.8	2.35
	2.67	37.5	85.9	2.29
	1.84	54.4	124.2	2.29

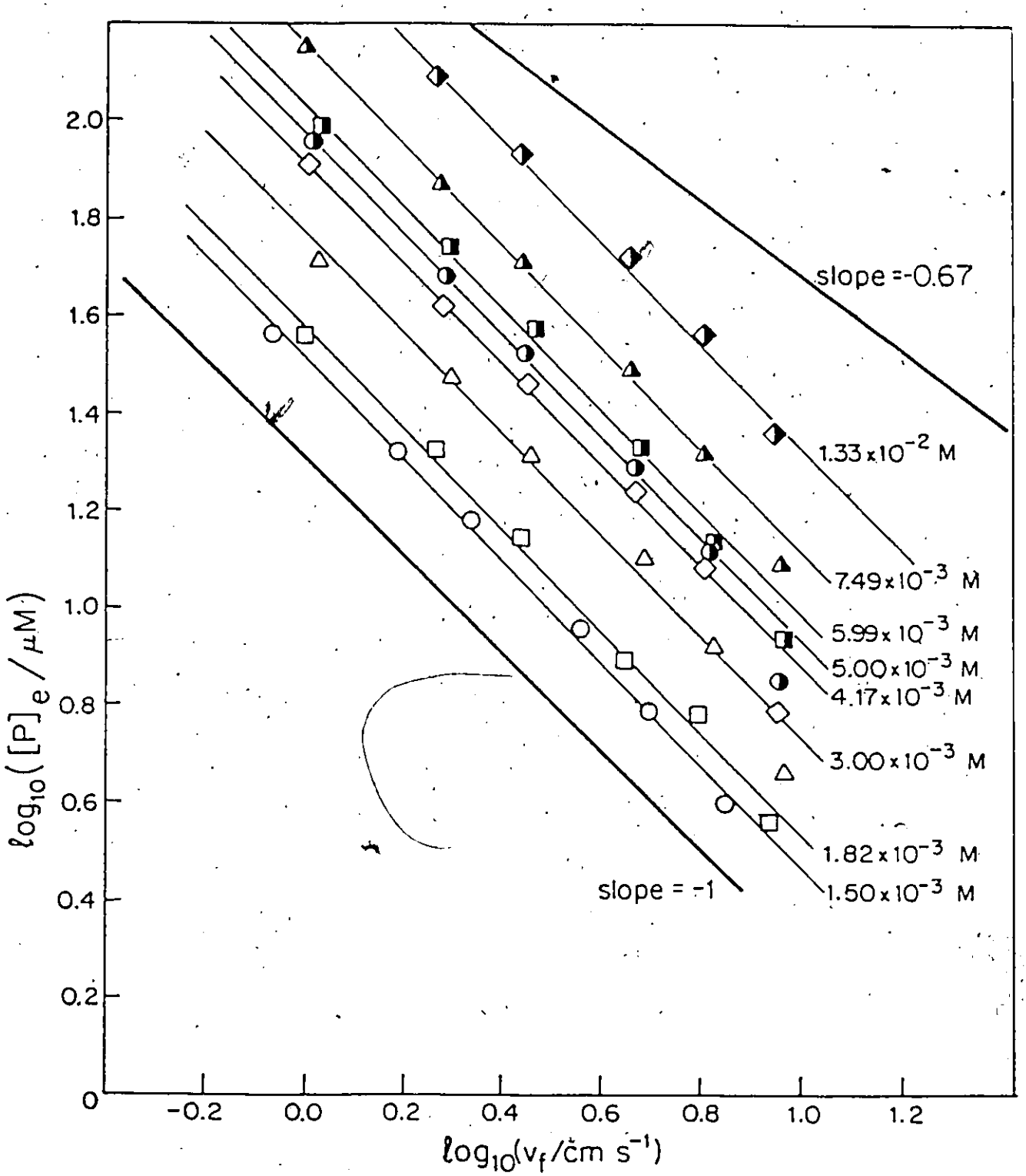

Figure 32. Double-logarithmic plots of the concentration $[P]_e$ of glucose at the exit against flow rate v_f, for different substrate concentrations as indicated. T = 25.0°C; pH = 5.87.

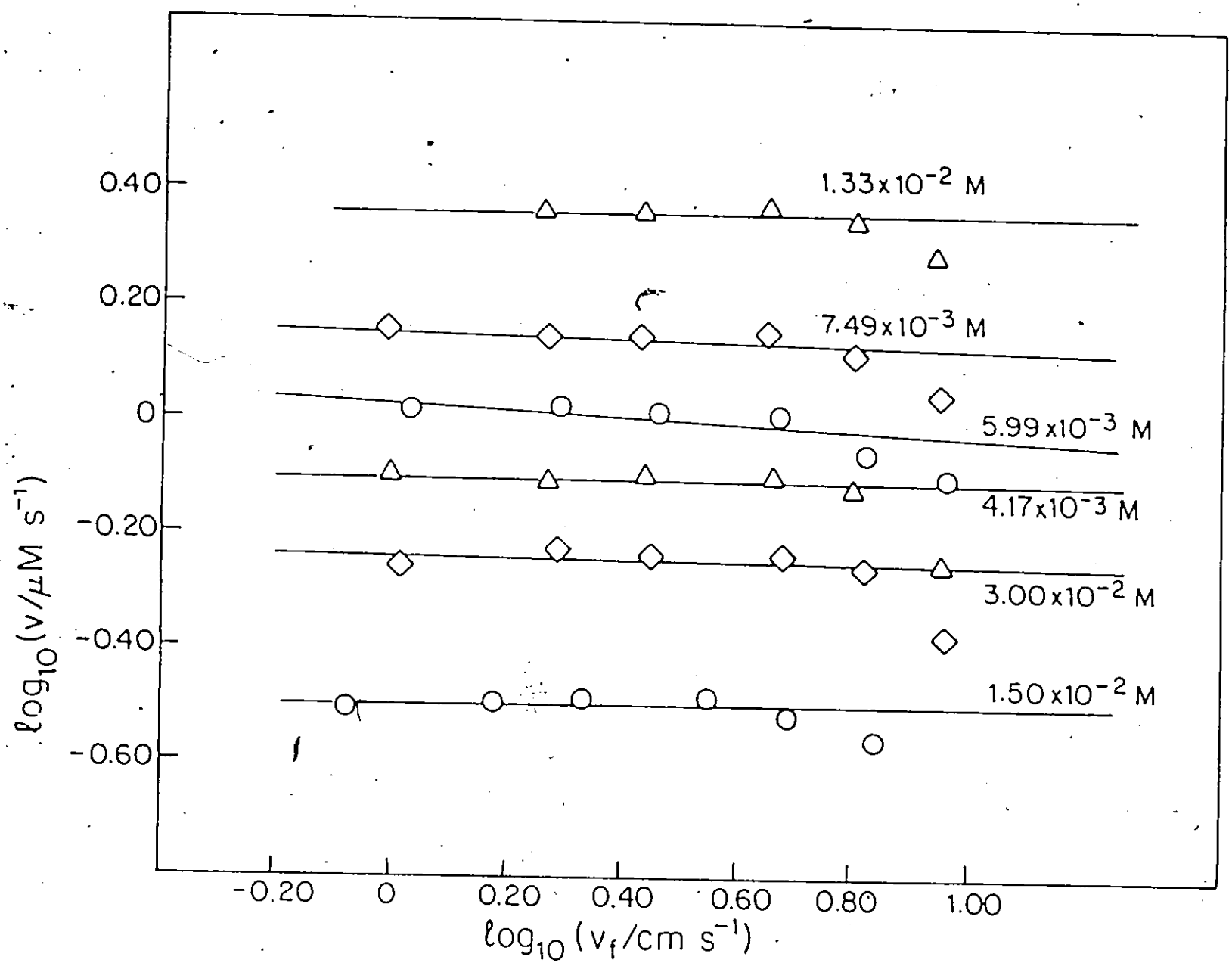

Figure 33. Double-logarithmic plots of the apparent reaction rate v against the flow rate v_f, for different substrate concentrations. T = 25.0°C; pH = 5.87.

tube reactions were carried out at pH 5.87 and 25.0±0.1°C, flow rates varying from 0.98 to 9.18 cm s^{-1}, with the substrate concentration ranging from 1.50 to 13.3 mM. Table 15 lists the product concentrations obtained at the exit of the tube and the reaction rates for these conditions. A double-logarithmic plot of product concentration against flow rate is shown in Fig.32, all of the slopes being close to -1. The corresponding double-logarithmic plots of the apparent reaction rate against flow rate, in Fig.33, show that the reaction rate is almost independent of the flow rate. These results indicate that under the conditions used in the present work, the reaction is free from diffusion control.

Dependence of product concentration on residence time

Fig.34 shows plots of product concentration against residence time. The linearity between the product concentration and the residence time, in accordance with eq.(49), is further evidence that there is essentially no diffusion control.

Lineweaver-Burk plots

The Lineweaver-Burk plot is linear; here the reaction rates were obtained from the slope of a plot of product concentration against the residence time, this being equivalent to taking the average of the reaction rates at different flow rates. Similar linear plots were obtained at other pH values and other temperatures (see Figure 39 and 42 in the next Chapter.) The

lack of curvature is consistent with there being no diffusion control in the system. Since there is no diffusion control the K_m(app) values obtained from these plots (the slopes of which are K_m(app)/V and the intercepts, 1/V) can be regarded as the inherent Michaelis constants K_m'. Table 18 shows K_m' values at various pH values, compared with the values for the free enzyme. The immobilization has brought about some increase in K_m', but the effect is much less than if there had been substantial diffusion control (eq.52).

Dimensionless parameters

Table 16 shows the experimental values of ρ and ϕ , calculated on the basis of eq.(53) and (54). In the calculation of ϕ , the diffusion coefficient was taken as $3X10^{-6}cm^2s^{-1}$; this is based on the values for sugars(184,185), and should be not far from the value for the present substrate. Figure 35 shows the theoretical plot of ϕ against ρ , together with the experimental points. All of the points lie well within region 1, the diffusion-free region.

7.5 Stability of the nylon-tube-supported β-glucosidase

Storage stability

Tests were made to determine the stability of the enzyme-coated tube used in the experiments. Its storage stability was investigated by making activity measurements at various times after storage at 5°C. The activity was determined as the rate of

Figure 34. Plots of product concentration $[P]_e$, against residence time, for different substrate concentrations. T = 25.0°C; pH = 5.87.

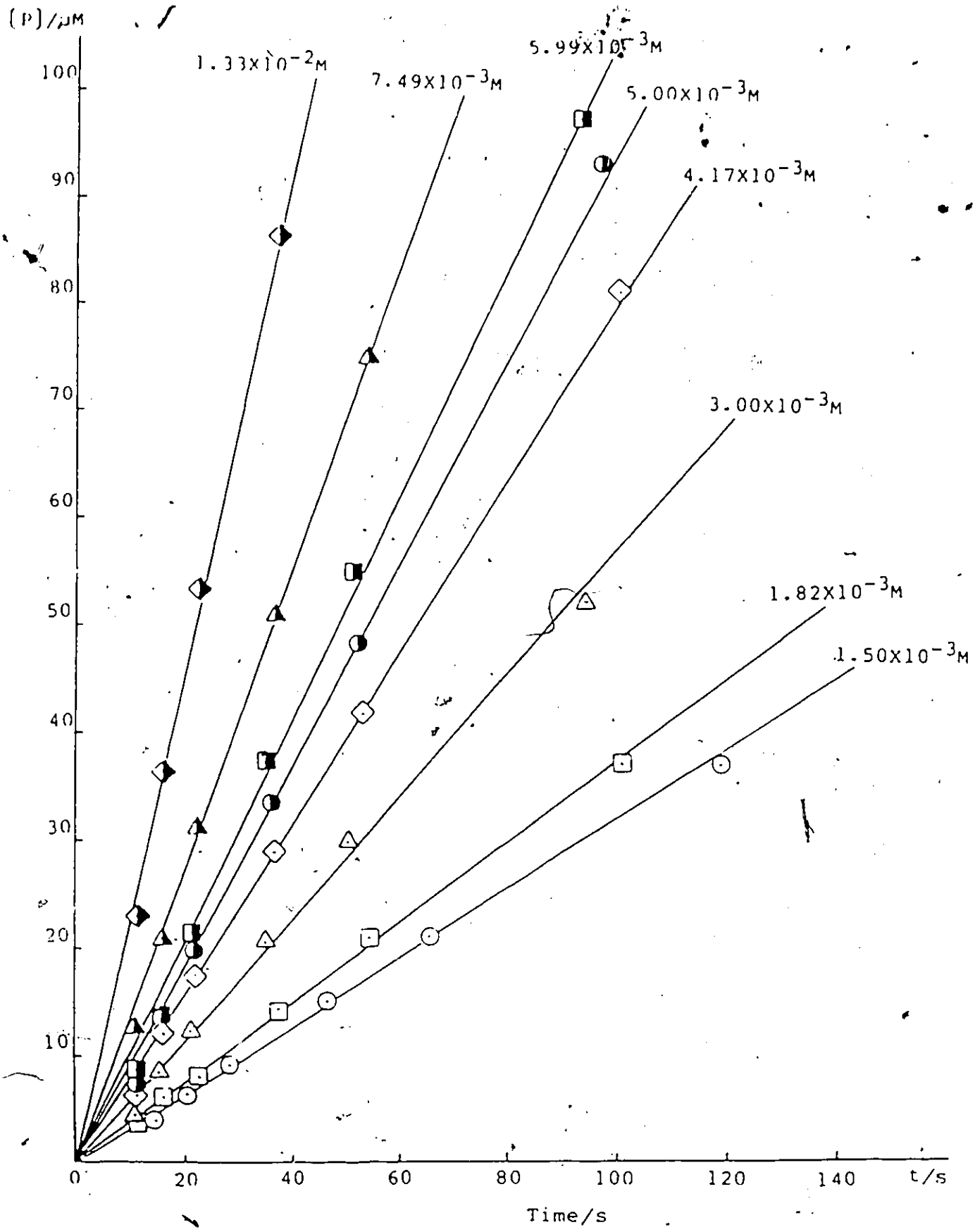
[P]/μM
1.33X10⁻²M
7.49X10⁻³M
5.99X10⁻³M
5.00X10⁻³M
4.17X10⁻³M
3.00X10⁻³M
1.82X10⁻³M
1.50X10⁻³M
100
90
80
70
60
50
40
30
20
10
0
20
40
60
80
100
120
140
t/s
Time/s

Table 16.

Values of dimensionless parameters ϕ and ρ for different substrate concentrations at various flow rates

T = 25.0°C pH = 5.87

v_f/cm.s^{-1}	[S]/mM											
	1.50		3.00		4.17		5.99		7.49		13.3	
	ρ	ϕ x10^3	ρ	ϕ x10^3	ρ	ϕ x10^3	ρ	ϕ x10^3	ρ	ϕ x10^3	ρ	ϕ x10^3
9.17			10.2	27								
9.14							5.13	26				
8.99					7.38	26						
8.82									4.11	29		
8.65											2.31	30
6.93	20.5	39										
5.00	20.5	52	10.2	45	7.38	46	5.13	43	4.11	43	2.31	41
2.86	20.5	62	10.2	55	7.38	55	5.13	51	4.11	54	2.31	50
2.00	20.5	69	10.2	61	7.38	62	5.13	57	4.11	60	2.31	56
1.43	20.5	77	10.2	69	7.38	69	5.13	64	4.11	68		
1.06			10.2	73			5.13	69				
0.99					7.38	79			4.11	78		
0.84	20.5	89										

Figure 35. Theoretical double-logarithmic plot of ϕ against ρ, those parameters being defined by eq.(53) and (54). The experimental points are for the following flow rates:

◇ 0.84-1.06 cm s^{-1}
□ 1.48 cm s^{-1}
△ 2.00 cm s^{-1}
× 2.86 cm s^{-1}
○ 5.00 cm s^{-1}
◑ 8.58-9.17 cm s^{-1}

Region 1, little diffusional control (<5%);
Region 2, moderate diffusional control (5-60%);
Region 3, considerable diffusional control (>60%).

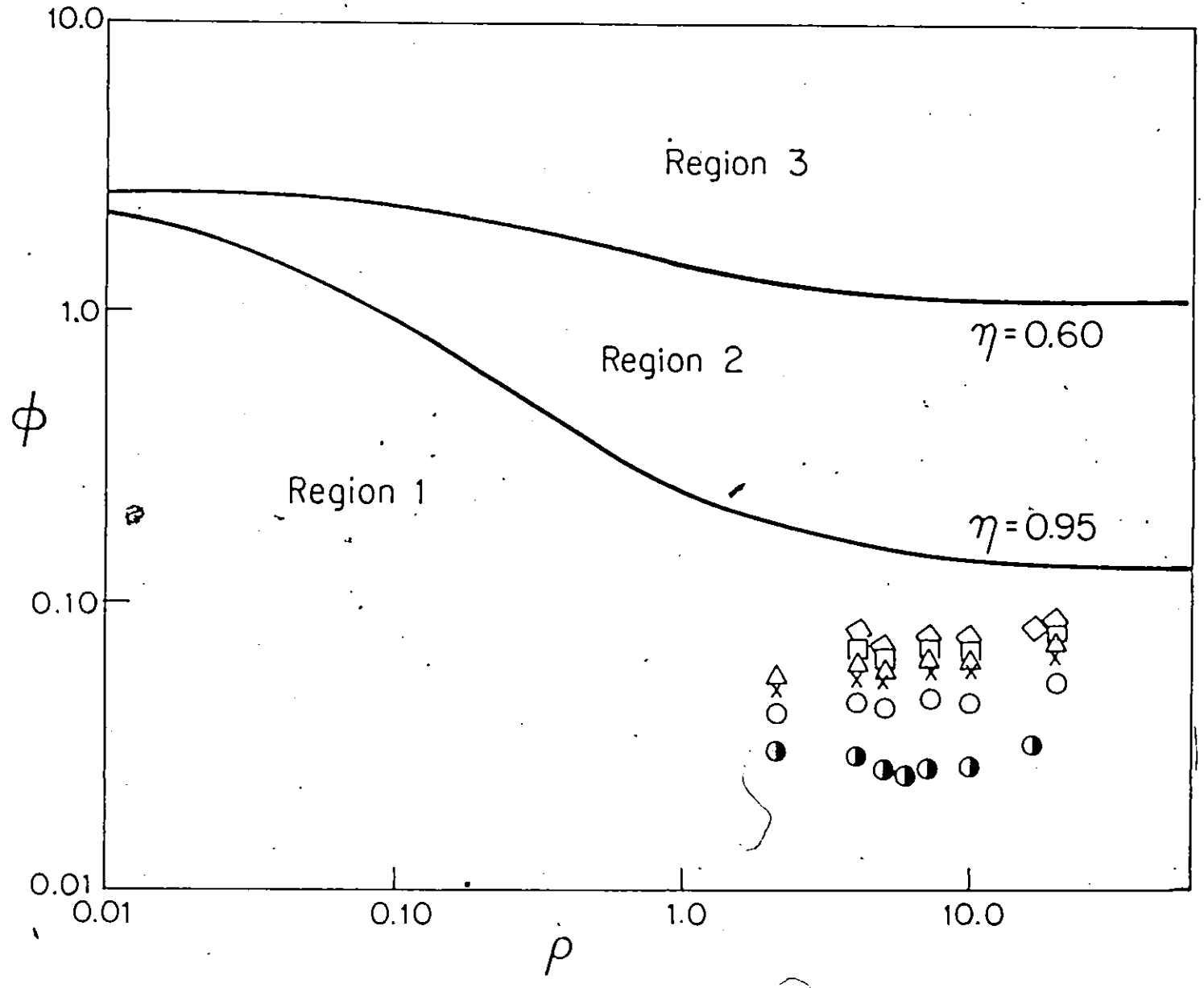
10.0
1.0
0.10
0.01
0.01
0.10
1.0
10.0
Region 3
Region 2
Region 1
η = 0.60
η = 0.95
φ
ρ

Figure 36a. Variation of the activity of the free enzyme and the immobilized enzyme on storage at 5°C and at pH 5.87
○ free enzyme
□ immobilized enzyme

b. Activity of β-glucosidase after incubation at 45°C and at pH = 5.87
○ free enzyme
□ immobilized enzyme

c. Variation of activity with operation time for the enzyme-tube used for kinetic measurements at temperatures up to 45°C.

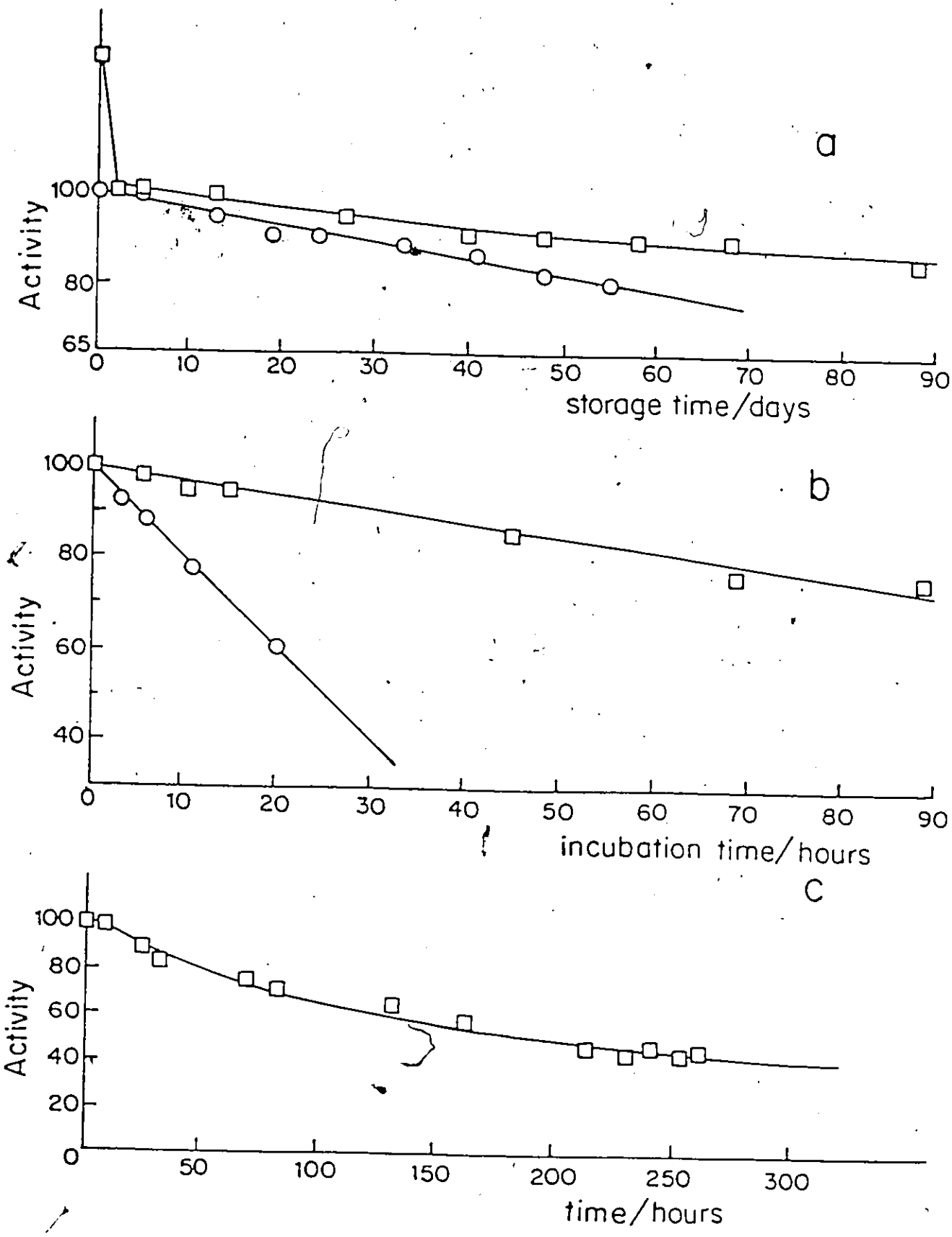
a
Activity
100
80
65
0
10
20
30
40
50
60
70
80
90
storage time/days
b
Activity
100
80
60
40
0
10
20
30
40
50
60
70
80
90
incubation time/hours
c
Activity
100
80
60
40
20
0
50
100
150
200
250
300
time/hours

hydrolysis at pH 5.87, at a temperature of 25.0°C and at a flow rate of 2.74 cm s^{-1}, of cellobiose at a concentration of 5.99 mM. The results, for both the immobilized enzyme and the free enzyme, are shown in Figure 36a. During the first two days the activity of the immobilized enzyme decreased by about 22%, presumably due to detachment of loosely-bound enzyme. After that the activity decreased about half as rapidly as that of the free enzyme. After 55 days, the solution of free enzyme became cloudy, while the activity of the immobilized enzyme is 90%, indicating that the immobilization makes the enzyme more stable.

Figure 36b shows corresponding plots for storage at 45°C. The loss of activity is, of course, much more rapid, but the enzyme attached to the tube is again substantially more stable than the free enzyme. An improvement in thermal stability of enzyme upon immobilization is not attained with all enzymes and immobilization methods. The present immobilization technique singificantly improves the thermal stability of the enzyme.

Reusage stability

Figure 36c shows the plot of variation of activity during the performance of kinetic measurements for enzyme-tube which has been maintained when not in use at 5°C, but which has been used for kinetic measurements at temperature up to 45°C. The rate of loss is now greater than for continuous storage. The half life of the enzyme tube is about 200 hours. In view of the much smaller decrease in activity during the storage without usage, the

decrease of activity with the reuse time may indicate some inactivation of β-glucosidase by the substrate cellobiose.

Thermal stability

Fig.37 gives the effect of temperature on the activity of immobilized enzyme. The optimum temperature is about 65°C, but the activities at temperatures 74°C and 85.5°C are still high.

The immobilization has brought about a significant improvement in stability, and the technical application of this type of immobilized β-glucosidase is therefore promising. Since the system can be used a considerable number of times before becoming ineffective, it offers considerable improvement over the use of the enzyme in a batch system.

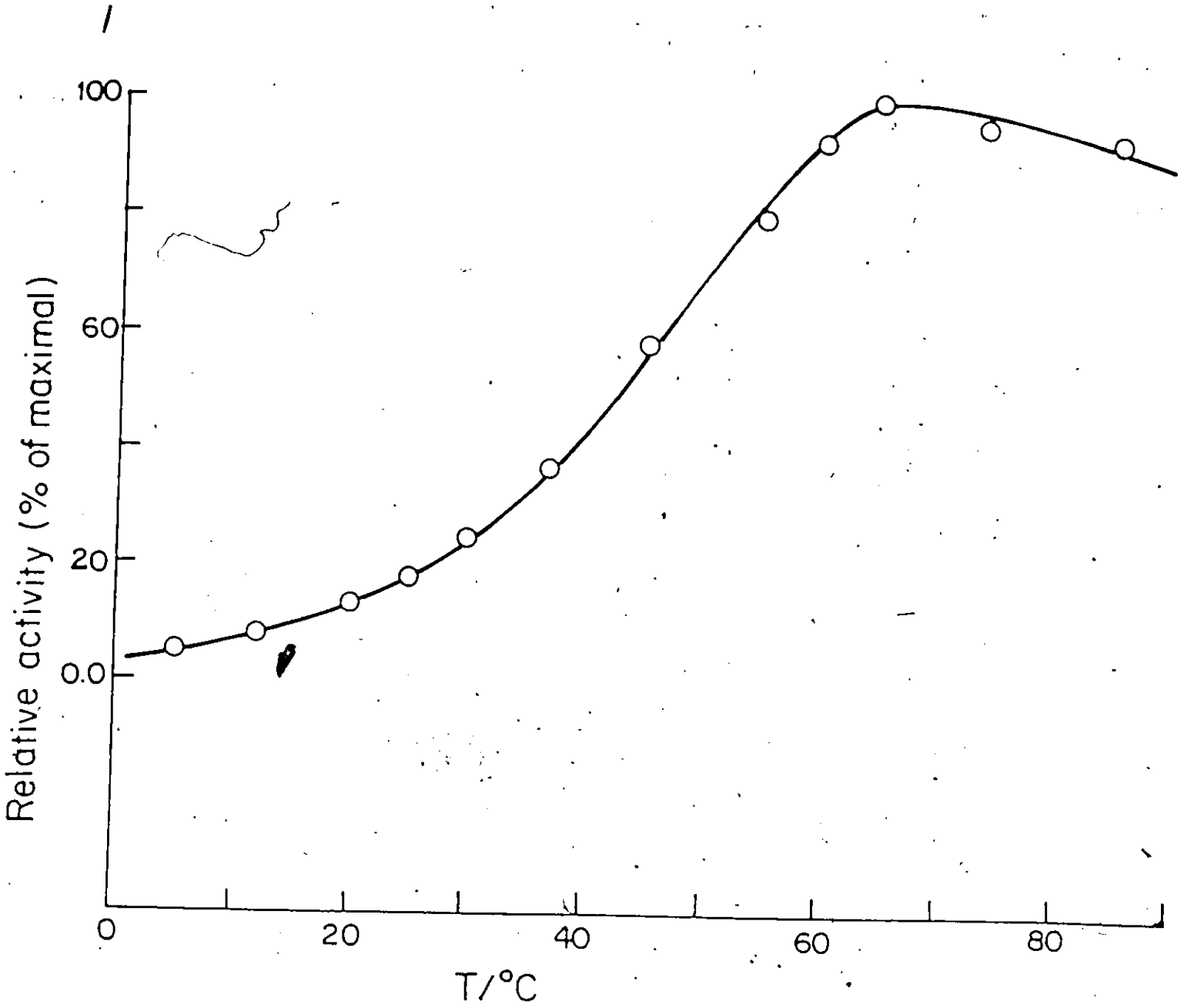

Figure 37. Effect of temperature on the activity of immobilized β-glucosidase

CHAPTER VIII

PH AND TEMPERATURE EFFECTS ON THE KINETICS OF IMMOBILIZED β-GLUCOSIDASE

8.1 Introduction

In general, the influence of pH on the rates of enzyme reactions will be different for an immobilized enzyme compared with an enzyme in free solution, due to microenvironmental effects caused by electrostatic, partitioning and diffusional effects.

Goldstein, Levin, and Katchalski(28) treated the problem in terms of the distribution of hydrogen ions between the bulk solution and the support, and developed a quantitative treatment for the situation in which the support contains ionizing groups and bears an electrostatic charge. The relative concentration of hydrogen ions in the near neighbourhood of a charged support will be different from that of the solution because of the electrostatic interaction between the charge on the support and the hydrogen ions. If the support is positively charged, the hydrogen-ion concentration will be lower than in the bulk of the solution, whereas if the support is negative the hydrogen ion concentration will be higher. Thus the enzyme attached on the charged support will be exposed to a pH which is different from that in the bulk of the solution; therefore the pH-activity profile for the immobilized enzyme should be shifted towards

higher or lower pH values, depending on whether the support is negatively or positively charged(94). This is also important if the enzyme-catalyzed reaction produces or consumes protons(129). When the acid is being produced or consumed, the pH in the vicinity of the enzyme active-site will be lower or higher than in the bulk solution so that the pH profile will be displaced.

The local electrostatic effects also cause a shift in pK values. Due to electrostatic interaction the excess of negatively charged groups on the support will decrease the acid dissociation constants of active groups of the enzyme and increase the pK values, while the positive groups on the support will reduce the pK values(129).

The studies of temperature effects on the kinetics of immobilized enzymes are very useful in estimating the extent of diffusion contol. Activation energies for diffusion in water lie within a certain narrow range, and may differ from those for the chemical interaction. Therefore, an analysis of the temperature dependence with an immobilized enzyme under different conditions can provide information about the reaction mechanism. These studies are also important for the design of enzyme reactions for practical purposes.

In Chapter VII, the flow kinetics of the immobilized β-glucosidase has been presented at a single pH of 5.87 and at a single temperature of 25°C. This chapter discusses the kinetic results obtained over a pH range of 4.44 to 6.82 and a temperature range from 5°C to 45°C.

8.2 Experimental

The methods for the kinetic measurements were essentially the same as described in Chapter VII; the thermostatted substrate solution was passed through the coiled enzyme tube in a temperature-controlled waterbath and the product was collected at the other end of the tube, and analyzed spectrophotometrically by use of ATP, hexokinase coupled with glucose-6-phosphate dehydrogenase and NADP. For studies of pH effects, the reaction rates were measured at seven different pH values from 4.44 to 6.82 and at a temperature of 25.0°C. The substrate concentrations range from 1.30 to 13.3 mM. For investigation of temperature effects, the rate measurements were carried out at seven different temperatures ranging from 5°C to 45°C, and over a range of substrate concentration from 1.30 to 13.3 mM for pH 5.87, and at one substrate concentration 2.30 mM for pH 5.22 and pH 6.38. Since the kinetics of the present immobilized preparation is free from diffusion control, the reaction rate is independent of the flow rate of the substrate solution. All the kinetic measurements in the present studies were carried out at one flow rate in a range from 2.05 to 2.29 cm s^{-1}. The flow rate was determined for each run.

The same enzyme tube was used for all of the measurements.

The substrate solutions were prepared in two different buffer systems according to the pH values desired. In the pH range of 4.44 to 5.59, 0.2 M acetate-acetic acid was used as buffer, while for pH values above 5.60, 0.1 M phosphate buffer was used.

8.3 Results and discussion of pH effects

Lineweaver-Burk plots

Reaction rates obtained at different pH values for various substrate concentrations are given in Table 17; Figure 38 shows the plot of apparent rate against pH. The shape of these curves is similar to that for the free enzyme.

Table 18 shows values of inherent Michaelis constants K_m' and inherent limiting rates V' at 25.0°C and at different pH values, obtained from Lineweaver-Burk plots shown in Figure 39. For comparison the values of the Michaelis parameters for the free enzyme are also given in Table 18. An inefficient immobilized enzyme system has a K_m(app) value much larger, sometimes by several orders of magnitude, than that for the enzyme in free solution. The fact that, for the present immobilized preparation these values of K_m' are not much larger than those for the free enzyme shows that the present system is quite efficient.

The pattern of pH behaviour

The pH dependences of the Michaelis parameters V' and V'/K_m', expressed as percentage of the corresponding value at optimum pH, are shown in Figure 40, with the curves for the free enzyme superimposed. The optimum pH, for immobilized β-glucosidase, is about 5.9, about 0.3 units higher than the values for the free enzyme. In addition there is a small change in the pattern of the pH curves, in that at low pH the relative rates are higher for the immobilized enzyme, while at high pH the relative rates are

Table 17.

Product concentrations and apparent reaction rates for immobilized β-glucosidase at different substrate concentrations and at different pH values

$T = 25.0^{o}C$; v_f = 2.08 to 2.23 $cm \cdot s^{-1}$

pH	4.44	4.82	5.21	5.59	5.87	6.27	6.82
[S]/mM	$[P]_e/\mu M$						
1.30	7.69	9.90	11.7	13.9	16.3	11.9	6.50
1.82	10.5	14.4	17.9	19.0	22.0	16.4	8.85
3.00	17.3	20.8	27.6	29.2	35.4	27.2	13.8
4.17	22.0	28.4	38.7	41.6	47.1	34.1	18.6
7.49	31.5	53.0	63.4	71.8	83.3	60.1	29.4
	$v/\mu M\ s^{-1}$						
1.30	0.165	0.208	0.241	0.290	0.336	0.256	0.136
1.82	0.228	0.301	0.371	0.404	0.465	0.353	0.188
3.00	0.372	0.432	0.573	0.618	0.738	0.585	0.293
4.17	0.486	0.587	0.807	0.877	0.982	0.733	0.394
7.49	0.697	1.09	1.31	1.51	1.74	1.28	0.621

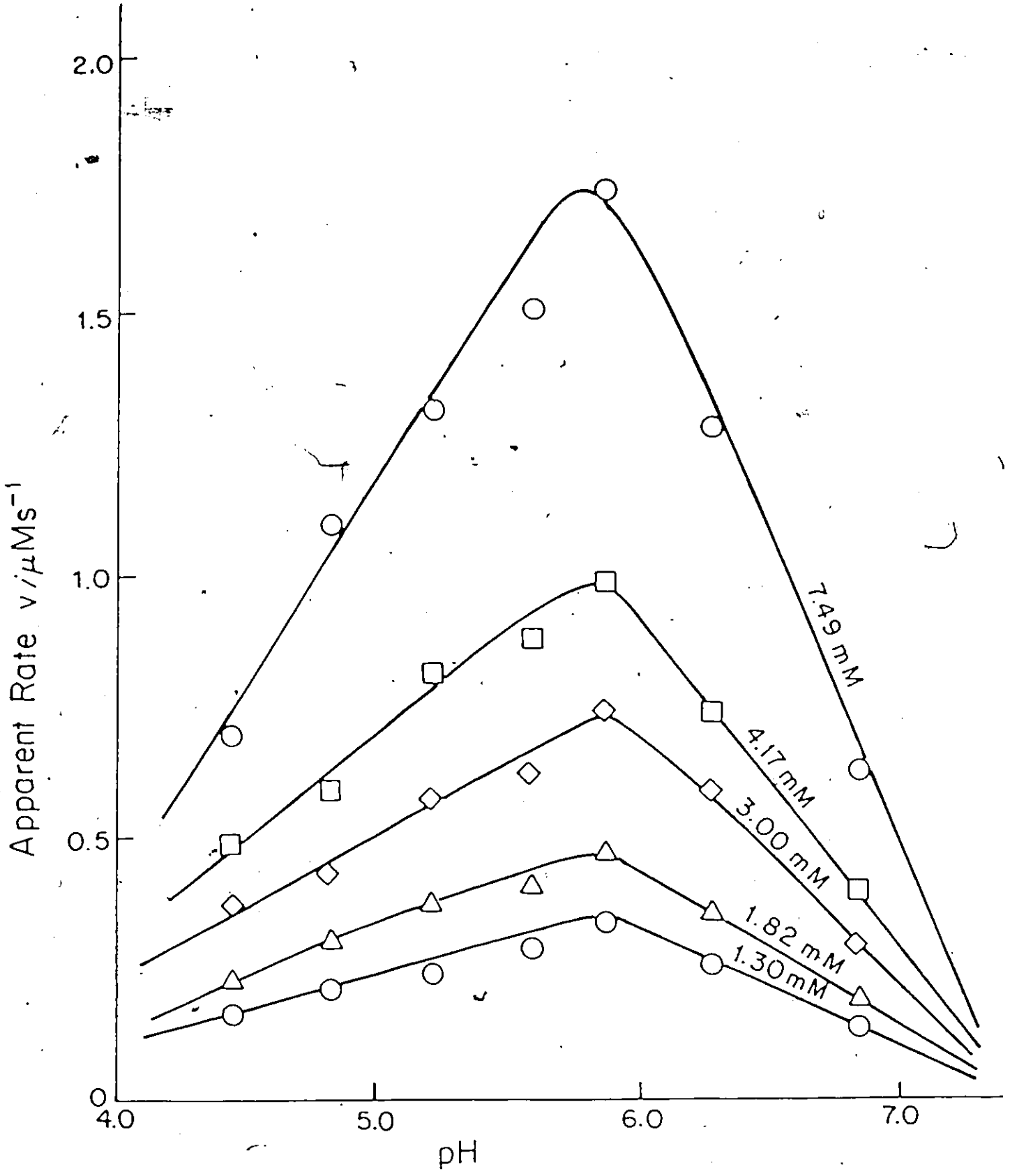

Figure 38. pH dependence of apparent rates at 25.0°C and at different substrate concentrations, as indicated for immobilized β-glucosidase at flow rates from 2.05 to 2.16 cm s^{-1}

Table 18.

Michaelis parameters for free and immobilized β-glucosidase at various pH values; T = 25.0°C; percentage error in both V' and K'_m < ± 6%

β-glucosidase immobilized on nylon tube			β-glucosidase in free solution		
pH	$V/\mu m \cdot s^{-1}$	K'_m/mM	pH	$V/\mu m \cdot s^{-1}$	K_m/mM
4.44	3.42	25.5	5.00	0.667	5.38
4.82	4.70	27.6	5.32	0.952	5.80
5.21	7.14	33.4	5.53	1.25	6.60
5.59	9.09	37.0	5.92	0.980	7.05
5.87	9.43	35.2	6.19	0.870	7.62
6.27	6.49	31.7	6.48	0.714	7.93
6.82	3.14	28.6	6.90	0.606	12.0

The errors were obtained in the same way as for the values for the free enzyme (Table 11).

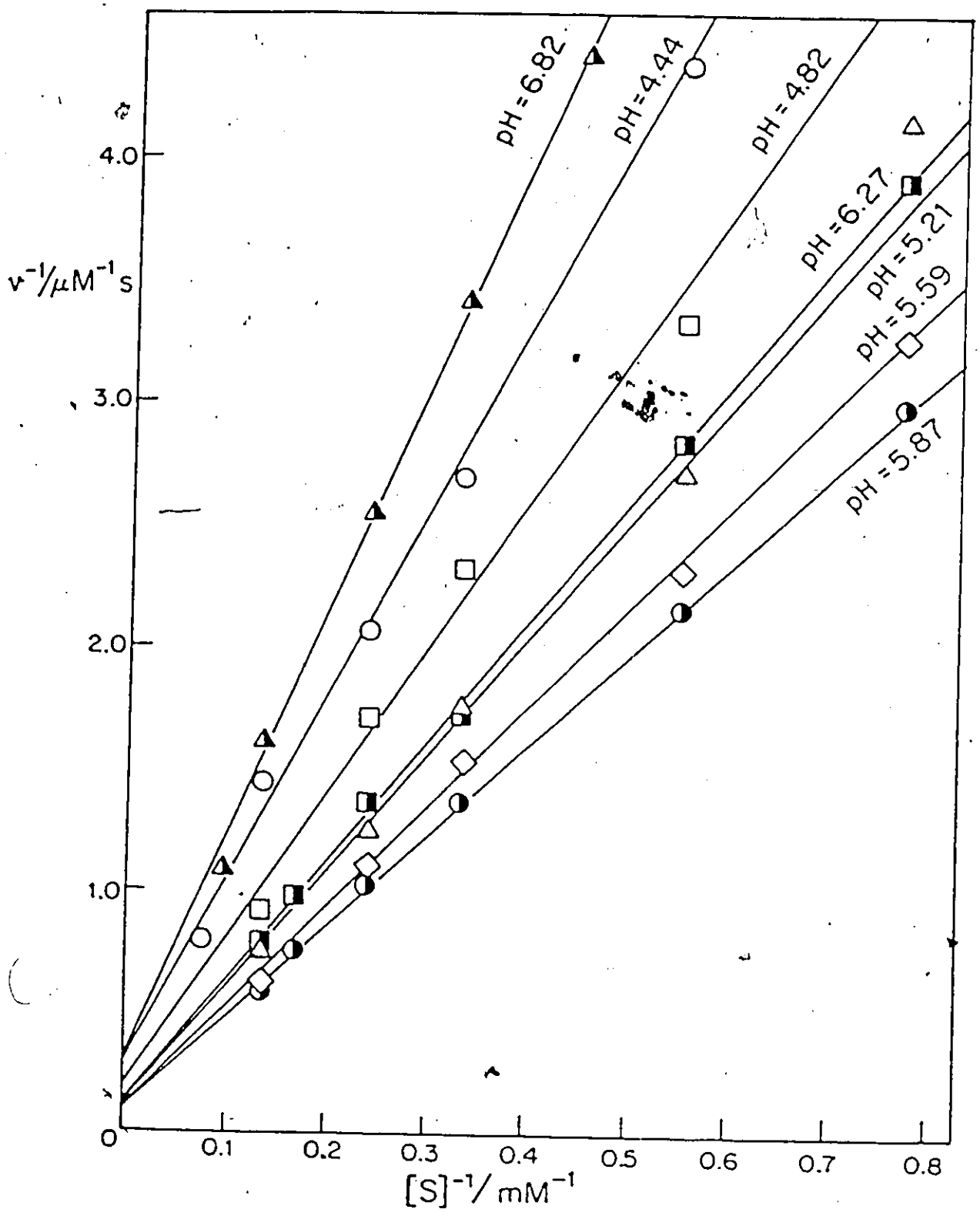

Figure 39. Lineweaver-Burk plots of 1/v against 1/[S] for immobilized β-glucosidase; T = 25.0°C; pH values as indicated

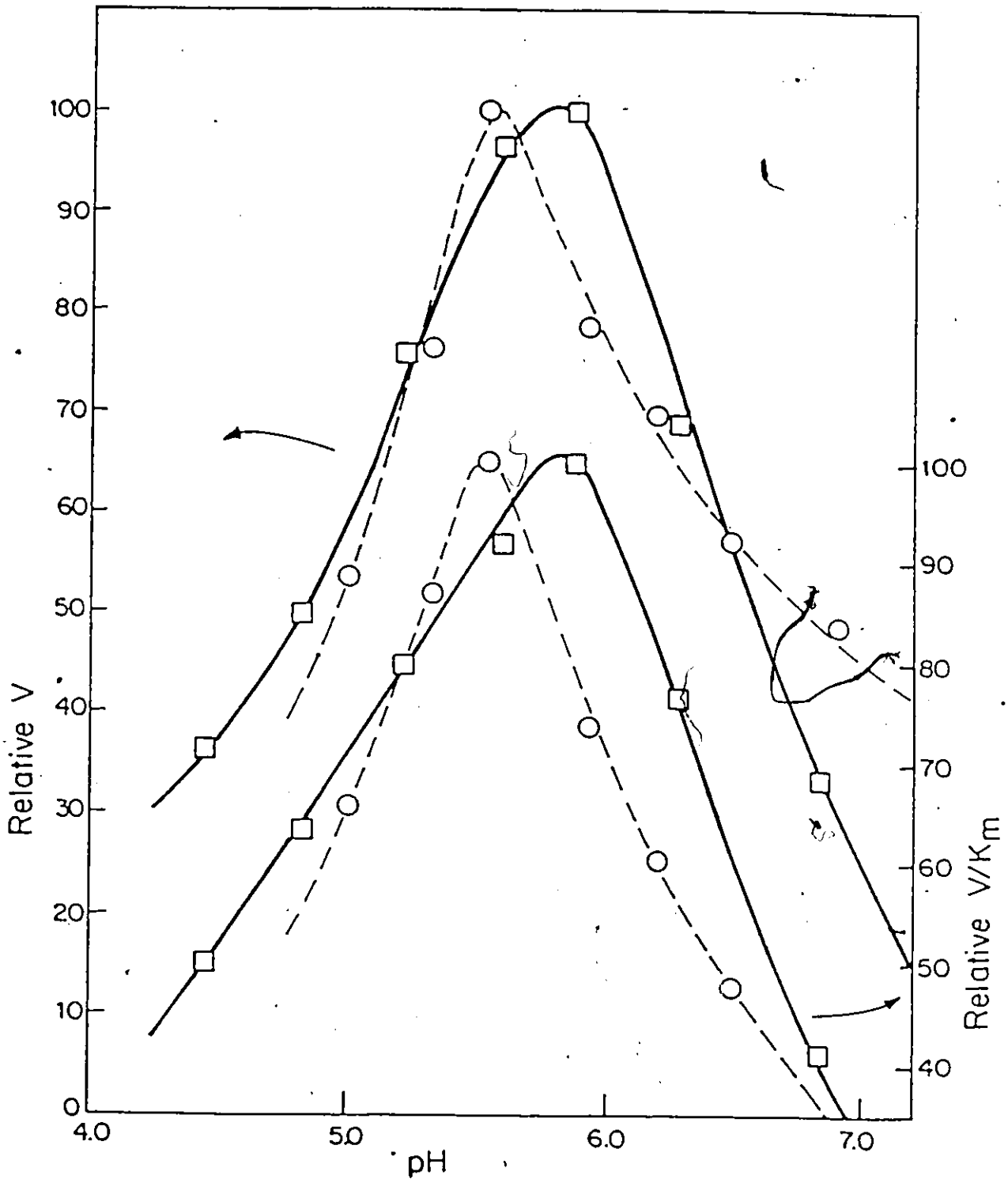

Figure 40. The pH dependence of V' and of V'/K_m' for the immobilized enzyme (□) and the free enzyme (o); T=25.0°C.

lower, compared with the free enzyme.

This difference between the free and immobilized enzyme may be caused by microenvironmental pH effects due to a slight positive residual charge on the surface of the support. The positive charge repels hydrogen ions from the surface and therefore causes the local pH near the surface to be higher than the value measured in the bulk of the solution. At low pH values this increase of local pH increases the rates, as observed. At high pH values the effect is to lower the rates. A similar result was also found by Bissett and Sternberg(19) with β-glucosidase attached to chitosan. At lower pH values the amino groups of the chitosan matrix were protonated, thereby attracting hydroxyl ions which caused the microenvironmental pH near the matrix to be higher than in the bulk solution; this resulted in stabilization and thus greater activity of the immobilized enzyme at lower pH values. Ngo and Laidler(180), for the acetylcholinesterase system, observed a similar effect which was also attributed to changes in the local pH at a surface, but there it was due to acid liberated in the reaction.

Ionization constants of catalytically active groups

The pK values for immobilized enzyme, calculated from Michaelis parameters V' and V'/K_m' by use of the computerized procedure described in Chapter III, are given in Table 19 where they are compared with the values for the free enzyme. The pK values are slightly lowered as a result of the immobilization.

Table 19.

Dissociation Constants obtained by use of statistical procedures for immobilized β-glucosidase
T = 25.0°C
(error in pK_a and $pK_b \leqslant \pm 0.1$)

	Immobilized β-glucosidase	Free enzyme
pK_b	4.5	4.9
pK_a	6.6	6.4
pK'_b	4.8	5.0
pK'_a	6.4	6.5

The errors were obtained in the same way as for the values for the free enzyme (Table 8).

This result is consistent with there being a small positive residual charge on the surface. The repulsion of hydrogen ions by the positive residual charge of the surface makes it easier for the proton ionizations to occur, and therefore increases the dissociation constants and lowers the pK values.

A similar effect, the perturbation of the dissociation constant of an active group due to the microenvironmental charge, has been found with the enzyme chymotrypsin. By chemical modification, the conversion of 14 positively charged lysines on the enzyme surface to negatively charged carboxylates causes the pK_a to increase from 7.0 to 8.0, while the conversion of 13 negatively charged surface carboxyls to positively charged amines lowers the pK_a to 6.1. Similarly the acylation of the surface amino groups of trypsin causes an increase of 0.2 units in the pK_a of the free enzyme, These are summarized in the Table 20 (186). Here the change of the dissociation constants of the active groups is due to the charge on the surface of the enzyme molecule itself, and not to the surface charge of the support, but the effects are similar.

Table 20.

Influence of surface charge on pK_a

Enzyme	Modification	pK_a	k_c/s^{-1}
Chymotrypsin	---	7.0*	47
Succiny-chymotrypsin	$Lys(-NH_3^+) \longrightarrow -NHOCCH_2CH_2COO^-$	8.0*	74
Ethylenediamine-chymotrypsin	$Asp,Glu(-CO_2^-) \longrightarrow -CONH(CH_2)_2NH_3^+$	6.1*	50
Trypsin	---	7.0**	0.7
Acetyl-typsin	$Lys(-NH_3^+) \longrightarrow -NHCOCH_3$	7.2**	1.2

* The pK_a for k_c for the hydrolysis of acetyl-L-tryptophan-methyl ester

** The pK_a for k_c/K_m for the hydrolysis of benzoyl-L-arginine amide.

8.4 Results and discussion of temperature effects

Arrhenius plots of apparent rate

Figure 41 shows the temperature dependence of apparent reaction rates in the Arrhenius form, for immobilized enzyme at pH value of 5.87 and at different substrate concentrations; these data are given in Table 21. As with the free enzyme these plots show a slight change in slope at about 22°C. The inherent Michaelis parameters V' and K_m' at pH 5.87 and at different temperatures, obtained from Lineweaver-Burk plots in Figure 42, are given in Table 22; the Arrhenius plots of $\log_{10}V'$ and $\log_{10}V'/K_m'$ are shown in Figure 43. Again there is an intersection at 22°C in both curves. Similar behaviour was shown at other pH values. Figure 44 shows plots of $\log_{10}v$ against 1/T for pH values of 5.22 and 6.38; here v is the apparent rate measured at substrate concentration of 3.00 mM and its values are listed in Table 23. In all cases there is an intersection at about 22°C.

Activation energies

Table 24 shows the activation energies obtained at pH 5.87 and the corresponding values obtained for the free enzyme. The subscript c indicates the activation energy corresponding to V', and o that corresponding to V'/K_m'; the subscript h indicates the activation energy in the higher temperature range and l that in the lower temperature range. The fact that the activation energies for the immobilized enzyme are very close to that obtained for the free enzyme confirms further the conclusion that

Table 21.

Product concentrations and apparent reaction rates for immobilized β-glucosidase at different substrate concentrations and at different temperatures

pH = 5.87 ; v_f = 2.08 to 2.23 cm s^{-1}

T/°C	5	12	20	25	30	37	45
[S]/ mM	$[P]_e$/μM						
1.30	4.58	6.94	12.0	15.8	21.0	33.3	47.9
1.82	5.66	8.98	15.6	21.2	28.9	43.2	66.7
3.00	9.74	15.0	23.9	35.4	46.9	70.0	107
4.17	12.8	19.0	33.5	52.4	63.4	97.9	146
7.49	21.1	36.3	58.8	84.2	116	174	254
	v/μM s^{-1}						
1.30	0.094	0.147	0.258	0.339	0.460	0.736	1.07
1.82	0.122	0.198	0.345	0.470	0.637	0.956	1.48
3.00	0.203	0.326	0.535	0.737	1.02	1.52	2.40
4.17	0.284	0.423	0.747	1.09	1.35	2.10	3.14
7.49	0.462	0.797	1.30	1.86	2.57	3.87	5.68

Figure 41. Temperature dependence of apparent reaction rate for immobilized β-glucosidase at different substrate concentrations; pH = 5.87 and at flow rates from 2.08 to 2.23 cm s^{-1}.

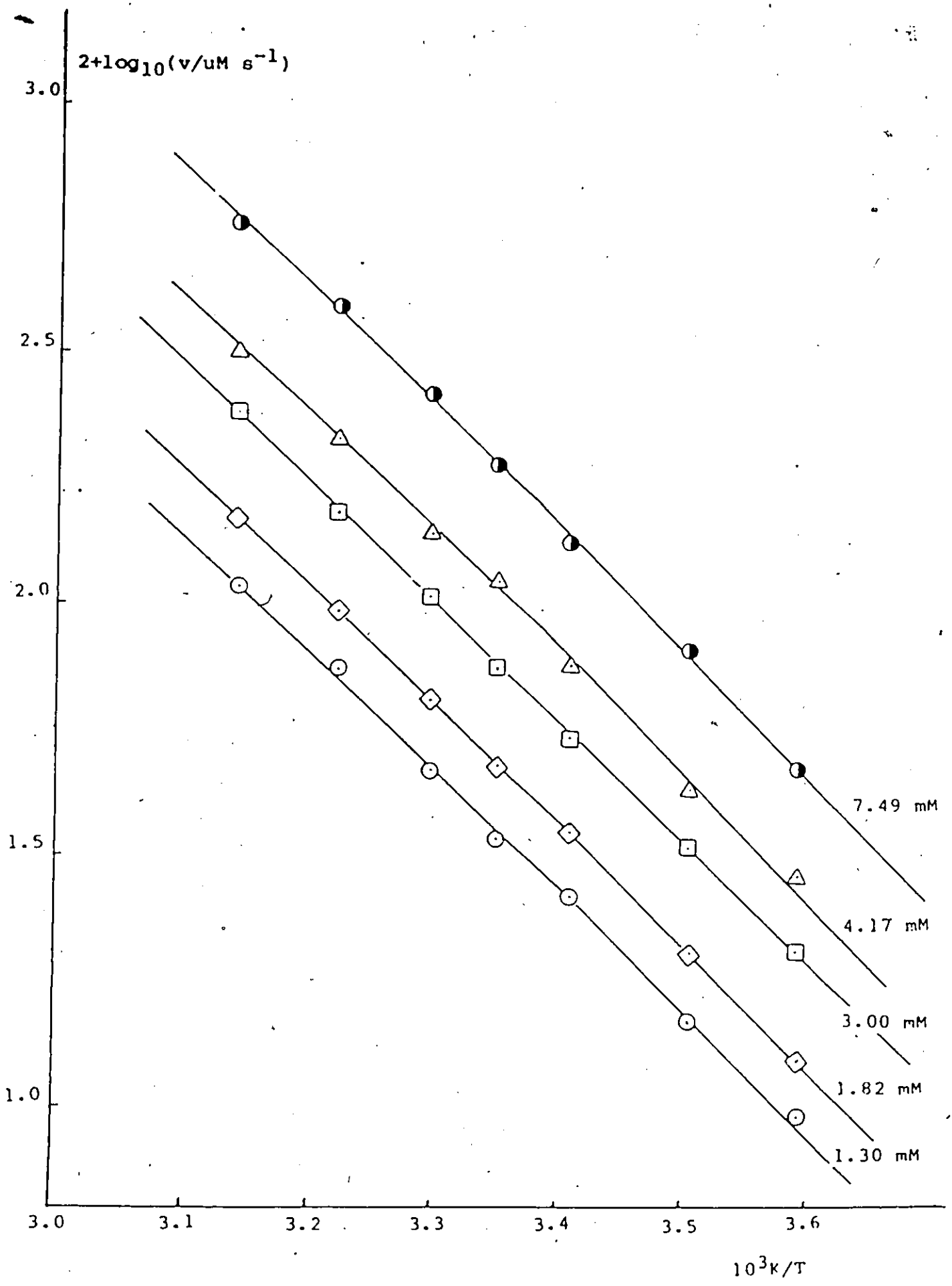
2+log10(v/uM s-1)
3.0
2.5
2.0
1.5
1.0
7.49 mM
4.17 mM
3.00 mM
1.82 mM
1.30 mM
3.0
3.1
3.2
3.3
3.4
3.5
3.6
10³K/T

Figure 42. Lineweaver-Burk plots of immobilized ß-glucosidase at pH = 5.87 and at various temperatures as indicated.

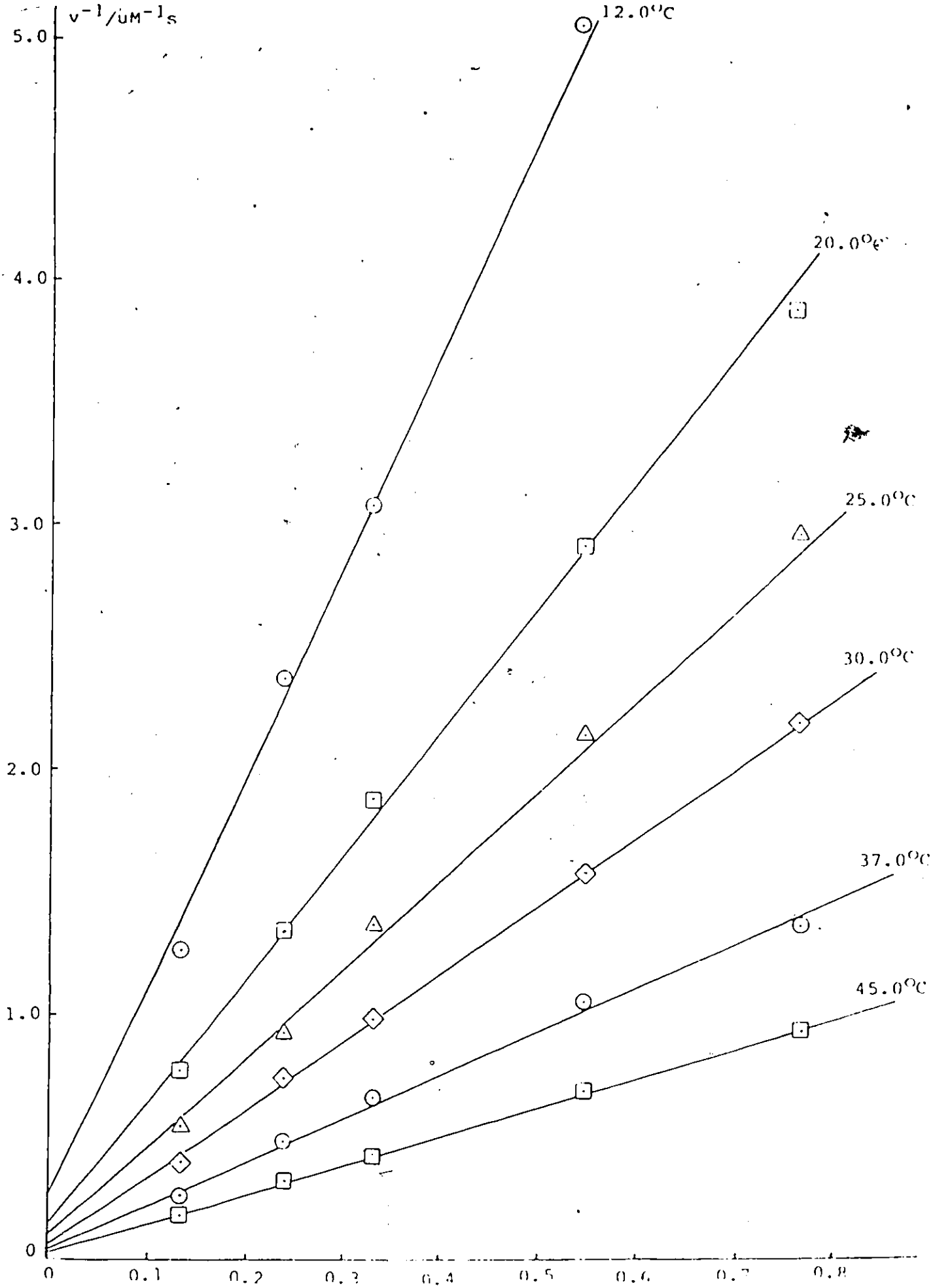
$v^{-1}/\mu M^{-1}s$
5.0
4.0
3.0
2.0
1.0
0
0
0.1
0.2
0.3
0.4
0.5
0.6
0.7
0.8
12.0°C
20.0°C
25.0°C
30.0°C
37.0°C
45.0°C

Table 22.

Inherent Michaelis parameters for immobilized β-glucosidase at various temperatures

pH = 5.87

(percentage error in both V' and K_m' $\lesssim \pm 5\%$)

T/°C	5	12	20	25	30	37	45
$V'/\mu Ms^{-1}$	2.38	3.85	6.67	9.52	13.3	21.3	29.4
K_m'/mM	31.9	32.9	33.5	34.8	36.4	37.4	34.4

The error was estimated in the same way as for the free enzyme (Table 7).

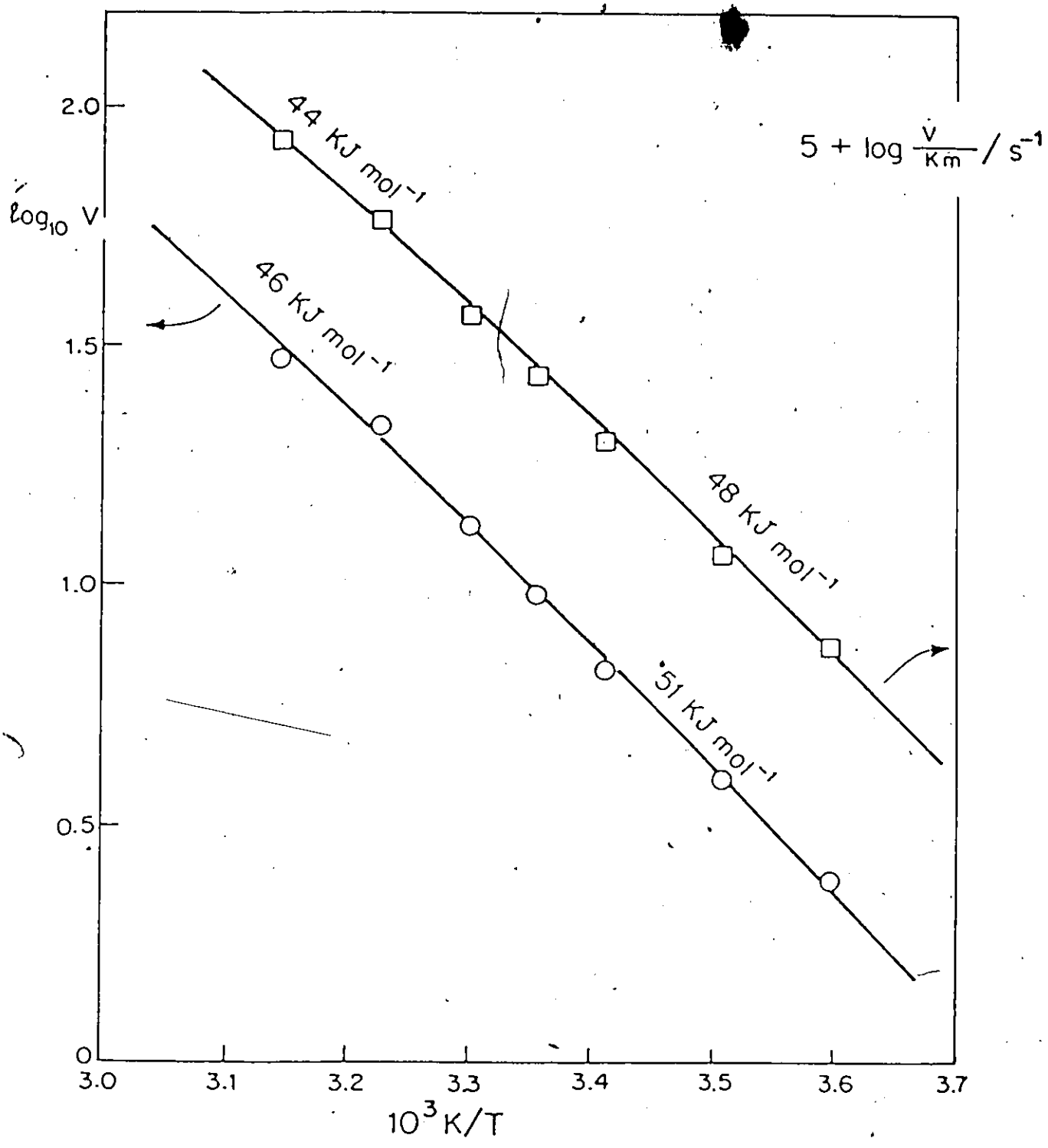

Figure 43. Arrhenius plots of inherent Michaelis parameters V' and V'/K_m' at pH 5.87

Table 23.

Apparent reaction rates of immobilized β-glucosidase at different temperatures for pH values of 5.22 and 6.38

$[S] = 3.00$ mM

pH	5.22		6.38	
T/°C	$[P]_e/\mu M$	$v/\mu Ms^{-1}$	$[P]_e/\mu M$	$v/\mu Ms^{-1}$
5	4.94	0.109	5.26	0.120
12	8.82	0.195	9.23	0.211
20	17.2	0.382	17.3	0.395
25	25.5	0.567	21.6	0.495
30	37.8	0.836	30.9	0.704
37	56.4	1.26	44.9	1.03
45	81.4	1.82	66.0	1.51

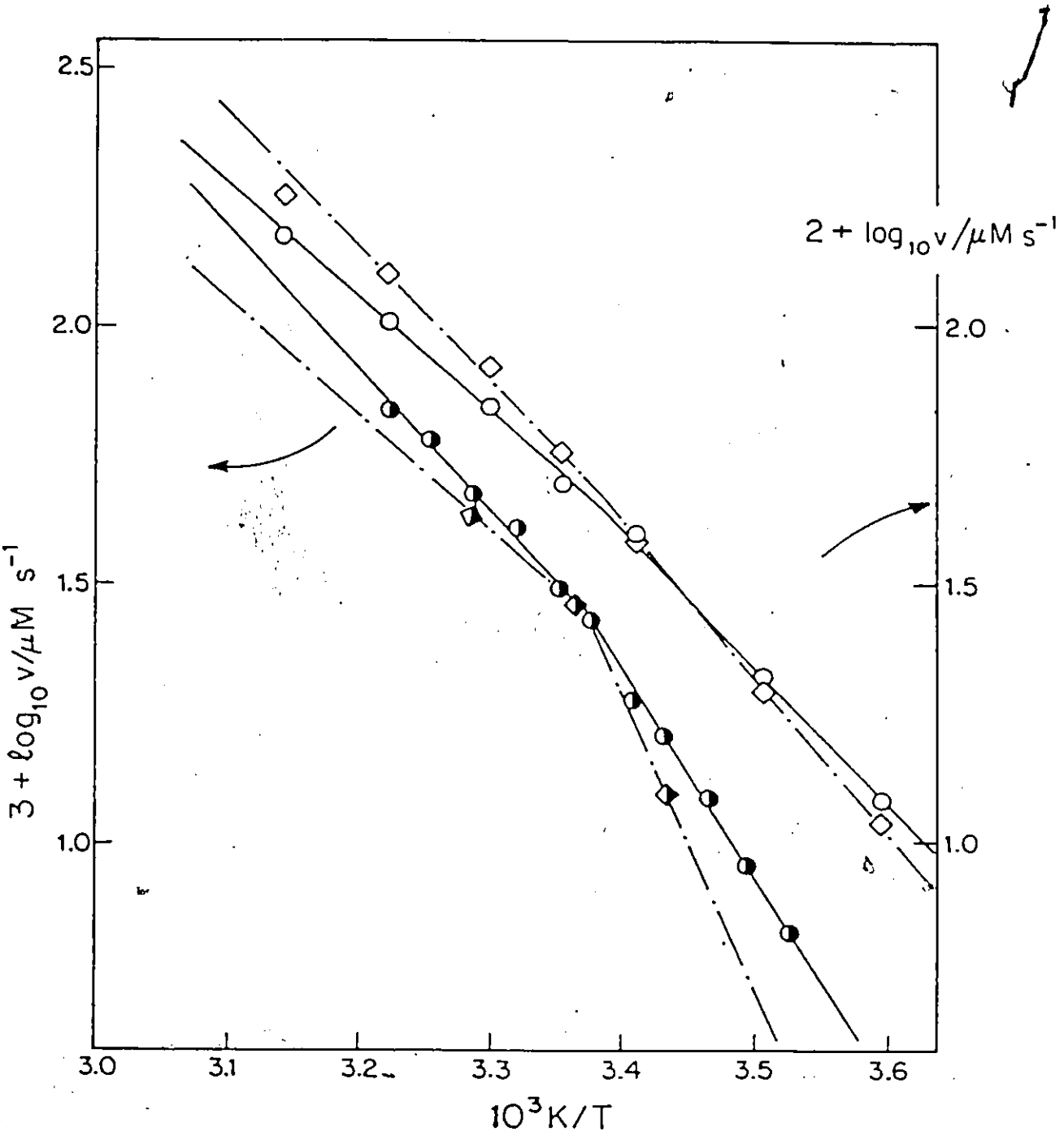

Figure 44. Plots of $\log_{10} v$ against 1/T. The upper curves relate to the immobilized enzyme and to the right-hand scale; ○, pH = 6.38 and [S] = 3.00 mM; ◇, pH = 5.22 and [S] = 3.00 mM. The lower curves are for the free enzyme ([E] = 0.1 mg mL^{-1}) and relate to the left-hand scale; ◑, pH = 6.39 and [S] = 0.299 mM; ◈, pH = 5.22 and [S] = 0.599 mM.

Table 24.

Activation energies, E/kJ mol^{-1}, for immobilized β-glucosidase and free enzyme.
Estimated error < ±6%

	immobilized enzyme	free enzyme	
	pH 5.87	pH 5.76	pH 6.19
E_{ch}	46.4	44	42
E_{cl}	50.5	49	55
E_{oh}	43.7	44	47
E_{ol}	48.3	70	65

Subscripts: c activation energy for V'
o activation energy for V'/K_m'
h higher temperature range
l lower temperature range

The error was estimated in the same way as for the free enzyme (Table 12).

there is no diffusion control in the kinetics of the present immobilized preparation.

For the free enzyme it was shown previously (Chapter V) that the changes in slope in the Arrhenius plots, at a temperature of about 23°C, become much more pronounced as the pH is either raised or lowered from the optimum value. This is clearly demonstrated in Figure 21 of Chapter V which shows that activation energies in the high and low temperature ranges come very close together at a pH of about 5.9, and diverge at higher and at lower values. A similar effect was found in the present work on the immobilized enzyme. The changes in slope shown in Figure 43 for a pH value of 5.87, the optimum pH for immobilized enzyme, are not very pronounced. By contrast, in Figure 44 in the plots of $\log_{10} v$ against 1/T for pH values of 5.22 and 6.38, the changes in slope are substantially more marked than at pH 5.87. In order to compare the behaviour of immobilized enzyme with free enzyme, the corresponding curves for the free enzyme are also presented in Figure 44. The apparent activation energies obtained from these data are given in Table 25. The interpretation for the changes in slope and for the variation of activation energy with pH has been discussed in some detail for the free enzyme in Chapter V and VI.

8.5 Conclusions

This investigation has shown that the immobilization has not brought about any important changes as far as the catalytic

Table 25.

Activation energies, E/kJ mol^{-1}, obtained from apparent reaction rates for pH = 5.22 and pH = 6.39
Estimated error < ± 6%

pH	immobilized enzyme		free enzyme	
	E_h^*	E_l^*	E_h^{**}	E_l^{***}
5.22	50.6	58.1	43.3	110
6.39	42.7	51.3	52.9	76.8

Subscripts : h higher temperature range

l lower temperature range

rates were measured at

* [S] = 3.00 mM

** [S] = 0.299 mM

*** [S] = 0.599 mM

The error was estimated in the same way as for the free enzyme (Table 12).

activity of the enzyme is concerned. The activity is still due largely to chemical effects, with negligible diffusion control, and the pH dependence remains much the same. The activation energies were not changed significantly, and the activation energy varies with pH in a similar way. The kinetics of cellobiose hydrolysis by the immobilized enzyme is similar to that by the free enzyme, indicating that the procedure used in the present work of immobilization of β-glucosidase on nylon tubing is quite efficient; the coupling process has very little influence on this aspect of the kinetic behaviour of the enzyme.

The immobilization has, however, brought about a significant improvement in stability, and the immobilized preparation can be used repeatedly for a considerable number of times. The utilization of β-glucosidase immobilized on nylon tubing in the saccharification of cellulose with cellulase enzymes is therefore promising. Absolute rates of hydrolysis could easily be increased by attaching more enzyme to a given surface area, or by increasing the surface area. The latter can be effected by increasing the length of the tube, or better by passing the substrate solution through a group of tubes in parallel.

CLAIMS TO ORIGINAL RESEARCH

1. A new method, which involves only one step and allows the reaction to be followed continuously, was developed for the kinetic studies of the hydrolysis of cellobiose catalyzed by β-glucosidase; a coupled system containing ATP, hexokinase, glucose-6-phosphate dehydrogenase and NADP was employed for the continuous spectrophotometric determination of the product glucose.

2. Two procedures, the glucose-concentration method ('GCM') and the glucose-slope-method ('GSM'), were devised for calculating the initial rates of the enzyme reaction under different conditions. At pH values above 6.2, where the enzyme reaction is the rate-determining step, the initial rates were calculated from the initial slopes of the corresponding absorbance-time curves by use of the conventional calibration curve with the absorbance plotted against the glucose concentration (the glucose concentration method). At pH values below 6.2, where the enzyme reaction is not the rate-controlling step, the initial rates were calculated by the glucose slope method, which involves obtaining an average rate at a sufficiently short period of time by use of an alternative type of calibration curve with initial slope of absorbance-time curves plotted against concentration. This type of calibration curve was proposed for the first time.

3. The pH-dependence of β-glucosidase kinetics was investigated

at three temperatures, 18°, 24° and 31°C. The dissociation constants for two ionizing groups involved in the enzymic catalysis were determined at these temperatures by a computerized least-squares procedure.

4. Temperature effects on the kinetics of the hydrolysis of cellobiose by β-glucosidase were studied at different pH values ranging from 5.0 to 7.0. There is consistently an intersection at about 23°C in Arrhenius plots of initial rates and of Michaelis parameters. The present study is the first to determine activation energies over a pH range and to investigate the variation of activation energy with pH for any enzyme system.

5. Theories of enzyme kinetics have so far dealt only with pH effects or with temperature effects; cooperation between both temperature and pH effects on the rates of enzyme-catalyzed reactions has not been considered. In the present work, both effects were considered together and a unified treatment of pH and temperature effects was presented to interpret the Arrhenius behaviour and the dependence of activation energy with the pH. Equations were obtained which indicate how the apparent activation energy varies with pH and temperature, for one-intermediate and two-intermediate mechanisms.

6. A mechanism involving two intermediates was first proposed for the hydrolysis of cellobiose by β-glucosidase. A successive approximation procedure was employed to estimate the values of

the activation energies and preexponential factors for individual steps, which provide good quantitative agreement with experiment.

7. Enthalpy and entropy changes have been measured for the ionization processes of catalytically active groups. The present work was the first to measure the thermodynamic parameters of the ionization processes from the temperature effects on the dissociation constants for any enzyme system.

8. β-glucosidase has been chemically attached to the inner surface of nylon tubing, and the detailed flow kinetics and stability have been studied for the first time.

9. Various tests suggested by the Kobayashi-Laidler theory showed that the extent of diffusion control was negligible.

10. The pH dependence of the Michaelis parameters for the immobilized enzyme has been studied.

11. Temperature effects on the kinetics of immobilized enzyme were investigated at several different pH values.

12. The kinetic behaviour of immobilized β-glucosidase indicated that the procedure of attachment of β-glucosidase on nylon tubing is quite efficient; the coupling process has very little influence on the function and activity of the enzyme.

REFERENCES

1. Eriksson, K. E. and Pettersson, B. (1975) Eur. J. Biochem. 51, 193-206.

2. Eriksson, K. E. and Pettersson, B. (1975) Eur. J. Biochem. 51, 213-218.

3. Pettersson, L. G. (1975) In Symposium on Enzymatic Hydrolysis of Cellulose (Edited by Bailey, M., Enari, T. M. and Linko, M.) pp.255-261. Helsinki, Finland.

4. Wood, T. M. and McCrae, S. I. (1972) Biochem. J. 128, 1183-1192.

5. Wood, T. M. and McCrae, S. I. (1975) In Symposium on Enzymatic Hydrolysis of Cellulose (Edited by Bailey, M., Enari, T. M. and Linko, M.) pp. 319-336. Helsinki, Finland.

6. Sadana, J. C., Lachke, A. H. and Patil, R. V. (1984) Carbohydr. Res. 133(2), 297-312.

7. Bergheim, L. E. R. and Pettersson, L. G. (1974) Eur. J. Biochem. 46, 295-305.

8. Halliwell, G. and Vincent, R. (1977) In Bioconversion of Cellulosic Substances into Energy, Chemicals and Microbial Protein (Edited by Ghose, T.K.) pp.413-434. Aroon Pureat Thomas Press, India.

9. Enari,Tor-Magnus and Nybergh, Paula M. A. (1979) Kemia-Kemi 6(6), 301-302. C.A. 91, 170462y (1979).

10. Shewale, J. G. (1982) Int. J. Biochem. 14, 435-443.

11. Rabirovich, M. L., Klesov, A. A. and Berezin, I. V. (1979) Dokl. Akad. Nauk SSSR. 246(2), 500-504.

12. Sadana, J. C., Shewale, J. G., Patil, R. V. (1983) Carbohydr. Res. 118, 205-214.

13. Berghem, L. E. R., Pettersson, L. G. and Axiofedriksson, U. (1975) Eur. J. Biochem. 53, 55-62.

14. Focher, B., Marzetti, A., Sarto, V., Beltrane, P. L. and Carniti, P. (1981) Ekman-Days 1981, Int. Symp. Wood Puling Chem., 1981(5), 61-64. C.A. 95 128283y (1981).

15. Shewale, J. G., Sadana, J. C. (1981) Archs Biochem. Biophys. 207, 185-196.

16. Joglekar, A. V., Karanth, N. G. and Srinivasant, M. C. (1983) Enzyme Microbiol. Tech. 5, 25-29.

17. Sternberg, D., Vijayakumar, P. and Reese, E. T. (1977) Can. J. Microbiol. 23, 139-147.

18. Sundstrom, D. W., Klei, H. E., Coughlin, R. W., Biederman, G. J. and Brouwer, C. A. (1981) Biotech. Bioeng. 23, 473-485.

19. Bissett, F. H. and Sternberg, D. (1978) Appl. Environ. Microbiol. 35, 750-755.

20. Allen, A. L., Blodgett, C. R. and Nystrom, J. M. (1979) Proc. AIChE Symp. Ser. 75(184), 20-23.

21. Ghose, T. K. and Bisaria, V. S. (1979) Biotech. Bioeng. 21, 131-146.

22. Knapp, J. S. and Howell, J. A. (1980) Top. Enzyme Ferment. Biotechnol. 4, 85-143.

23. Jermyn, M. A. (1955) J. Biol. Sci. 8, 577-602.

24. Umezurike, C. M. (1971) Biochim. Biophys. Acta 227, 419-428.

25. Grover, A. K. and Cushley, R. J. (1977) Biochim. Biophys. Acta 482, 109-124.

26. Bruyne, C. K. K., Aerts, G. M. and Gussen, R. L. (1979) Eru. J. Biochem. 102, 257-267.

27. Anthony, M. and Coughlan, M. P. (1981) Biochim. Biophys. Acta, 662, 152-159.

28. Goldstein, L., Levin, Y. and Katchalski, E. (1964) Biochemistry, 3, 1913.

29. Woodward, J. and Alan Wiseman (1982) Enzyme Microbiol. Tech. 4, 73-79.

30. Rabinovich, M. L., Klesov, A. A. and Berezin, I. V. (1979) Dokl. Akad. Nauk SSSR 246(2), 500-504. C.A. 91, 86394 (1979).

31. Han, Y. W. and Srinivasan, V. R. (1969) J. Bact. 100, 1355-1363.

32. Duerksen, J. D. and Halvorson, H. (1958) J. Biol. Chem. 233 1113-1120.

33. Hultson, G. H. (1964) Biochem. J. 92, 142-146.

34. Deshpande, V., Eriksson, K. E. and Petterson, B. (1978) Eur. J. Biochem. 90, 191-198.

35. Daniels, L. B. and Glew, R. H. (1982) Clin. Chem. 28(4), 569-577.

36. Emert, G. H., Gum, E. K., Lang, J. A., Liu, T. H. and Brown, R. D. (1974) in Advances in Chemistry Ser. 136, pp. 79-100.

37. Herr, D., Baumer, F. and Dellweg, H. (1978) Eur. J. Appl. Microbiol. Biotechnol. 5, 29-36.

38. Hirayama, T. Horie, S., Nagayama, M. and Matsuda, K. (1978) J. Biochem. 84, 27-37.

39. Reese, E. T., Parrish, F. W. and Eitlinger, M. (1971) Carbohydr. Res. 18, 381-388.

40. Chibata, I. (1978) Immobilized Enzymes, Research and Development, Halsted Press Book and John Wiley & Sons. pp.10 .

41. Conchie, J., Gelman, A. L. and Levvy, G. A. (1967) Biochem. J. 103, 609-615.

42. Kelemen, M. V. and Whelan, W. J. (1966) Arch. Biochem. Biophys. 117, 423-428.

43. Van Opstal O., Aerts, G. M., Kersters-Hilderson, H. and De Bruyne, C. K. (1979) Arch. Int. Physiol. Biochim. 87 (4), 856-857.

44. Legler, G. and Harder, A. (1978) Biochim. Biophys. Acta, 524, 102-108.

45. Legler, G. (1979) Forschungsber. Landes Nordrhein-Westfalen. 2846, 32pp. C.A. 93, 2994w (1980).

46. Heyworth, R. and Walker, P. G. (1962) Biochem. J. 81, 331-335.

47. Kiss, Laszlo; Berki Lili K. and Nanasi, Pal; (1981) Biochem. Biophy. Research Communications 98(3), 792-799.

48. Hirayama, T., Nagayama, H. and Matsuda, K. (1979) J. Biochem. 85, 591-599.

49. Maguire, R. J. (1977) Can. J. Biochem. 55, 19-26.

50. Umezurike, G. M. (1977) Biochem. J. 167, 831-833.

51. Umezurike, G. M. (1978) Biochem. J. 175, 455-459.

52. Umezurike, G. M. (1979) Biochem. J. 179, 503-507.

53. Rupley, J. A., Banerjee, S. K., Kregar, I., Lapanje, S., Shrake, A. F. and Turk, V. (1974) in Lysozyme (Edited by Osserman, F. F., Canfield, R. E. and Beychok, S.), pp.251-268. Academic Press, New York.

54. Aerts, G. M. and Bruyne, C. K. K. (1981) Biochim. Biophys, Acta 660, 317-324.

55. Weber, J. P. and Fink, A. L. (1980) J. Biol. Chem. 255(19), 9030-9032.

56. Alfani, F., Albanesi, D., Cantarella, M., Scardi, V. and Vetromile, A. (1982) Biomass 2, 245-253.

57. Fan, L. T., Lee, Yong-Hyun and David, H. (1980) Biotech. Bioeng. 22, 177-199.

58. Ladisch, M. R., Gong, C. S. and Tsao, G. T. (1976) Dev. Ind. Microbiol. (pub. 1977) 18, 157-168.

59. Cheng-Sung, G., Ladisch, M. R. and Tsao, G. T. (1977) Biotech. Bioeng. 19, 959-981.

60. Goldman, R., Kedem, O. and Katchalski, E. (1968) Biochemistry, 7, 4518-4532.

61. Miyairi, S., Suguira, M. and Vukui, S. (1978) Agric. Biol. Chem., 42, 1661-1667.

62. Venardos, D., Klei, H. E. and Sundstrom, D. W. (1980) Enzyme Microbiol. Tech. 2, 112-116.

63. Beltrame, Pier Luigi; Carniti, P., Focher, B., Marzetti, A. and Sarto, V. (1983) Chim. Ind. (Milan) 65(6), 398-401. C.A. 99, 154354z (1983).

64. Han, Y. W. and Srinivasan, V. R. (1969) J. Bacteriol 100, 1355-1363.

65. Laidler, K. J. and Bunting, P. S. (1973) The Chemical Kinetics of Enzyme Action, 2nd ed. Clarendon Press. Oxford pp. 69-79.

66. Wurtz, A. (1880) Comp. rend., 91, 787.

67. Chance, B. (1943) J. Biol. chem., 151, 553; Acta Chem. Scand., 1, 236 (1947); cf. also Stern, K. G. (1936) J. Biol. Chem., 114, 473; Keilin, D. and Mann, T. (1936) Proc. R. Soc., B122, 119.

68. Velick, S. F. (1958) J. Biol. Chem., 233, 1455.

69. Blum, J. J. and Morales, M. F. (1953) Arch. Biochem. Biophys., 43, 208-230.

70. Spector, L. B. and Anthony, R. S. (1970) J. Biol. Chem., 245, 6739-6741; Tsuda, Y., Stephani, R. A. and Meister, A. (1971) Biochem., 10, 3186-3189.

71. Lineweaver, H. and Burk, D. (1934) J. Am. Chem. Soc., 56, 658-666.

72. Royer, G., Wildnauer, R., Cuppett, C. C. and Canady, W. J. (1971) J. Biol. Chem., 246, 1129; and references therein: Valenzuela, P. and Bender, M. L. (1969) Proc. Nat. Acad. Sci. U.S., 63, 1214-1221.

73. Winstead, J. A. and Wold, F. (1965) J. Biol. Chem., 240, 3694-3696.

74. Eadie, G. S. (1942) J. Biol. Chem., 146, 85; cf. Hofstee, B. H. J. (1952) Science, 116, 329; (1959) Nature, 184, 1296.

75. Keston, A. S. (1956) Abstracts of Papers, 129th Meeting, A. C. S. pp. 31c.

76. Teller, J. D. (1956) Abstracts of Papers, 130th Meeting, A. C. S. pp. 69c.

77. Sols, A. and de la Fuente, G. (1961) Methods in Medical Research, Vol.9, Year Book Publishers, Chicago.

78. Meyers, S. P., Prindle, B. and Reynolds, E. S. (1960) Tappi, 43, 534-538.

79. Slein, M. W. (1965) in: Methods of Enzymatic Analysis (Bergmeyer, H. U. ed.), pp.117, Academic Press, New York.

80. Widdowson, G. M. and Penton, J. R. (1972) Clin. Chem. (Winston-Salem, N.C.) 18, 299-300.

81. Ek, J. and Hultman, E. (1958) Nature, 181, 780-781.

82. Hultman, E. (1959) Nature, 183, 108-109.

83. Dragovic, Danica; Majkic, Nada; Spasic, Slavica and Berkes, Ivan (1981) Arh. Farm. 31(1-2), 7-15 (Serbo-Croatian). C.A. 96, 118384 (1982).

84. Pomeranz, Y. and Meloan, C. E. (1971) in: Food Analysis: Theory and Practice, pp. 534-577, Avi, Westport, Connecticut.

85. Zabriskie,Dane W., Outubuddin, A. S. M. and Downing, Kim M. (1980) Biotech. and Bioeng. Symp. No.10, 149-162.

86. Winckers, P. L. M. And Jacobs, Ph. (1971) Clin Chim. Acta 34, 401-408.

87. Berghem, L. E. R. and Pettersson, L. G. (1973) Eur. J. Biochem. 37, 21-30.

88. Chan, A. H. and Cotter, D. A. (1980) Microbios Lett. 15, 7-15.

89. Nelson, N. (1944) J Biol. Chem., 153, 375-380.

90. Bergmeyer, H. and Bernt, E. (1963) in: Bergmeyer, E. (Ed.) Methods of Enzymatic Analysis, Academic Press, New York, pp. 321-325.

91. Morris, D. L., Campbell, J. and Hornby, W. E. (1975) Biochem. J. 147, 593-603.

92. Day, D. F. and Workman, W. E. (1982) Anal. Biochem. 126, 205-207.

93. Danielsson, B., Rieke, E., Mattiasson, Bo G., Winquist, F. and Mosbach, K. H. (1981) Appl. Biochem. and Biotech. 6, 207-222.

94. Engasser, J. M. and Horvath, C. (1976) in: Applied Biochemistry and Bioengineering (Wingard, L. B.,Jr.et al. eds.) Vol.1, pp.127, Academic Press, New York.

95. Tipton, K. F. and Dixon, H. B. F. (1979) in: Methods in Enzymology (Purich, D. L., ed.) Vol. 63A, pp.183, Academic Press, New York.

96. Michaelis, L. and Davidsohn, H. Biochem. Z., (1911) 35, 386-412.

97. Michaelis, L. and Pechstein, H. Biochem. Z., (1914) 59, 77-99.

98. Michaelis, L. and Rothstein, M. Biochem. Z., (1920) 110, 217-233.

99. von Euler, H., Josephson, K. and Myrback, K. (1924) Z. physiol. Chem., 134, 39-49.

100. Waley, S. G. (1953) Biochim. Biophys. Acta, 10, 27-34.

101. Laidler, K. J., (1955) Trans. Faraday Soc., 51, 528-539; see Ottolenghi, P. (1971) Biochem. J., 123, 445.

102. Kaplan, H. and Laidler, K. J. (1967) Can. J. Chem., 45, 539-546

103. Krupka, R. M. and Laidler, K. J. (1960) Trans. Faraday Soc. 56, 1467-1476.

104. Dixon, M. (1953) Biochem. J. 55, 161-170.

105. Alberty, R. A. and Massey, V. (1954) Biochem. Biophys. Acta 13, 347-353.

106. Cleland, W. W. (1967) Adv. Enzymol. 29, 1-32.

107. Wilkinson, G. N. (1961) Biochem. J. 80, 324-332.

108. Hinberg, I. and Laidler, K. J. (1973) Can. J. Biochem. 51, 1096-1103.

109. Mazid, M. A. and Laidler, K. J. (1982) Can. J. Biochem. 60, 100-107.

110. Draper, N. R. and Smith, H. (1966) Applied Regression Analysis, Chapts. 1 and 10, pp.1-43; 263-304, John Wiley and Sons, New York.

111. Barker, S. A., Doss, S. H., Gray, C. J., Kennedy, J. F., Stacey, M. and Yeo, T. H. (1971) Carbohyd. Res., 20, 1.

112. Srinivasan, V. R. and Bumm, M. W. (1974) Biotech. Bioeng. 16, 1413-1418.

113. Rao, M., Vasanti Deshpande, V. and Mishra, C. (1983) Biotech. Letters 5(2), 75-78.

114. Rudick, M. J. and Elbein, A. D. (1975) J. Bacteriol. 124, 534-541.

115. Herr, D., Baumer, F. and Dellweg, H. (1978) Eur. J. Appl. Microbiol. Biotechnol. 5, 29-36.

116. Wang, D. I. C., Cooney, C. L., Demain, A. L., Dunnill, P., Humphrey, A. E. and Lilly, M. D., eds. (1979) Fermentation and Enzyme Technology, John Wiley and Sons.

117. Sober, H. A.(ed.) (1984) Handbook of Biochemistry. Chemical Rubber Co.

118. Laidler, K. J. and Bunting, P. S. (1973) The Chemical Kinetics of Enzyme Action, 2nd Ed. Clarendon Press, Oxford, Chapter 13.

119. Levy, M. and Benaglia, A. E. (1950) J. Biol. Chem. 186, 829-847.

120. Steinhardt, J. (1937) K. danske Vidensk. Selsk. Mathfys. Medd., 14, No.11, 1-53.

121. Gibbs, R. J., Bier, M. and Nord, F. F. (1952) Arch. Biochem. Biophys. 35, 216-228.

122. Tanford, C. (1961) Physical Chemistry of Macromolecules, John Wiley & Sons, Inc., Publishers.

123. Laidler, K. J. and Peterman, B. F. (1979) in: Methods in Enzymology, 63, 234-257.

124. Laidler, K. J. (1959) Trans. Faraday Soc., 55, 1725-1730.

125. Kirk, J. E. (1969) Enzymes of the Arterial Wall, Academic Press, New York.

126. Brown, G., Thomas, D., Gellf, G., Domurado, D., Berjonneau, A. M. and Guillon, C. (1973) Biotech. Bioeng. 15, 359-375.

127. Bunting, P. S. and Laidler, K. J. (1972) Biochemistry, 11, 4477-4483.

128. Ngo, T. T. and Laidler, K. J. (1975) Biochem. Biophys. Acta 377, 303-316.

129. Laidler, K. J. and Bunting, P. S. (1980) in: Methods in Enzymology, 64, 234. Academic Press, New York.

130. Weetall, H. H. (ed.) Immobilized Enzyme, Antigens, Antibodies and Peptides (1975) Marcel Dekker.

131. Laidler, K. J. and Bunting, P. S. (1980) Method. Enzymol. 64B, 227.

132. Engasser, J. M. and Horvath, C. (1976) Appl. Biochem. Bioeng. 1, 127-220 (Wingard, L. B., Katchalski, K. E. and Goldstein, L. eds.) Academic Press.

133. Wang, S. S. and King, C. K. (1979) in: Advances in Biochemical Engineering (Gose, T. K., Fiechter, A. and Blakebrough, N., eds.) Springer-Verlag.

134. Kobayashi, T. and Laidler, K. J. (1974) Biotech. Bioeng. 16, 77-97.

135. Sundaram, P. V., Tweedale, H. and Laidler, K. J. (1970) Can. J. Chem. 48, 1498-1504.

136. Kobayashi, T. and Laidler, K. J. (1973) Biochim. Biophys. Acta 302, 1-12.

137. Kobayashi, T. and Moo-Young, M. (1973) Biotech. Bioeng. 15, 27-45, 47-67.

138. Berezin, I. V., Antonov, V. K. and Martinek, K., eds. (1976) Immobilized Enzymes, Moscow University Press, Moscow.

139. Goldman, R., Goldstein, L. and Katchalski, E. (1971) in: Biochemical Aspects of Reactions on Solid Supports, Stark, G. R. ed., Academic Press, New York, pp.1-78.

140. Zaborsky, O. R. (1973) Immobilized Enzymes, CRC Press, Cleveland.

141. Weetall, H. H. and Suzuki, S., eds. (1975) Immobilized Enzyme Technology, Plenum Press, New York.

142. Mosbach, K., ed. (1976) Methods in Enzymology, Vol.44, Academic Press, New York.

143. Brodelius, P.(1978) in: Advances in Biochemical Engineering (Ghose, T. K., Fiechter, A., Blakeborough N. eds.), Vol.10, Springer-Verlag, Berlin Heidelberg, New York, p.75 .

144. Barker, S. A. (1980)in: Economic Microbiology (Rose, A. H. ed.) Vol.5, Academic Press, New York and London. p.330 .

145. Chibata, I., Tosa, T. and Matuo, Y. (1972) in: Fermentation Technology Today (Terui, G., ed.), Soc Fermentation Technology, Osaka Japan, p.383 .

146. Chibata, I. and Tosa, T. (1977) Adv. Appl. Microbiol. 22, 1-27.

147. Vandamme, E. J. (1976) Chem. Ind. 24, 1070.

148. Abbott, B. J. (1976) Adv. Appl. Microbiol. 20, 203-257.

149. Abbott, B. J. (1977) in: Annual Reports on Fermentation Processes (Perlman, D., ed.) Vol.1, Academic Press, New York, p.205 .

150. Jack, T. R. and Zajic, J. E. (1977) in: Advances in Biochemical Engineering (Fiechter A., ed.), Vol.5, Springer-Verlarg Berlin Heidelberg, New York, p.125 .

151. Venkatasubramanian, K. and Vieth, W. R. (1979) in: Progress in Industrial Microbiology (Bull, M. J., ed.), Vol.15, Elsevier Amsterdam, Oxford, New York, p.61 .

152. Chibata, I. and Tosa, T.(1981) Annu. Rev. Biophys. Bioeng. 10, 197-216.

153. Durand, G. and Navarro, J M. (1978) Process Biochemistry 13(9), 14-23.

154. Klein, J. and Wagner, F. (1978) In Dechema Monogr 82--Biotechnology-. Verlag Chemie, Weinheim New York, 142-164.

155. Klein, J. and Eng, H. (1979) Biotechnol Lett, 1, 171-176.

156. Mosbach, K. (1982) J. Chem. Tech. Biotechnol. 32,179-188.

157. Klaus-Dieter Vorlop and Joachim Klein, (1983) in: Enzyme Technology III. Springer-Verlag, Berlin Heidelberg, pp.219-235.

158. Hagerdal, B. and Mosbach, k. (1980) in: Linko, P. and Larinkari, J. (eds.) Food process engineering Vol.2. Applied Science Publishers. London. pp.129-132.

159. Hartmeier, W. (1981) in: Moo-Young, M. (ed.) Advances in biotechnology Vol. 3. Pergamon, Toronto. pp.377-382.

160. Hartmeier, W. (1983) in: Lafferty, R. M.(ed.) Enzyme Technology III. Springer-Verlag, Berlin Heidelberg. pp.207-217.

161. Silman, I. H. and Katchalski, E. (1966) Ann. Rev. Biochem., 35, 873-908.

162. Kay, G. (1968) Process Biochem., August; see also Sundaram, P. V. and Hornby, W. E. (1970) FEBS Lett., 10, 325.

163. Goldstein, L. and Manecke, G. (1976) in: Applied Biochem. Bioeng. (Wingard, L. B., Katchalski, E. and Goldstein, L. eds.) 1, 23-110, Academic Press, New York.

164. Chibata, I. (1978) Immobilized Enzymes, Research and Development, Halsted Press, New York.

165. Hahn-Haegerdal, B. (1984) Biotech. Bioeng. 26(7), 771-774.

166. Magae, Y., Kawashima, K., Kashiwagi, Y. and Sasaki, T. (1984) Nippon Shokuhin Kogyo Gahkaishi 31, 231-5 (Japan) C. A. (1984) 101, 68459r.

167. Lomako, O. V., Menyailova, I. I., Nakhapetian, L. A., Kozlovskaya, L. I. and Rodionova, N. A. (1982) Acta Biotechnol. 2(2), 179-185.

168. Klibanov, A. M. (1979) Analytical Biochemistry 93, 1-25.

169. Ory, R. L. and St. Angelo, A. J. eds. (1977) Enzymes in Food and Beverage Processing, A.C.S. Symposium Series.

170. Hornby, W. E., Campbell, J., Inman, D. J. and Morris, D. L. (1974) in: Enzyme Engineering (K. Pye and Wingard, L. Jr., eds.) Vol. 2, Plenum, New York. pp.401.

171. Itoh, N., Hagi, N., Iida, T., Tanaa, A. and Fukui, S. (1979) J. Appl. Biochem. 1, 291-300.

172. Inman, D. J. and Hornby, W. E. (1973) Biochem. J. 137, 25-32.

173. Campbell, J. and Hornby, W. E. (1977) in: Biomedical Applications of Immobilized Enzymes and Proteins (T.M. S. Chang, ed.) Vol. 2, Plenum Press, New York.

174. Kobayashi, T. and Laidler, K. J. (1974) Biotech. Bioeng. 16, 99-118.

175. Van Dongen, David B. and Cooney, D. O. (1977) Biotech. Bioeng. 19, 1253-1258.

176. Bunting, P. S. and Laïdler, K. J. (1974) Biotech. Bioeng. 16, 119-134.

177. Ngo, T. T. and Laidler, K. J. (1975) Biochim. Biophys. Acta 377, 317-330.

178. Narinesingh, D., Ngo, T. T. and Laidler, K. J. (1975) Can. J. Biochem. 53, 1061-1069.

179. Ngo, T. T., Narinesingh, D. and Laidler, K. J. (1976) Biotech. Bioeng. 18, 119-127.

180. Ngo, T. T. and Laidler, K. J. (1978) Biochim. Biophys. Acta 525, 93-102.

181. Daka, N. J. and Laidler, K. J. (1978) Can. J. Biochem. 56, 774-779.

182. Daka, N. J. (1981) Ph.D. Thesis, University of Ottawa, Canada.

183. Fasman, G. D. (ed.) (1975) Handbook of Biochemistry and Molecular biology; Physical and Chemical Data Vol. 1 (3rd Ed.), pp.153-212 CRC Press.

184. Longsworth, L. G. (1953) J. Am. Chem. Soc. 75 5705-5709.

185. Clarke, D. M. and Dole, M. (1954) J. Am. Chem. Soc. 76, 3745-3751.

186. Fersht, A. (1985) Enzyme Structure and Mechanism, 2nd Ed. W. H. Freeman and Company, New Youk.